# University of Alberta

Chemical Synthesis and Biological Evaluation of Naturally Occurring Cyclic Peptides and their Analogues: Lacticin 3147 A2 and Neopetrosiamides

by

Hongqiang Liu

A thesis submitted to the Faculty of Graduate Studies and Research
in partial fulfillment of the requirements for the degree of

Doctor of Philosophy

Department of Chemistry


Fall, 2010
Edmonton, Alberta

*Your file Votre référence*
*ISBN:* 978-0-494-81318-8
*Our file Notre référence*
*ISBN:* 978-0-494-81318-8

## Examining Committee

Dr. John C. Vederas (Supervisor)
*Department of Chemistry*

Dr. Derrick L. J. Clive
*Department of Chemistry*

Dr. David R. Bundle
*Department of Chemistry*

Dr. Charles A. Lucy
*Department of Chemistry*

Dr. David C. Bressler
*Department of Agricultural, Food and Nutritional Science*

Dr. Sarah E. O'Connor (External)
*Department of Chemistry*
*Massachusetts Institute of Technology*

*To my wife, Hua, and daughter, Tracy*

# ABSTRACT

Lantibiotics, such as lacticin 3147 A1 (**16**) and A2 (**17**) are antibacterial peptides that exhibit great promise for application in food preservation, veterinary medicine and human therapeutics. However, use of lantibiotics is limited due to the chemical lability of the sulfur atoms in lanthionine rings. To improve oxidative stability of lacticin A2, an analogue (**45**) with oxygen replacing sulfur atoms was designed and synthesized. The preliminary biological evaluation suggests that the oxygen analogue (**45**) displays the inherent activity of the parent peptide, but lacks the synergistic activity with lacticin 3147 A1 (**16**).

To verify the proposed structure of the natural lacticin A2 (**17**), its total synthesis was initiated. A practical synthetic methodology for the large-scale synthesis of methyllanthionine with orthogonal protecting groups was developed. The synthesis of the post-translationally modified *N*-terminal portion (residues 1-5) of lacticin A2 was also explored.

Neopetrosiamides are disulfide-rich peptides that are potent inhibitors of metastasis. Their total synthesis was explored using a stepwise disulfide formation approach. During the course of the synthesis, it was found that the disulfide connectivity in the originally proposed structure was misassigned. A revised structure was proposed and confirmed by chemical synthesis. To evaluate the necessity of the methionine sulfoxide at position 24, four analogues in which this residue is replaced by methionine (**175**), norleucine (**176**), *O*-methyl homoserine (**180**) and glutamine (**181**) were synthesized. The methionine and norleucine analogues (**175** and **176** respectively) were found to be as active as the

natural peptide, suggesting that this unusual functional group is not essential for biological activity. In an effort to simplify the structure of neopetrosiamides, three analogues (**182**, **183** and **184**) were prepared, each having one of the three disulfides replaced with a pair of phenylalanine residues. Their lack of biological activity suggests the importance of disulfides in maintaining an active conformation. In order to elucidate the detailed mode of action of neopetrosiamides, a fluorescently labeled analogue (**196**) was prepared via a "click" reaction. The peptide conjugate (**196**) is inactive, but its synthetic precursor (**194**) with an azido linker attached is fully active, suggesting that the design of active labeled analogues for further investigation is an attainable goal.

# ACKNOWLEDGEMENTS

This work would not have been possible without the support of many different people around me. First of all, I would like to acknowledge my research supervisor, Professor John C. Vederas, for his constant support, encouragement and endless guidance. The time spent in his research lab has been rewarding and memorable. The people that I have met in his group, both past and present, deserve acknowledgement for creating a stimulating and enjoyable working environment. I would specially like to thank Avena Ross, Dr Jennifer Chaytor and Dr. Wei Liu for their valuable insight and assistance in proofreading this manuscript. I also would like to acknowledge our collaborators, Prof. Michel Roberge, Prof. Raymond Andersen and Pamela Austin (University of British Columbia) for their assistance and hardwork in neopetrosiamide project. I would like to thank the dedicated support staff in the Chemistry Department, especially Dr. Randy Whittal and Jing Zheng for the help with mass spectrometry. All of the funding agencies, the University of Alberta and Alberta Heritage Foundation for Medical Research, are gratefully acknowledged for their financial support.

My deep appreciation also goes to my family and friends for their constant support throughout my graduate studies. My parents especially deserve the particular gratitude for their encouragement in my life.

Finally, I would like to thank my wife Hua and daughter Tracy for everything that you have sacrificed for me. My wife's endless supply of encouragement, patience, and support has been source of strength throughout the

duration of my graduate study. My daughter's smile has been such wonderful source of joy and delight. Words cannot describe how appreciative I am. Thank you!

# TABLE OF CONTENTS

# LIST OF TABLES

# LIST OF FIGURES

# LIST OF SCHEMES

# LIST OF ABBREVIATIONS

| | |
|---|---|
| $[\alpha]_D^{25}$ | specific rotation |
| A or Ala | alanine |
| Abu | aminobutyrine |
| Ac | acetyl |
| Acm | acetamidomethyl |
| $Ac_2O$ | acetic anhydride |
| AcOH | acetic acid |
| Alloc | allyloxycarbonyl |
| app | apparent |
| Ar | aryl |
| $BF_3$ | boron trifluoride |
| Bn | benzyl |
| Boc | *tert*-butoxycarbonyl |
| *t*-Bu | *tertiary*-butyl |
| *t*-BuOH | *tertiary*-butanol |
| br | broad |
| *c* | concentration |
| C or Cys | cysteine |
| *C*-terminus | carboxy terminus |
| calc'd | calculated |
| Cbz | benzyloxycarbonyl |

| | |
|---|---|
| $Cys_2$ | cystine |
| d | doublet |
| D or Asp | aspartic acid |
| DBU | 1,8-diazabicyclo[5.4.0]undec-7-ene |
| DCC | 1,3-dicyclohexylcarbodiimide |
| DCE | 1,2-dichloroethane |
| DCM | dichloromethane |
| Dha | didehydroalanine |
| Dhb | didehydrobutyrine |
| DIC | diisopropylcarbodiimide |
| DIPEA | diisopropylethylamine |
| DMAP | 4-dimethylaminopyridine |
| DMF | N,N-dimethylformamide |
| DMSO | dimethylsulfoxide |
| DNs | 2,4-dinitrobenzenesulfonyl |
| E or Glu | glutamic acid |
| EDCI | 1-ethyl-3-(3'-dimethylaminopropyl)carbodiimide |
| EDT | 1,2-ethane dithiol |
| EI | electron impact |
| equiv | equivalents |
| ES | electrospray |
| Et | ethyl |
| $Et_3N$ | triethylamine |

| | |
|---|---|
| $Et_2O$ | diethyl ether |
| EtOAc | ethyl acetate |
| F or Phe | phenylalanine |
| FDA | US food and drug adminstration |
| Fmoc | 9*H*-fluorenylmethoxycarbonyl |
| g | gram |
| G or Gly | glycine |
| h | hour |
| H or His | histidine |
| HBTU | 2-(1H-benzotriazole-1-yl)-1,1,3,3-tetramethyluronium hexafluorophosphate |
| HIV | human immunodeficiency virus |
| HOBt | 1-hydroxybenzotriazole |
| HPLC | high performance liquid chromatography |
| HRMS | high resolution mass spectrometry |
| I or Ile | isoleucine |
| IR | infrared |
| *J* | coupling constant |
| K or Lys | lysine |
| L or Leu | leucine |
| LAB | lactic acid bacteria |
| Lan | lanthionine |
| LC | liquid chromatography |

| | |
|---|---|
| LC-MS/MS | liquid chromatography tandem mass spectrometry |
| μM | micromolar |
| m | multiplet |
| M or Met | methionine |
| MALDI-TOF | matrix-assisted laser desorption ionization / time of flight |
| Me | methyl |
| MeCN | acetonitrile |
| MeLan | methyllanthionine |
| Mmt | monomethoxytrityl |
| mol | mole |
| MHz | megahertz |
| MS | mass spectrometry |
| MsCl | methanesulfonyl chloride |
| MS/MS | tandem mass spectrometry |
| MQ | Milli-Q |
| MW | molecular weight |
| nM | nanomolar |
| N or Asn | asparagine |
| Nle | norleucine |
| Nmm | *N*-methylmaleimide |
| NMM | *N*-methylmorpholine |
| NMP | *N*-methylpyrrolidone |
| NMR | Nuclear magnetic resonance |

| | |
|---|---|
| Neo | neopetrosiamide |
| NOE | nuclear Overhauser effect / enhancement |
| NOESY | NOE spectroscopy |
| P or Pro | proline |
| $Pd(PPh_3)_4$ | tetrakis(triphenylphosphine)palladium |
| Ph | phenyl |
| $PhSiH_3$ | phenylsilane |
| PMB | *para*-methoxybenzyl |
| Pmc | 2,2,5,7,8-pentamethyl chroman-6-yl sulfonyl |
| pNZ | *para*-nitrobenzyloxycarbonyl |
| ppm | part per million |
| *n*-PrSH | *n*-propyl mercaptane |
| PTSA | *para*-toluene sulfonic acid |
| Py-BOP | benzotriazole-1-yl-oxy-*tris*-pyrrolidino-phosphonium hexafluorophosphate |
| q | quartet |
| Q or Gln | glutamine |
| R or Arg | arginine |
| RCM | ring closing metathesis |
| RP | reverse phase |
| rt | room temperature |
| s | singlet |
| S or Ser | serine |

| | |
|---|---|
| SA | sinapinic acid, 3,5-dimethoxy-4-hydroxycinnamic acid |
| SAR | structure activity relationship |
| SPPS | solid phase peptide synthesis |
| t | triplet |
| T or Thr | threonine |
| TFA | trifluoroacetic acid |
| THF | tetrahydrofuran |
| TIPS | triisopropylsilane |
| TLC | thin layer chromatography |
| $t_R$ | retention time |
| Tris | trihydroxymethylaminomethane |
| Trt | trityl |
| UV | ultraviolet |
| V or Val | valine |
| W or Trp | tryptophan |
| Y or Tyr | tyrosine |

# Chapter 1. Cyclic peptides in drug development

Since the discovery of their activities as hormones, neurotransmitters and antibiotics,[1,2,3] peptides have gained enormous importance in drug development.[4] They possess great potential as therapeutic agents because they offer high selectivity and potency with minimal toxicity.[5] The development of peptide-based drugs coincides with the advancement of techniques for chemical modification and production of such compounds on a large scale. For example, the synthetic anti-HIV drug Fuzeon (enfuvirtide), a linear peptide with 36 amino acids, can be produced at a capacity of about 3700 kg per year according to a report in 2005.[6] However, peptide drugs have been used therapeutically to only a limited extent, as they often lack metabolic stability *in vivo* and are not orally available.[4]

Fortunately, not all peptides suffer from these shortcomings. Naturally occurring cyclic peptides frequently display enhanced metabolic stability, along with high receptor affinity and selectivity and improved bioavailability due to conformationally constrained structural features.[7] Cyclic peptides often contain unusual moieties, such as D-amino acids, β-amino acids, *N*-alkyl amino acids and α, β-didehydro amino acids. Due to the increased metabolic stability resulting from these unusual structures, cyclic peptides become excellent leads for drug discovery.[7] Some are directly utilized as drugs. A prominent representative is caspofungin (**1**), which was approved by the US Food and Drug Adminstration (FDA) in 2001 and has become a best selling anti-fungal drug (Figure 1).[8] A novel class of plant-derived cyclic peptides named cyclotides has been recently

discovered. Cyclotides show a wide range of biological activities, including anti-HIV, antimicrobial, uterotonic, cytotoxic, hemolytic, neurotensin antagonistic, trypsin inhibitory and insecticidal activity.[9] Cyclotides, such as kalata B1 (**2**), comprise a head to tail macrocycle together with a knotted arrangement of three conserved disulfide bonds (Figure 1). This characteristic framework gives cyclotides exceptional resistance to chemical and enzymatic degradation (and even stability to boiling), thereby making oral administration of these peptides possible. Cyclotides are excellent drug candidates. In addition, the cyclotide framework can also be used as a scaffold for drug design.[10]

**Figure 1.** Structures of representative cyclic peptides

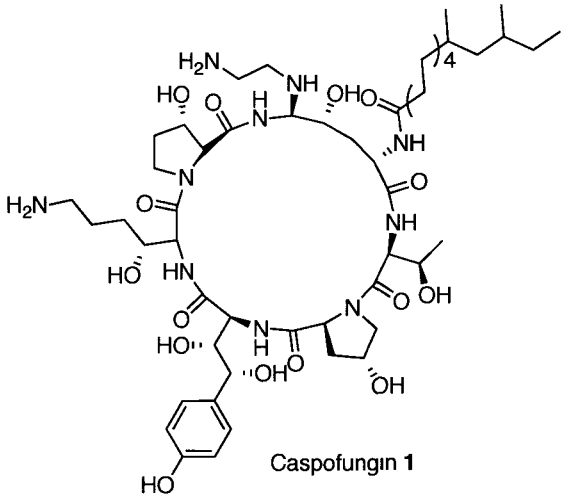

Caspofungin **1**

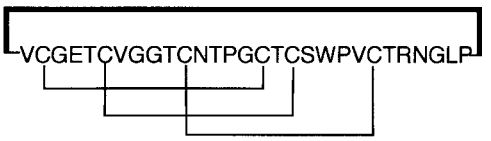


Prototypic cyclotide, Kalata B1 **2**

Peptides can be cyclized in several different ways. As illustrated in the structure of caspofungin (**1**), the *N*-terminal amino group of the linear peptide can be linked to the *C*-terminal carboxylic acid through amide bond formation. This is termed "backbone *N*-to-*C* cyclization." In addition, most cysteine-rich linear peptides can also be cyclized via the formation of covalent bonds by free thiols (Scheme 1). The most common form of cyclization is a disulfide bridge formed

by oxidation of two cysteine residues, which stabilizes the three-dimensional structure of peptides and plays a crucial role in their biological activities. A wide variety of peptide drugs in clinical use, such as the hormones insulin and oxytocin[1] and the toxin ω-conotoxin ziconotide (Prialt),[11] contain these cyclic motifs. The majority of drug development utilizing cyclic peptides has focused on the study of disulfide bond-containing compounds.

A less common type of cyclization is the formation of thio-ether rings, often called lanthionine bridges.[12] These unusual motifs are commonly present in lantibiotic (lanthionine containing antibiotic) peptides, such as nisin, which has broad antimicrobial activity and is used as a food preservative worldwide.[13] The formation of lanthionine bridges involves the Michael addition of a free thiol of cysteine onto an α, β-unsaturated amino acid that is derived from the dehydration of either serine or threonine residues.[14] The detailed biosynthetic pathway for lanthionine formation will be discussed in Chapter 2. Cyclic peptides containing lanthionine rings have received much attention as potential antimicrobial drugs to fight resistant bacterial infections.[15]

**Scheme 1.** Formation of cyclic peptides containing disulfide or thio-ether bridges

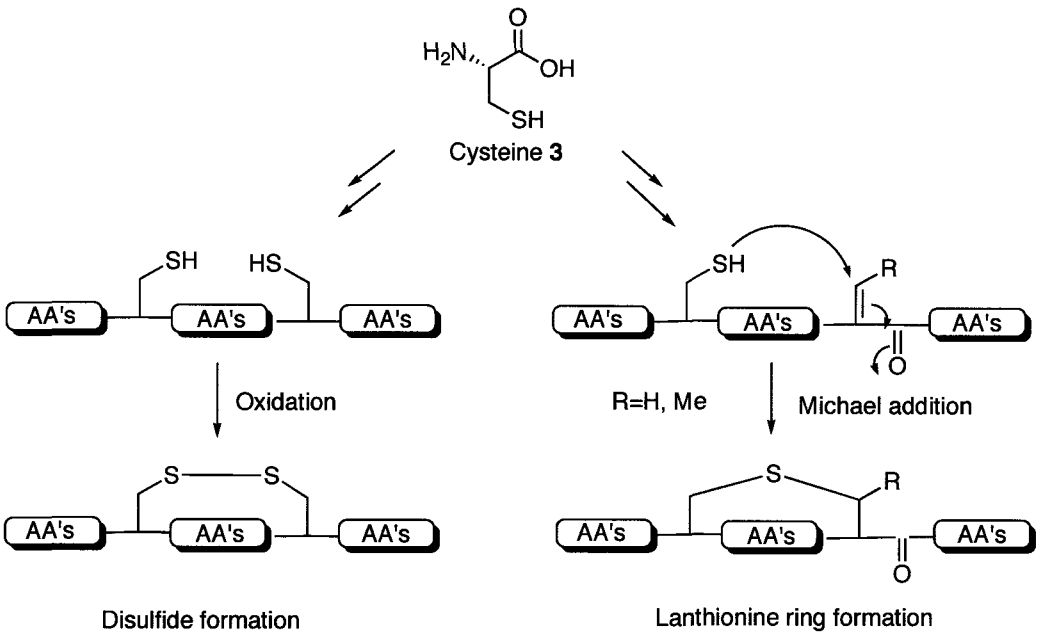


Although naturally occurring cyclic peptides are important for drug development, it is often difficult to isolate a large amount of them because the producing organisms often make only minute quantities. In addition, collecting the organisms can be problematic.[16] Performing precise structure elucidation and biological activity screens for a peptide can be very challenging when only a limited amount of sample is available. Therefore, final structural proof for naturally occurring cyclic peptides often relies on chemical total synthesis of the proposed structure. Synthesis also offers opportunities for large-scale production and enables facile access to a wide variety of analogues that would be difficult to produce via biological methods. In this thesis, the central theme is chemical synthesis of naturally occurring cyclic peptides and their analogues combined with the examination of their biological activities.

# Chapter 2. Antimicrobial peptides: lacticin 3147 A2 and its stable analogue

## 2.1. Introduction

### 2.1.1. Bacteriocins from lactic acid bacteria

The discovery of antibiotics has had an immense impact on the treatment of human bacterial infections.[17] Over the past few decades, the widespread emergence of bacterial resistance to current antibiotics has presented a serious problem that imposes a huge financial burden on patients and healthcare systems globally.[18,19] To date, bacterial resistance has developed to almost all antibiotics used in clinical settings.[20] The imperative need for novel and more effective antimicrobial agents that are active against resistant bacteria is prompting scientists to investigate a variety of natural sources.[17,16, 21] Among them, bacteria are a very promising source of a vast variety of antimicrobial peptides known as bacteriocins.[22,23] As an important part of the defense system of bacteria, bacteriocins often only kill bacteria that are closely related to their producer strains (narrow spectrum). In some cases, they also extend their activity spectrum to species and/or genera different from the producer (broad spectrum), potentially including strains resistant to conventional antibiotics.[22] The producer organism is protected from its own bacteriocin through a specific immunity protein.[24] It is believed that bacteriocins can be found in almost every bacterial species.[25] Both Gram-positive and Gram-negative bacteria can produce bacteriocins by ribosomal peptide synthesis and post-translational modification.[26] The bacteriocins from

Gram-positive bacteria normally possess a broader killing spectrum.[27] In particular, bacteriocins produced by food-grade lactic acid bacteria (LAB) show great promise as antimicrobial agents.

With the remarkable diversity of bacteriocins discovered, the scientific community has attempted to classify the peptides from lactic acid bacteria into several groups. However, the classification is continually evolving as new bacteriocins are identified and understanding of the existing bacteriocins is developed. Nevertheless, two distinct families have become evident: the lantibiotics (class I) and the non-lantibiotics (class II). The widely accepted classification of LAB bacteriocins is listed in Table 1.[27]

**Table 1. Classification of LAB bacteriocins according to Nes *et al.*** [27, 28]

| | | | |
|---|---|---|---|
| Class I. Lantibiotics<br><br>*- Presence of lanthionine or methyllanthionine;*<br><br>*- Extensive post-translational modifications* | Type A | Elongated, flexible, cationic peptides | Nisin<br>Gallidermin<br>Lacticin 3147 A2 |
| | Type B | Globular, rigid, anionic or neutral peptides | Mersacidin<br>Lacticin 3147 A1 |
| Class II. Non-lantibiotics<br><br>*-Non-lanthionine containing peptides;*<br><br>*-No extensive post-translational modifications* | Type IIa | Highly anti-listerial, conserved "Pediocin-box" motif in the *N*-terminus (YGNGV) | Leucocin A<br>Pediocin PA-1<br>Piscicolin 126 |
| | Type IIb | Two-component bacteriocins – full antimicrobial activity depends on the presence of both peptides | Lactococcin G |
| | Type IIc | Miscellaneous peptides (do not easily fit into the other categories) | Lactococcin A |
| | Type IId | Leaderless peptides | Enterocin L50 |
| | Type IIe | Derived from fragmentation of larger proteins | HP |
| Class III.<br>*-Large, heat-labile bacteriocins* | | | Helveticin J |
| Class IV. Circular<br><br>*-backbond cyclized bacteriocins* | Class i | Low sequence homology, high pI (~10) | Enterocin AS-48<br>Carnocyclin A |
| | Class ii | High sequence homology, low pI (~6) | Gassericin A |

## 2.1.2. Lantibiotics

As illustrated in Table 1, lantibiotics are a subclass of bacteriocins that are small (< 5 kDa) bactericidal peptides characterized by the presence of the unusual amino acid lanthionine (Lan) **4** or β-methyllanthionine (MeLan) **5**.[14, 12, 13] The name lantibiotic was actually coined as an abbreviation for *lan*thionine-containing an*tibiotic*. Lantibiotics are ribosomally synthesized and post-translationally modified to their active forms. The extensive post-translational modifications not only produce the characteristic Lan **4** and MeLan **5** but also generate other modified amino acids, such as 2,3-didehydroalanine (Dha) **6**, (*Z*)-2,3-didehydrobutyrine (Dhb) **7**, 2-oxopropionyl **8**, 2-oxobutyryl **9**, D-alanine (D-Ala) **10**, *S*-[(*Z*)-2-aminovinyl]-D-cysteine (AviCys) **11** and *S*-[(*Z*)-2-aminovinyl]-(3*S*)-3-methyl-D-cysteine (AviMeCys) **12** (Figure 2).[14]

**Figure 2.** Structures of common post-translationally modified residues in lantibiotics

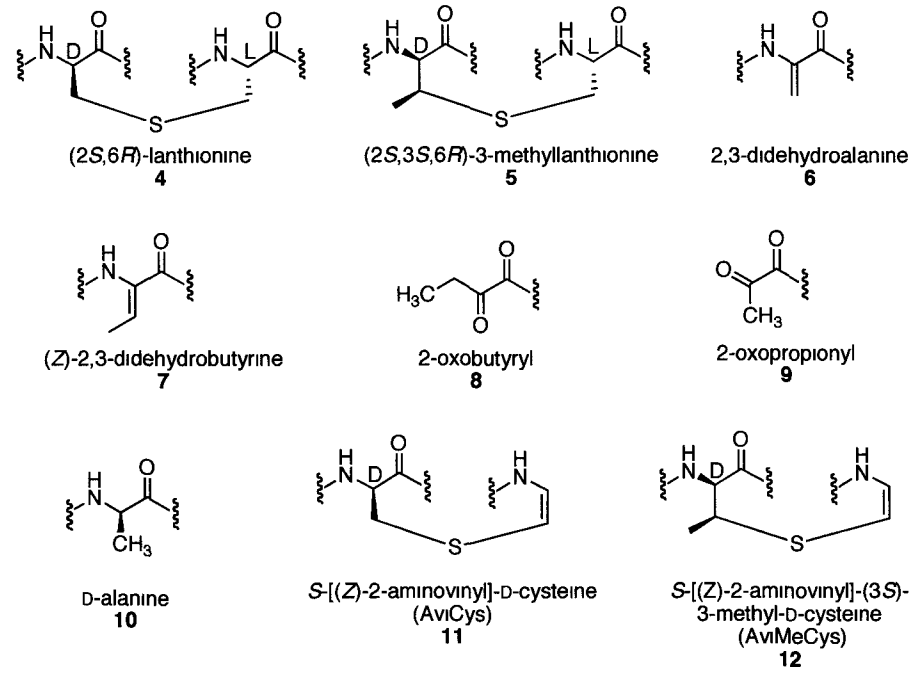

To date, nisin (**13**) is the most intensively studied lantibiotic, as it has been used as a food preservative for almost 50 years in over 80 countries worldwide and has been examined by total synthesis[29] and NMR studies[30] (Figure 3). Nisin not only effectively kills Gram-positive food-borne pathogens such as staphylococci, bacilli, clostridia and mycobacteria, but also exhibits activities against clinically significant bacteria such as methicillin resistant *Staphylococcus aureus* (MRSA), vancomycin resistant *Enterococci* (VRE) and *Clostridium difficile*.[27] Their broad spectrum of antibacterial activity as well as lack of toxicity to humans make lantibiotics attractive as therapeutic agents. For example, nisin has been commercialized in antibiotic wipes for treatment and prevention of bacterial mastitis in animals.[31] Mersacidin (**14**) has become a promising compound for treatment against methicillin resistant *Staphylococcus aureus* (MRSA).[32] Gallidermin **15** has been used topically to treat acne due to its potent activity against *Propionibacterium acne*.[33] More recently, it has been demonstrated that nisin also shows spermicidal activities and could be used as a potential ingredient in contraceptive agents.[34]

**Figure 3.** Structures of representative lantibiotics

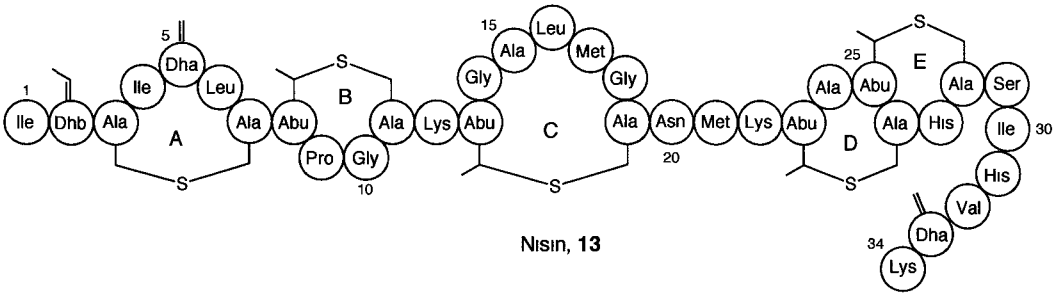


Nisin, **13**

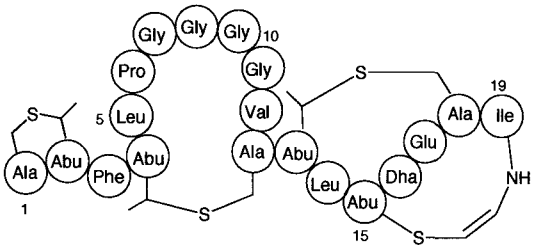


Mersacidin, **14**

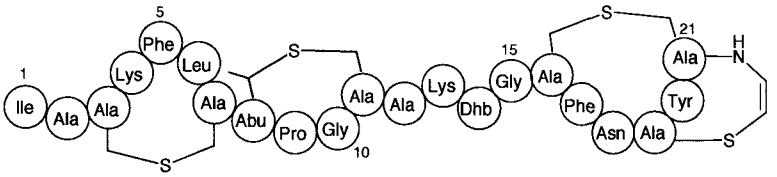


Gallidermin, **15**

Lantibiotics are usually produced as individually active peptides, but they can also occur as pairs of synergistic peptides. The first identified two-peptide lantibiotics are lacticin 3147 A1 (**16**) & A2 (**17**) (Figure 4).[35] Lacticin 3147 A1 & A2 are produced by *Lactococcus lactis* sub species *lactis* DPC 3147, which was isolated from an Irish kefir grain.[35] The individual A1 and A2 peptides display weak antibacterial activity (μM concentration), but when combined together, they show potent synergistic activity (nM concentration). The structures of lacticin 3147 A1 and A2 have been elucidated by NMR analysis. However, unlike nisin,

the stereochemistry of the lanthionine and methyllanthioine residues within lacticin 3147 A1 and A2 had not been confirmed by total synthesis. (2*S*,6*R*) Lanthionine and (2*S*,3*S*,6*R*) 3-methyllanthionine stereochemistries were assigned by analogy to the configurations found in a small number of other lantibiotics that have undergone chiral analysis. Although two-peptide lantibiotics are rare compared to singly active peptides, eight such systems have been described since the discovery of the first two-peptide lantibiotics in 1996.[35] These two-peptide systems include lacticin 3147, staphylococcin C55, plantaricin W, Smb, BHT-A, cytolysin, haloduracin and lichenicidin. [36,37]

**Figure 4.** Structures of the two-peptide lantibiotics: lacticin 3147 A1 (**16**) & A2 (**17**)

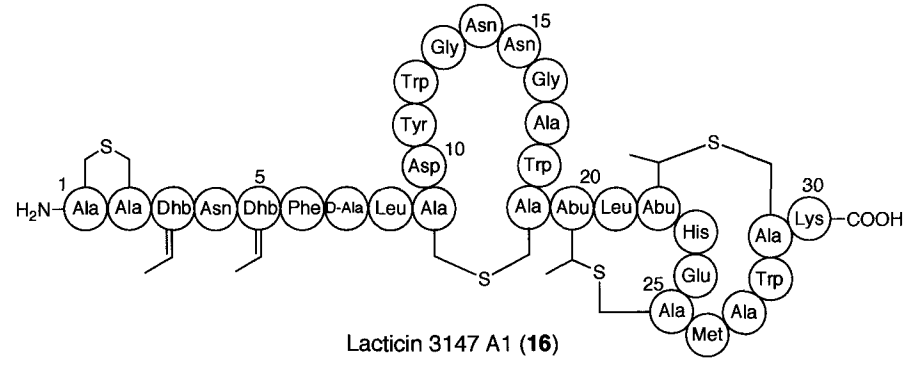


Lacticin 3147 A1 (**16**)

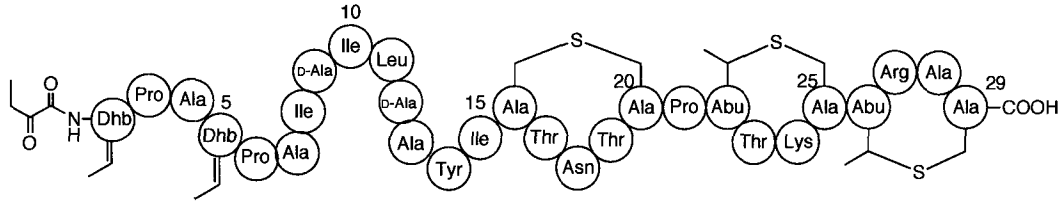


Lacticin 3147 A2 (**17**)

Lacticin 3147 has activity against an impressive list of the "superbugs" including MRSA, VRE, and penicillin resistant *Pneumococcus*. Therefore, there

is particular interest in developing this peptide system for medical use. Lacticin 3147 can be incorporated into a commercial teat seal product for prevention and treatment of mastitis in cows.[38] It can also be exploited for application in oral hygiene.[37]

Despite widespread application in the food industry and promising potential as therapeutic agents, use of lantibiotics can be limited due to their chemical lability.[39] For example, the sulfur in the characteristic lanthionine ring is prone to aerobic oxidation to a sulfoxide, greatly diminishing biological activity.[35, 40] Therefore, extensive research focuses on exploring the possibility of modifying lantibiotics to enhance oxidative and metabolic stability as well as antimicrobial activity.

### 2.1.3. Biosynthesis of lantibiotics

Lantibiotics are first synthesized as precursor peptides via ordinary protein synthesis machinery, namely the ribosome. The precursor peptides (prepeptide) contain an *N*-terminal leader sequence and a *C*-terminal structural region (propeptide) that undergoes post-translational modification.[14] The role of the leader peptide is generally accepted to fuction as a recognition motif for enzymatic modification or proteolysis. It is also believed to provide protection to the producing bacteria by keeping the lantibiotic inactive in the cell, and to assist transport of the peptide from the bacterial cell. [41]

As illustrated in Figure 5, a generic biosynthetic pathway has been proposed for the post-translational modifications of lacticin 3147 A2.[42, 43] The serine and threonine residues in the linear peptide undergo enzymatic dehydration

to yield didehydroalanine (Dha) and didehydrobutyrine (Dhb) residues, respectively. Subsequent enzymatically catalyzed Michael additions of free thiols of cysteines onto Dha and Dhb residues result in the formation of lanthionine and β-methyllanthionine, respectively.[44] Additional dehydrated residues either remain in the mature peptide or are converted into D-amino acid residues by a enzymatic reduction.[45] The proteolytic removal of the leader peptide with concomitant export generates the mature lantibiotic.

**Figure 5.** Schematic representation of the post-translational modification of lacticin 3147 A2 (**17**)

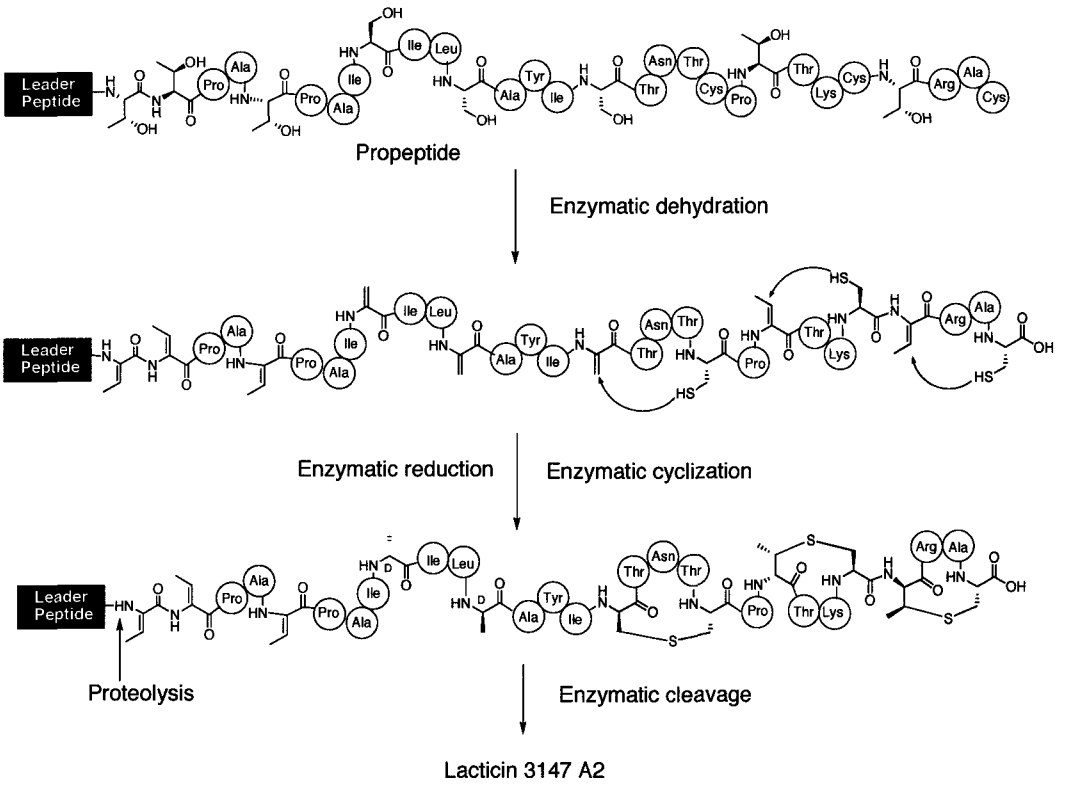


When the *N*-terminus of the propeptide is a dehydro amino acid, such as in lacticin 3147 A2, the removal of the leader peptide may trigger a deamination and hydrolysis process that yields an α-keto amide moiety (Figure 6).[14]

**Figure 6.** Schematic representation of α-keto amide formation

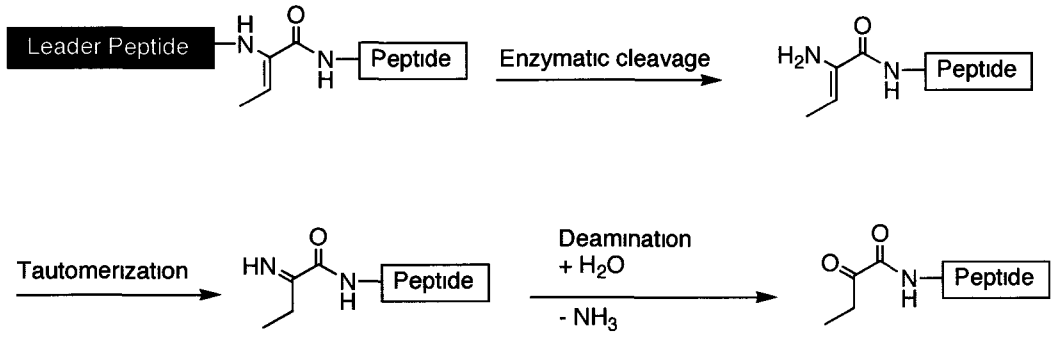


In some cases when a *C*-terminal cysteine is present in a propeptide, an enzymatic oxidative decarboxylation can lead to a transient ene-thiol species that then undergoes Michael addition to a neighboring dehydro residue to give an unsaturated lanthionine derivative, such as aminovinyl-D-cysteine (**11**) in mersacidin (Figure 7).[46]

**Figure 7.** Schematic representation of aminovinyl-D-cysteine formation

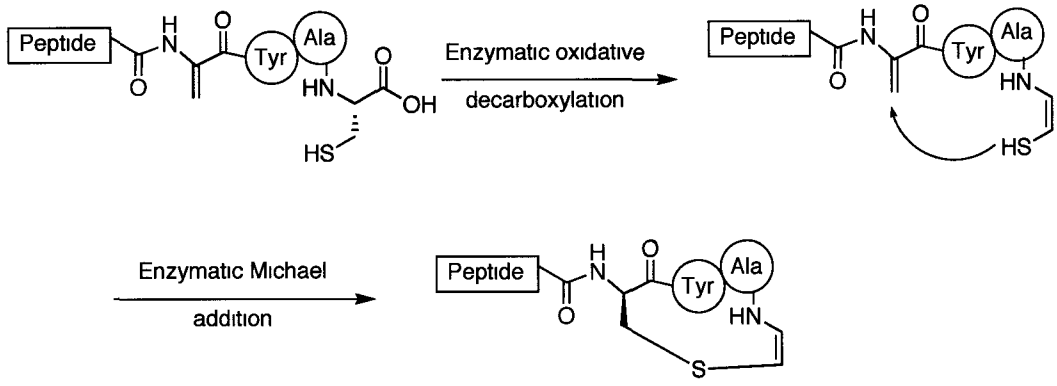


## 2.1.4. Modes of action of lantibiotics

While more than 50 lantibiotics have been identified to date, there are only a few whose modes of action are elucidated.[12] Most lantibiotics target the cell wall

of bacteria.[42] To help better understand this interaction of lantibiotics and the bacterial cell wall, the structure and biosynthesis of the cell wall are described briefly below.

To maintain structural rigidity of the cell and mechanical strength, the bacterial cell wall utilizes peptidoglycan, which is a polymer network of alternating amino sugars, *N*-acetylglucosamine (GlcNAc) and *N*-acetylmuramic acid (MurNAc) (Figure 8).[47, 48] These polymer chains introduce a continuous and covalent network via cross-linking pentapeptide chains that are attached to MurNAc sugars. The thickness of peptidoglycan varies from organism to organism. Generally, the cell wall of Gram-positive bacteria is much thicker and contains around 20 peptidoglycan layers, while Gram-negative bacteria have much thinner cell walls with an average thickness of around 1.5 layers. However, Gram-negative bacteria have an outer membrane that provides additional protection.

The fundamental building block for peptidoglycan biosynthesis is known as lipid II (**18**). In addition to amino sugars and a pentapeptide chain, a lipid II monomer also contains a C55 carbon chain that is attached to the disaccharide via a pyrophosphate linkage (Figure 9). After being assembled in the cytosol, lipid II is translocated across the plasma membrane. This monomer is then incorporated into the peptidoglycan network via enzymatic transglycosylation and transpeptidation.[48]

**Figure 8.** Schematic representation of peptidoglycan in the bacteria cell wall

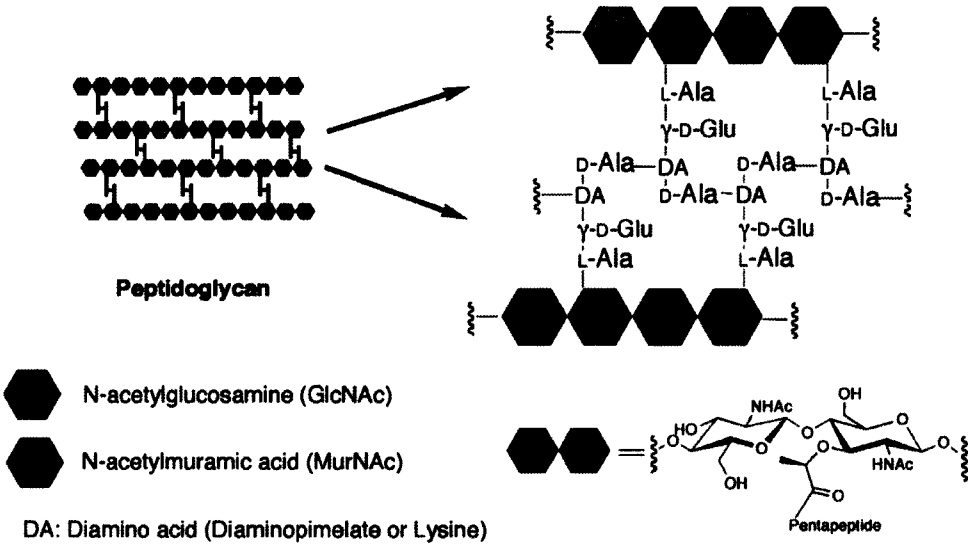


Lipid II, the "Achilles heel" of the Gram-positive cell wall, represents a promising target for the development of an antibiotic with low human toxicity, as lipid II has an essential role in bacterial cell wall biosynthesis, but no known metabolic function in humans.[47, 49] Vancomycin targets lipid II by binding to the D-Ala-D-Ala residues of the pentapeptide chain (Figure 9) through a specific hydrogen-bonding network and thereby inhibits cell wall biosynthesis.[50, 51] However, this specific binding is reduced in certain antibiotic-resistant bacteria wherein the terminal D-Ala in the pentapeptide chain of lipid II is mutated to D-lactate, leading to the decreased bacterial susceptibility of vancomycin.[48]

**Figure 9.** Chemical structure of lipid II (**18**) and the binding sites of antimicrobial agents

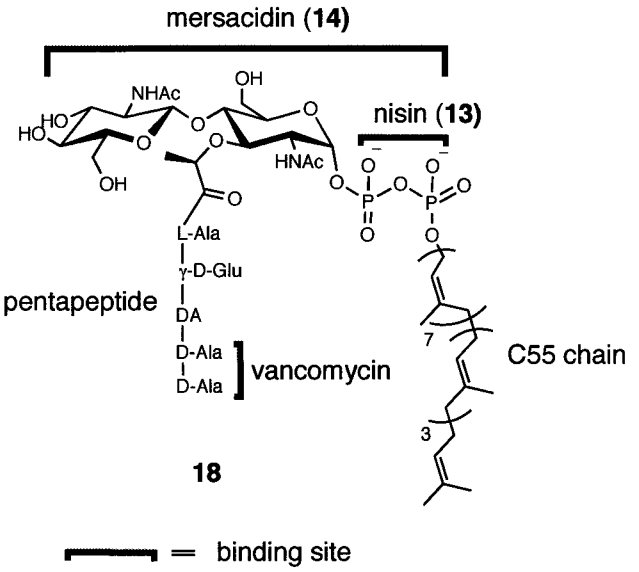


Lantibiotics also act on lipid II to kill bacteria by targeting a different structural region.[47] Nisin, the most studied lantibiotic, exhibits a dual mode of action entirely different from that used by vancomycin. It not only inhibits cell wall biosynthesis by specifically binding to lipid II with high affinity, but also triggers the formation of stable pores in the cell membrane that leads to rapid efflux of ions, dissipation of membrane potential, and eventually causing cell death.[14, 42, 52, 53] Recent NMR investigations reveal the interaction of nisin and lipid II at the molecular level.[54] Specifically, the *N*-terminal portion (ring A and B) of nisin binds to the pyrophosphate of lipid II to form a cage-like structure through a specific hydrogen-bonding network (Figure 10). Upon docking on lipid II, the *C*-terminus of nisin inserts into the cell membrane and forms highly ordered oligomers with other complexes of lipid II and nisin, ultimately resulting in pore formation and the leakage of cell contents. This dual mode of action may offer an

explanation for the exceptional potency of nisin against antibiotic-resistant bacteria and partially explain why no significant bacterial resistance has developed for nisin.

**Figure 10**. Hydrogen bond network between nisin *N*-terminal residues and the lipid II pyrophosphate moiety (*Reproduced from Nature Structural & Molecular Biology, Hsu et al., 2004*)[54]

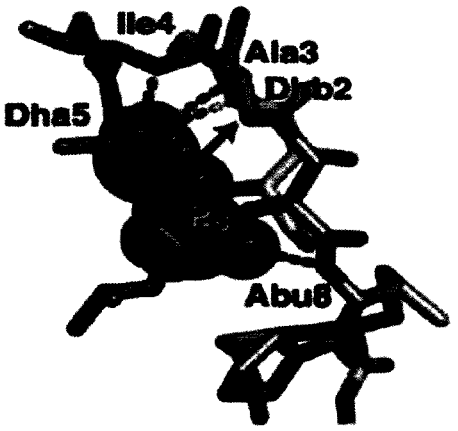


*Hydrogen bonds are indicated in yellow dashed lines and the corresponding residues are labeled (pyrophosphate group in spheres). The sulfur atoms in the lanthionine rings are orange. A green arrow indicates the position of Ala3-Cβ, at which the addition functional group can disrupt bioactivity.*

In two-peptide lantibiotics, such as lacticin 3147 A1 & A2 and haloduracin α & β, the individual peptides exhibit only moderate antimicrobial activity. When both peptides work together, a synergistic effect is observed with the resulting activity at low nanomolar concentrations. Recent investigations have provided further insight into their modes of action.[55] The two-peptide lantibiotics have a similar mode of action to nisin, which involves inhibition of cell wall biosynthesis and pore formation. However, the interesting feature is that the dual modes of action appear to be divided between the separate peptides. In the case of lacticin 3147 A1 & A2, it is postulated that the individual peptides bind to lipid II to inhibit the peptidoglycan biosynthesis, thereby exerting the peptides' individual

activities (Figure 11).[48, 56 52, 57] This also triggers a sequence of events resulting in pore formation in the cell membrane. The binding of A1 to lipid II is believed to induce a conformational change in the A1 peptide. This exposes a high-affinity binding site for A2 and then facilitates formation of an A1:A2:lipid II trimeric complex. Upon binding A1 and A2, the complex inserts into the membrane and induces pore formation, thereby leading to the observed potent synergistic activity. Haloduracin α & β peptides appear to operate by a similar mechanism to lacticin A1 & A2.[58]

**Figure 11.** Simplified representation of the mode of action of lacticin 3147 A1 (**16**) & A2 (**17**)

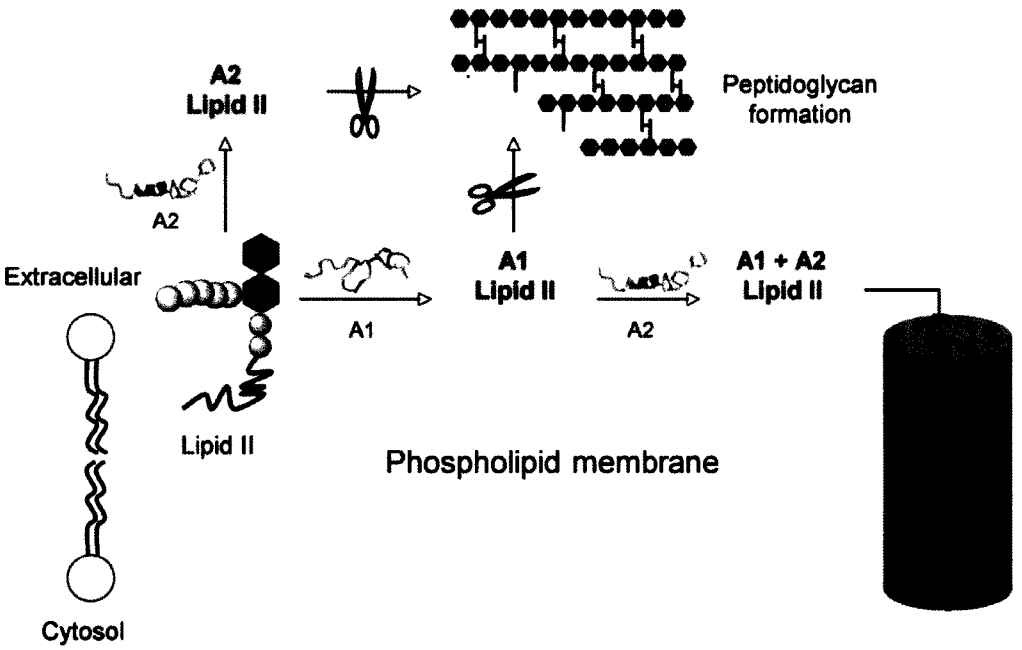


Not all lantibiotics are believed to trigger bacterial cell death by dual modes of action. Studies suggest that mersacidin, the most studied type B lantibiotic, targets lipid II but in a different manner to nisin. Mersacidin binds to the terminal sugar moiety in lipid II (Figure 9).[59] This intimate binding sequesters

lipid II, inhibits cell wall biosynthesis and eventually causes cell death without forming pores on the cell membrane. This may be due to mersacidin's smaller and more compact structure, rendering it incapable of inserting into the cell membrane. [52]

## 2.1.5. Chemical synthesis of lantibiotics and their analogues

### 2.1.5.a. Total synthesis of natural lantibiotics

Due to the intriguing structural features and promising biological activities of lantibiotics, chemical synthesis of these compounds has attracted attention. The pioneering solution phase synthesis of nisin by Shiba and co-workers represents the first total chemical construction of a lantibiotic peptide (Figure 12). [29,60 61-63]

**Figure 12.** Fragment condensation approach for total synthesis of nisin (**13**)

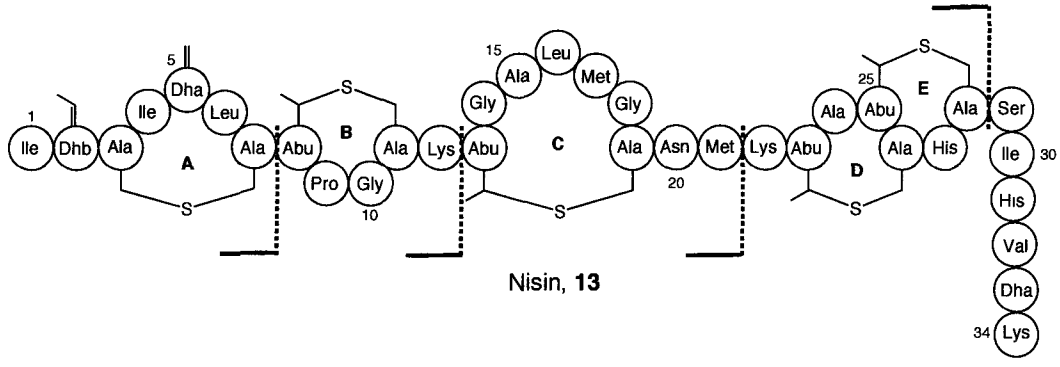


Nisin, **13**

This synthesis involves the fragment condensation of lanthionine and methyllanthionine containing rings using Boc chemistry in solution. The required building blocks, the A, B, and C rings as well as the fused D and E-rings of nisin, are prepared individually from the corresponding disulfide counterparts using a

sulfur extrusion method reported by Harpp and Gleason (Scheme 2).[64] Notably, this novel regioselective procedure affords the correct stereochemistry of the methyllanthionine ring with the retention of stereochemical configuration of the β-carbon in the 3-methyl-D-cysteine. Protecting group manipulations followed by sequential fragmental coupling of each ring complete the total synthesis of nisin in solution.

**Scheme 2.** Synthetic strategy for lanthionine and β-methyllanthionine ring formation by sulfur extrusion methodology

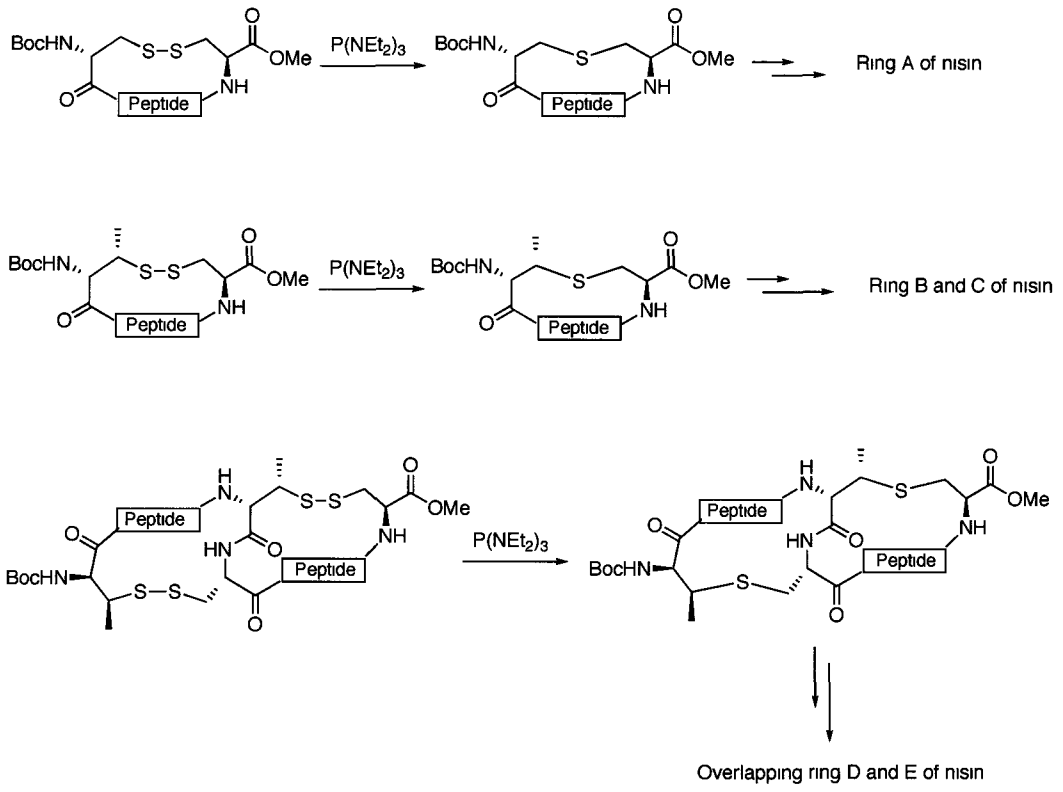


While the current thesis project was underway, Vederas and co-workers accomplished a total synthesis of a natural lantibiotic, lactocin S (**19**).[65] In contrast to Shiba's nisin synthesis, this peptide is assembled on a solid support through

sequential cyclizations to form the lanthionine rings and fragmental coupling to introduce the *N*-terminal modified residues (Figure 13).

**Figure 13.** Synthetic strategy for the total synthesis of lactocin S (**19**) on solid support[65]

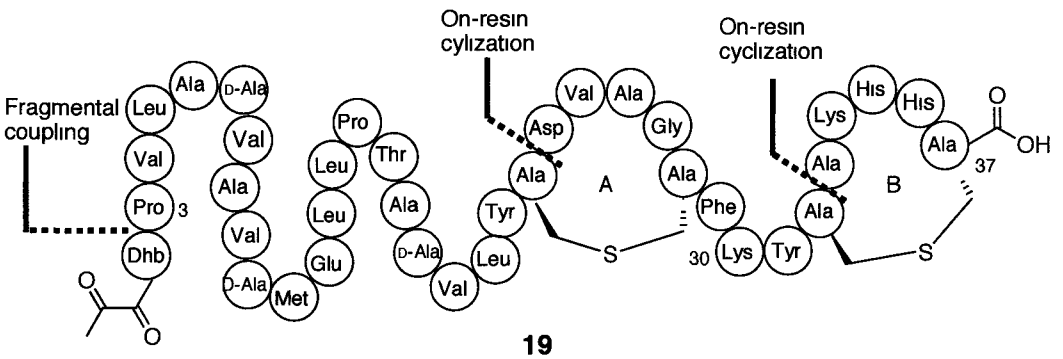


**19**

In this work, an orthogonally protected lanthionine building block **20** with Alloc, allyl and Fmoc protection is synthesized in solution and then loaded onto solid support (Scheme 3). Peptide elongation using standard Fmoc solid phase peptide synthesis (SPPS) affords the linear precursor **21**. The sequential deprotection of Aloc, allyl and Fmoc protecting groups using $Pd(PPh_3)_4$ and then 20% piperidine is followed by cyclization using PyBOP to give ring B **22** bound to the resin. The lanthionine ring A is formed in the same manner. Further chain extension, fragmental coupling using standard Fmoc chemistry and acidic hydrolysis/cleavage from the resin yields the natural peptide in 10 % overall yield.

**Scheme 3.** Total synthesis of lactocin S (**19**) on solid support

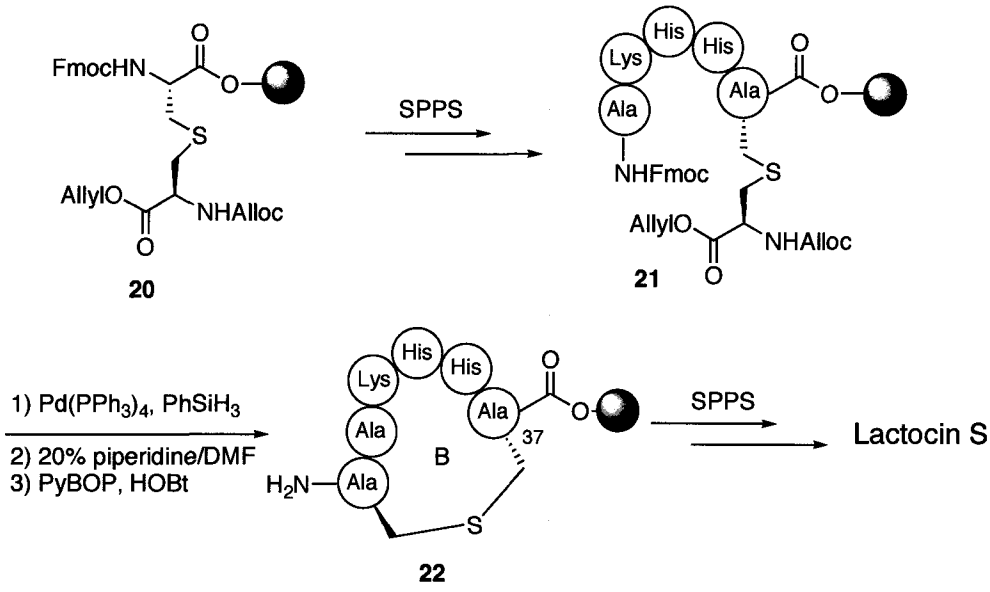


## 2.1.5.b. Synthesis of β-methyllanthionine (MeLan) with orthogonal protecting groups

Despite the significant developments in lantibiotic total synthesis, solid phase synthesis of lantibiotic peptides having β-methyllanthionine rings has not been reported prior to the work described in this thesis. This is due to the synthetic challenge of making the MeLan building block with orthogonal protection. The additional methyl group at the C-3 position makes stereoselective synthesis of MeLan more difficult than Lan. This is reflected by the limited synthetic methodologies for synthesizing MeLan reported in literature, even though syntheses of lanthionine are well documented. [66-70]

In 1983, Nakajima and co-workers reported the synthesis of MeLan **23** via the reaction of cysteine derivative **24** with aziridine **25** derived from D-threonine (Scheme 4).[71] However, this reaction suffers from low yields (22%). More

importantly, its application as a building block in peptide synthesis is limited as there is no orthogonality among the four protecting groups.

**Scheme 4.** Synthesis of β-methyllanthionine via aziridine ring opening

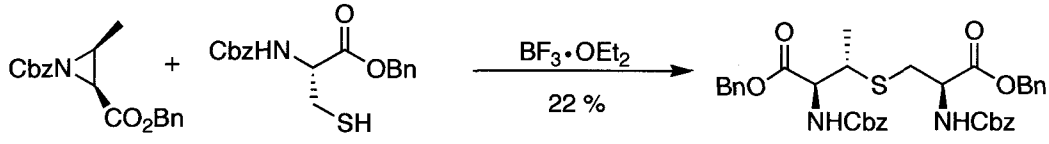


**25** **24** **23**

Van Nieuwenhze and co-workers have reported that the nucleophilic displacement of β-bromoalanine **26** with β-methylcysteine **27** under phase transfer conditions can afford the linear orthogonal protected MeLan **28** in good yield (Scheme 5).[72] However, further manipulations changing the existing protecting groups to orthogonal protecting groups that are compatible with solid phase peptide synthesis is still problematic. These manipulations involve the difficult removal of a benzyl carbamate (Cbz) and a benzyl ester (Bn) in the presence of sulfur.

**Scheme 5.** Synthesis of MeLan via nucleophilic substitution

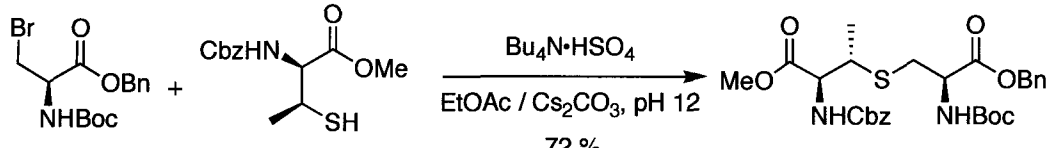


**26** **27** **28**

Recently, Vederas and co-workers discovered that a ring opening of sulfamidates **29** with cysteine derivatives **30** generates linear orthogonally protected MeLan **31** in good yields (Scheme 6).[73] However, further tedious protecting group manipulation is required for the application of this building

block to solid phase peptide synthesis. Additionally, the high price of D-allo-threonine for preparing the necessary sulfamidate limits practical application of this methodology.

**Scheme 6.** Synthesis of MeLan via ring opening of sulfamidate

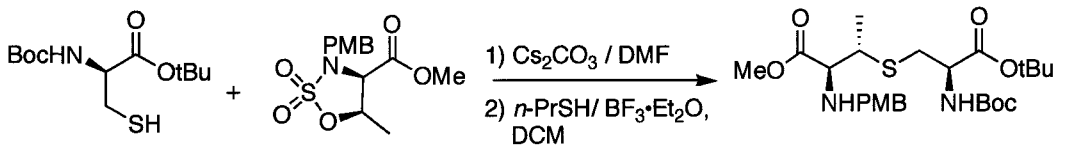


**29** **30** **31**

Despite the continuing development of synthetic methodology for MeLan synthesis, there was no general and efficient method that would give facile access to the orthogonally protected MeLan and allow for its installation on solid support for lantibiotic synthesis. In this regard, development of an orthogonally protected MeLan synthesis is undertaken in this thesis.

### 2.1.5.c. Chemical synthesis of lantibiotic analogues

In addition to total syntheses of natural lantibiotics, synthesis of their analogues has also received much attention with the aim of understanding the structure-activity relationship (SAR) and investigating modes of action of these peptides. Considerable effort has been focused on modifications of unusual amino acids, such as lanthionine and methyllanthionine.

To study the importance of the methyl group in MeLan, Vederas and co-worker reported the synthesis of an analogue of lacticin 3147 A2 (**32**) wherein

two methyllanthionine rings are replaced with lanthionine rings (Figure 14).[57] Their synthetic approach involves a similar strategy to the lactocin S synthesis described above. On-resin cyclizations of the orthogonally protected lanthionines that are prepared in solution and subsequent chain extension afford resin-bound tricylic peptide **33**. Fragment coupling with the *N*-terminal modified pentapeptide **34** gives bis(desmethyl) lacticin A2 (**32**). The biological testing of **32** found that the analogue retains synergistic activity with lacticin A1 but loses its inherent activity, suggesting the importance of the methyl group for direct binding of the lacticin A2 peptide to lipid II.

**Figure 14.** Synthetic strategy for bis(desmethyl) analogue **32** on solid support

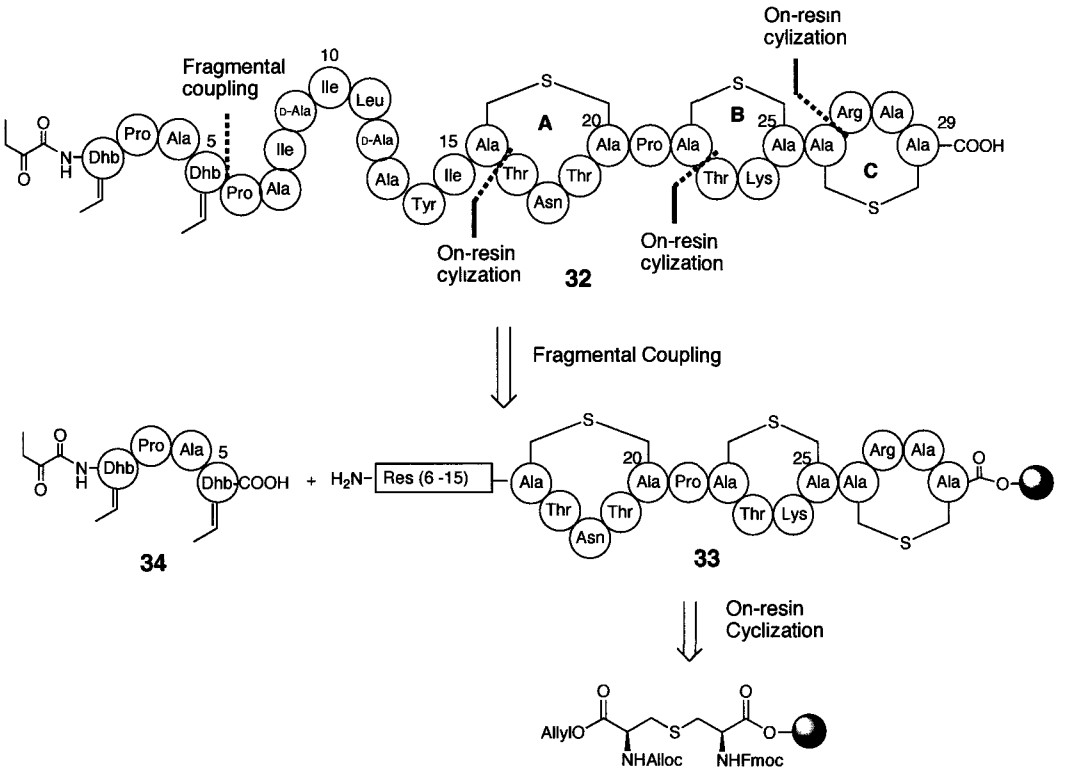


To shed light on the biological function of the sulfur atoms in lantibiotics, the syntheses of analogues with carbon atoms in place of the sulfur atoms have

been reported by several groups. Using lacticin 3147 A2 as a model peptide, Vederas and co-workers described the synthesis of a carbocyclic ring analogue **34** on a solid support (Figure 15).[74] The synthesis features the sequential on-resin ring closing metathesis (RCM) between two allyl glycine residues in the linear peptide **35**. After the three consecutive rings are formed by RCM, fragmental coupling affords the carbocyclic analogue **34**.

**Figure 15.** Synthetic strategy for synthesis of carbocyclic analogue **34** on solid support

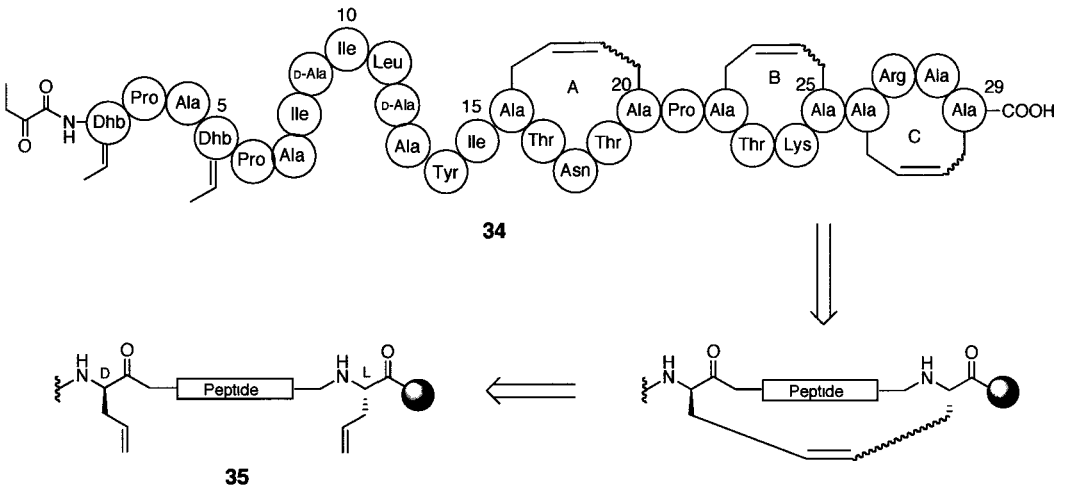


The RCM strategy can also be utilized to construct carbocyclic analogues of lantibiotics in solution phase. Using nisin Z (a natural nisin variant) as a template, Liskamp and co-workers have reported the solution phase synthesis of carbocyclic analogues of lantibiotic fragments (Figure 16).[75-78] An analogue of ring B **37** is constructed by RCM between two suitably protected allyl glycine residues in **38**. More interestingly, the analogue of the overlapping D and E rings (**40**) is also prepared using a combination of solid phase and solution phase RCM.

The synthesis begins with a cross-metathesis reaction between allyl glycines on solid support to give the ring E precursor **41**. This is followed by chain extension and on-resin cyclization to afford ring E **42**. The installation of another allyl glycine followed by cleavage of the peptide **43** from the resin gives the ring D precursor **44**. RCM in solution gives the overlapping D and E ring carbon analogue **40**.

**Figure 16.** Synthetic strategy for synthesis of carbocyclic analogue **37** and **40**

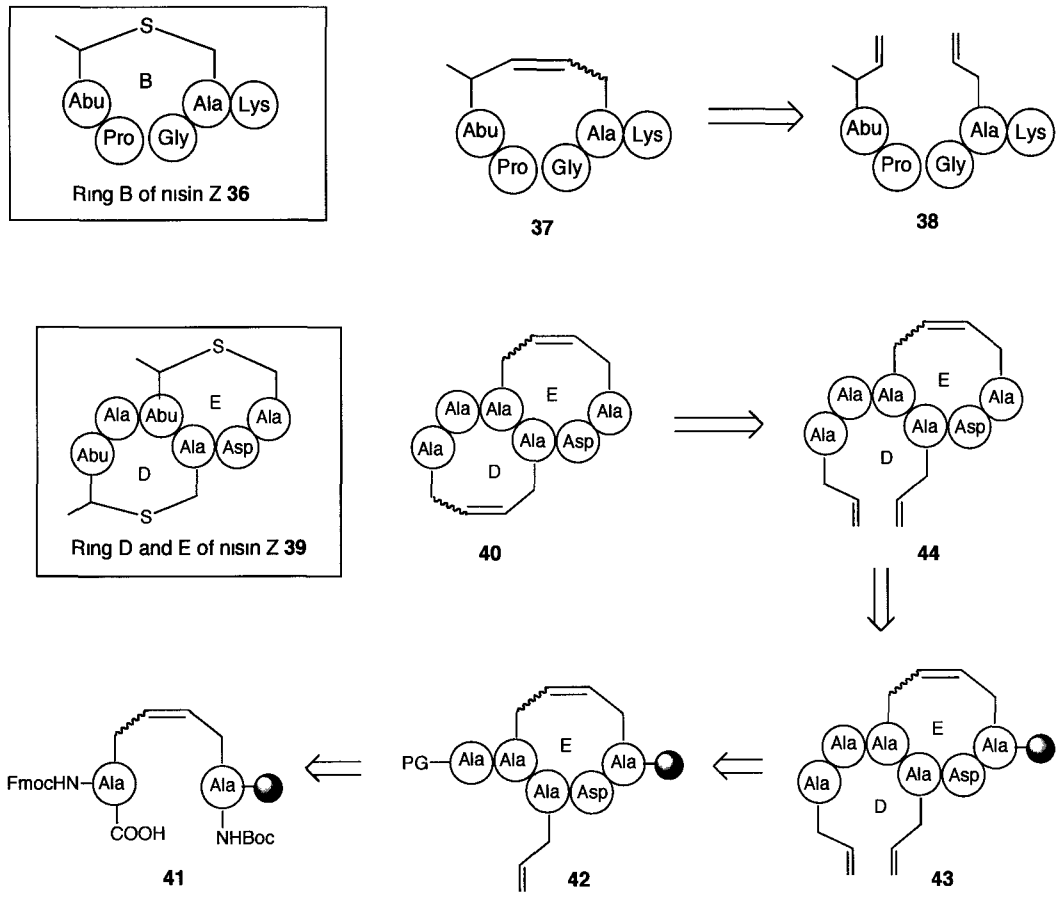

## 2.1.6. Research Goals

### 2.1.6.a. Design and synthesis of an oxygen analogue of lacticin 3147 A2

Given the increasing interest in understanding structure-activity relationships of lantibiotics, chemical synthesis of their analogues becomes a very important tool, as it can generate variants that are not readily accessible by biological methods.[57,74,78] Herein, the first project focuses on the design, synthesis and biological evaluation of a novel analogue of lacticin 3147 A2 (**45**) in which the sulfur atoms have been replaced by oxygen atoms (Figure 17). Such replacement would increase the oxidative stability of lantibiotics, as the sulfur atoms in the lanthionine rings are vulnerable to oxidation to a corresponding sulfoxide, which leads to loss of biological activity.

**Figure 17.** Structure of lacticin 3147 A2 (**17**) and its oxygen analogue (**45**)

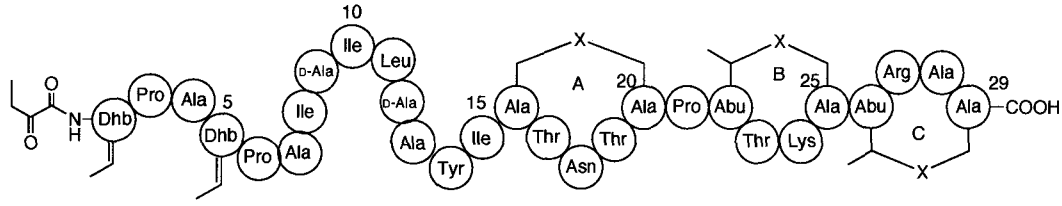


X = S, natural lacticin 3147 A2 (**17**)
X = O, oxa-lacticin 3147 A2 (**45**)

In addition to the enhanced oxidative stability, the oxygen analogue (**45**) is expected to maintain the biologically active conformation of the natural lantibiotic, due to the conformational similarity between lanthionine and its oxygen counterpart (Figure 18). Although sulfur to carbon and oxygen to carbon have different single bond lengths (1.80 Å vs. 1.43 Å), the more acute bond angle

of C-S-C compared to C-O-C bonds (101.4° vs. 111.4°) compensates to make the overall length of *meso*-lanthionine (Lan) and its oxygen analogue (Oxa-lan) very similar (ca. 6% difference).[79, 80] It is believed that this is also true for β-methyllanthionine as suggested by the overlaid energy minimized tertiary structure of ring B in lacticin A2 and its oxygen analogue (Figure 19).

**Figure 18.** Bond length and bond angle of Lan and Oxa-lan based on modeling*

Bond length: S-C vs. O-C

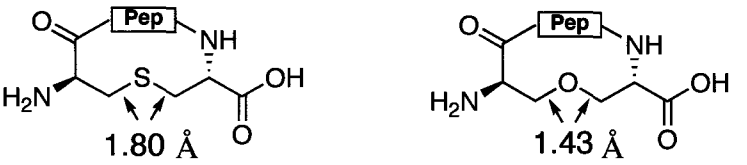


Bond angle: C-S-C vs. C-O-C

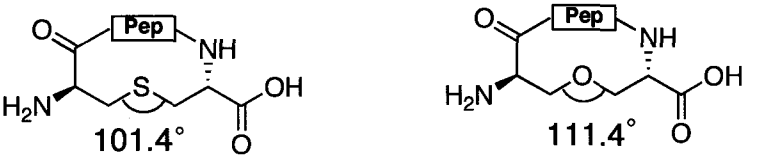


*The calculation was done using MacSpartan Pro™

**Figure 19.** The overlaid MacSpartan Pro™ energy minimized structures of ring B of lacticin A2 (**A**) and its oxygen analogue (**B**)*

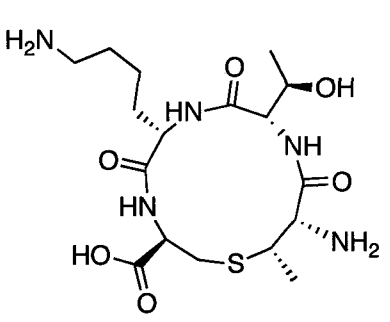


Ring B of lacticin 3147 A2

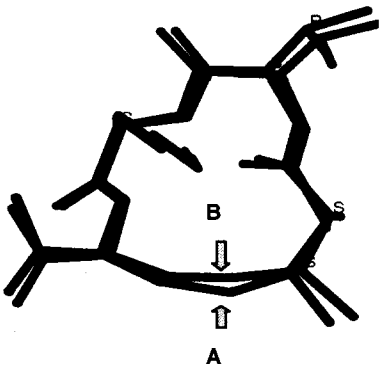

The successful completion of this study can shed light on the biological function of the sulfur atom in lanthionine rings. Thus, a guiding principle for the design of novel antimicrobial agents based on lantibiotic peptides could possibly be uncovered.

### 2.1.6.b. Chemical synthesis of natural lacticin 3147 A2 on solid support

Although the primary structure of the lacticin 3147 A2 has been elucidated for some time, the stereochemistry of lanthionine and methyllanthionine have only been assigned by analogy to that found in other lantibiotics,[35] and has not been proven conclusively. To confirm the proposed structure and stereochemistry of the lanthionine and methyllanthionine rings, the total synthesis of lacticin 3147 A2 (**17**) was undertaken.

More importantly, only one lantibiotic containing lanthionine rings has been synthesized on solid support to date.[65] Developing methodology for the total synthesis of methyllanthionine containing lantibiotics could allow access to many more lantibiotics through chemical synthesis, thereby enabling investigations of modes of action and SAR as well as simply obtaining practical amounts of material for clinical studies.

## 2.2. Results & Discussion

### 2.2.1. Synthesis and biological testing of oxa-lacticin 3147 A2

Our strategy for the synthesis of the oxygen analogue of lacticin 3147 A2 (**45**) involves a combination of solid and solution phase peptide synthesis as shown in Scheme 7.[81] The key building blocks, orthogonally protected oxa-lanthionine (Oxa-lan) **46** and oxa-methyllanthionine (Oxa-melan) **47**, could be prepared via solution phase synthesis. Loading of **47** on acid labile resin followed by peptide elongation using standard Fmoc methodology could give the ring C precursor **48**. Selective removal of protecting groups followed by on-resin intramolecular cyclization could lead to ring C. Sequential on-resin cyclizations of ring B and A in the same manner followed by chain extension could afford tricyclic peptide **49**. Fragment coupling with the modified *N*-terminal pentapeptide **34** prepared in solution could yield the oxygen analogue **45**.

**Scheme 7**. Retrosynthesis of oxygen analogue of lacticin 3147 A2 (**45**)

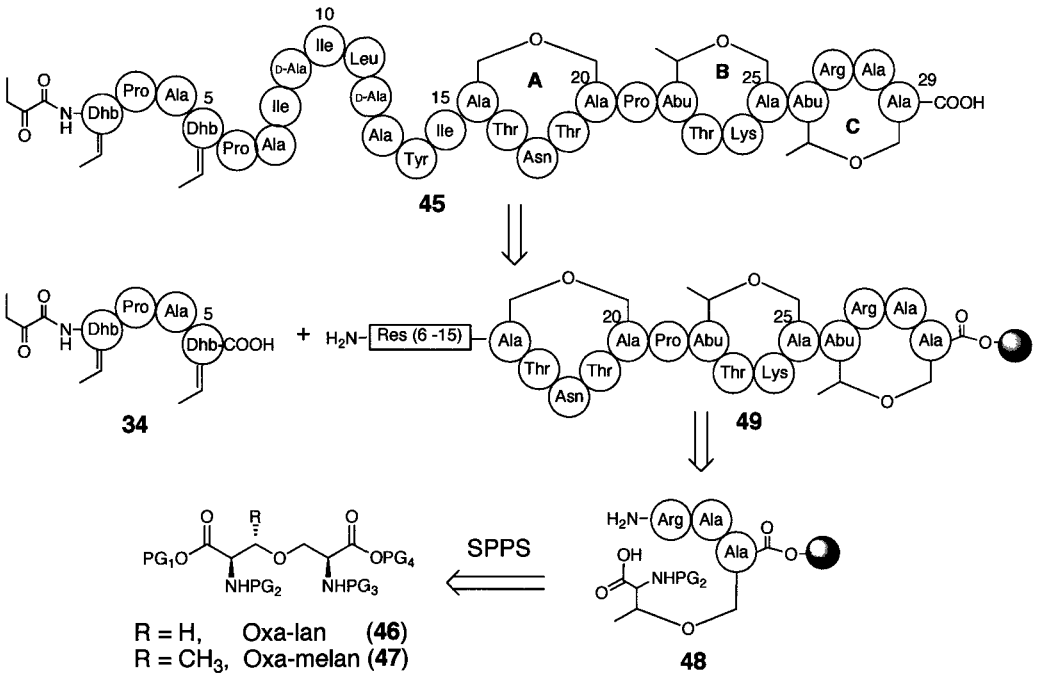

### 2.2.1.a. Development of synthetic methodology for oxa-lanthionine and its derivatives

The synthesis of highly functionalized ether-bridged bisamino acids represents significant synthetic challenges. Two important factors need to be considered: the maintenance of stereochemical integrity during synthesis; and the compatability of orthogonal protecting groups with Fmoc SPPS. As there are no general methods for synthesis of such compounds reported in the literature, the development of suitable synthetic methodology was undertaken.

Our synthetic strategy to the tetra-functionalized oxa-lanthionine and its derivatives involves the regio- and stereoselective ring opening of serine and threonine-derived aziridines **50** by the hydroxyl nucleophile of serine derivatives **51** in the presence of a Lewis acid catalyst (Scheme 8).[82]

**Scheme 8.** Strategy for synthesis of orthogonally protected Oxa-lan and its derivatives

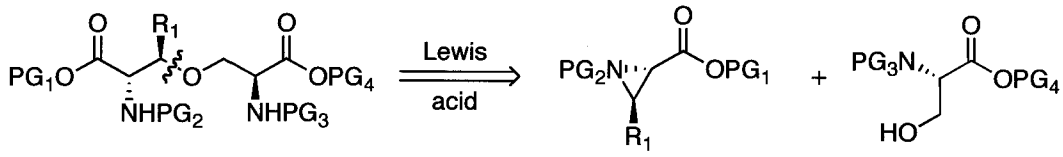


**50** **51**

$R_1$ = H, Oxa-lan
= $CH_3$, Oxa-melan

$PG_1$, $PG_2$, $PG_3$, $PG_4$ = orthogonal protecting groups

The chemistry of aziridine ring opening with a variety of nucleophiles in the presence of Lewis acids is well documented in the literature.[83, 84] However, due to the poor nucleophilicity of hydroxyl groups, successful examples of ring openings with oxygen nucleophiles are usually limited to a solvolysis reaction in the corresponding alcohol.[85-87] In order to activate the aziridine ring opening reaction, the electron-withdrawing *para*-nitrobenzyloxycarbonyl group (pNZ) was

selected for protecting the azridine nitrogen.[85, 88] In addition, the pNZ protecting group is compatible with Fmoc SPPS conditions.[89]

The synthesis of the aziridinocarboxylate ester **52** starts with protection of the serine methyl ester **53** with a trityl group to give **54** (Scheme 9). Mesylation of the hydroxyl side chain followed by intramolecular cyclization gives *N*-Trt protected aziridine **55.** Removal of the Trt group with TFA followed by introduction of the pNZ group on nitrogen with *para*-nitrobenzyloxycarbonyl chloroformate affords **52**.[85]

**Scheme 9.** Synthesis of aziridine-2-carboxylate (**52**)

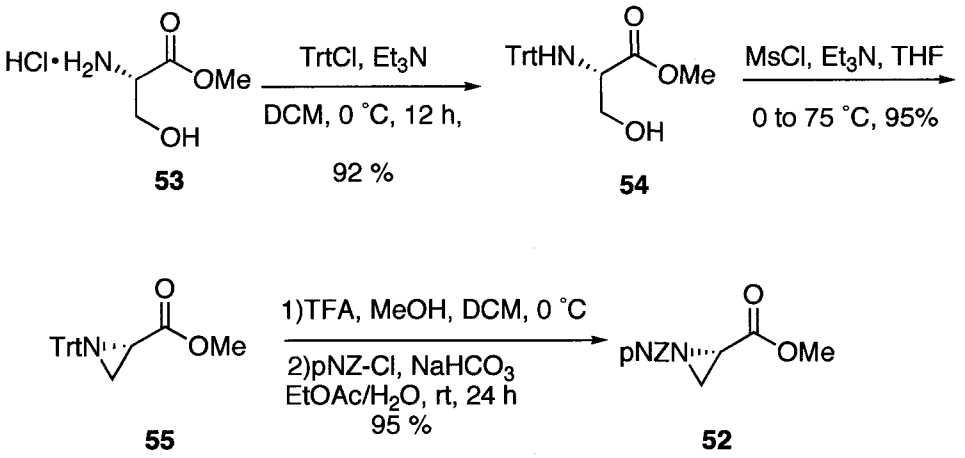


In order to use serine and threonine as nucleophiles in lower concentrations for the aziridine ring opening reaction, the poor reactivity of the hydroxyl needs to be enhanced. The weak nucleophilicity of the hydroxyl group presumably arises from the unfavorable hydrogen bonding between the oxygen lone pair and the hydrogen of its monoprotected neighboring amine (Figure 20-A). Bisprotection of the amino group could lead to favorable reversal of the hydrogen bonding thus increasing the electron density on the oxygen, improving

its nucleophilicity (Figure 20-B).[90, 91] The phthalimido (Pht) group was chosen for bisprotection of the amino group, because of its ease of preparation and removal (Figure 20-C).

**Figure 20.** Hydrogen-bonding patterns and effects on nucleophilicity of hydroxyls in protected serine or threonine derivatives

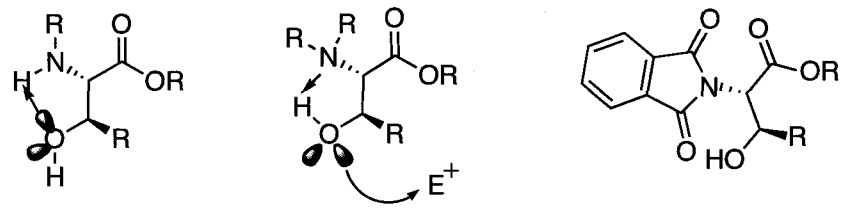

mono-protected: weak OH nucleophile (A)

bis protected: better OH nucleophile (B)

Pht (phthalimido) protected Ser/Thr (C)

*N*-phthalimido serine derivative **56** can be prepared according to the literature procedure (Scheme 10).[92] Reaction of serine methyl ester hydrochloride **53** with phthalic anhydride under Dean-Stark conditions yields the corresponding *N*-phthalimido serine derivatives.

**Scheme 10.** Synthesis of *N*-phthalimido serine (**56**)

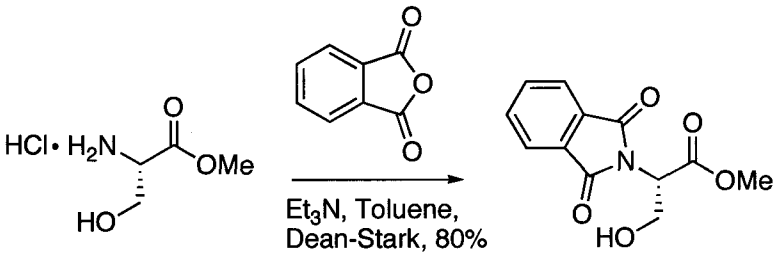


**53** **56**

With the electrophile and nucleophile available, the ring opening of pNZ-aziridinocarboxylate ester **52** with 5 equivalents of Pht-Ser-OMe **56** in the presence of $BF_3$•$OEt_2$ affords the desired product **57** (Scheme 11). Although the

reaction is sluggish and requires 2 days for completion, the yield (57%) is comparable to those using oxygen nucleophiles as solvent.[85,87]

**Scheme 11.** Synthesis of oxa-lanthionine (**57**) via aziridine ring opening with **56**

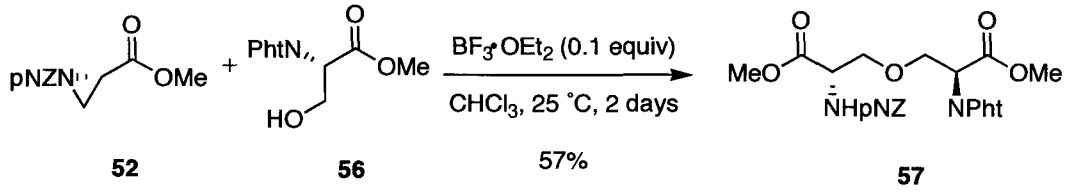


**52** **56** 57% **57**

Encouraged by this positive result, the reaction was examined with respect to the catalyst, solvent, temperature and reagent stoichiometries (Table 2). Among the screened catalysts, only $BF_3$•$OEt_2$ can promote the ring opening reaction. Although the reaction yield has not been improved dramatically with use of $BF_3$•$OEt_2$, optimization shows that using 0.5 equiv $BF_3$•$OEt_2$ in refluxing toluene (Table 2, entry 6) shortens the reaction time significantly from 4 days to 1.5 h and improves the yield.

**Table 2.** Optimization of aziridine ring opening reactions

| Entry | Nu/E$^+$ | Catalyst equiv | Solvent | Temp | Time | Yields (%) |
|---|---|---|---|---|---|---|
| 1 | 5:1 | $Yb(OTf)_3$ 0.1 | $CHCl_3$ | rt | 2 d | no reaction |
| 2 | 5:1 | $Ti(O\textit{i}\text{-}Pr)_3$ 0.1 | $CHCl_3$ | rt | 2 d | no reaction |
| 3 | 5:1 | TsOH 0.1 | $CHCl_3$ | rt | 2 d | no reaction |
| 4 | 2:1 | $BF_3$•$OEt_2$ 0.2 | $CHCl_3$ | rt | 4 d | 60 |
| 5 | 2:1 | $BF_3$•$OEt_2$ 0.2 | Toluene | 110 °C | 5 h | 70 |
| 6 | 2:1 | $BF_3$•$OEt_2$ 0.5 | Toluene | 110 °C | 1.5 h | 72 |

With the reaction conditions optimized, the scope of this methodology was explored using several primary and secondary hydroxyl side chain containing amino acids as nucleophiles and the pNZ protected aziridines as electrophiles. The serine-derived aziridines (**58** and **59**) can be prepared following a procedure similar to that used for the preparation of **52** (Scheme 12). The commercially available *N*-Trt-serine **60** is converted to its allyl ester **61** with allyl bromide.[93] Mesylation of the hydroxyl group with MsCl followed by intramolecular cyclization gives **62**. Removal of the trityl group with TFA followed by introduction of the electron-withdrawing pNZ protecting group affords **58**. The corresponding enantiomer **59** was synthesized using the same method.

**Scheme 12.** Synthesis of aziridine-2-carboxylates from serine

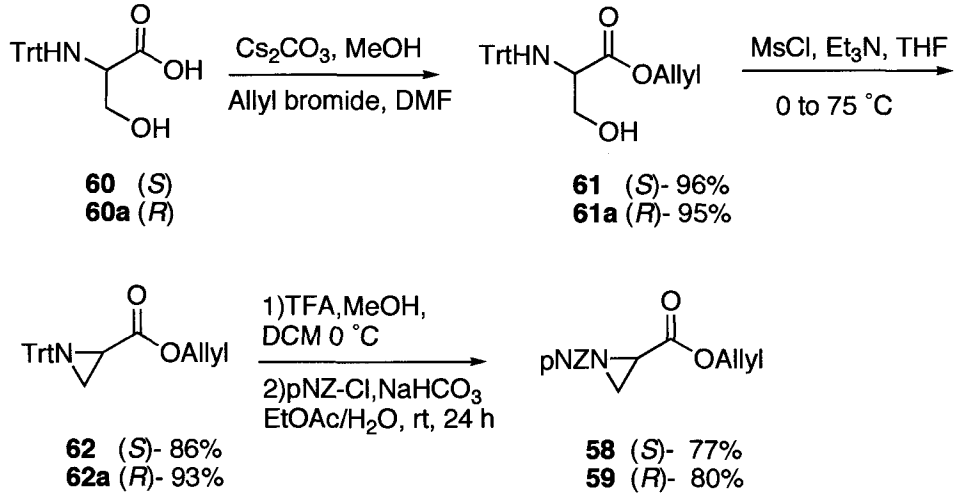


**60** (*S*)
**60a** (*R*)

**61** (*S*)- 96%
**61a** (*R*)- 95%

**62** (*S*)- 86%
**62a** (*R*)- 93%

**58** (*S*)- 77%
**59** (*R*)- 80%

The synthesis of β-substituted aziridine **63** starts with the condensation of the carboxyl group of D-threonine **64** with allyl alcohol under Dean-Stark conditions catalyzed by *p*-toluenesulfonic acid (PTSA) to yield the allyl ester as the *p*-toluenesulfonate salt (Scheme 13). Addition of triethylamine to neutralize the acid followed by reaction with trityl chloride affords the bis-protected D-

threonine **65**. In a similar manner to preparation of **58**, aziridine formation followed by protecting group manipulation gives the bis-protected aziridine **63** in very good yield.

**Scheme 13.** Synthesis of aziridine-2-carboxylate (**63**) from threonine

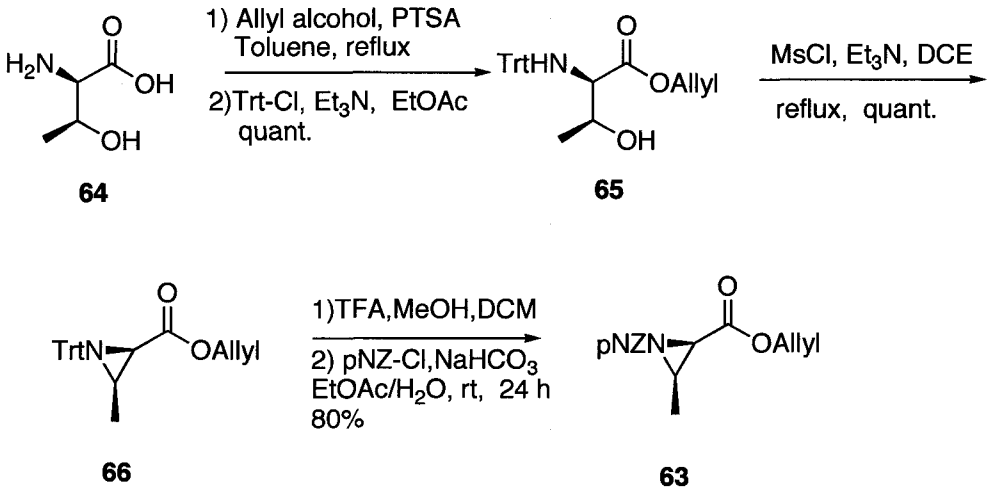


**64** **65** **66** **63**

To provide bis-*N*-protected nucleophiles, a variety of *N*-phthalimido protected serine and threonine derivatives (**66a-d**) were prepared in a manner similar to that used for formation of **56** (Scheme 14).

**Scheme 14.** Synthesis of *N*-phthalimido serine and threonine derivatives (**66a-d**)

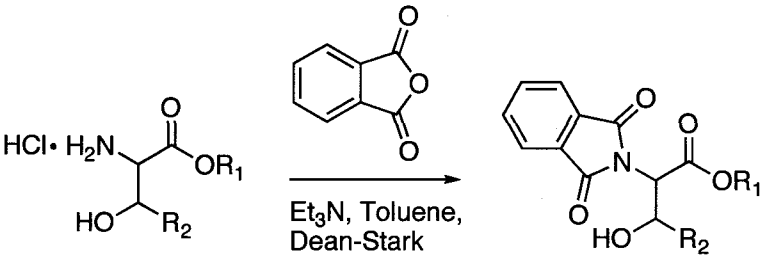


**66a** (2*R*) $R_1$= Me, $R_2$= H 80%
**66b** (2*R*) $R_1$= Et, $R_2$= H 78%
**66c** (2*S*, 3*R*) $R_1$= Me, $R_2$= Me 86%
**66d** (2*R*, 3*S*) $R_1$= Me, $R_2$= Me 80%

The azridine ring opening reactions used $BF_3 \bullet OEt_2$ as the catalyst under the optimized conditions. In all cases, the reaction proceeds smoothly to give a single isomer of the oxygen bridged bis-amino acids in moderate to good yields (Scheme 15). Interestingly, the stereochemically pure *sec-sec* dimethyl ethers **67f** and **67g** can be formed in good yields. Reactions leading to *sec-sec* ethers are often reported to undergo stereocenter scrambling,[94] but this was not observed in this case.

**Scheme 15.** Preparation of bis-amino acid ether derivatives (**67a-g**)

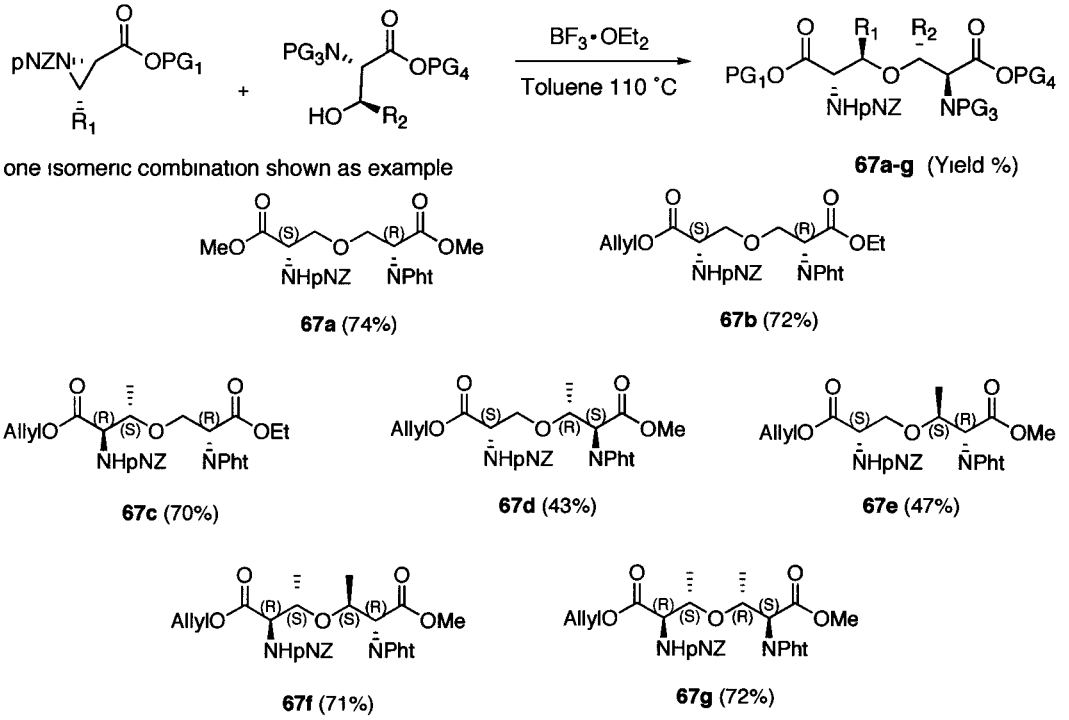


Upon closer analysis of the ring opening reaction mixtures of **67c** and **57**, two interesting byproducts are identifiable by NMR and mass spectrometry, repectively. One is the oxazolidinone derivative **68** (5% yield) due to intramolecular aziridine rearrangement;[95,96] the other is the benzyl ether derivative

**69** (6% yield) resulting from the attack of OH on the benzylic position.[97] The proposed mechanism for byproduct formation is shown in Scheme 16.

**Scheme 16.** Proposed mechanism for byproduct formation during aziridine ring opening

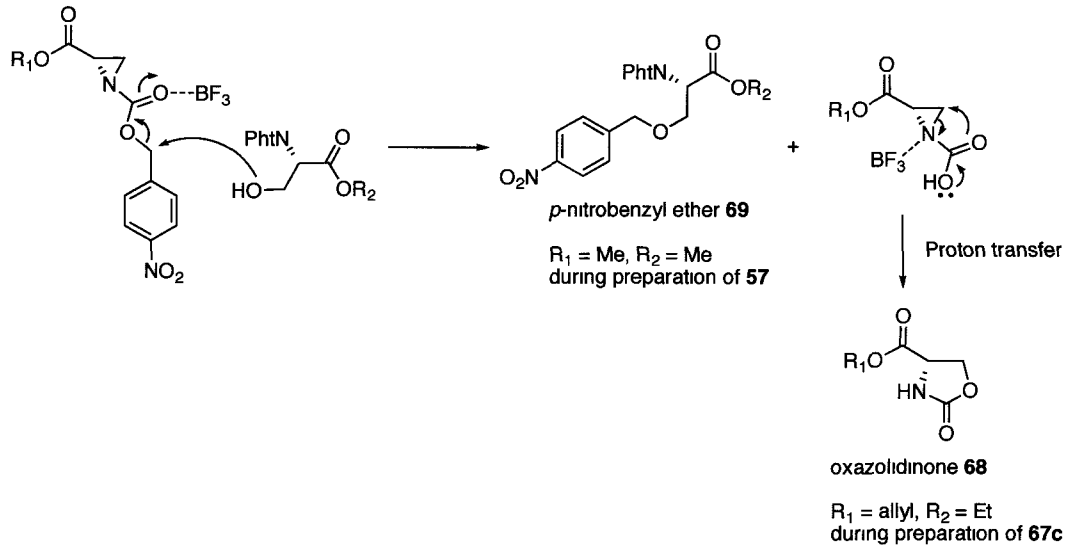


To further explore the scope of this methodology, the sterically demanding cyclic alcohol, Fmoc-Hyp-OMe, was tested as an oxygen nucleophile. It can be prepared according to literature procedure (Scheme 17).[98] Reaction of Fmoc-OSu with **70** in the presence of $Na_2CO_3$ gives the Fmoc protected **71**. Ring opening of aziridines **59** or **63** with **71** successfully affords **72a** and **72b,** respectively in moderate to good yields (Scheme 18).

**Scheme 17.** Synthesis of Fmoc-Hyp-OMe (**71**)

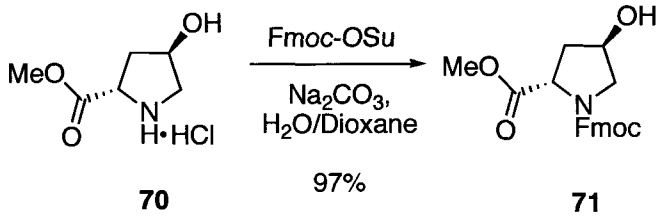


**70** **71**

**Scheme 18.** Aziriding ring opening reactions with **71**

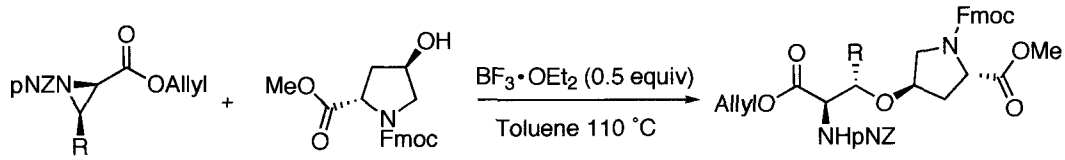


R = H **59**
R = $CH_3$ **63**

**71**

**72a**, R = H, 62%
**72b**, R = $CH_3$ 47%

Having successfully developed synthetic methodology to generate the ether-bridged bisamino acids stereoselectively, focus was shifted to the investigation of orthogonal protecting groups that are suitable for Fmoc SPPS. All four protecting groups on these building blocks need to be manipulated selectively. Hence, the ring opening reaction was investigated using the aziridine with pNZ and allyl protection and the serine nucleophile having Fmoc and *t*-Bu protecting groups. The Fmoc-Ser-O*t*-Bu **73** can be prepared from the serine *tert*-butyl ester using Fmoc-OSu in good yield (Scheme 19).[161]

**Scheme 19.** Synthesis of Fmoc-Ser-O*t*-Bu (**73**)

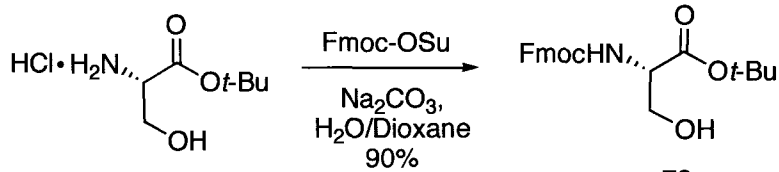


**74** **73**

However, all attempts to use Fmoc-Ser-O*t*-Bu (**73**) as a nucleophile under the optimized conditions (toluene, 110° C) led to a complex mixture of products, presumably due to the instability of the *t*-Bu group. Fortunately, milder conditions using 0.2 equiv $BF_3 \bullet OEt_2$ in ethanol-free $CHCl_3$ at 40 °C yield the orthogonally protected Oxa-lan (**75a, 75b**) and Oxa-melan (**76**) in moderate yields (Scheme 20). The lower yields can be attributed to the decreased nucleophilicity of the oxygen lone pairs resulting from unfavorable H-bonding as described in Figure 20, as well as the decreased temperature. Nonetheless, the yields in these cases are still preparatively useful. The *tert*-butyl groups are selectively removed under acidic conditions to give **77** and **78**, respectively, which can be incorporated into solid phase peptide synthesis.

**Scheme 20.** Synthesis of orthogonally protected Oxa-lan and its derivatives

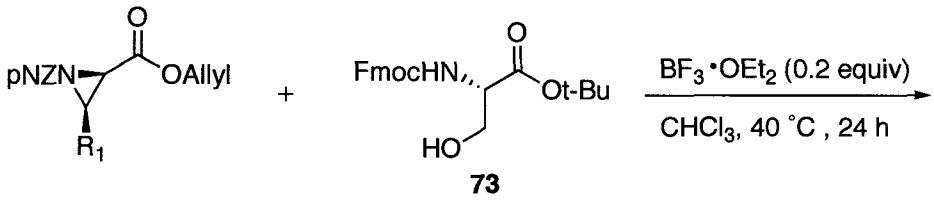


one isomeric combination shown as example

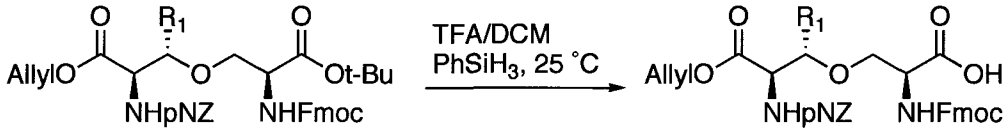


$R_1$ = H, **75a** (*2S,6S*) 36%
= H, **75b** (*2R,6S*) 37%
= $CH_3$ **76** (*2R,3S,6S*) 40%

$R_1$ = H, **77** (*2S,6S*) 90%
= $CH_3$ **78** (*2R,3S,6S*) 87%

At this point, to verify the stereochemical integrity of the aziridine ring opening, $^{13}C$ NMR spectra of a mixture of stereochemically pure **75a** and **75b**

were examined. Appearance of individual peaks for each diastereomer at different ppm values (Figure 21) clearly illustrates the stereochemical integrity of the ring opening reaction.

**Figure 21.** Portion of the 125 MHz $^{13}C$ NMR spectra of diastereomers **75a**, **75b**, and a mixture of **75a** and **75b** at 27 °C in $CDCl_3$

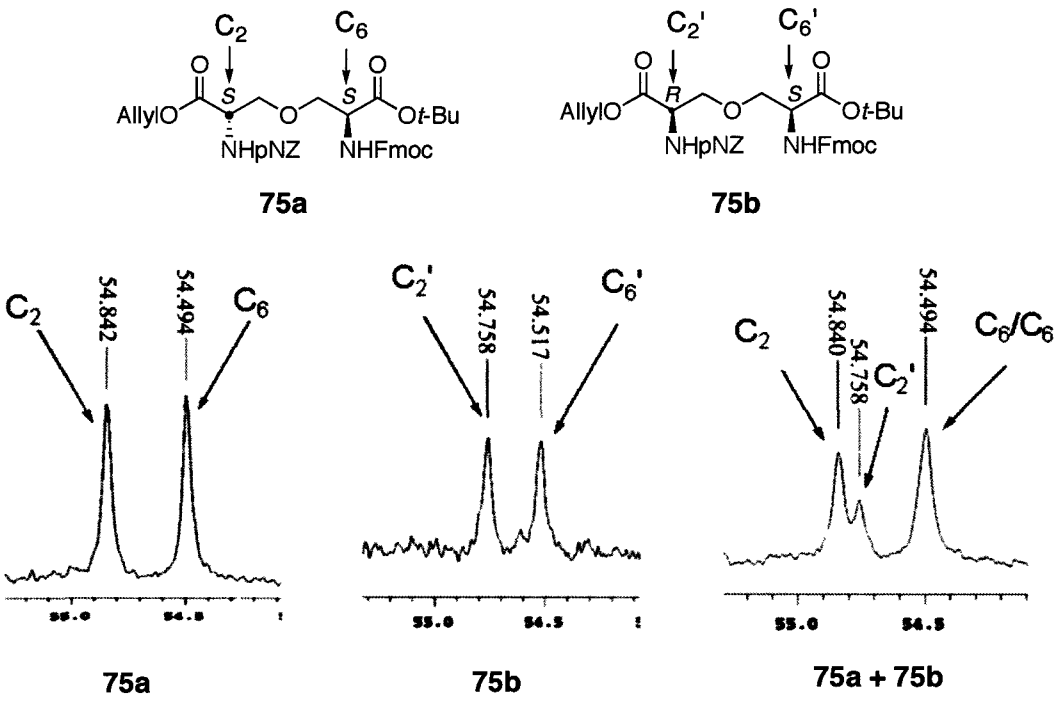


### 2.2.1.b. Synthesis of *N*-terminal pentapeptides

The synthesis of the highly modified *N*-terminal residues (1→5) of lacticin 3147 A2 was accomplished according to a method developed in the Vederas lab.[74] A graduate student in this group, Vijaya R. Pattabiraman (Ph.D. thesis, 2007) prepared the pentapeptide **34.** The synthesis is briefly summarized for clarity and completeness.

The pentapeptide is synthesized in solution by fragmental coupling of dehydrodipeptide **79** with dehydrotripeptide **80**. The dehydrodipeptide **82** is formed by the treatment of dipeptide **81** with MsCl/DBU. Hydrolysis of the methyl ester with LiOH affords **79** (Scheme 21).

**Scheme 21.** Synthesis of dehydrodipeptide (**79**)

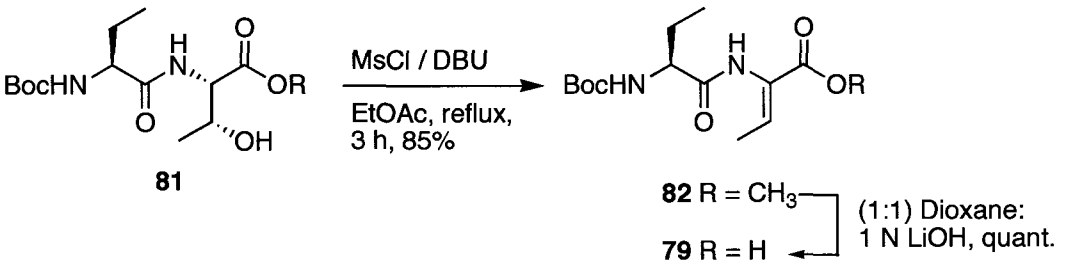


The dehydrotripeptide **80** is synthesized from the dehydrodipeptide **83** via peptide coupling. The dehydro moiety in **83** is introduced from dipeptide **84** in a similar manner to **82** via an activation and elimination procedure (Scheme 22). Removal of the Boc protecting group of **83** with TFA followed by coupling with Boc-Pro-OH affords **80**. Boc deprotection followed by fragment coupling with **79** in the presence of DIC yields the dehydropentapeptide **85**. The *N*-terminal amino group of **85** is liberated with TFA followed by transamination using 4-pyridinecarboxaldehyde-acetic acid salt and hydrolysis to give the α-ketoamide containing pentapeptide **86.** Removal of the *C*-terminal carboxyl allyl protection with $Pd(PPh_3)_4$ affords the desired pentapeptide **34** that is ready for SPPS.

**Scheme 22.** Synthesis of the modified pentapeptide (**34**)

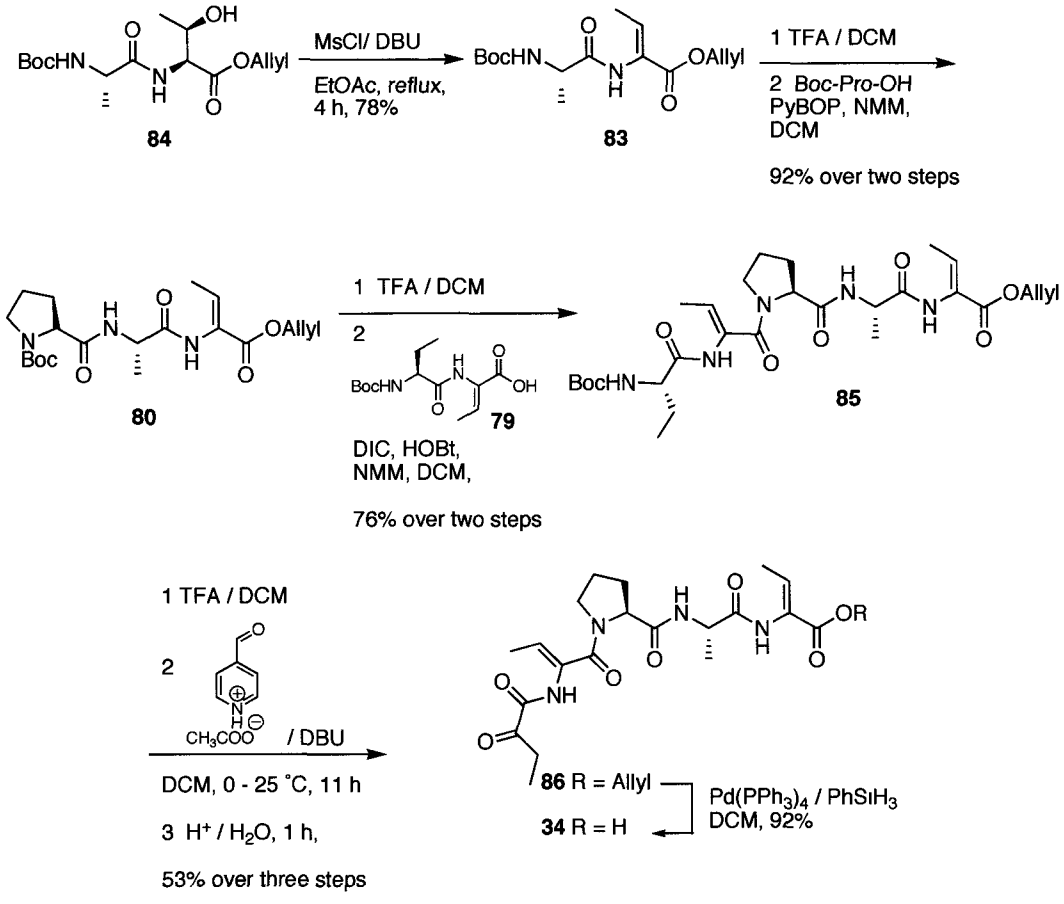


### 2.2.1.c. Solid Phase Peptide Synthesis of oxa-lacticin 3147 A2 (45)

With the successful preparation of key building blocks using solution phase synthesis, the Fmoc SPPS was initiated by loading the protected Oxa-melan (**78**) onto Wang resin with a loading of 0.65 mmol/g. Standard Fmoc SPPS furnishes the linear sequence of ring C (**88**) by sequentially coupling Fmoc-Ala-OH and Fmoc-Arg(Pmc)-OH using PyBOP. The selective removal of the allyl group on the Oxa-melan residue with $Pd(PPh_3)_4$ followed by Fmoc deprotection on the arginine residue with 20% piperidine affords the on-resin cyclization precursor **89**. The cyclization between the amino group of the arginine residue

and the carboxylic acid of the Oxa-melan proceeds readily using PyBOP/HOBt to give **90** in 2 h (Scheme 23).

**Scheme 23.** Attempted solid phase peptide synthesis with 0.65 mmol/g resin loading

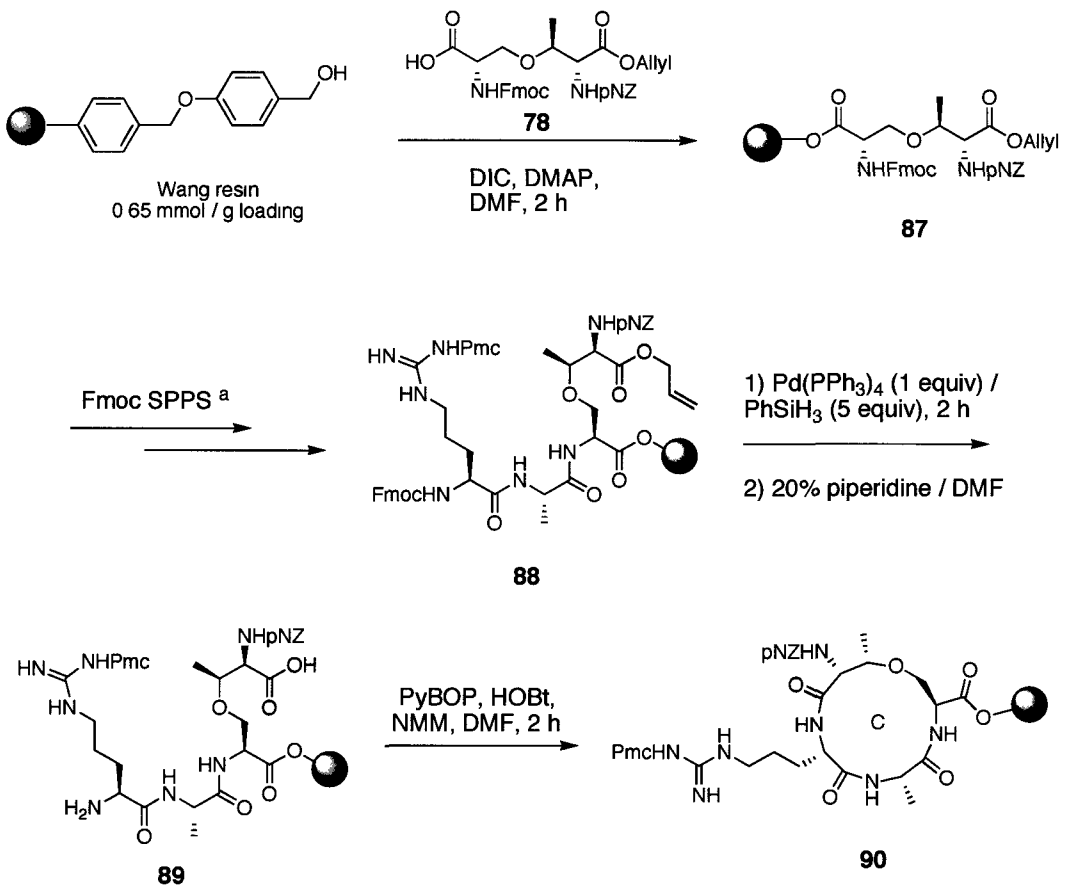


[a] Conditions used for synthesis of **88** from **87**: (i) 20% piperidine in DMF (ii) PyBOP, HOBt, NMM, DMF (iii) Fmoc-Ala-OH, (iv) repeat steps (i) and (ii) with Fmoc-Arg(Pmc)-OH.

A small sample of the resin-bound **90** was treated with TFA/$H_2O$/TIPS (95:2.5:2.5) to cleave the peptide from the resin. Analysis of this peptide by mass spectrometry suggested the formation of ring C **90** [595.7 (M+H)]. However, the dimer **91** [1189.7 (M+H)] resulting from interstrand cross-linking was observed as well. A similar dimer formation reaction has been reported in the synthesis of lactocin S.[99] This arises from the favorable diketopiperizine (DKP) formation

between two lanthionine moieties in growing peptide chains during cyclization when the two peptide chains are in close proximity (Scheme 24).

**Scheme 24.** The dimer formation via diketopiperizine formation in the synthesis of lactocin S

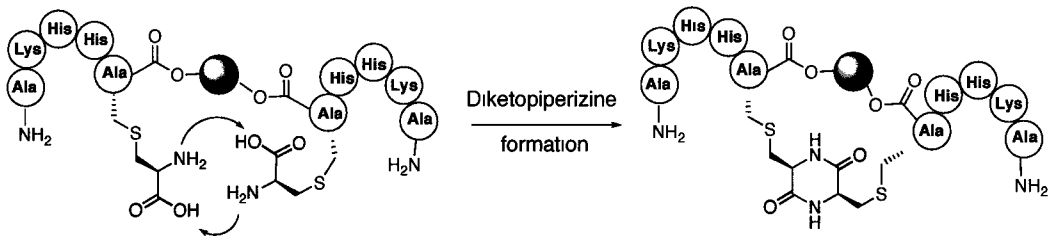


However, the presence of the pNZ protecting group on the amino group of Oxa-melan should prevent this dimer formation. Therefore, one possible reason for this side reaction is that high resin loading increases the possibility of two growing peptide strands being close and coupling to each other to form the larger macrolactam during the cyclization step (Scheme 25). Based on this reasoning, the problem of the formation of dimer can be overcome by lowering the resin loading.

**Scheme 25.** The proposed pathway of dimer formation during cyclization of ring C of oxa-lacticin A2

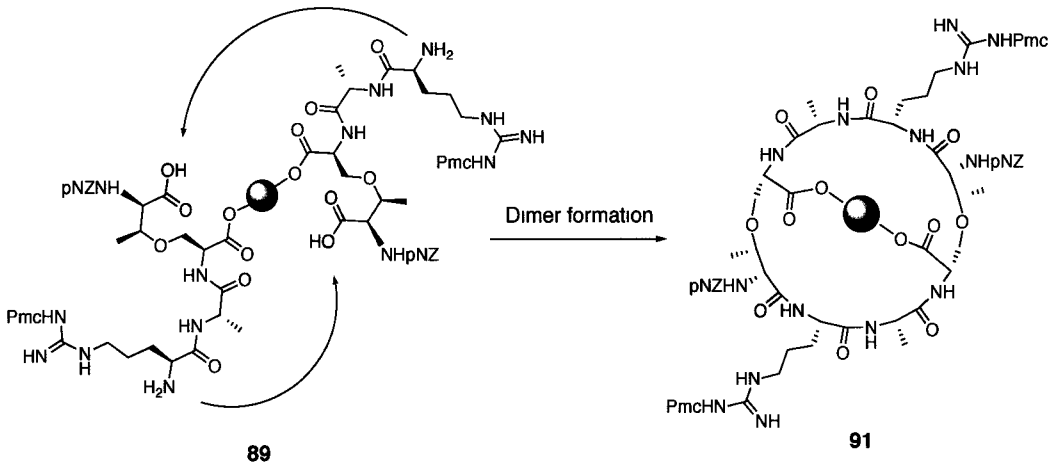

Based on the above result, a new synthesis of oxa-lacticin A2 with a lower resin loading of 0.1 mmol/g was undertaken. The Oxa-melan (0.1 mmol/g) was first loaded on the commercially available Wang resin (0.44 mmol/g). The remaining sites are capped with $Ac_2O$ to ensure the lower resin loading for further synthesis. Following the same synthetic steps as described above, cyclization affords the resin-bound ring C **90** smoothly without any observable dimers. This observation suggests that our proposed explanation for the formation of dimer (Scheme 25) is plausible.

The pNZ group on ring C is removed under reductive conditions with $SnCl_2$/DMF in the presence of a low concentration of acid (1.6 mM HCl/dioxane) to give **92** (Scheme 26).[89] Completion of the reaction is ascertained by MALDI-TOF MS analysis after treatment of a small portion of the resin with TFA/TIPS/$H_2O$ to liberate the peptide. Fmoc SPPS can then introduce the required amino acids for the formation of ring B. The following amino acids are coupled using Fmoc SPPS in the following order: orthogonal protected Oxa-melan **78**, Fmoc-Lys(Boc)-OH and Fmoc-Thr(*t*-Bu)-OH. After removal of the allyl and Fmoc groups as before, the cyclization proceeds on-resin with PyBOP/HOBt for 2.5 h. Cleavage of a small portion of the peptide under acidic condition followed by MALDI-TOF MS analysis showed a major peak corresponding to the bicyclic product **94** [994.8 (M+H)].

After removal of the pNZ group with $SnCl_2$, Fmoc SPPS can be continued to introduce the linear precursor for ring A. The amino acids are coupled in the following sequence: Fmoc-Pro-OH, orthogonal protected Oxa-lan **77**, Fmoc-

Thr(*t*-Bu)-OH, Fmoc-Asn(Trt)-OH, Fmoc-Thr(*t*-Bu)-OH. Removal of the allyl and Fmoc protecting groups and on-resin cyclization gives the tricylic product **95** (Scheme 26). Mass spectrometric analysis of a small fraction of the peptide cleaved from resin confirmed the generation of the tricyclic peptide as the major product. The observed mass [1563.4 (M+H)] agreed with the calculated mass [1562.6 (M+H)]. More importantly, no dimerized or oligomerized peptides are observed.

With the successful formation of the tricylic peptide on solid support, Fmoc SPPS was continued to introduce residues 6-15 after removal of the pNZ protecting group (Scheme 27). The amino acids are introduced in the following sequence: Fmoc-Ile-OH, Fmoc-Tyr(*t*-Bu)-OH, Fmoc-Ala-OH, Fmoc-D-Ala-OH, Fmoc-Leu-OH, Fmoc-Ile-OH, Fmoc-D-Ala-OH, Fmoc-Ile-OH, Fmoc-Ala-OH, Fmoc-Pro-OH. A small portion of the peptide was cleaved from the resin with TFA/TIPS/$H_2O$ and subjected to MALDI-TOF MS analysis. The major peak at 2603.3 (M+H) indicates formation of the desired product **96**.

**Scheme 26.** Synthesis of rings B and A of oxa-lacticin A2

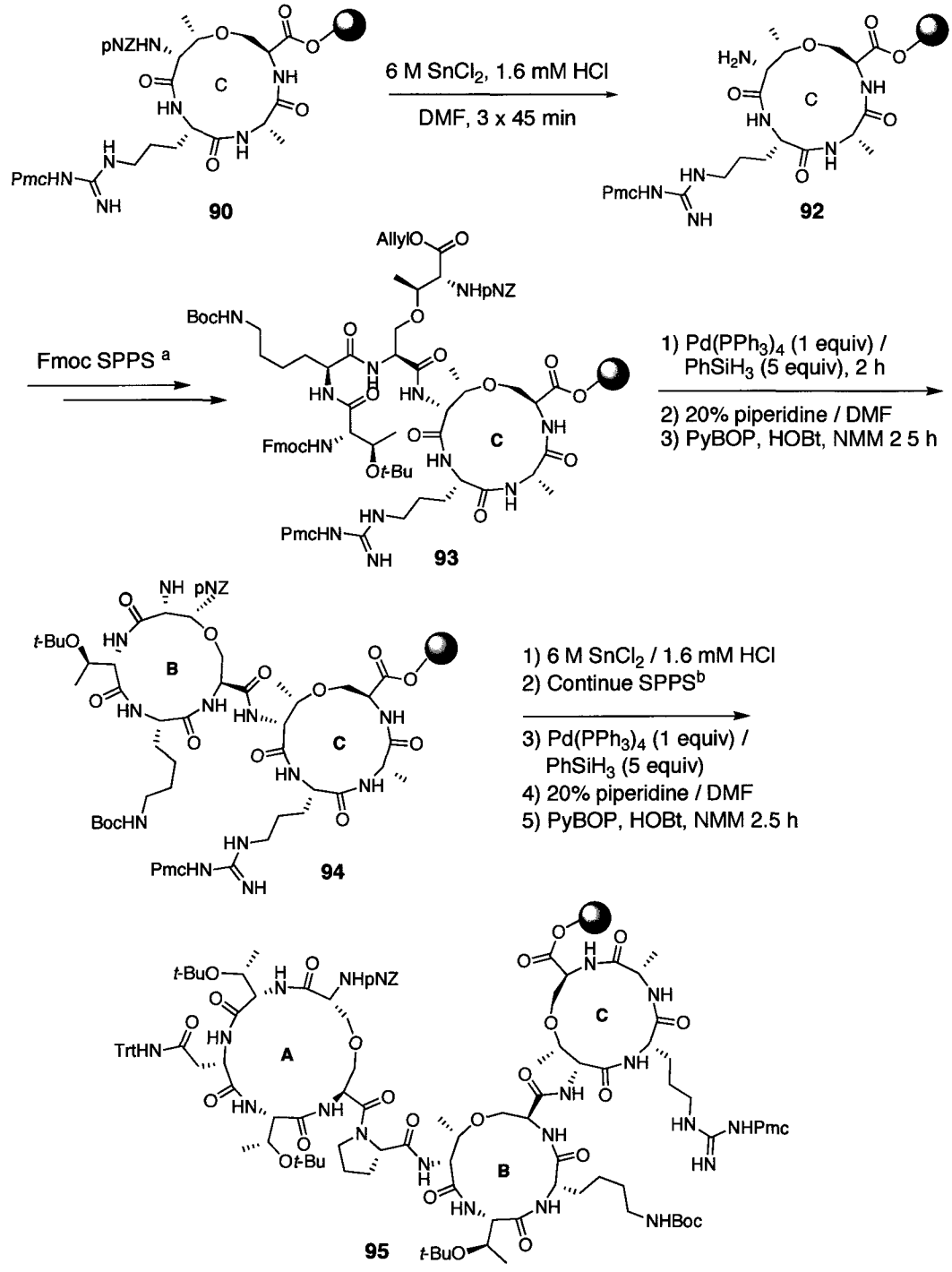


Fmoc-SPPS conditions: [a] (i) PyBOP, HOBt, NMM, DMF (ii) Orthogonal Oxa-melan **78** (iii) 20% piperidine in DMF (iv) Repeat steps (iii) and (i) for amino acids: Fmoc-Lys(Boc)-OH, Fmoc-Thr(*t*-Bu)-OH [b] Perform step (i) with Fmoc-Pro-OH, repeat steps (iii) and (i) with orthogonal Oxa-lan **77**, Fmoc-Thr(*t*-Bu)-OH, Fmoc-Asn(Trt)-OH, Fmoc-Thr(*t*-Bu)-OH.

**Scheme 27.** Introduction of residues (6→15) of oxa-lacticin A2

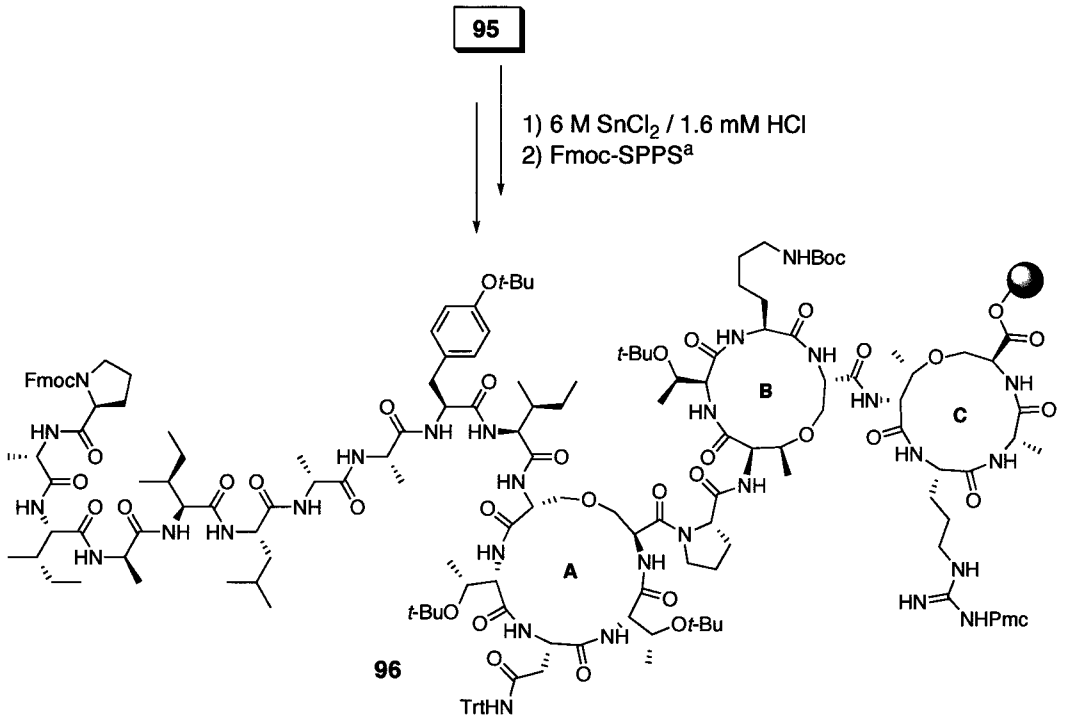


[a] Conditions used for synthesis of **96** from **95**: (i) Fmoc-Ile-OH, PyBOP, HOBt, NMM (ii) 20% piperidine in DMF, (iii) PyBOP, HOBt, NMM, DMF, [b] Repeat (ii) and (iii) for amino acids: (iv) Fmoc-Tyr(*t*-Bu)-OH, (v) Fmoc-Ala-OH, (vi) Fmoc-D-Ala-OH, (vii) Fmoc-Leu-OH, (viii) Fmoc-Ile-OH (ix) Fmoc-D-Ala-OH, (x) Fmoc-Ile-OH: (xi) Fmoc-Ala-OH (xii) Fmoc-Pro-OH.

To complete the synthesis, on-resin fragmental coupling was performed with the pentapeptide **34** (Scheme 28). Treatment of resin-bound peptide **96** with 20% piperidine removes the Fmoc group on proline. The pentapeptide is pre-activated with PyBOP/HOBt/NMM. To avoid aggregation of the long hydrophobic peptide chain, *N*-methylpyrrolidone (NMP) is used as the solvent for the coupling. This difficult fragment coupling between the secondary amine group of the proline residue on the resin and the relatively unreactive carboxyl group of the dehydropentapeptide is sluggish, and thus requires 7 h for completion.

**Scheme 28.** Completion of the synthesis of oxa-lacticin A2 (**45**)

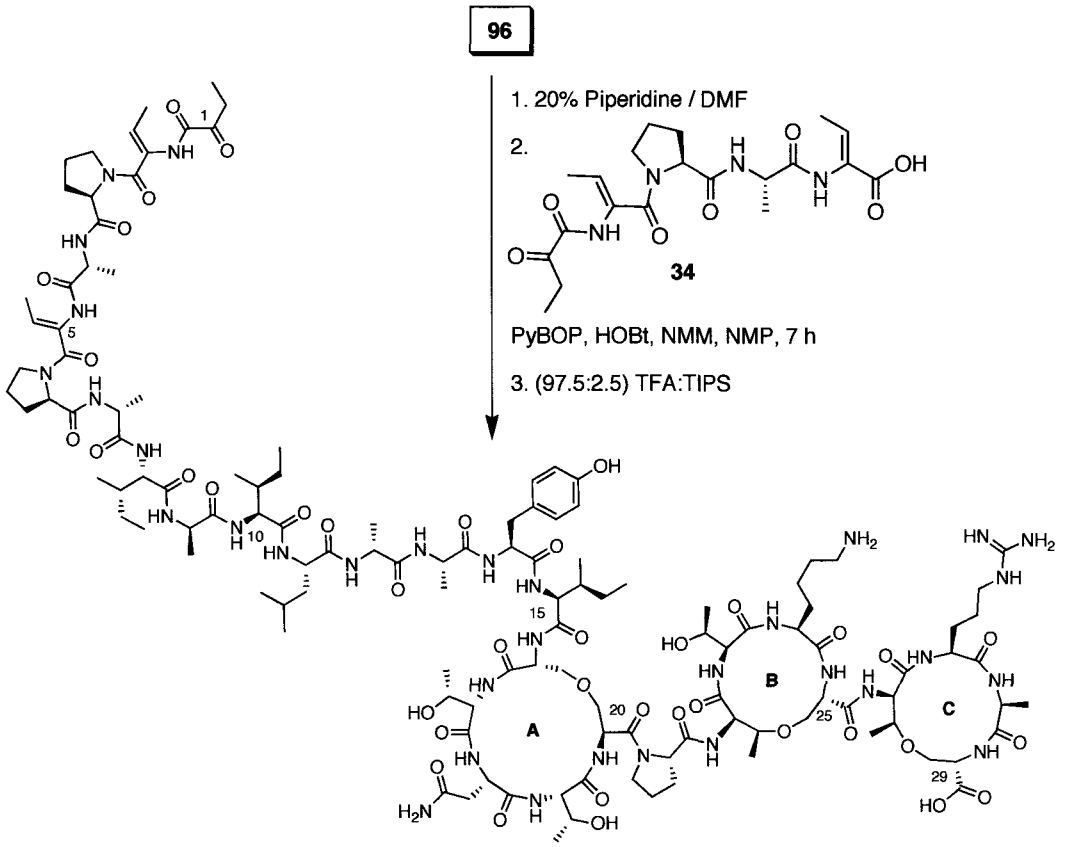


Oxa-lacticin A2, **45**

The final deprotection and cleavage of oxa-lacticin A2 from the resin was effected with (97.5:2.5) TFA/TIPS. The crude compound was purified by reverse phase C18 HPLC to yield 1.1 mg of **45**. The overall yield is 0.3% over ca. 53 steps (22 deprotections and couplings, 3 macrocyclizations, 3 pNZ removals and 3 allyl deprotections). The MALDI-TOF MS analysis of **45** shows a clean peak at 2799.2 (M+H) corresponding to the calculated mass of oxa-lacticin A2. A detailed LC-MS/MS analysis gives fragments corresponding to the masses of ring C (416.2 Da), rings CB (815.4 Da) and rings CBA (1384.6 Da) of **45** (Figure 22).

This result confirms the correct sequence and connectivity of the ether rings in oxa-lacticin A2.

**Figure 22.** LC-MS/MS analysis of oxygen analogue of lacticin A2 (**45**)

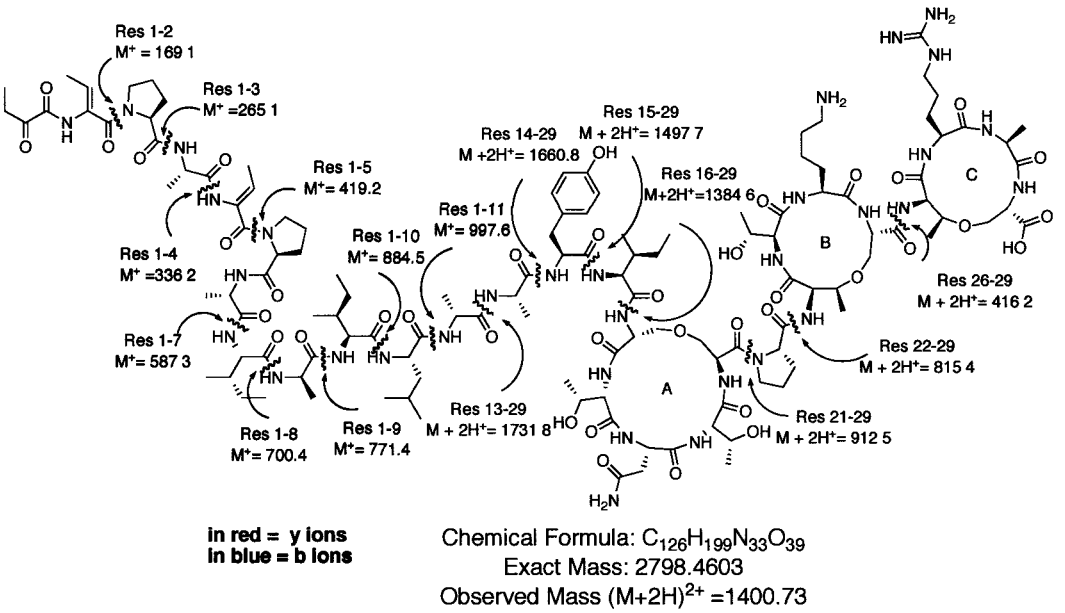


## 2.2.1.d. Biological testing of oxa-lacticin A2 (45)

A preliminary biological evaluation of oxa-lacticin A2 (**45**) was done using spot-on-lawn assay, wherein a compound of interest is spotted on the surface of a bacteria-growing agar plate and the zone formed during incubation indicates the compound's inhibitory activity. The oxa-lacticin A2 was tested in conjunction with natural lacticin A1 (**16**) against a panel of Gram-positive bacteria that are sensitive to natural lacticin A2.[100] Oxa-lacticin A2 (Oxa-A2) exhibited only individual antibacterial activity against *L. lactis* subsp. *cremoris* HP (Figure 23a) and *Leuconostoc mesenteroides* Y105 and no biological activity

against five other Gram-positive bacteria: *Staphylococcus aureus* ATCC 29213; *Enterococcus faecalis* ATCC 7080; *Enterococcus faecium* BFE900; *Lactobacillus sakei* 706 and *Pediococcus acidilactici* PAC 1.0. The results suggest that oxa-lacticin A2 (**45**) shows a reduced spectrum of activity compared to natural A2. A serial dilution assay indicates that the inherent antimicrobial activity of oxa-lacticin A2 is approximately 20 times less than natural lacticin A2. Interestingly, when oxa-lacticin A2 (**45**) is spotted beside natural lacticin A1 (**16**) at a series of different distance, it shows no synergistic antimicrobial activity against *L. lactis* subsp. *cremoris* HP at any distance (Figure 23b).

**Figure 23**. Spot-on-lawn tests for antimicrobial activity of oxa-lacticin A2 (**45**) against *L. lactis* subsp. *cremoris* HP

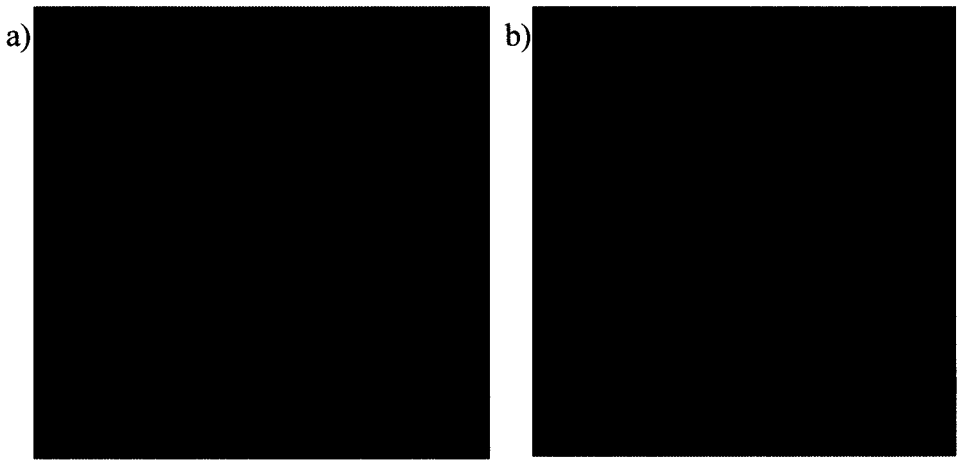


a) the synergisic and inherent activity of natural A1 (**16**) & A2 (**17**) [top]; the inherent independent activity of natural A1 (**16**) & oxa-A2 (**45**) [bottom]; b) the activity of A1(**16**) and oxa-A2 (**45**) at differing distances (no synergism).

These results support the hypothesis that the two-peptide lantibiotic lacticin 3147 has at least two modes of action. In the natural system, it is believed that synergistic activity results from pore formation in the cell membrane via the

interaction of the A2 peptide with the lacticin A1-lipid II complex.[56] The loss of synergistic activity for oxygen analogue **45** presumably results from poor recognition of the A1-lipid II complex. This may be due to an additive effect of the three modification sites or perhaps to differences in the size of sulfur vs. oxygen (van der Waals radius 1.80 Å vs. 1.52 Å) or their electrostatic properties (Pauling scale electronegativity 2.5 vs. 3.5). However, the small conformational changes between oxa-lacticin A2 and natural A2 may be tolerated for the direct binding to lipid II. This would result in inhibition of cell wall biosynthesis and the observed antimicrobial activity for the lone peptide.[52]

### 2.2.1.e. Preliminary SAR analysis for Lan and MeLan rings in two-peptide lantibiotics

To date, three analogues of lacticin 3147 A2, a carbon analogue (**34**)[74], a bis(desmethyl) analogue (**32**)[57] and the oxygen analogue (**45**)[81], have been synthesized on solid support and examined for activity in the Vederas lab. These analogues exhibit different and interesting activities in the spot-on-lawn assay (Table 3). Comparing their features helps to generate a clearer picture about the relationship between activities and structures of methyllanthioine/lanthionine rings in two-peptide lantibiotics.

**Table 3.** Biological activity of lacticin 3147 A2 (**17**) and its analogues

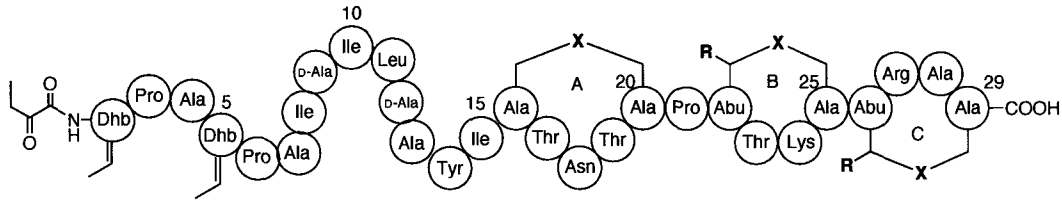


(**17**) R = $CH_3$, X = S, natural lacticin $A_2$

(**45**) R = $CH_3$, X = O, oxa-lacticin A2

(**32**) R = H, X = S, bis(desmethyl) lacticin A2

(**34**) R = H, X = CH=CH carbocyclic lacticin A2

| Compound | Synergistic activity | Inherent activity |
|---|---|---|
| **17** | + | + |
| **45** | - | + |
| **32** | + | - |
| **34** | - | - |

Upon closer examination of the structure of lacticin A2, the ring size may play an important role in binding the A1:lipid II complex or lipid II alone. Significant change in ring size in lacticin A2 cannot be tolerated as demonstrated by the complete loss of activity for carbocyclic analogue (**34**). The complementary biological testing results for the bis(desmethyl) analogue (**32**) and oxygen analogue (**45**) highlight the importance of methyl groups and sulfur atoms in the dual modes of action of two-peptide lantibiotics. The loss of inherent activity of bis(desmethyl) analogue (**32**) suggests that the methyl groups in the methyllanthionine rings are crucial for direct binding to lipid II, which is responsible for the observed inherent activity. In contrast, the sulfur atoms of lacticin A2 have an essential role in recognition of the A1:lipid II complex as illustrated by the loss of synergistic activity for the oxygen analogue (**45**). The

preliminary SAR analysis for methyllanthionine and lanthionine rings is summarized in Figure 24.

**Figure 24.** Preliminary SAR analysis of Lan and MeLan rings in lacticin A2 (**17**)

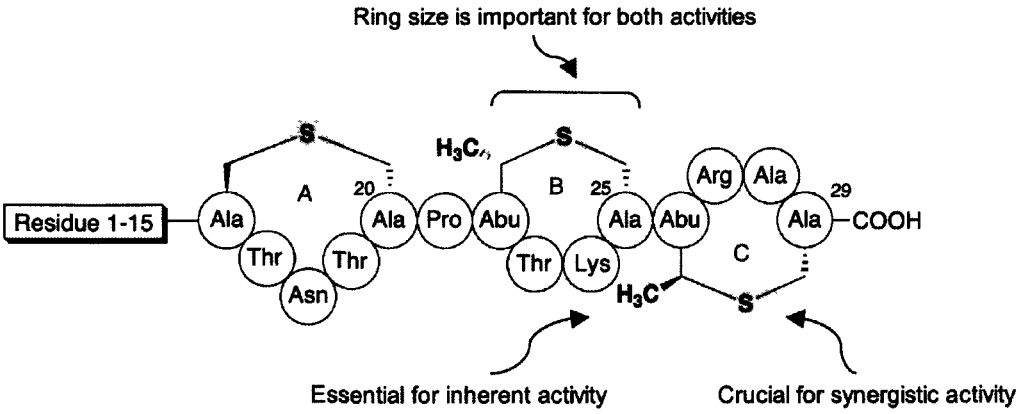


### 2.2.1.f. Conclusions and future direction

In conclusion, a facile, regio- and stereoselective methodology to prepare ether bridged bis-amino acids via aziridine ring opening with oxygen nucleophiles has been developed. The orthogonal protection of the oxygen analogues of lanthionine and methyllanthionine allows them to be readily incorporated into peptides using solid phase peptide synthesis. Multiple on-resin cyclizations together with a fragmental coupling are successfully utilized for the chemical synthesis of oxa-lacticin 3147 A2 (**45**). This oxidatively stable analogue exhibits inherent activity against Gram-positive bacteria but lacks the synergistic activity with natural lacticin A1 that is characteristic of the native lacticin A2 peptide. The

biological evaluation results support the proposal of dual modes of action for two-peptide lacticin 3147 A1 & A2.

Future studies may be directed towards the synthesis of an analogue of lacticin 3147 A2 with a single carbon atom in place of the sulfur atom in the lanthionine rings. Given the close similarity between carbon and sulfur in terms of electronegativity and their bond angles as well as bond lengths to carbon, the replacement of sulfur with carbon would lead to an analogue with minimal ring conformational change, thereby potentially retaining biological activity and enhancing oxidative stability.

## 2.2.2. Chemical synthesis and testing of natural lacticin A2

Our strategy envisioned for the synthesis of natural lacticin 3147 A2 (**17**) (Scheme 29) was similar to the synthesis of its oxygen analogue **45**. This involves the on-resin synthesis of a tricyclic peptide from lanthionine and methyllanthionine building blocks and then a fragmental coupling with the *N*-terminal pentapeptide **97**. Notably, the α-ketoamide moiety in the mature peptide could be installed as a Boc protected enamine, which would undergo hydrolysis during acidic cleavage from the resin to reveal the α-ketoamide functionality.

**Scheme 29**. Retrosynthetic analysis of lacticin 3147 A2 (**17**)

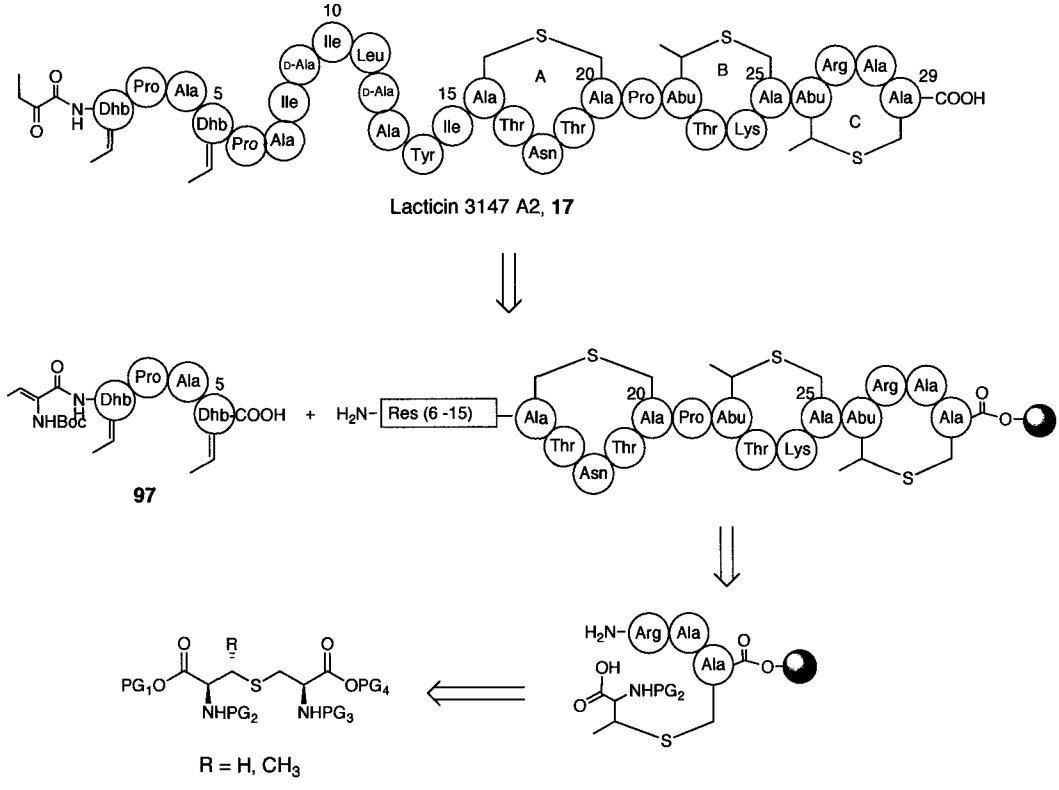

### 2.2.2.a. Synthesis of the *N*-terminal pentapeptide via a biomimetic approach

The previous synthesis of the α-ketoamide containing *N*-terminal pentapeptide **34** described in section 2.2.1.b is challenging and contains several low yielding steps. The coupling of the pentapeptide to the rest of the resin-bound peptide is also problematic. Thus, an alternative synthetic strategy was investigated. Inspired by the biosynthetic pathway for *N*-terminal ketoamide moieties in lantibiotics (Figure 6), a strategy involving spontaneous deamination of dehydrobutyrine during cleavage of the peptide from the resin was designed (Figure 25).

**Figure 25.** Strategy for formation of an α-ketoamide containing peptide

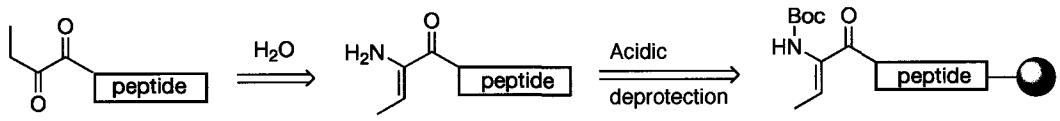


The synthesis of the pentapeptide begins with coupling of Boc-Thr-OH (**98**) and H-Thr-OMe (**99**) using EDCI to give the dipeptide **100** (Scheme 30). Double dehydrations are triggered by activation of the hydroxyl group with MsCl followed by DBU-promoted elimination to yield peptide **101**. At this point, the conversion from the enamine to keto amide moiety was tested. Removal of the Boc protecting group with TFA followed by hydrolysis affords the desired product **102** smoothly.

**Scheme 30.** Synthesis of ketoamide containing dipeptide (**102**)

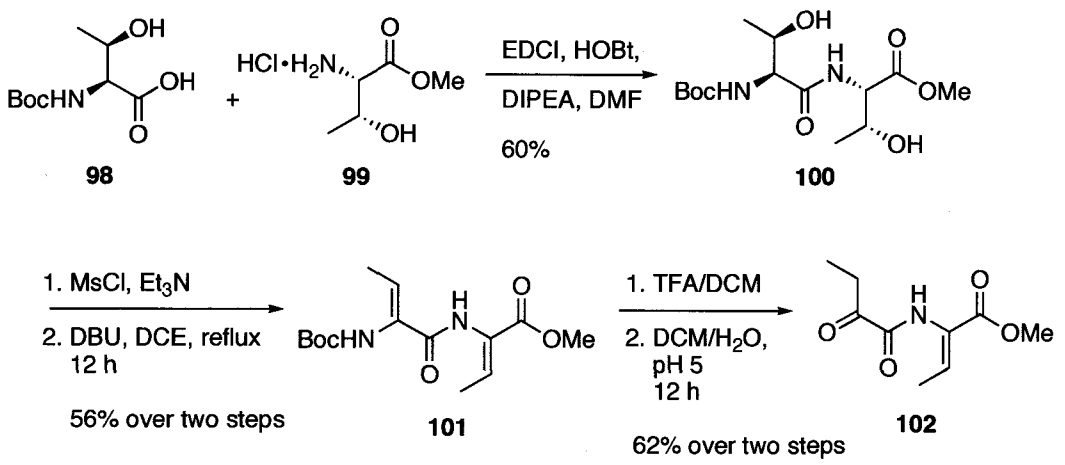


With the success of the biomimetic deamination strategy, the dehydrodipeptide **101** needs to be coupled with dehydrotripeptide **80** to afford the desired pentapeptide **97**. Hydrolysis of the methyl ester of **101** using LiOH can be expected to give **103** (Scheme 31). However, upon closer examination of the $^1$H NMR for **103**, two sets of peaks for the olefin adjacent to *N*-terminus were observed, suggesting scrambling of the geometry of this double bond. The loss of stereochemical integrity is possiblely due to an unselective intramolecular Michael addition followed by elimination under very strongly basic conditions. A proposed mechanism is shown in Scheme 32.

**Scheme 31.** Attempted hydrolysis of methyl ester in dehydrodipeptide (**101**)

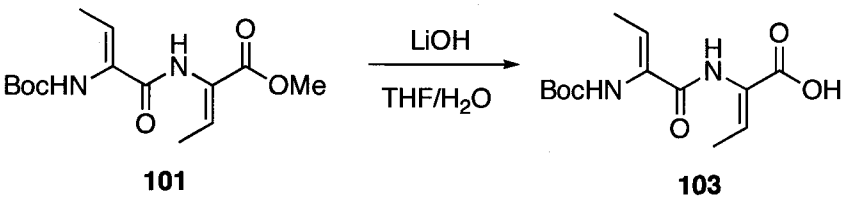

**Scheme 32.** Proposed mechanism for the scrambling of double bond geometry in **103**

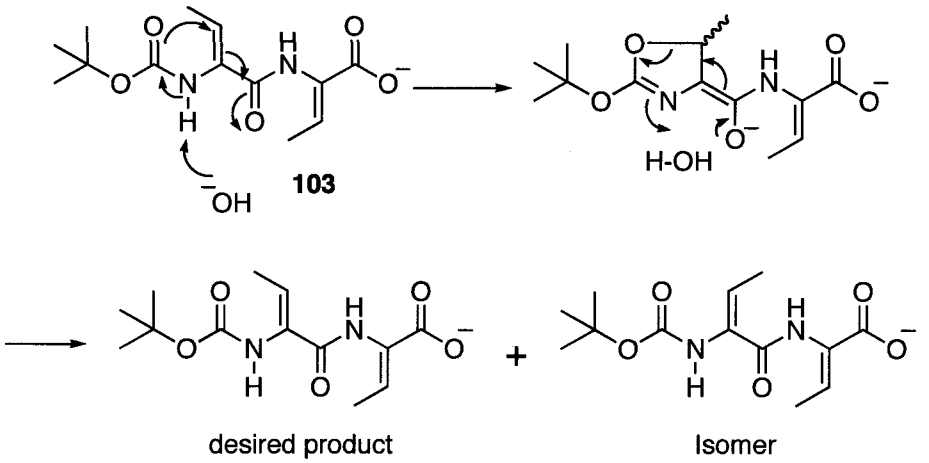


To overcome the problem associated with hydrolysis of the methyl ester, an allyl ester was used to protect the carboxylic acid functional group. The synthesis starts with the coupling reaction between commercially available Boc-Thr-OH (**104**) and D-threonine allyl ester (**105**) mediated by PyBOP to give the dipeptide **106** (Scheme 33). The activation and double elimination of the hydroxyl side chains by MsCl and DBU afford **107**. Deprotection of the allyl ester with $Pd(PPh_3)_4$ in the presence of the scavenger $PhSiH_3$ gives **108**.

**Scheme 33.** Synthesis of dehydrodipeptide (**108**)

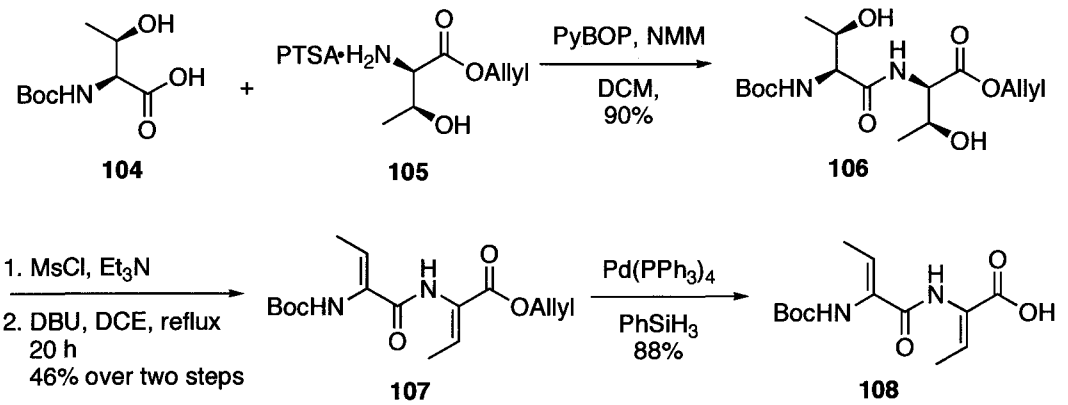

Having successfully obtained dipeptide **108**, a fragmental coupling is performed in solution between **108** and dehydrotripeptide **80** that is prepared according to the procedure described in Scheme 22. Removal of the Boc group on **80** followed by coupling with **108** in the presence of DIC gives **109** (Scheme 34). Deprotection of the allyl ester with $Pd(PPh_3)_4$ affords **110** that can subsequently be incorporated onto solid support.

**Scheme 34.** Synthesis of modified pentapeptide (**110**)

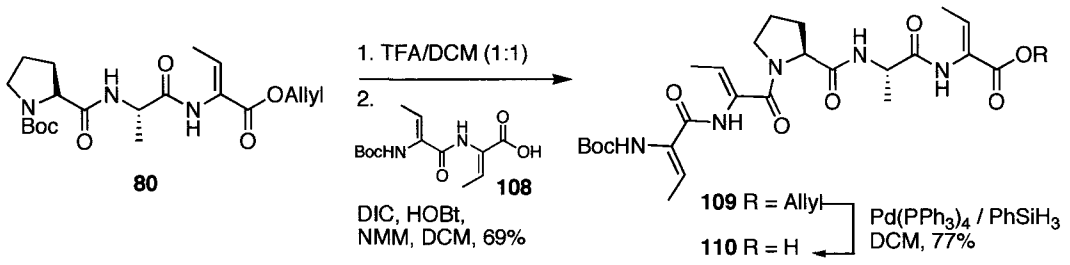


### 2.2.2.b. Synthesis of methyllanthionine with orthogonal protecting groups

In order to synthesize the natural lacticin 3147 A2 on the solid support, an orthogonally protected methyllanthionine building block is required. However, as mentioned in Section 2.1.5.b., only a few methods for the stereoselective synthesis of methyllanthionine have been reported in the literature.[71,72,73] None of them can be readily used on solid phase due to the difficulty in protecting group manipulations. Therefore, effort focused on methodology development to gain facile access to multigram quantities of methyllanthionine with orthogonal protecting groups.

Given the successful synthesis of the oxygen analogue of methyllanthionine via regio- and stereo-selective aziridine ring opening with oxygen nucleophiles,[82] the logical extension is to use the free thiol of cysteine (**111**) to open the activated aziridines (**112**). This ring opening reaction could stereoselectively give access to not only methyllanthionine **114** but also lanthionine **113** (Scheme 35).

**Scheme 35.** Strategy for synthesis of methyllanthionine and lanthionine

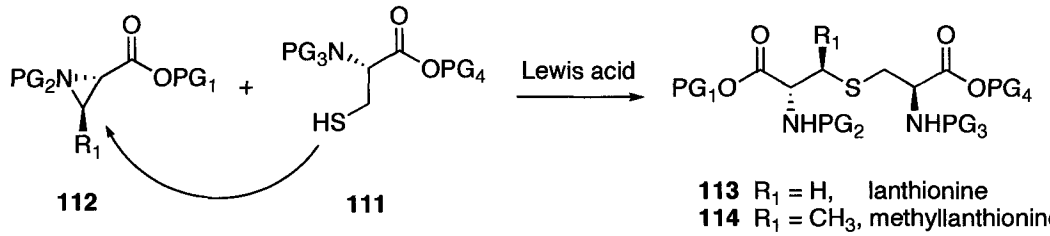


To test the possibility of regio- and stereo-selective ring opening of activated aziridines by thiol nucleophiles, a model reaction was performed using *para*-methoxybenzyl thiol (**115**) as a nucleophile and the pNZ protected aziridine (**63**) as an electrophile (Scheme 36). However, under the optimized condition described in Section 2.2.1.a, the azridine ring opening only leads to a mixture with the major product (based on $^1$H-NMR) corresponding to the proposed structure **117**. This byproduct could come from the attack of the thiol on the benzylic position in the pNZ protecting group.

**Scheme 36.** Model reaction of aziridine ring opening with a thiol nucleophile

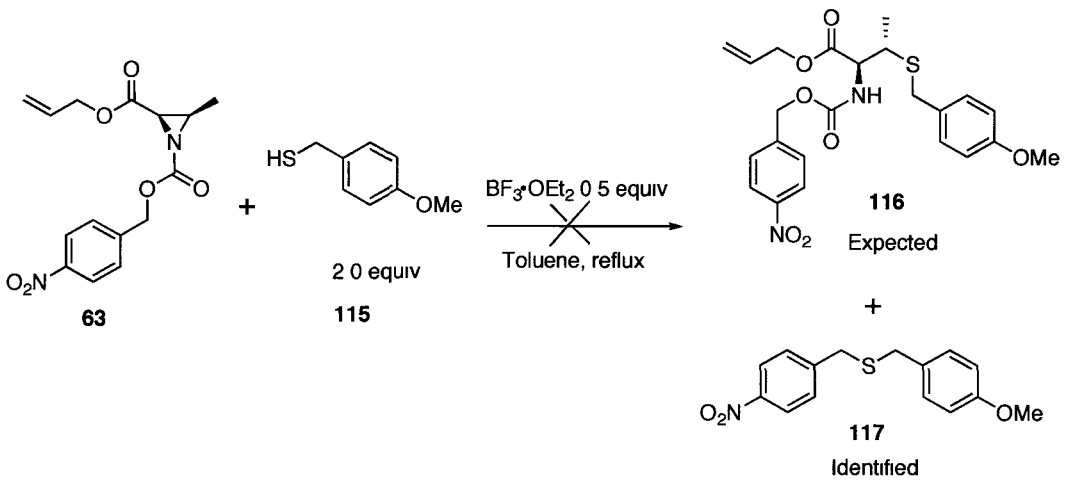


With the failure of the model reaction, another activated aziridine electrophile was designed wherein the 2,4-dinitrobenzenesulfonyl (DNs) group is used as a temporary amino protecting group.[101] Although nucleophilic ring openings with *N*-nosyl (*o*- or *p*- nitrobenzenesulfonyl) activated aziridines have been well documented in the literature,[72, 102, 103] the aziridine activation with DNs has not been explored. The DNs group could offer several advantages over the pNZ group in our synthesis: stronger electron withdrawing ability to facilitate the aziridine ring opening; and also compatibility with 2-chlorotrityl chloride resin for the subsequent SPPS.[104] In contrast, pNZ deprotection conditions ($SnCl_2$, 1.6 mmol HCl) are not compatible with the acid labile 2-chlorotrityl chloride resin, which would result in potential cleavage of peptide from the solid support during deprotection. The reason for using 2-chlorotrityl chloride resin is that it can suppress side reactions, such as epimerization and thiol elimination when the *C*-terminal residue is cysteine or a cysteine derivative.[105-107] The DNs protected aziridine can be prepared through protecting group manipulations from the *N*-

trityl protected aziridine. Removal of the trityl group from **66** with TFA followed by introduction of the DNs group under Schotten-Baumann conditions affords **118** (Scheme 37).

**Scheme 37.** Synthesis of the DNs protected aziridine (**118**)

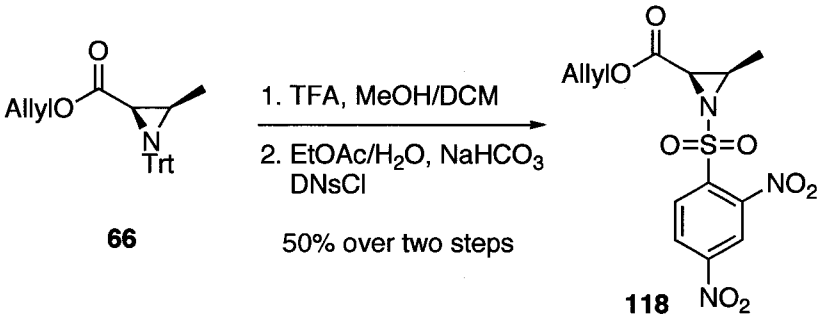


With the DNs protected aziridine available, the aziridine ring opening with the thiol side chain of Fmoc-Cys-O*t*-Bu (**119**) is performed to afford protected methyllanthionine **120**. Interestingly, the number of equivalents of $BF_3 \bullet OEt_2$ plays a crucial role in promoting the reaction. When 0.2, 0.5 or 1.0 equivalents of Lewis acid are used, there is no observed reaction as assessed by TLC. However, the reaction is triggered with 2.0 equivalents of $BF_3 \bullet OEt_2$. Formation of the desired product is then observed by mass spectrometry (Scheme 38). The possible reason for this is that $BF_3 \bullet OEt_2$ preferentially coordinates to the free thiol instead of the aziridine nitrogen; therefore excess Lewis acid is required to promote the ring opening reaction. However, TLC shows a complex mixture of products for this reaction. This is likely due to the instability of the *tert*-butyl protecting group in the presence of excess Lewis acid.

**Scheme 38.** Attempted synthesis of methyllanthionine with orthogonal protecting groups

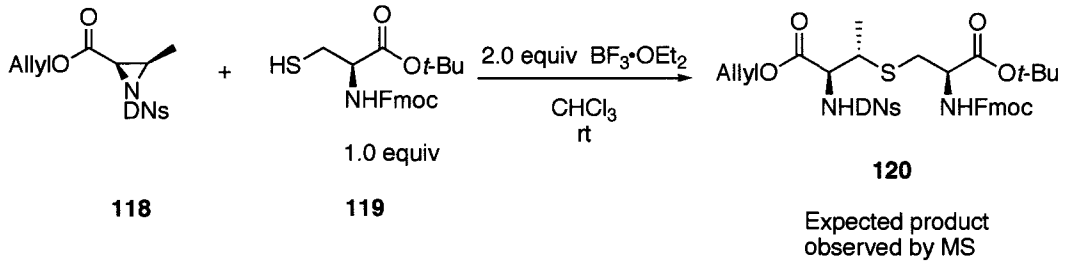


1.0 equiv

**118** **119** **120**

Expected product observed by MS

To circumvent this problem, a possibility is to use alternative acid stable protecting groups for the carboxylic acid. However, the required orthogonality with the other three protecting groups makes it difficult to find a suitable protecting group. Ideally, the best protecting group is no protecting group at all. Given the nucleophilic difference between a free thiol and carboxyl group under the reaction conditions, we envisioned that there may be no need to protect the carboxylic acid of the cysteine nuclophile. Thus, another model reaction with mercaptoacetic acid **121** as a nucleophile was performed (Scheme 39). With 2 equivalents of Lewis acid as catalyst, the DNs-activated aziridine is regio- and stereo-selectively opened by this thiol nucleophile to give the desired product **122** in good yield.

**Scheme 39.** Aziridine ring opening with an unprotected nucleophile

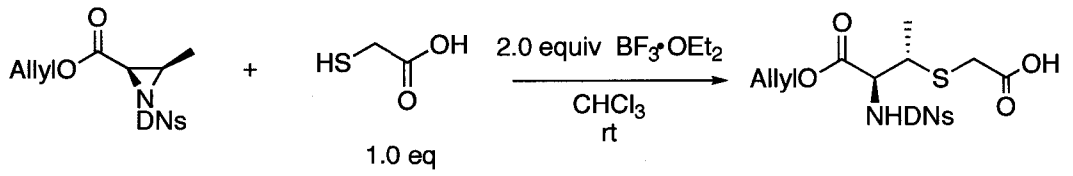


1.0 eq

45%

**118** **121** **122**

With this encouraging result, our attention refocused on the synthesis of methyllanthionine with orthogonal protecting groups. The Fmoc protected thiol **123** is prepared from commercially available cysteine **124** using Fmoc-OSu (Scheme 40). Aziridine ring opening with **123** under $BF_3 \bullet OEt_2$ catalysis at room temperature gives **125** smoothly in moderate yield (Scheme 41).

**Scheme 40.** Synthesis of Fmoc-Cys-OH (**123**)

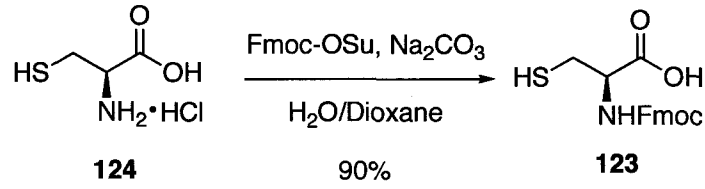


**124** 90% **123**

**Scheme 41.** Synthesis of methyllanthionine via aziridine ring opening

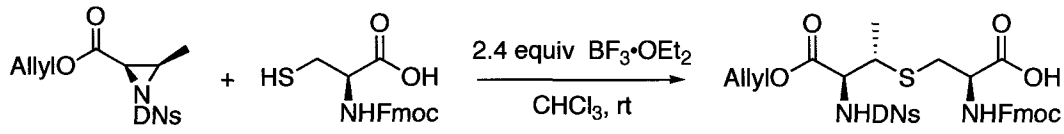


**118** **123** 32 % **125**

At this point, no further attempt for reaction optimization was made. Focus was directed to the solid phase peptide synthesis. Before loading the methyllanthionine onto the resin, the orthogonality between DNs and Fmoc was examined. Surprisingly, based on $^1$H-NMR analysis, the DNs protecting group is not stable under Fmoc deprotecting conditions using 20% piperidine. This is possibly due to the strong nucleophilicity of piperidine. A mechanism for DNs deprotection with piperidine is proposed in Scheme 42.

**Scheme 42.** Proposed mechanism for DNs deprotection with piperidine

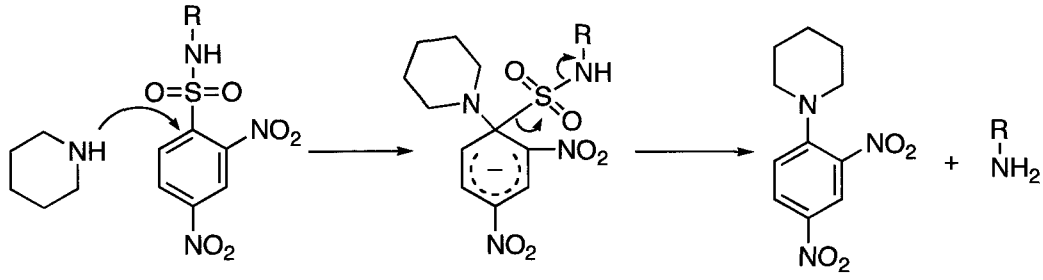

It may be possible to find suitable deprotection conditions for removal of an Fmoc group without affecting the DNs group. Another approach is to replace the DNs group with a different protecting group, such as Alloc, that will be orthogonal to Fmoc. For the first approach, several attempts were made using weak nucleophilic basic systems to effect Fmoc deprotection (Figure 26).[108] However, these conditions also affect the DNs group to various extents based on $^1$H-NMR analysis. Therefore, attention shifted to the second possibility.

**Figure 26.** Attempted Fmoc deprotection conditions with weak nucleophiles

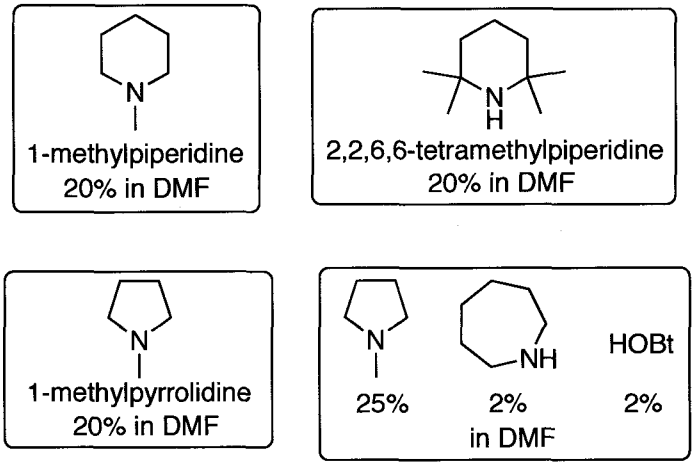

A mild reagent for the removal of DNs is a solution of mercaptoacetic acid and $Et_3N$ in DCM (**126**).[101] These conditions should be suitable for removing DNs in the presence of the Fmoc group. Model reactions on solid support were performed to test the compatibility of the Fmoc protecting group to the DNs deprotection conditions (Figure 27). The reaction can be monitored using a colorimetric test (Kaiser test), wherein the characteristic dark blue color indicates the presence of primary amino groups on the resin.[109] The results suggest that the DNs group can be selectively removed without affecting the Fmoc group.

**Figure 27.** Test of compatibility of the Fmoc group to DNs deprotection conditions

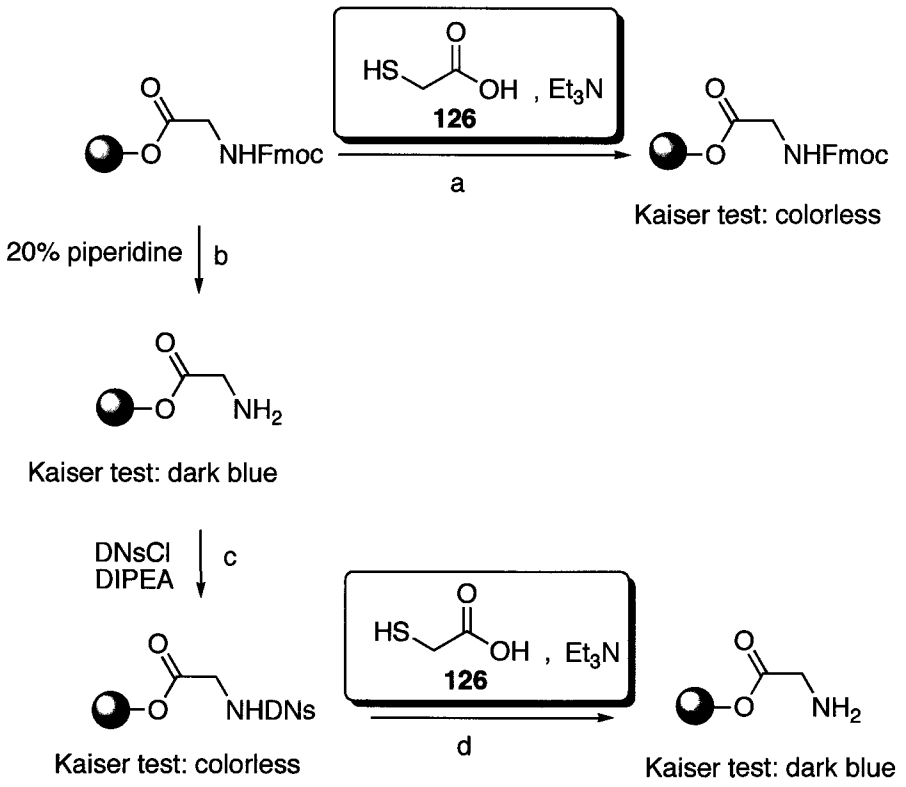


a) Treatment of resin-bounded Fmoc-Gly with **126** results in no deprotection of Fmoc group. b) Treatment of resin-bounded Fmoc-Gly with piperidine leads to Fmoc deprotection; c) Treatment of free amino group with dinitrobenzenesulfonyl chloride (DNsCl) and base introduces DNs group onto resin; d) Treatment of DNs protected glycine with **126** affords the free amino group.

Having identified the conditions for DNs deprotection, protecting group manipulation could be performed readily. At this point, this project was taken over by a postdoctoral fellow, Dr. Wei Liu, due to time constraints. For completion and clarity, further protecting group manipulation for methyllanthionine and the completion of total synthesis of natural A2 is briefly described below.

The DNs protecting group was removed with mercapoactic acid in the presence of $Et_3N$. Subsequent reaction with allyl chloroformate affords **127** that can be incorporated onto solid support directly (Scheme 43). The developed methodology also allows for the preparation of lanthionine with orthogonal protecting groups (**128**) via the ring opening of aziridine derived from serine (**129**) (Scheme 44).

**Scheme 43.** Protecting group manipulations of methyllanthionine

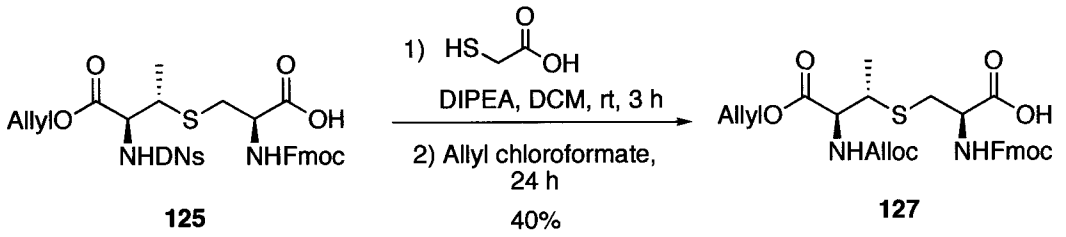


**125** 40% **127**

**Scheme 44.** Synthesis of lanthionine via aziridine ring opening

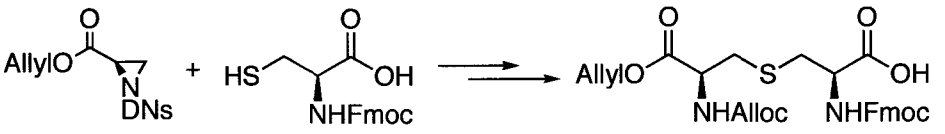


**129** **123** **128**

### 2.2.2.c. The completion of the chemical synthesis of lacticin 3147 A2 on solid support

The completion of total synthesis was accomplished by Dr. Wei Liu. Briefly, utilizing a similar synthetic strategy to that adopted for oxa-lacticin A2 (**45**), the tricylic peptide was assembled via sequential on-resin cyclizations (Scheme 45). The methyllanthionine **127** is loaded onto 2-chlorotrityl chloride resin with a low loading of 0.15 mmol/g. Fmoc SPPS was performed using PyBOP to couple the amino acids required for ring C. The Alloc, allyl and Fmoc protecting groups are removed on solid support using $Pd(PPh_3)_4$ with $PhSiH_3$ as scavenger and 20% piperidine in DMF repectively. The cyclization to form ring C is performed on solid support using PyBOP as the coupling reagent. In a similar manner, ring B and ring A are also formed. Standard Fmoc SPPS can be continued to give the resin-bound peptide **129**.

**Scheme 45.** Synthesis of tricyclic moiety of lacticin A2 on solid support

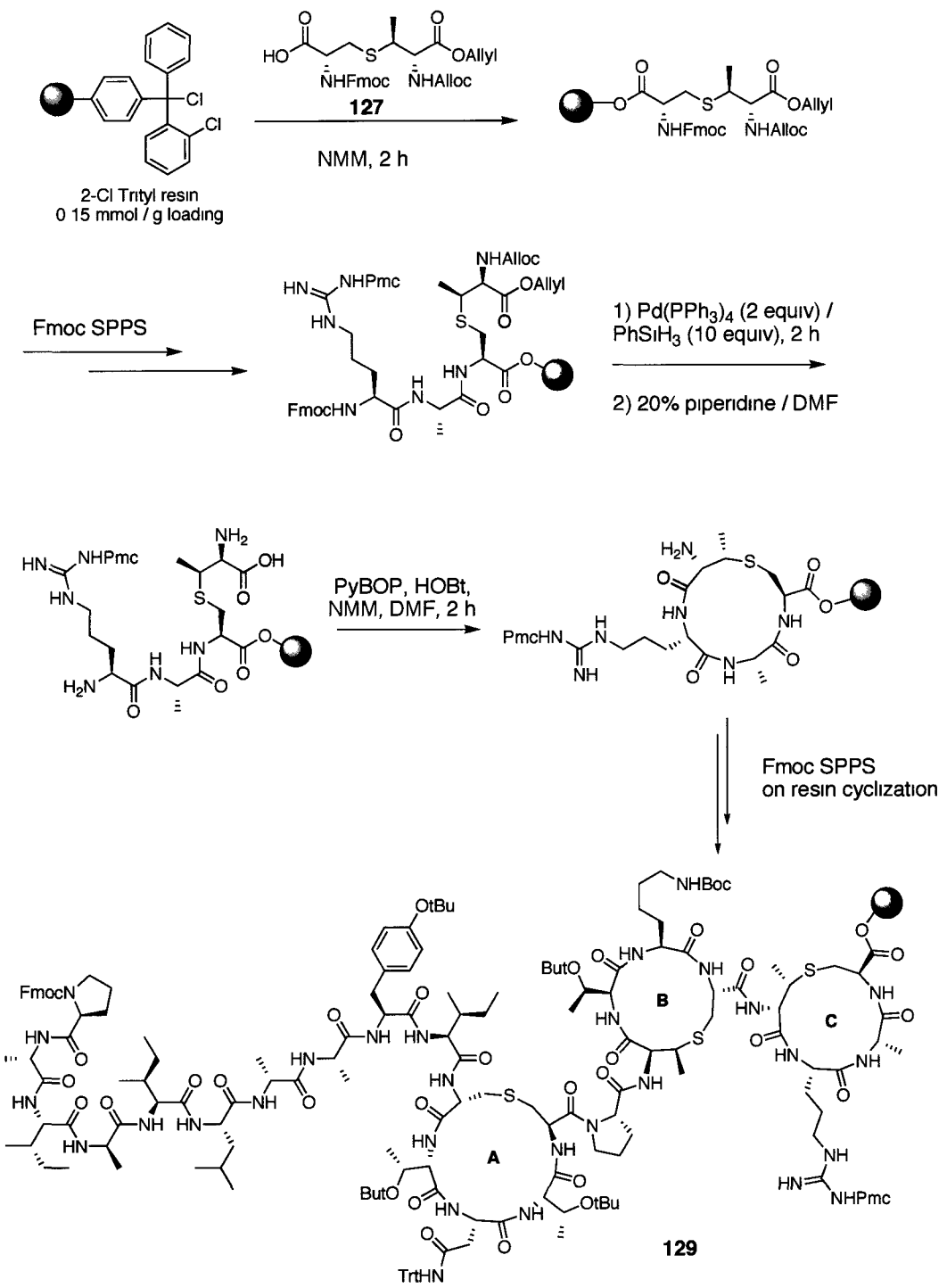

Fragment coupling between tricylic peptide **129** and pentapeptide **110** prepared in solution as described in Section 2.2.2.a, was performed using PyBOP (Scheme 46). Final deprotection with a 95:2.5:2.5 TFA/Anisole/$H_2O$ cocktail cleaves the peptide from the resin with concomitant removal of all the side chain protecting groups including the *N*-terminal Boc group. This triggers the formation of the α-ketoamide moiety through the hydrolysis of the unprotected enamine functionality. The desired peptide (**17**) was purified and characterized by MALDI-TOF MS and MS/MS sequencing. Biological testing and ananlytical RP-HPLC analysis confirms that the synthetic peptide is the same as the natural lacticin 3147 A2. Thus by chemical synthesis, we are able to confirm that the proposed stereochemistry of the lanthionine and methyllanthionine residues in natural lacticin 3147 A2 are indeed (2*S*, 6*R*) lanthionine and (2*S*, 3*S*, 6*R*) methyllanthionine, respectively.

**Scheme 46.** The completion of the synthesis of lacticin 3147 A2 **(17)**

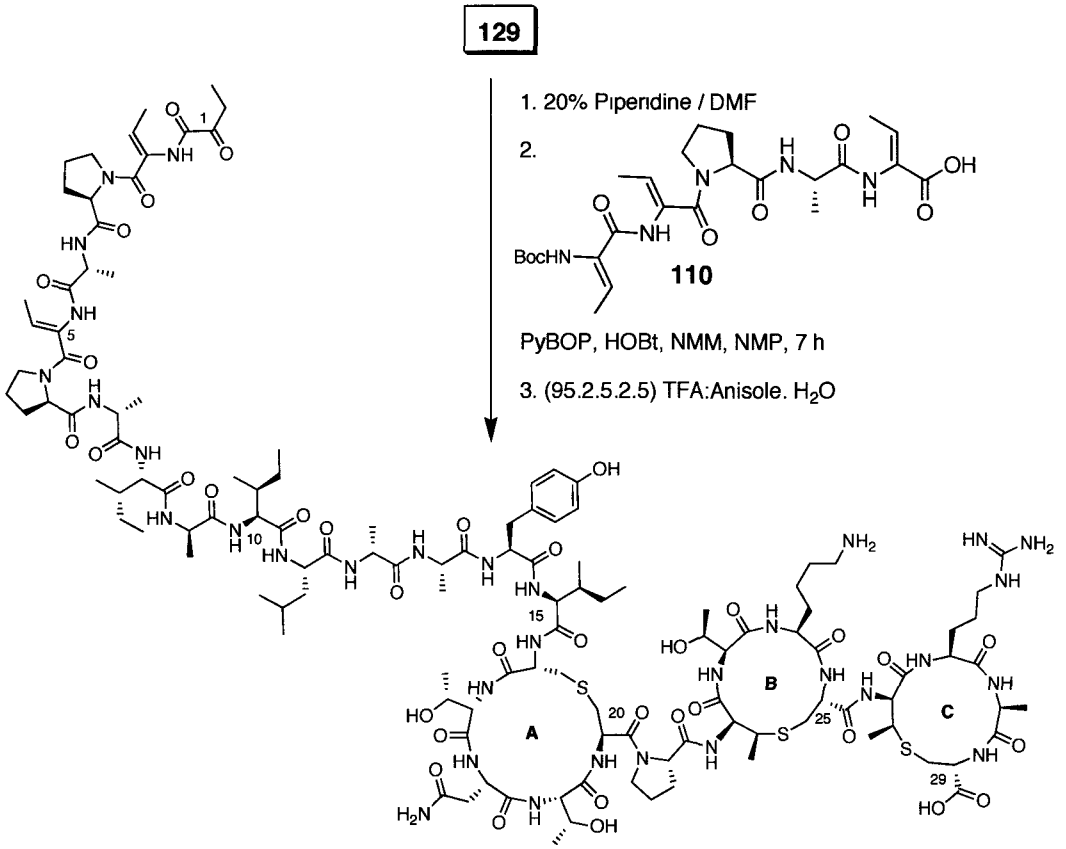


## 2.2.2.d. Conclusions and future work

In an effort for the total synthesis of natural lacticin 3147 A2, a biomimetic synthesis of an *N*-terminal α-keto amide moiety has been achieved by incorporation of a Boc-protected enamine onto solid support followed by hydrolysis during final TFA-mediated global deprotection/cleavage. This synthesis not only facilitates the chemical total synthesis of lacticin A2, but also further supports the proposed mechanism for the biosynthesis of α-keto amide moieties in lantibiotics.

A methodology for synthesizing orthogonally protected methyllanthionine and lanthionine has been developed via a regio- and stereo-selective aziridine ring opening reaction. This practical and reliable synthetic approach enables facile access to multigram quantities of methyllanthionine with orthogonal protecting groups that are compatible with solid phase peptide synthesis. The stereoselective synthesis of lanthionine and methyllanthionine also allows for the confirmation of stereochemistry of these unusual residues in natural peptides.

These syntheses provide access to more structurally diverse lantibiotics. Utilizing the established synthetic methodology, future studies can focus on the challenge of synthesizing lantibiotics with interlocking rings, such as lacticin 3147 A1 (**16**) and nisin (**13**).

# Chapter 3. Anticancer peptides: neopetrosiamides

## 3.1. Introduction

Cancer is currently responsible for about 13% of human deaths worldwide and is a leading cause of death in the United States and the western world, second only to heart disease.[110, 111] Cancer is a group of diseases that are characterized by the uncontrolled growth of cells that invade and destroy adjacent tissues. Cancer cells can also spread to other locations in the body through a process known as metastasis, which is responsible for about 90% of cancer deaths.[112] Although significant advances in cancer therapies have been made through surgery, radiotherapy or systemic chemotherapy, about half of cancer patients are not cured by these treatments.[112] Moreover, anticancer drug development suffers from the problems of nonspecific toxicity and multidrug resistance. Therefore, there is a clear and urgent need for effective new anticancer drugs. Even though high throughput screening (HTS) and combinational chemistry are playing important roles in anticancer drug development, natural products from plants, insects and more recently marine organisms continue to be valuable sources for drug prototypes.[16, 113] This is reflected by almost half of the anticancer drugs in the clinic are of natural origin.[114]

### 3.1.1. Neopetrosiamide A & B

Recently, Andersen and co-workers reported the isolation and structure elucidation of neopetrosiamide A and B (**130**) from a marine sponge (*Neopetrosia sp.*) collected in Papua New Guinea.[115] They have been found to be potent inhibitors (6 $\mu$g/mL) of human cancer cell invasion associated with metastasis. The two peptides contain 27 standard amino acids and a methionine sulfoxide at position 24. They are diastereomeric, differing only in the stereochemistry of the methionine sulfoxide functionality and contain three intramolecular cross-linking disulfides (Cys 3-26, Cys 7-12 and Cys 18-28) (Figure 28) as determined by 2D NMR spectroscopy and mass spectrometry.

**Figure 28.** Proposed structures of neopetrosiamide A and B (**130**)

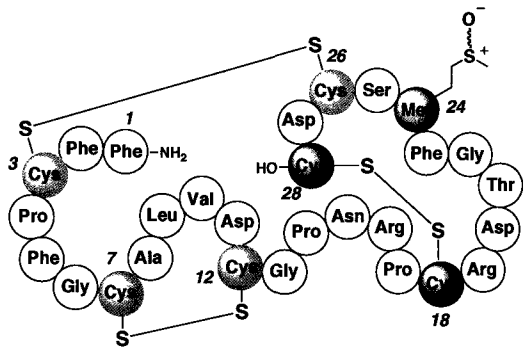


The lethal spread of cancer cells requires that cells invade and migrate through the extracellular matrix (ECM), the structural support of mammalian cells.[116] This attachment of a cell to the ECM is mediated by cell surface receptors, integrins. To move through ECM barriers, cancer cells utilize two distinct mechanisms.[115] One is a path-generating process (mesenchymal migration) wherein the cancer cells clear a way for forward motion by

enzymatically degrading the ECM using proteases; the other is a path-finding process (amoeboid migration), in which cancer cells change their shapes and escape out of the ECM for migration. During metastasis, when the mesenchymal migration pathway is blocked through inhibition of proteases, the cancer cells can simply switch to the amoeboid migration process (Figure 29).[117] This transition makes the cancer therapies based on protease inhibitors less efficient. Therefore, the simultaneous inhibition of both pathways in cancer cell migration might be a powerful way to effectively control metastasis. Fortunately, neopetrosiamides inhibit both cancer migration pathways.

**Figure 29.** Schematic representation of mesenchymal-amoeboid transition of a cancer cell in ECM (*adapted from the Journal of Cell Biology, Wolf et al.* [117])

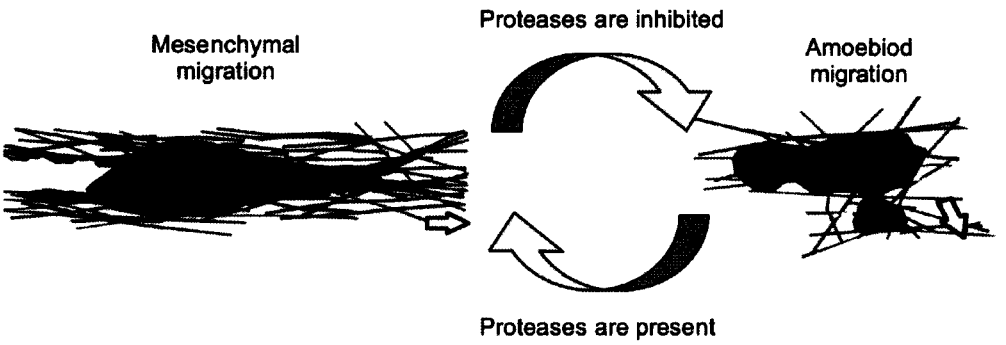


In addition to inhibiting cancer cell invasion, neopetrosiamides also decrease cell surface integrin levels, thereby inhibiting cancer cell adhesion to the rigid ECM.[118] Even though the detailed inhibition mechanism of the neopetrosiamides is still unclear, their intriguing anticancer features make them appealing candidates for use in the therapeutic control of cancer metastasis.

Neopetrosiamides possess unique structural features that differ from those of many other peptides from sponges. Most sponge-derived peptides have either

one or no disulfide bond, whereas neopetrosiamides contain three cross-linking disulfides.[115] As one of the most common post-translational modifications, disulfide bonding plays an important role in maintaining the three-dimensional structures and biological activities of proteins and peptides. Bioactive disulfide-rich peptides are also found in other natural sources. For example, the venom produced by carnivorous marine snails from the genus *Conus* provides biologically active, short disulfide-rich peptides known as conotoxins. Ziconotide (Prialt) (**131**), a ω-conotoxin, was approved by US FDA in 2004 for treatment of chronic pain (Figure 30).[119] In plants, a class of circular, small disulfide-rich peptides known as cyclotides (**2**) has been discovered,[9] which exhibit a range of biological activities as described in Chapter 1. The cyclic backbone and three intramolecular cross-linking disulfides give cyclotides exceptional stability, even to boiling. In mammals, the short antimicrobial peptides known as β-defensins (**132**) are also characterized by the presence of three intramolecular disulfide bonds.[120]

**Figure 30.** Structures of representative bioactive disulfide-rich peptides

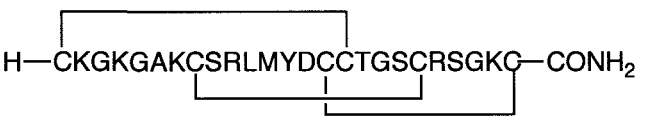


Ziconotide **131**

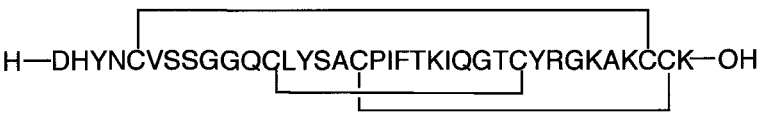


β–Defensin: hBD-1 **132**

### 3.1.2. Characterization of disulfide connectivity in disulfide-rich peptides

Despite the diversity of structures and biological activities of short disulfide-rich peptides, it is believed that only a small fraction of this naturally occurring resource has been discovered and characterized to date.[121] This is partly due to the significant challenge in rapid characterization of disulfide bond connectivity in these peptides.[122]

Traditional disulfide mapping methods involve the digestion of the peptide chain with protease followed by isolation and characterization of the bridged fragments to deduce the overall connectivity.[123] Resistance to enzyme digestion can make it difficult to obtain diagnostic fragments for further analysis. Many short peptides lack convenient proteolytic cleavage sites.

The advance of multidimensional NMR techniques has made it possible to elucidate the three-dimensional structure of peptides. In particular, the disulfide bridge can be confirmed by the NOESY cross-peaks between the side chain protons in two cysteines paired in a disulfide bond.[124] The disulfide bond connectivity of the neopetrosiamides was proposed based on 2D NOESY data.[115] Although NMR-based methods offer a convenient way to map disulfide connectivity, correct assignment can be difficult if there is overlap of resonances. When two or more disulfides are in close proximity in the molecule's tertiary structure, the local Cys-Cys NOEs can be misleading because proton pairs in the non-connected Cys residues can be closer in space than those paired within a disulfide bond.[125]

Another commonly used method to determine disulfide connectivity is based on a mass spectrometry technique that was originally introduced by Gray.[126] In contrast to the traditional disulfide mapping, Gray's method features the cleavage of disulfides while leaving the peptide chain intact. This method involves the partial reduction of disulfides in combination with stepwise disulfide-specific tagging. Since its first introduction in 1993, several modifications on this strategy have been reported.[123, 127] Recently, Craik and co-workers presented a new approach for mapping disulfides in highly clustered cyclotides.[128] A brief description for this strategy is given in Figure 31. The method starts with the disulfide partial reduction of the folded cyclotide peptide (**2a**) at low pH using phosphine-based reducing agents, such as tris(2-carboxyethyl)phosphine (TCEP). The disulfide reduction generates many partially reduced species, such as **2b** and **2c** that contain one or two original disulfide bridges. HPLC purification of these intermediates followed by sulfhydryl alkylation with *N*-ethylmaleimide (Nem) under acidic condition affords the first labeled peptides (**2d, 2e**). The low pH for partial reduction and alkylation is crucial to prevent disulfide exchange between the reduced and intact disulfides, which is a serious side reaction under basic conditions. The alkylated peptides are subjected to complete reduction followed by a second alkylation with 2-bromoethylamine to give **2f** and **2g**, respectively. The aminoethylation ($Ae^+$) introduces charges as well as enzymatic digestion sites, which make the following enzymatic digestion and MS/MS sequencing more feasible. After enzymatic digestion, the cleaved fragments in **2h** and **2i** are then identified and thus the cysteine pairs involved in disulfides (**2j, 2k**) are

determined. The disulfide bond connectivity of cyclotides is deduced as shown in **2l**.

**Figure 31.** Overview of partial reduction and selective alkylation strategy for disulfide bond mapping for cyclotides

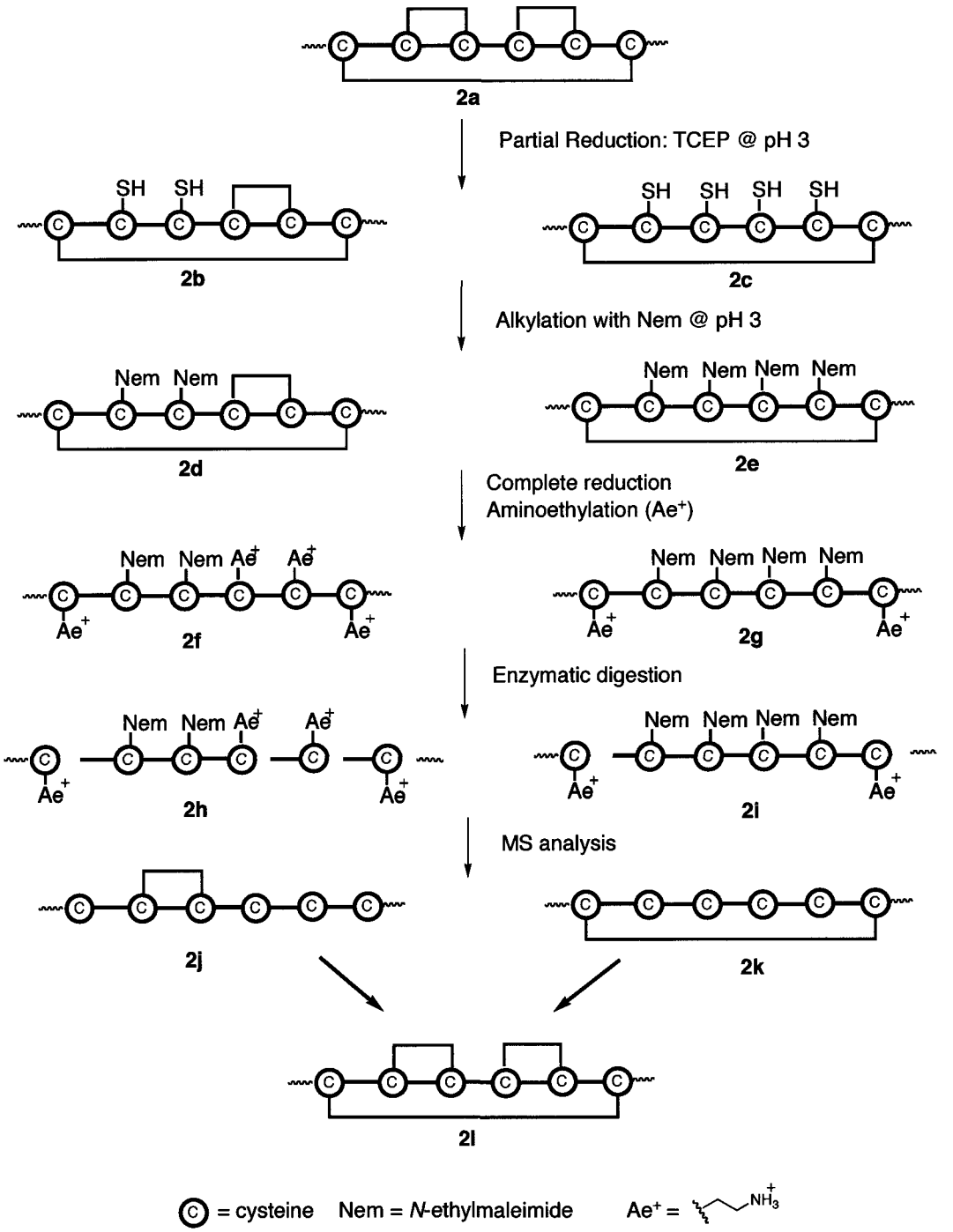

Although progress in analytical techniques has been made, in some cases the final structural proof is obtained only by chemical synthesis.[129]

### 3.1.3. Chemical synthesis of small and disulfide-rich peptides

A classic goal of chemical total synthesis is to confirm the proposed structure of a compound. In addition, chemical synthesis of naturally occurring peptides makes it possible to obtain practical amounts of material for clinical studies. It also provides access to peptide analogues with the aim of enhancing their stability and bioactivity, elucidating structure-activity relationships (SAR), or unravelling modes of action.

To date, many synthetic approaches to disulfide-rich peptides have been developed.[130, 131] The most favoured method involves construction of the linear peptide on a solid support followed by directed oxidative folding from a polythiol precursor in solution to yield the native isomer (Scheme 47). While this is the most simple and straightforward approach, it is limited to the synthesis of peptides where the native form of the peptide is thermodynamically favoured.

**Scheme 47.** General strategy for formation of multiple disulfides via directed oxidative folding

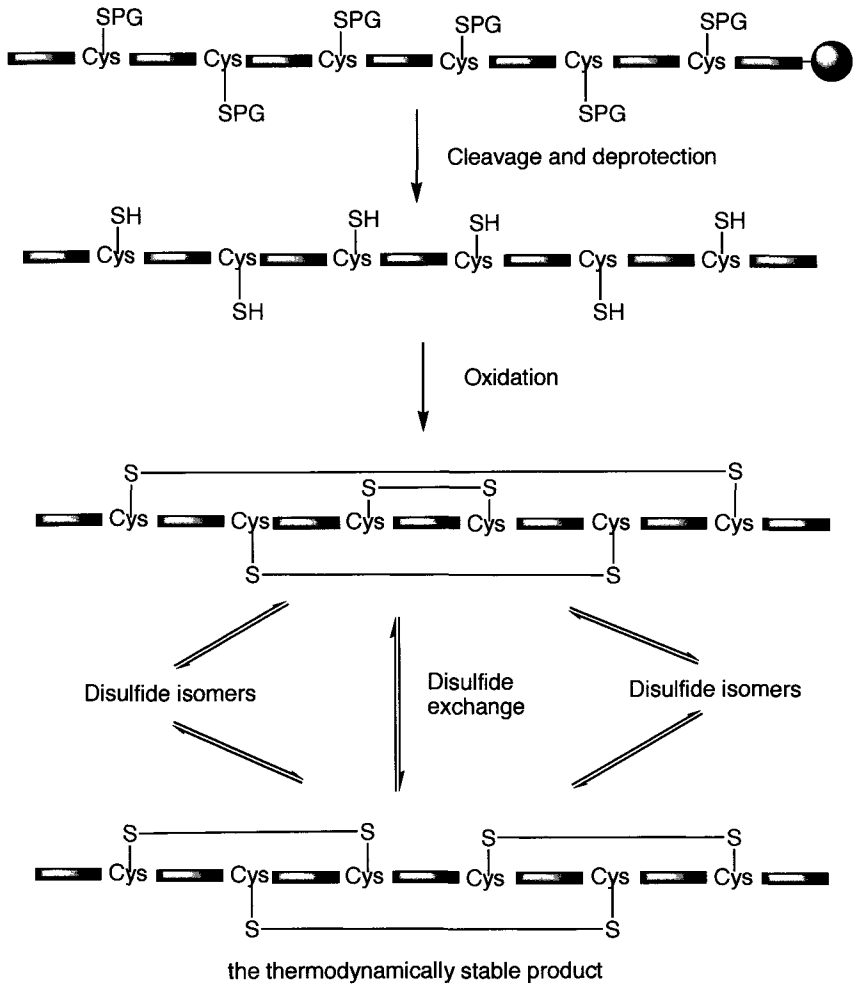


PG = protecting group

Alternatively, disulfide bonds can be introduced sequentially using orthogonal protections on cysteine residues (Scheme 48). This method is suited to the synthesis of peptides where the native isomer is not the most thermodynamically favoured. More importantly, controlled disulfide formation can provide information about disulfide connectivity in peptides not available by directed oxidative folding.

**Scheme 48.** General strategy for stepwise formation of multiple disulfides

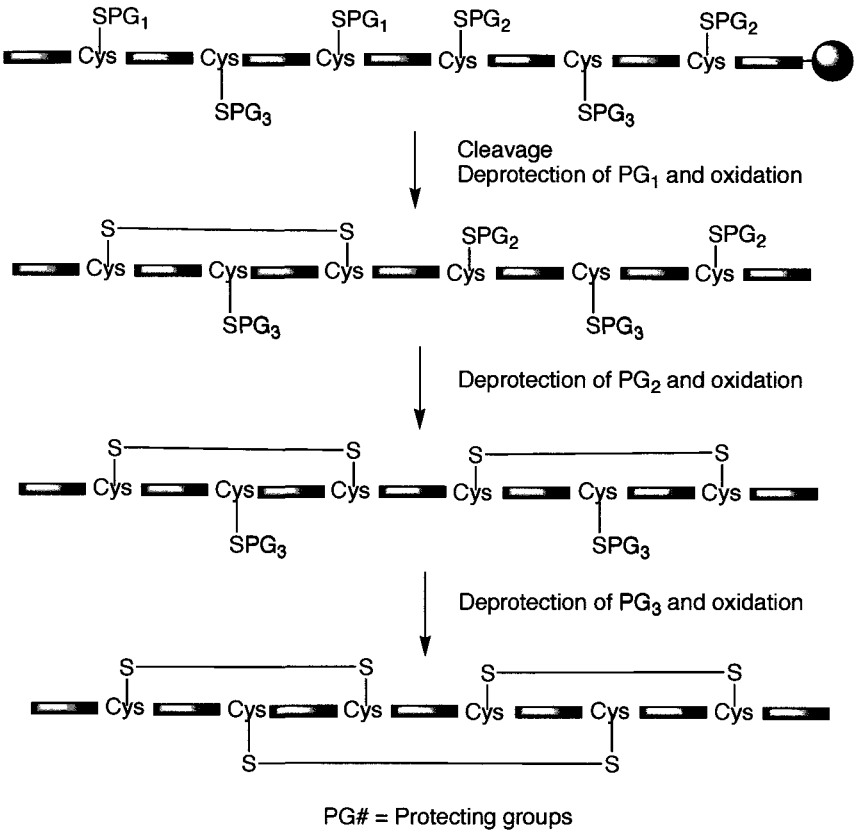


Multiple disulfides can also be introduced to a circular peptide precursor. This methodology has been demonstrated in the synthesis of circulins by Tam and co-workers (Scheme 49).[132] This synthesis features a thia-zip mechanism for backbone cyclization where the precursor with an electrophilic *C*-terminal thioester group and a nucleophilic *N*-terminal Cys residue undergoes cyclization through intramolecular transthioesterifications. The process is facilitated by the various cysteine side chains, which act as intermediate nucleophiles and zip the activated *C*-terminus along the peptide toward the *N*-terminus. Eventually, the largest thiolactone rearranges to the head to tail cyclic peptide via irreversible *S*, *N*-acyl migration at an *N*-terminal cysteine. Once cyclized, the reorganized

conformation facilitates the oxidation of the first two disulfide bonds to give the desired connectivity. The last disulfide is introduced by a selective deprotection and oxidation process.

**Scheme 49.** Synthesis of a complex cyclic peptide with cystine knot pattern

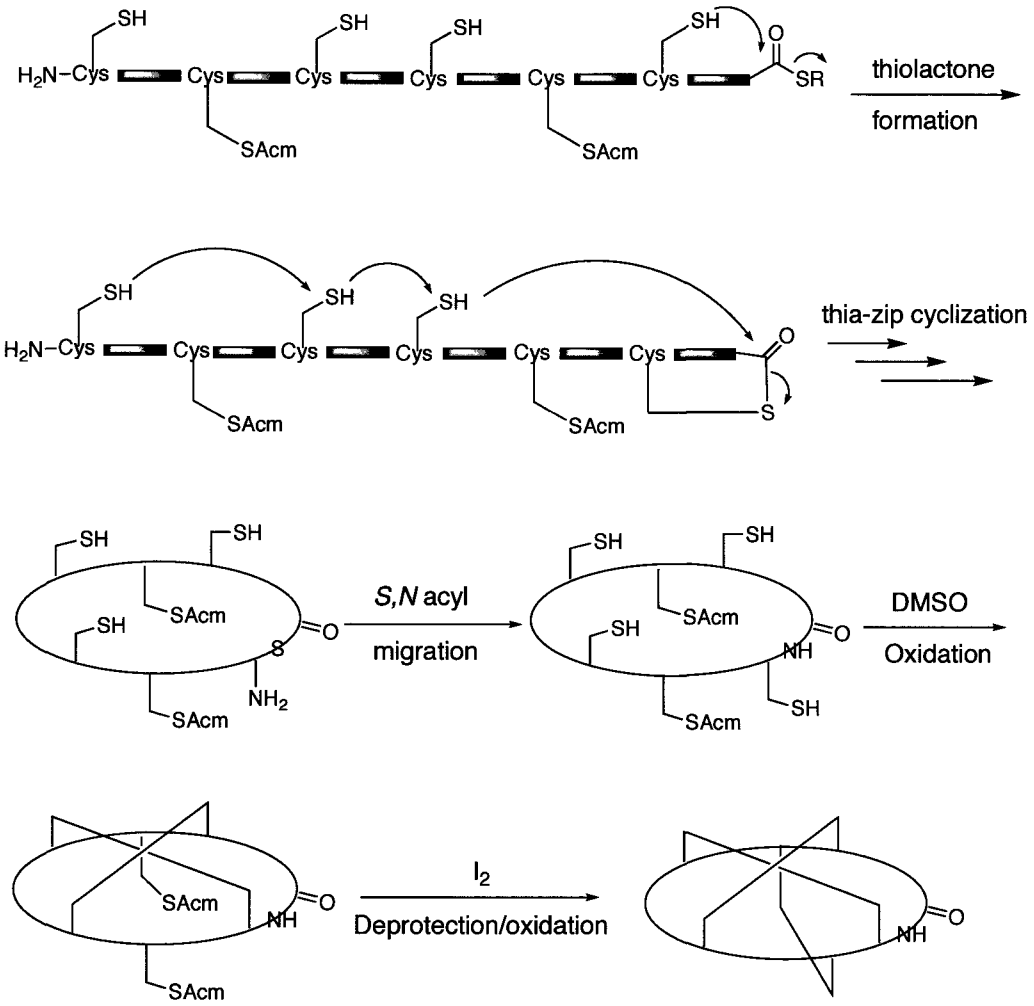

### 3.1.4. Peptide analogues that mimic disulfides

Various groups are investigating peptidomimetics in which the disulfide linkages have been modified. These analogues may overcome the inherent instability of disulfides in metabolically reducing environments and could provide important clues to the biological importance of the disulfide bridges.

Vederas and co-workers showed the disulfide bridge in oxytocin (**133**), a peptide hormone used to induce labour, can be replaced with an olefin moiety (Figure 32).[133] This analogue **134** exhibits increased stability and comparable biological activity. The synthesis utilizes the on-resin RCM strategy described in Chapter 2.

**Figure 32.** Structures of oxytocin (**133**) and its carbon analogue (**134**)

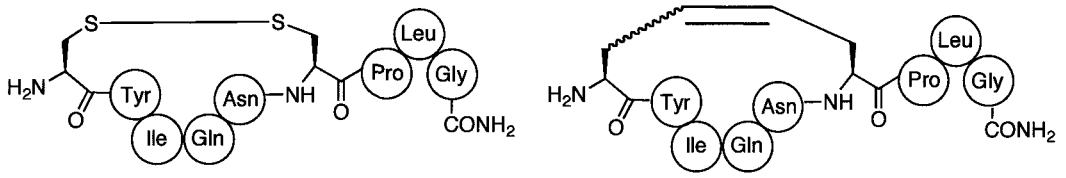


Oxytocin **133** Carba oxytocin **134**

Recently, Alewood and co-workers reported the synthesis of novel diselenide analogues of α-conotoxins in which one disulfide is replaced by a diselenide.[134] The structures of a diselenide analogue (**135**) and its parent peptide (**136**) are shown in Figure 33. These analogues generally have comparable (sometimes improved) activity compared to the corresponding native α-conotoxins. The interesting regioselective diselenide ring formation takes advantage of the different reactivity of selenocysteine and cysteine. Diselenide

formation from selenocysteines occurs more readily than the corresponding disulfide formation.

**Figure 33.** Structures of α-conotoxin MI (**136**) and its diselenide analogue (**135**)

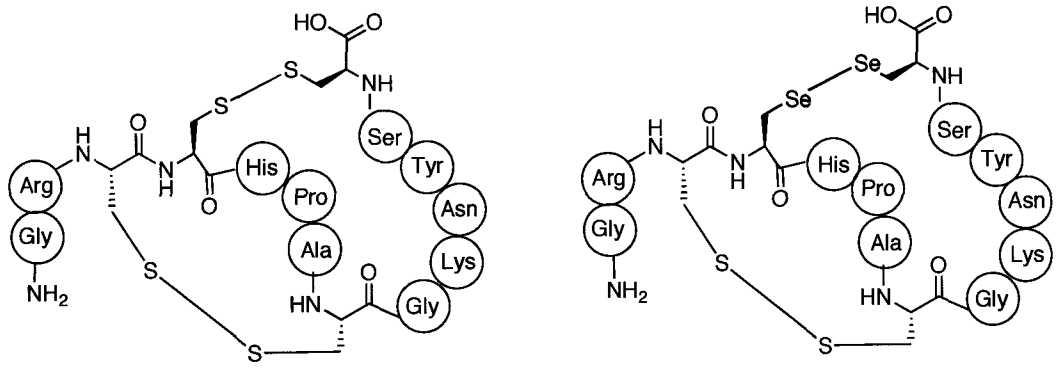


α–Conotoxin MI **136**

α-Conotoxin Sec [2, 4]-MI **135**

Interestingly, the disulfide bond even can be mimicked by noncovalent hydrophobic interactions. Vederas and co-workers have demonstrated this interesting concept in the synthesis of antimicrobial leucocin analogues (**137**) where one pair of cysteines is replaced by a pair of allyl glycine residues (Figure 34).[135, 136] Presumably due to the hydrophobic interaction of diallyl side chains that assist the formation of the bioactive conformation, the acyclic analogue displays activity as potent as the parent peptide (**138**).

**Figure 34.** Structures of leucocin A (**138**) and its acyclic analogue (**137**)

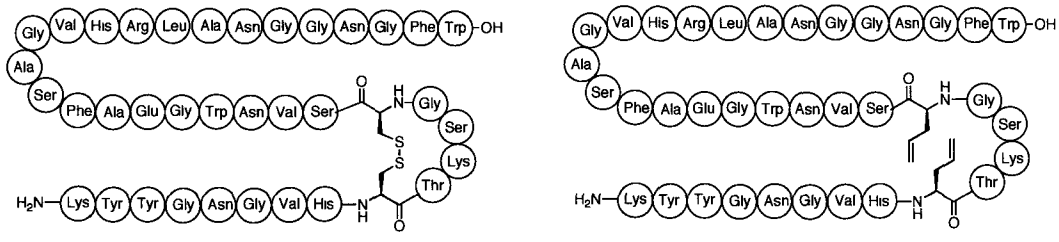


leucocin A **138**

9, 14 diallyl leucocin A **137**

## 3.1.5. Research goals

### 3.1.5.a. Total synthesis of naturally occurring neopetrosiamides

Given the promising and novel anticancer activity of neopetrosiamides, as well as their interesting structural features with complex disulfide connectivity, the first goal for this project is to chemically synthesize these naturally occurring peptides. The proposed structure of neopetrosiamides (Figure 28) was targeted for synthesis and comparison to the natural peptides that are isolated from marine sponges. This would also provide facile access to practical amounts of peptides for further studies.

### 3.1.5.b. Design and synthesis of analogues of neopetrosiamides

The development of a synthetic methodology for neopetrosiamides would also allow for access to various analogues for SAR and mode of action studies. To shed light on the biological importance of the methionine sulfoxide functional group, a variety of analogues could be synthesized in which the methionine sulfoxide at position 24 is replaced by other amino acids. These include either natural amino acids, such as methionine (**139**) and glutamine (**140**), or unnatural ones, such as norleucine (**141**) and *O*-methyl homoserine (**142**) (Figure 35). These compounds can then be tested for anticancer activity and compared to the parent peptides.

**Figure 35.** Possible substitutions for the methionine sulfoxide at position 24 of neopetrosiamides

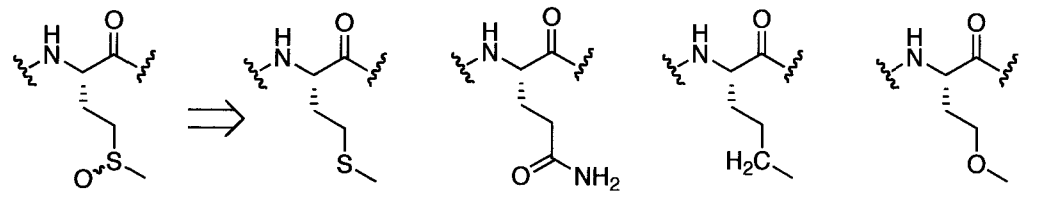


**139** **140** **141** **142**

In order to simplify the complex structure of neopetrosiamide and examine the concept that disulfides in this anticancer peptide can be replaced with hydrophobic or π-stacking interactions, three analogues **143**, **144** and **145** could be synthesized and tested, in which each pair of cysteine residues are individually replaced with one pair of phenylalanine residues. If those compounds are active, this will greatly simplify the chemical synthesis and make the large-scale production of the peptide through biological methods easier.

Given that the detailed mode of action for neopetrosiamides is still unclear, we also plan to embark on the synthesis of labeled neopetrosiamide analogues, which can be used to reveal how neopetrosiamides interact with a cancer cell. Neopetrosiamide analogues with a flexible linker attached would first be synthesized. If the modified peptide retained activity, the presence of a linker would allow neopetrosiamides to be attached to a variety of labelling molecules, such as fluorescent, biotin or photoactive affinity labels (Figure 36). In the case of a fluorescent tag, the target of neopetrosiamide in cancer cells could potentially be visualized using fluorescence microscopy. This study could aid understanding how the peptide acts on the cancer cell.

**Figure 36.** Schematic representation of chemical probe for mode of action study


## 3.2. Results & Discussion

### 3.2.1. Chemical synthesis of neopetrosiamides

#### 3.2.1.a. Synthesis of neopetrosiamides via directed oxidative folding

Our synthetic strategy involves the synthesis of the linear peptide precursor on solid support followed by introduction of multiple disulfide bonds and the methionine sulfoxide at position 24 in solution. The initial approach for multiple disulfide bond formation employs the common practice of using global deprotection of many cysteine residues followed by formation of multiple disulfides through directed oxidative folding (Scheme 50). The 2-chlorotrityl chloride resin with preloaded cysteine (**146**) is used in conjunction with standard Fmoc methodology for the coupling of amino acid residues. The reason for using the bulky trityl resin is to suppress unwanted side reactions associated with the *C*-terminal cysteine residue.[107] The 28 amino acids are assembled on solid support using a peptide synthesizer to give resin-bound linear peptide **147**. The acid labile trityl protecting groups are used for the six thiols of cysteine residues. Global deprotection is effected by TFA/TIPS/$H_2O$ (95:2.5:2.5) to yield the linear hexathiol precursor **148**.

**Scheme 50.** Synthesis of neopetrosiamide (**130**) via directed oxidative folding

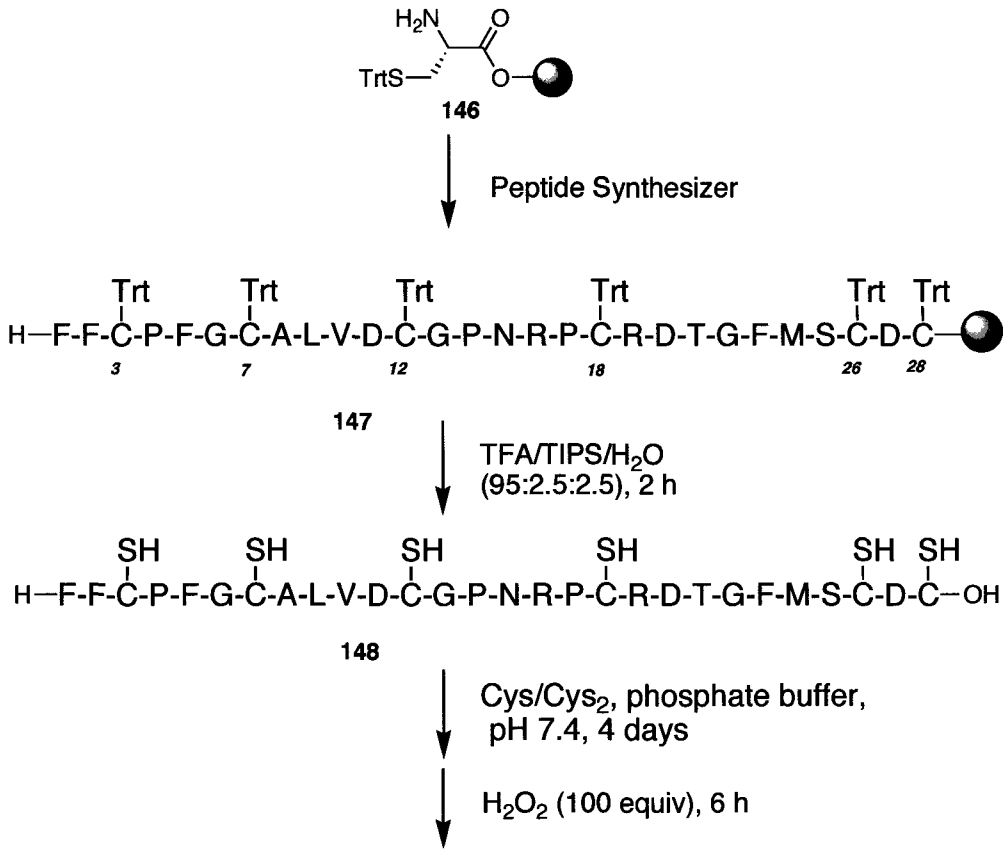


The treatment of the linear peptide **148** with a cysteine/cystine ($Cys/Cys_2$) redox system was attempted to afford the cyclic peptide with desired disulfide connectivity.[137] However, the formation of the desired native isomer is accompanied with the production of significant amounts of several other non-native isomers as shown by HPLC analysis (Figure 37). The subsequent oxidation of methionine sulfoxide with hydrogen peroxide only gives the native isomer as a minor product based on the comparison to natural peptides using HPLC. These results indicate that the native isomer is not the most thermodynamically stable product, which makes the directed oxidative folding synthesis impractical.

**Figure 37.** Semi-preparative RP-HPLC traces of the directed oxidative folding products (using HPLC purification method B listed in Chapter 5)

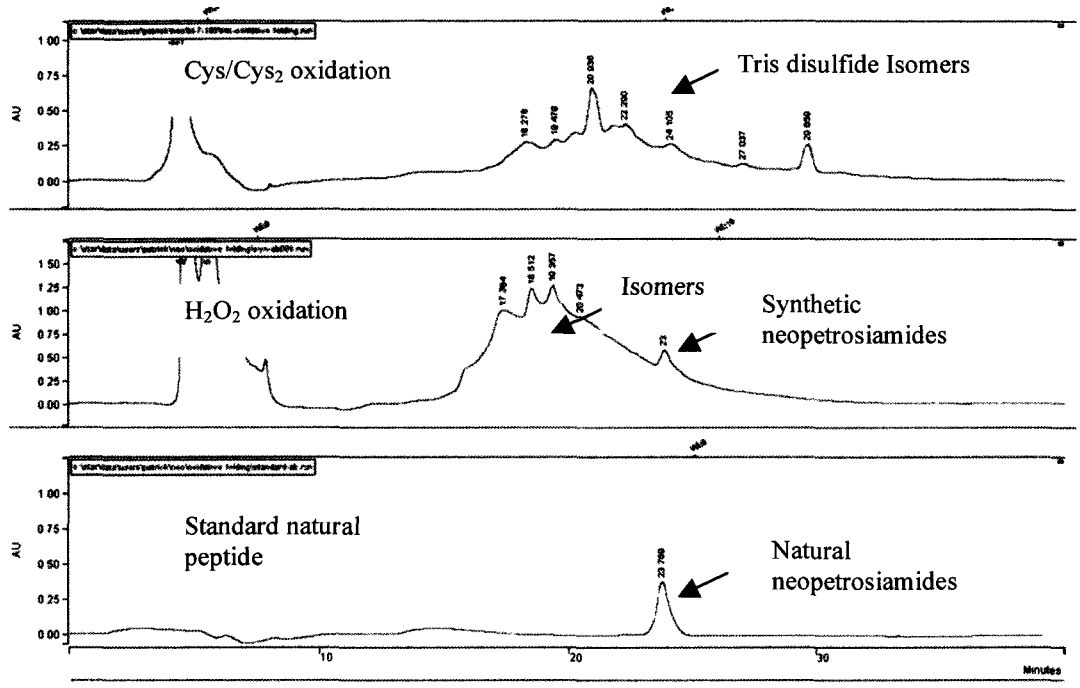


### 3.2.1.b. Synthesis of neopetrosiamide via stepwise disulfide formation

Following unsuccessful attempts to utilize oxidative folding for the synthesis of neopetrosiamide, focus shifted to a stepwise disulfide formation strategy. Such synthesis requires judicious choices of orthogonal protecting groups for cysteines and deprotection/oxidation conditions.

The initial studies using this strategy were investigated by Dr. Marc Boudreau. For clarity and completeness, the synthesis is briefly described (Scheme 51). The linear peptide (**149**) with three pairs of orthogonal protecting groups on six cysteine residues (Cys 3, 26 *t*-Bu, Cys 7, 12 Mmt and Cys 18, 28 Trt) was prepared on a peptide synthesizer using standard Fmoc chemistry.[138] Upon treatment with 1% TFA in DCM, the peptide (**150**) is cleaved from the 2-

chlorotrityl chloride resin with concomitant removal of the Mmt protecting groups whereas the remaining side chain protecting groups are left intact. The crude protected linear peptide is subjected to oxidation using DMSO in the presence of TFA to form the first disulfide (**151**) between Cys7 and Cys12. However, the reaction is very sluggish and requires 16 h and elevated temperature to reach completion. Although the disulfide bond is formed, the harsh reaction conditions appear to cause the instability of the trityl protecting groups on another pair of cysteines. This leads to the second disulfide formation (Cys 18-28) and even disulfide exchange, as suggested by mass spectrometry and HPLC analysis. Therefore, a milder reaction is required for the selective formation of the first disulfide bond.

**Scheme 51.** The attempted synthesis of neopetrosiamide (**130**) via stepwise disulfide formation

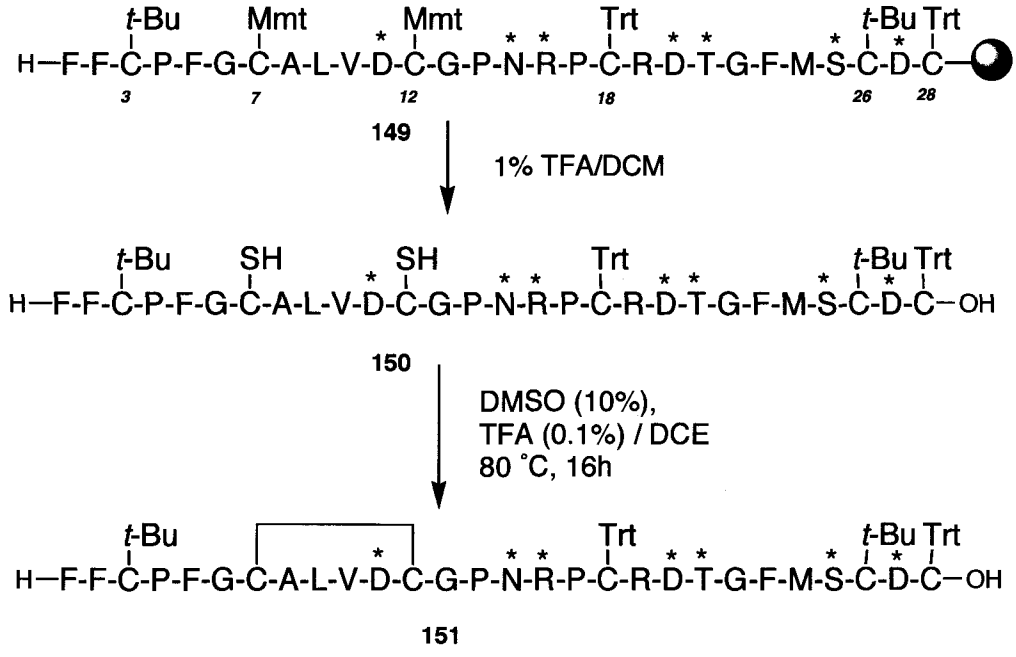


* = acid labile side chain protecting groups

Based on these initial studies, exploration of selective disulfide formation under milder conditions was continued. Oxidation of the protected linear peptide **150** was attempted using a variety of mild conditions, such as air oxidation, a polymer-supported oxidant (Clear-OX$^{TM}$)[139] and $CCl_4$/TBAF.[140] Unfortunately, all these conditions only afford the recovered starting material without any observable disulfide formation. Possibly, the presence of remaining side chain protecting groups, such as Asp(*t*-Bu), Asn(Trt), Arg(Pmc), Thr(*t*-Bu) and Ser(*t*-Bu), disrupt the proper folding conformation of the peptide and make the disulfide formation more difficult.

An alternative synthesis was then attempted using a peptide precursor with orthogonal protecting groups on cysteines and minimal protection for other side chains. Inspired by the synthesis of human β-defensins by Schulz[120], three pairs of orthogonal protecting groups (Trt, Acm and *t*-Bu) were chosen for cysteine protection. The resin-bound linear peptide (**152**) with orthogonal protecting groups on cysteine (Cys 3, 26-*t*-Bu, Cys 7, 12-Trt and Cys 18, 28-Acm) was prepared using a peptide synthesizer (Scheme 52). Cleavage of peptide from the resin with concomitant side chain deprotections is effected using TFA/Thioanisole/EDT/Anisole (90:5:2.5:2.5) to give the linear peptide (**153**) with *t*-Bu and Acm protecting groups intact. Interestingly, the first two disulfides can be formed sequentially in a one-pot two-step oxidation process to give peptide **154**. In analogy to a literature procedure[141], the treatment of the crude linear peptide with iodine in acetic acid affords the first disulfide (Cys 7-12) regioselectively. Upon adding water to the reaction mixture, the deprotection of

the Acm protecting group is accelerated dramatically with the half-life shortened to 50-60 s, thereby leading to the formation of the second disulfide. The high regioselectivity is presumably due to the significantly different reactivity of *S*-Acm and free thiols towards iodine in different solvents. The oxidation of free thiols by iodine proceeds rapidly in a variety of solvents. However, deprotection and oxidation of *S*-Acm by iodine in acetic acid is extremely slow with a half life of about 45 min.[142] Therefore, this reactivity difference allows for the selective formation of disulfides from free thiols in the presence of the *S*-Acm groups.

**Scheme 52.** One step formation of bis-disulfide of neopetrosiamide

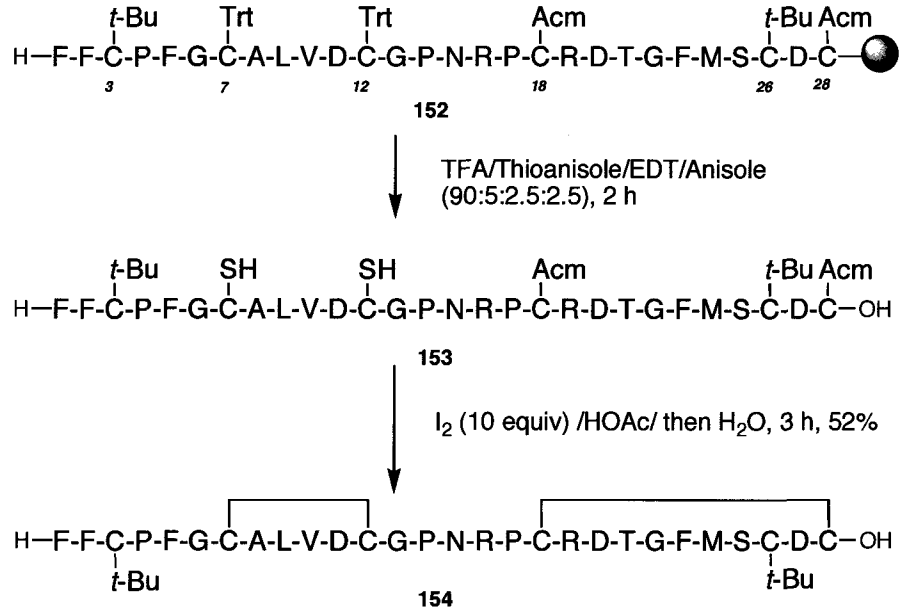


More importantly, the progress of the first disulfide formation and the *S*-Acm deprotection/oxidation can be easily monitored by mass spectrometry. The crude peptide was purified by RP-HPLC to give **154** with the expected mass of 3169.3 (M+H). At this point, the disulfide connectivity of **154** was verified by MS/MS sequencing. To further rule out the possibility that the desired bis-

disulfide formation was due to random disulfide exchanges that generate the most thermodynamically stable isomer, two other possible disulfide isomers (**155**, **156**) were synthesized using the same method by reshuffling Trt and Acm protecting groups on cysteines. These purified peptides (**154**, **155** and **156**) show different retention times by analytical HPLC (Figure 38). The co-injection of three isomers led to a triple peak in HPLC, suggesting that the desired disulfide connectivity is governed by the position of the protecting group pairs instead of the thermodynamic stability of the native isomer. This verification study also highlights the generality and reliability of this methodology for regioselective disulfide formation.

**Figure 38.** Structures of bis-disulfide isomers and analytical HPLC comparison (using HPLC method C listed in Chapter 5)

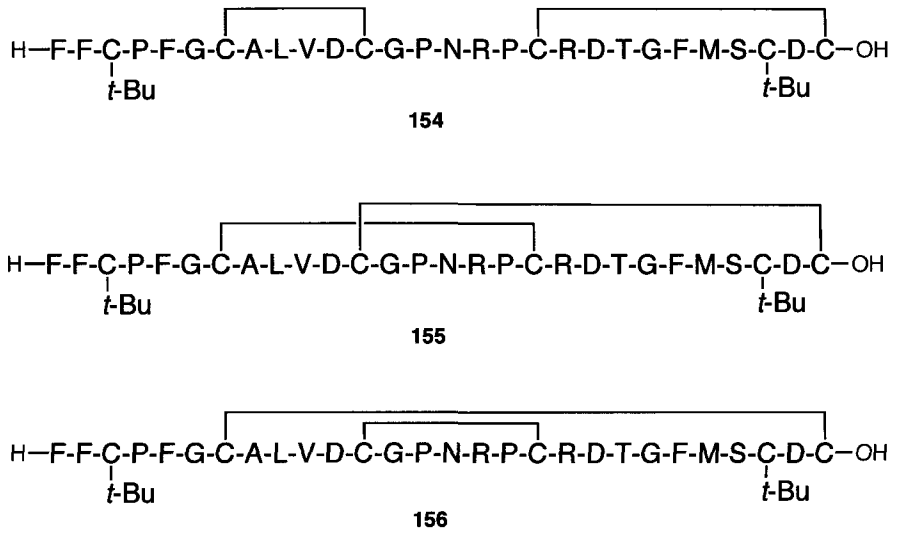


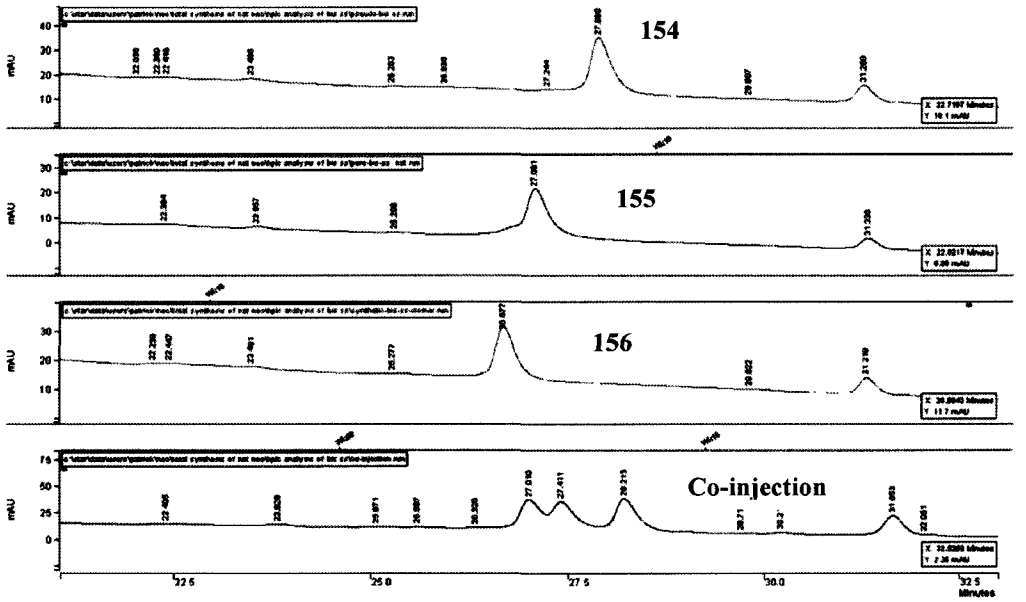


With the desired bis-disulfide intermediate in hand, efforts focused on the synthesis of the third disulfide and formation of the methionine sulfoxide. Deprotection of *t*-Bu protecting groups followed by disulfide formation can be

achieved using $PhS(O)Ph/CH_3SiCl_3$ as reported by Akaji and co-workers (Scheme 53).[143]

**Scheme 53.** Synthesis of third pair of disulfide via $PhS(O)Ph/CH_3SiCl_3$

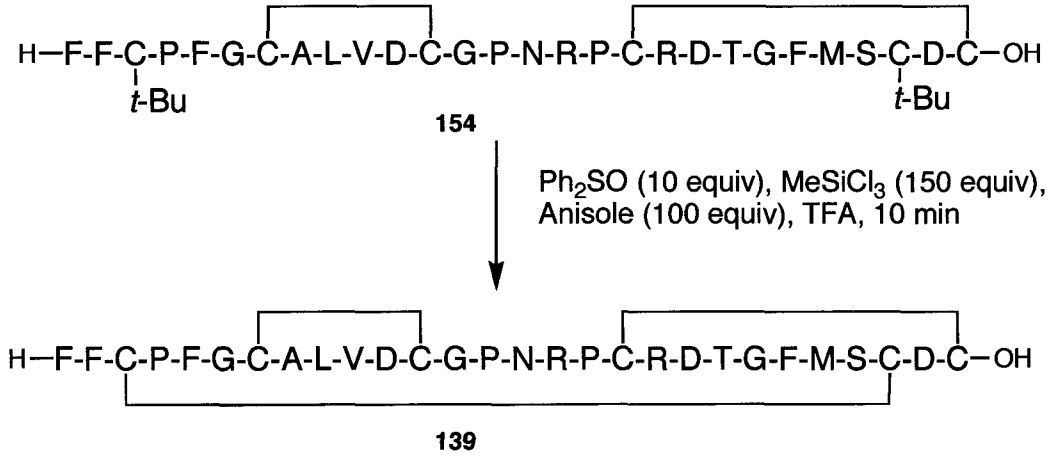


Although formation of the third disulfide is completed in 10 min as suggested by MALDI-TOF MS, extensive disulfide exchange was observed. HPLC analysis of reaction mixture shows the presence of multiple peaks with the same mass corresponding to the tris-disulfide peptide. Similar disulfide scrambling using the $PhS(O)Ph/CH_3SiCl_3$ system has also been seen by Meto and co-workers in the synthesis of α-conotoxin GI.[144] It is believed that disulfide exchange reactions normally happen under basic conditions due to the presence of thiolate.[145] Therefore, the disulfide scrambling under acidic conditions is likely related to the high reactivity of the silyl chloride-sulfoxide system towards disulfide formation.[146] This reaction system may activate the existing disulfides and then trigger the subsequent disulfide scrambling. The possible disulfide exchange mechanism is proposed in Figure 39. In addition, the oxidation of the methionine residue to methionine sulfoxide was also observed based on mass

spectrometry. This side reaction may also result from the high reactivity of the oxidizing reagents.

**Figure 39.** Proposed mechanism for disulfide exchange in $PhS(O)Ph/CH_3SiCl_3$

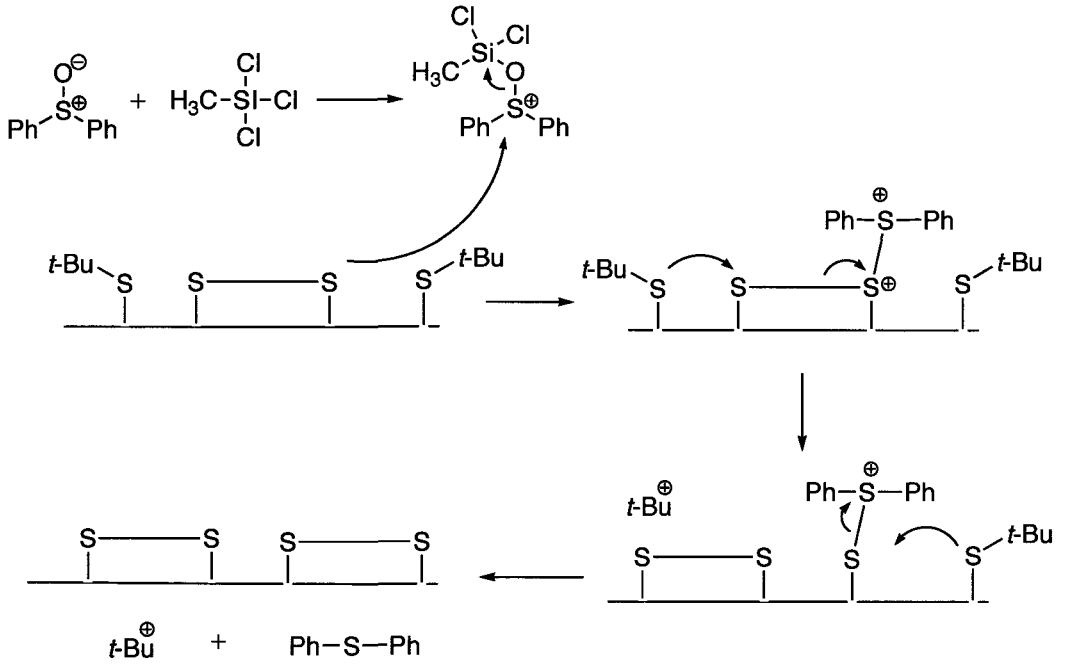


At this point, in order to optimize the reaction conditions for the third disulfide formation, efforts focused on the synthesis of a norleucine analogue **141** wherein the methionine sulfoxide at position 24 is replaced by a norleucine residue (Scheme 54). Such replacement would avoid problems associated with methionine oxidation and simplify the reaction system for the optimization of the disulfide formation. In addition, this analogue can be used to elucidate the biological function of the unusual methionine sulfoxide functionality in neopetrosiamides. The resin-bound linear peptide **157** was assembled using a synthesizer followed by acid cleavage to give peptide **158**. The bis-disulfide norleucine analogue **159** was prepared using the one step procedure described

above. Using **159** as a model system, a variety of reaction conditions for disulide formation were screened with respect to temperature, reagent equivalent, reaction time and the sequence of reagent addition. Unfortunately, all the attempts led to either no reaction or significant disulfide scrambling. As the oxidation with $PhS(O)Ph/CH_3SiCl_3$ was unsuccessful, attention shifted to other synthetic methods to form the third disulfide. Fortunately, oxidation with DMSO/Anisole/TFA gives a much better result with no significant disulfide scrambling even with a prolonged reaction time (5 h).[120] The synthesis of the norleucine analogue **141** was completed in this fashion.

**Scheme 54.** Synthesis of a norleucine analogue (**141**) via stepwise disulfide formation

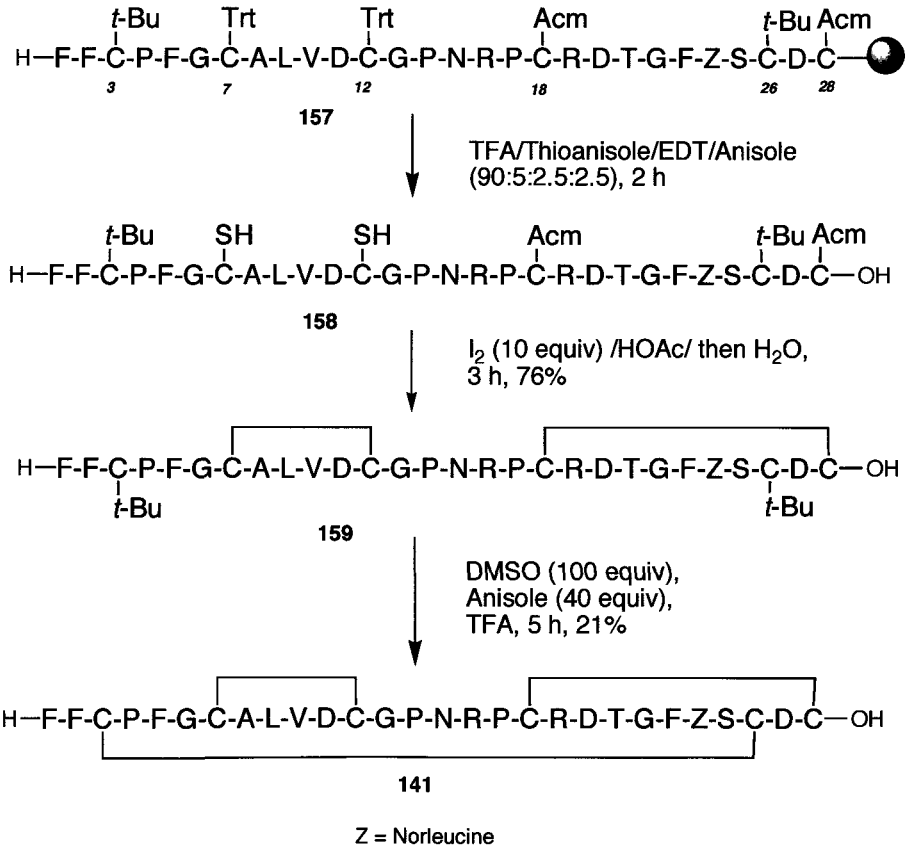

Utilizing the optimized conditions, the third disulfide of neopetrosiamide is readily constructed. No methionine sulfoxide formation is observed during oxidation, which allows access to another analogue **139** for SAR study. Oxidation of the methionine residue with hydrogen peroxide proceeds smoothly to afford neopetrosiamide **130** with the expected mass of 3071.3 (M+H) (Scheme 55).[147]

**Scheme 55.** Synthesis of neopetrosiamides with the originally proposed structure

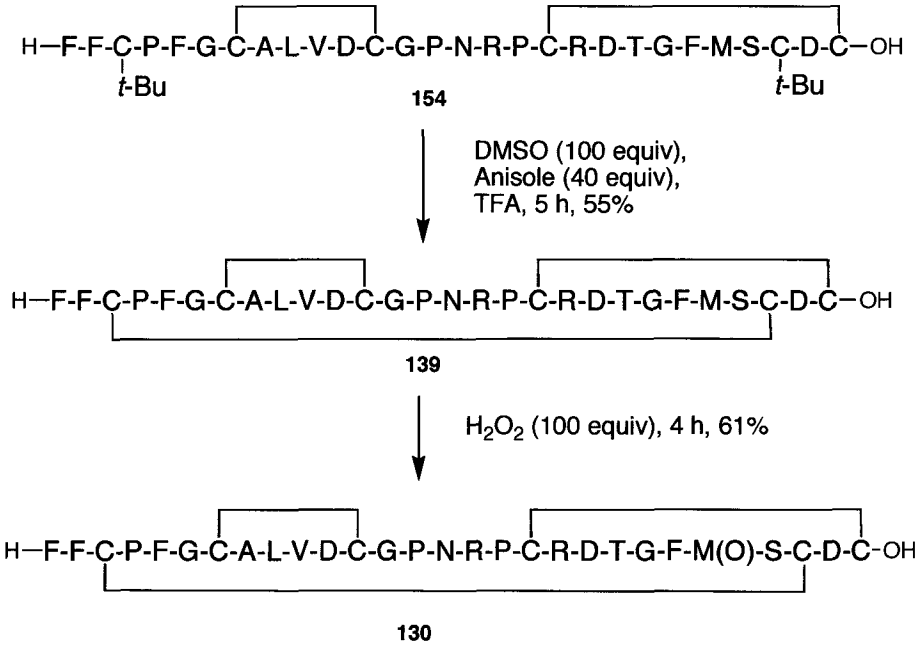


To confirm the identity of the synthetic neopetrosiamide **130**, extensive HPLC comparisons were done using the natural product as a standard (Figure 40). Surprisingly, the synthetic compound shows different retention times in analytical HPLC using a variety of conditions, demonstrating that the synthetic peptide **130** and the natural product are different. This result led us to question the proposed structure of neopetrosiamide, particularly the assignment of the disulfide connectivity. In the original structure elucidation, the assignment of the disulfide

connectivity was based on 2D NOESY experiments, which may be misleading when the non-bonded cysteine pairs are in close proximity to each other.

**Figure 40.** The RP-HPLC comparison of the synthetic neopetrosiamide (**130**) and the natural peptide from marine sponge (using HPLC method E listed in Chapter 5)

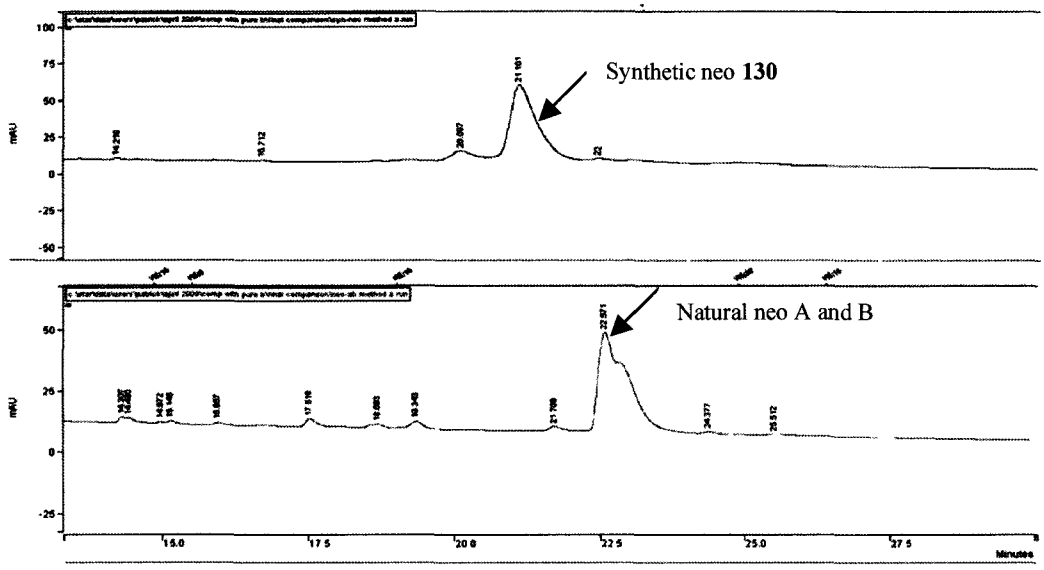


### 3.2.1.c. Characterization of disulfide connectivity in neopetrosiamides

MS-based disulfide mapping experiments were undertaken to provide disulfide connectivity information. With synthetic peptide **130** and norleucine analogue **141** available, initial investigation focused on these compounds. In analogy to the procedure reported by Craik,[128] the disulfide partial reduction and selective alkylation method was utilized to characterize the disulfide connectivity (Scheme 56). Briefly, the folded peptide (**130a**) was reduced with TCEP under acidic conditions to generate the partially reduced disulfide species (**130b**, **130c**).

Notably, the reaction conditions were optimized with respect to incubation time and temperature to give the highest ratio of partially reduced disulfide species relative to fully reduced peptide. These intermediates were separated by analytical RP-HPLC, manually collected and analyzed by MALDI-TOF MS. Interestingly, the reduced peptide(s) elutes before the native peptide on RP-HPLC. This behavior is likely due to the presence of multiple disulfides forces the hydrophobic residues to be surface-exposed and the reduction of disulfides releases this conformational constraint, leading to the burial of these exposed hydrophobic amino acids.

The alkylation of partially reduced intermediates was achieved via the Michael addition of free thiols onto *N*-ethylmaleimide (Nem) under acidic conditions that suppress disulfide exchange. After purification by RP-HPLC, the alkylated species (**130d, 130e**) are subjected to complete reduction using TCEP in citric acid buffer (pH = 3). The second alkylation is done using *N*-methylmaleimide (Nmm) as an alkylator in the same manner as the Nem alkylation to give **130f** and **130g**. To the best of our knowledge, this is the first example using Nmm as the second alkylator among the MS-based disulfide mapping methods.[123, 126, 128] This second alkylation under acidic conditions offers several advantages over the alkylation under basic conditions, which include suppressing potential reshuffling of alkylators between the labeled and non-labeled cysteines and preventing the possible ring opening of maleimide tags via hydrolysis under basic conditions.

The linear peptides with labeled cysteines were subjected to MS/MS sequencing that can identify the position of the cysteine labels and the connectivities of each disulfide in **130h** and **130i**. Once the individual disulfides are revealed, the overall disulfide bond connectivity as shown in **130j** can be deduced by piecing all the information together.

**Scheme 56.** Schematic representation of the MS-based disulfide mapping method

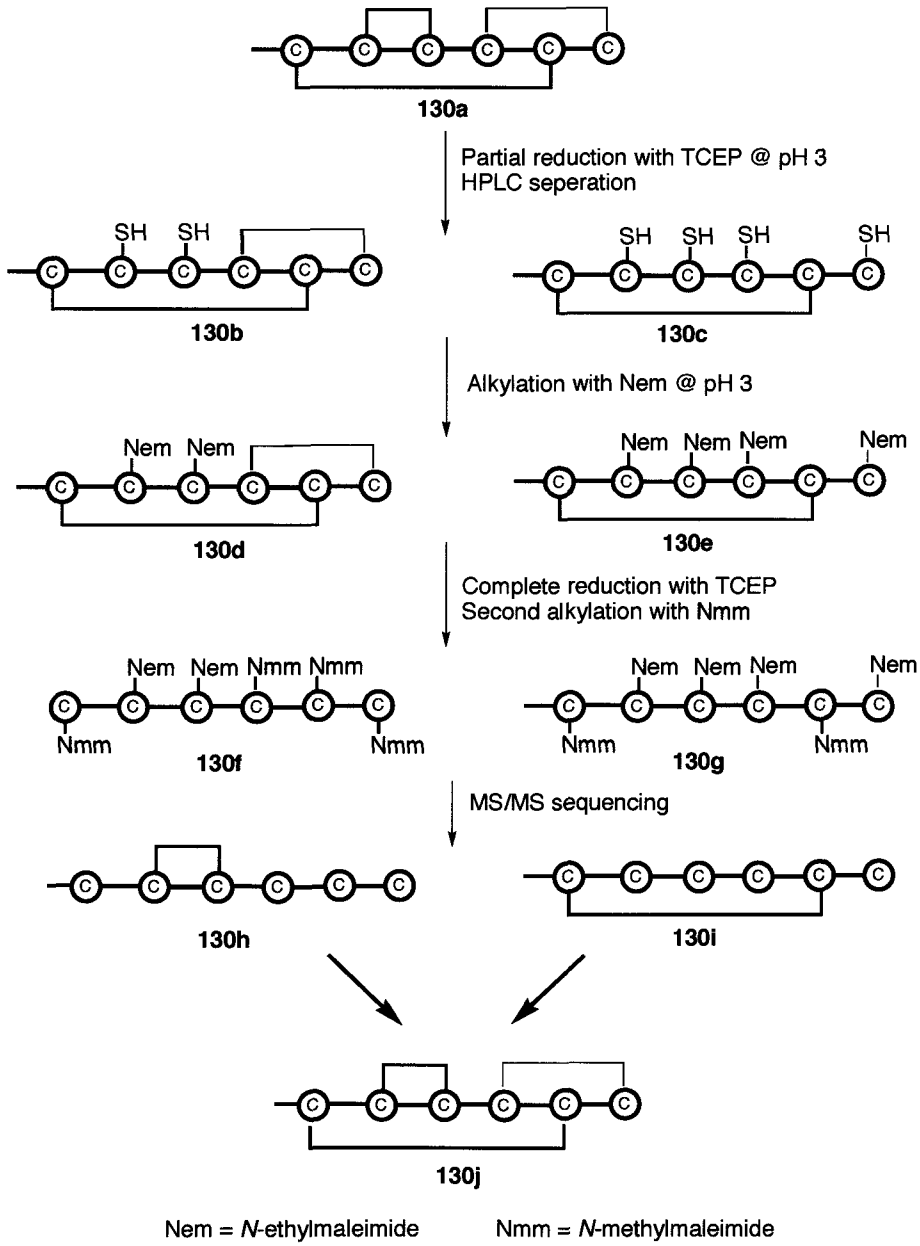

Notably, the second alkylation is often necessary for the linear peptide MS/MS sequencing, as the free thiols tend to be reoxidized to disulfides and this complicates data analysis. In the case of the norleucine analogue (**141**), only one species (**160**) underwent fragmentation in MS/MS sequencing without the second alkylation, but most partially reduced species originated from **141** fail to do so. The MS/MS sequencing of **160** confirmed the identity of one disulfide (Cys 7-12) in **161**, Therefore, the species (**162**) with the second alkylation was generated to obtain the connectivity of another disulfide (Cys 18-28) in **163**. Based on the information of the individual disulfides in **161** and **163**, the overall disulfide connectivity of **141** was deduced (Figure 41).

**Figure 41.** Disulfide mapping result for norleucine analogue **141**

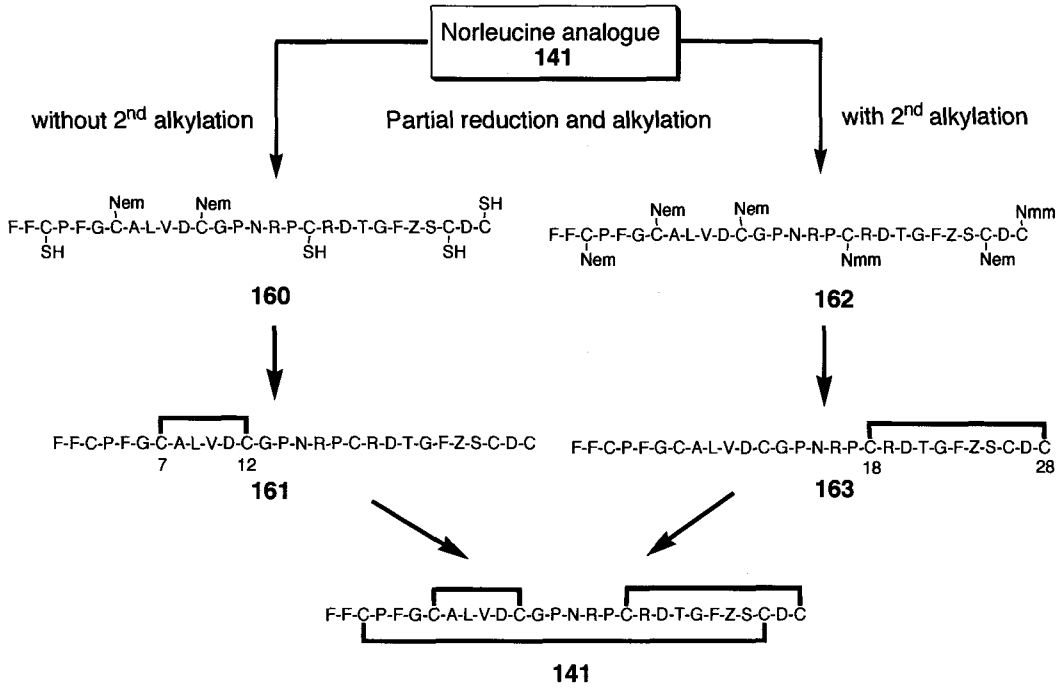

For the synthetic neopetrosiamide **130**, it is necessary to digest the labeled linear peptide into small pieces for further analysis due to the difficulties associated with MS/MS fragmentation of longer peptides. The labeled long peptides **164** and **165** were treated with trypsin that selectively cleaves peptides at arginine to yield two small fragments (Figure 42). MS/MS sequencing of these fragments reveals the individual disulfide connections as Cys 18-28 in **166** and Cys 7-12 in **167**. Thus, the overall disulfide connectivity in **130** is characterized. The disulfide mapping results of both the synthetic neopetrosiamide **130** and norleucine analogue **141** are in agreement with the originally proposed disulfide connectivity[115], which underlines the reliability of our methodology for stepwise disulfide formation. However, this synthetic compound does not match the natural product by HPLC analysis.

**Figure 42.** Disulfide mapping result for synthetic neopetrosiamide **130**

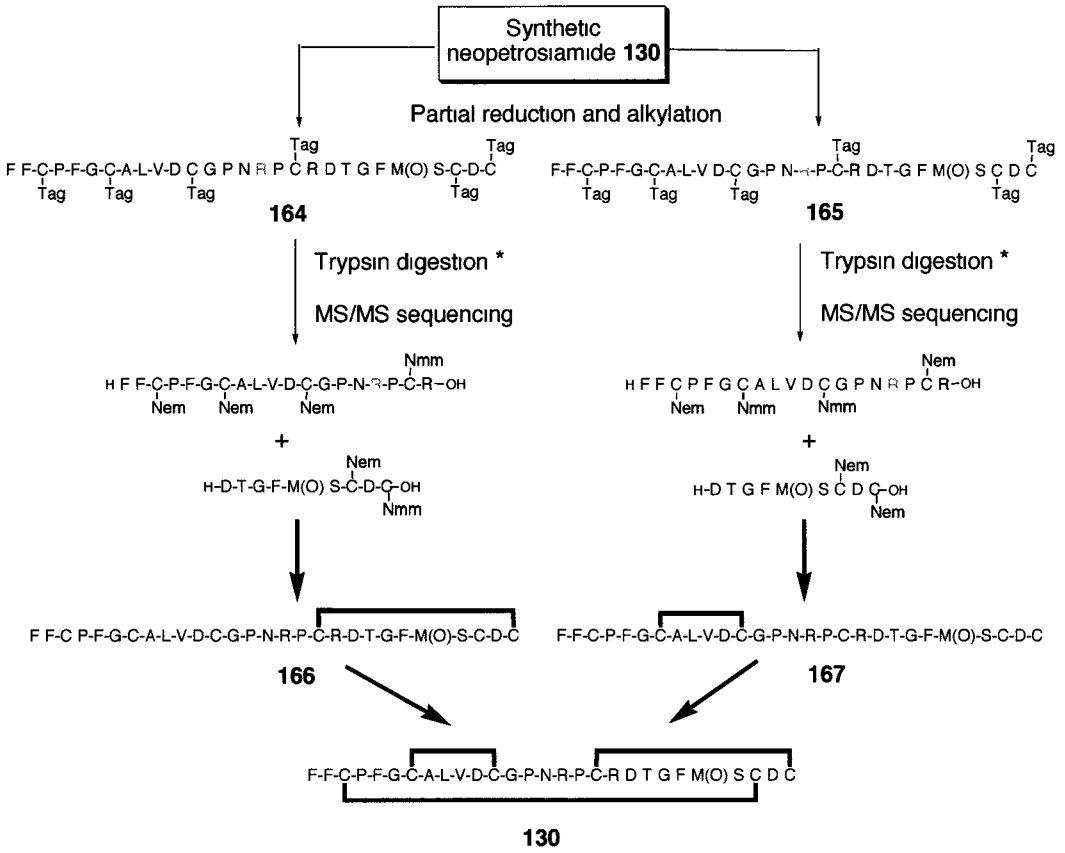


* *The trypsin digestion only cleaves the peptide at the arginine residue highlighted in red The arginine in green is resistant to proteolysis due to the presence of the adjacent proline*

Efforts refocused on the characterization of the natural peptide using this disulfide mapping methodology. Surprisingly, the partial reduction of folded natural peptide with TCEP behaves quite differently compared to the synthetic peptides. Under previously optimized condition, the reduction only generates the fully reduced peptide and the native peptide without any detectable partially reduced species. To obtain a significant quantity of partially reduced natural peptide, the reduction was optimized with respect to the amount of TCEP, reaction temperature and time. A lower concentration of TCEP (25 equiv) and

lower reaction temperature (4 °C) slow down the reduction and suppress the generation of fully reduced species. A longer reaction time (4 h) helps the accumulation of partially reduced species. However, only one partially reduced peptide was obtained even under the optimized conditions, which limits the deduction of overall disulfide connectivity. Nevertheless, the intermediate was subjected to alkylation with Nem followed by complete reduction and the second alkylation with Nmm to give the labeled linear peptide **168**. MS/MS sequencing unambigiously reveals the disulfide (Cys 12-28) in **169** (Figure 43).

**Figure 43.** Disulfide mapping of natural neopetrosiamide using the partial reduction and alkylation method.

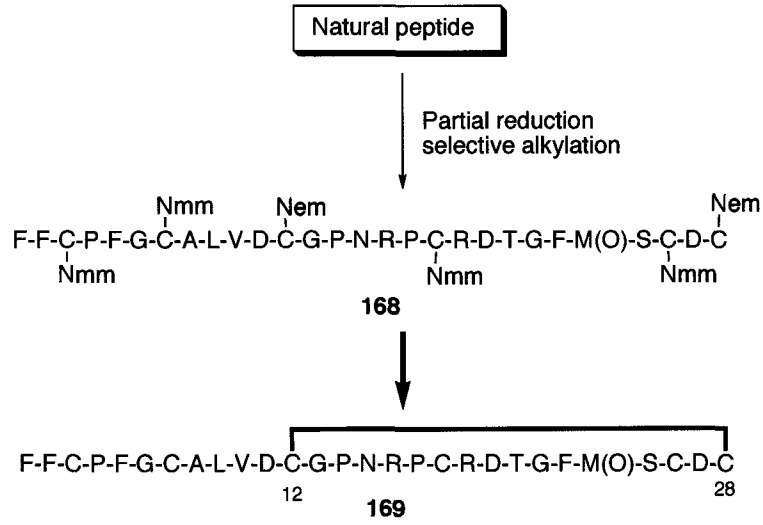


Given the limited partial reduction of the natural peptide, a classic enzymatic digestion strategy was investigated. The natural peptide was treated with endoprotease Asp-*N*, which selectively cleaves a peptide from the *N*-terminus of an aspartic acid. After incubation at 37 °C for 22 h, MALDI-TOF MS analysis of the reaction mixture displays a new peak 54 Da higher than the native peptide, which corresponds to the natural peptide plus an additional three water

molecules. Given that three aspartic acid residues are present in linear neopetrosiamide, the new peak is in agreement with the completely enzymatically cleaved peptide **170**. Although this result rules out the possibility of some disulfide isomers, the disulfide connectivity cannot be fully confirmed by this experiment. Fortunately, the MS/MS sequencing of the enzymatic digestion species **170** strongly supports the presence of a disulfide (Cys 3-26) in **171** as suggested by the y ion series (Figure 44).

**Figure 44.** Disulfide mapping of natural neopetrosiamide using enzymatic cleavage and MS/MS sequencing [a]

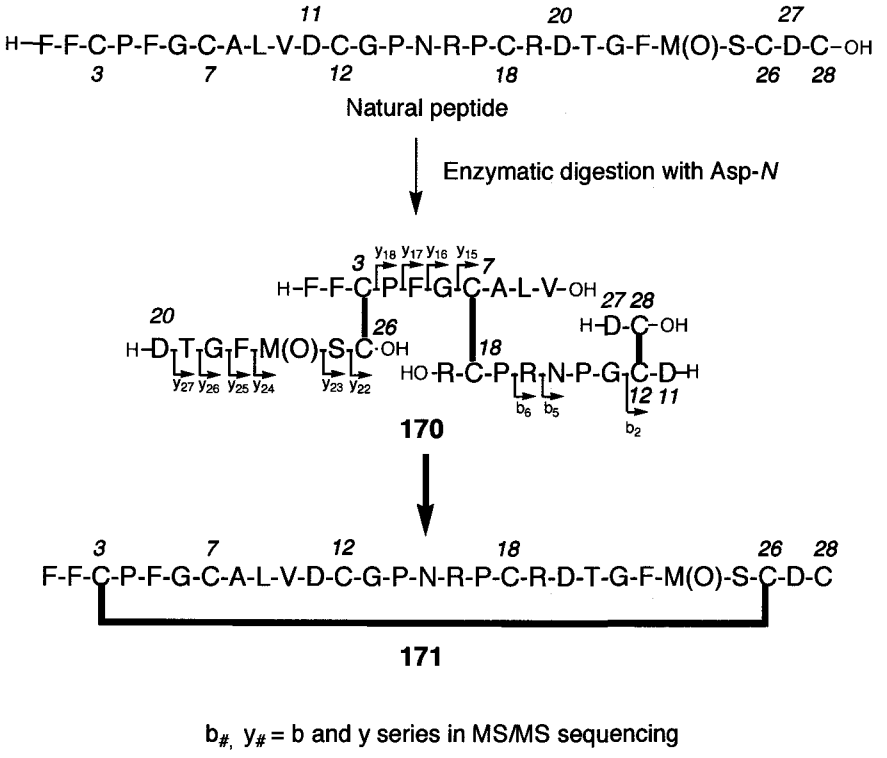


[a] *The disulfides Cys 12-28 and Cys 7-18 highlighted in thick black bonds are also suggested by b ion series in MS/MS sequencing.*

In combination with the disulfide (Cys 12-28) established using the partial reduction method, the results from the enzymatic digestion followed by MS/MS sequencing reveals the overall disulfide connectivity of natural neopetrosiamide (**172**) as shown in Figure 45. The newly proposed disulfide connectivity of the neopetrosiamides is different from that originally proposed in structure **130**.

**Figure 45.** Newly proposed disulfide connectivity of natural neopetrosiamide and its originally proposed structure

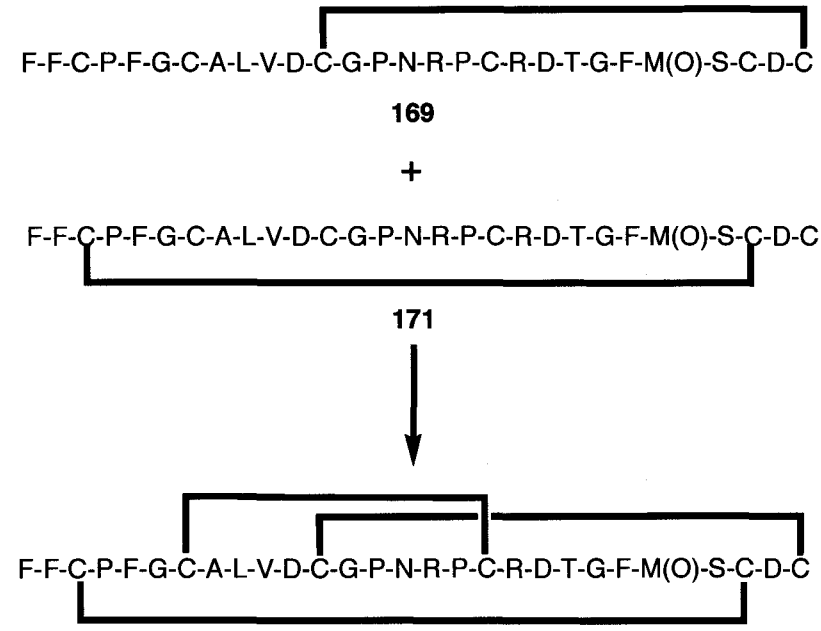


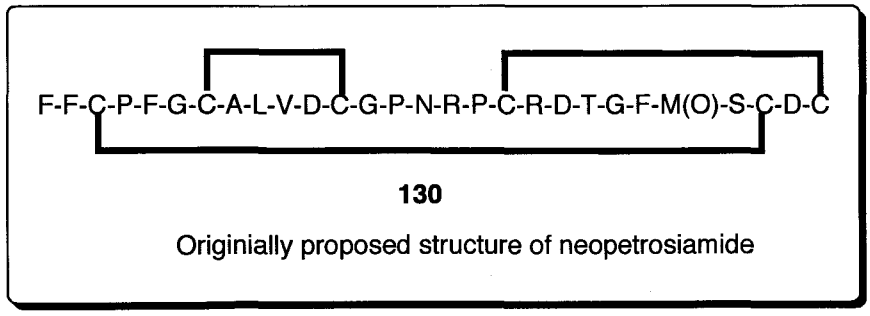

### 3.2.1.d. Synthesis of neopetrosiamide with revised disulfide connectivity.

Utilizing our stepwise disulfide formation methodology, the chemical synthesis of neopetrosiamide (**172**) with the newly proposed disulfide connectivity was undertaken. The resin-bound peptide **173** was assembled on a peptide synthesizer with reshuffled protecting groups on the cysteine residues (Cys 3, 26-*t*-Bu, Cys 7, 18-Trt and Cys 12, 28-Acm). Acidic cleavage with concomitant side chain deprotection gave linear peptide **174** (Scheme 57). Stepwise disulfide formation was performed as described above. The first two disulfides were sequentially introduced by iodine oxidation to afford **155**. The third was constructed by DMSO oxidation to yield **175**. Subsequent methionine oxidation with hydrogen peroxide afforded the product **172**. The desired disulfide connectivity of this synthetic neopetrosiamide (**172**) was also confirmed via enzymatic digestion and MS/MS sequencing in a similar manner to the natural peptide (Figure 44).

**Scheme 57.** Synthesis of neopetrosiamide (**172**) with the revised structure

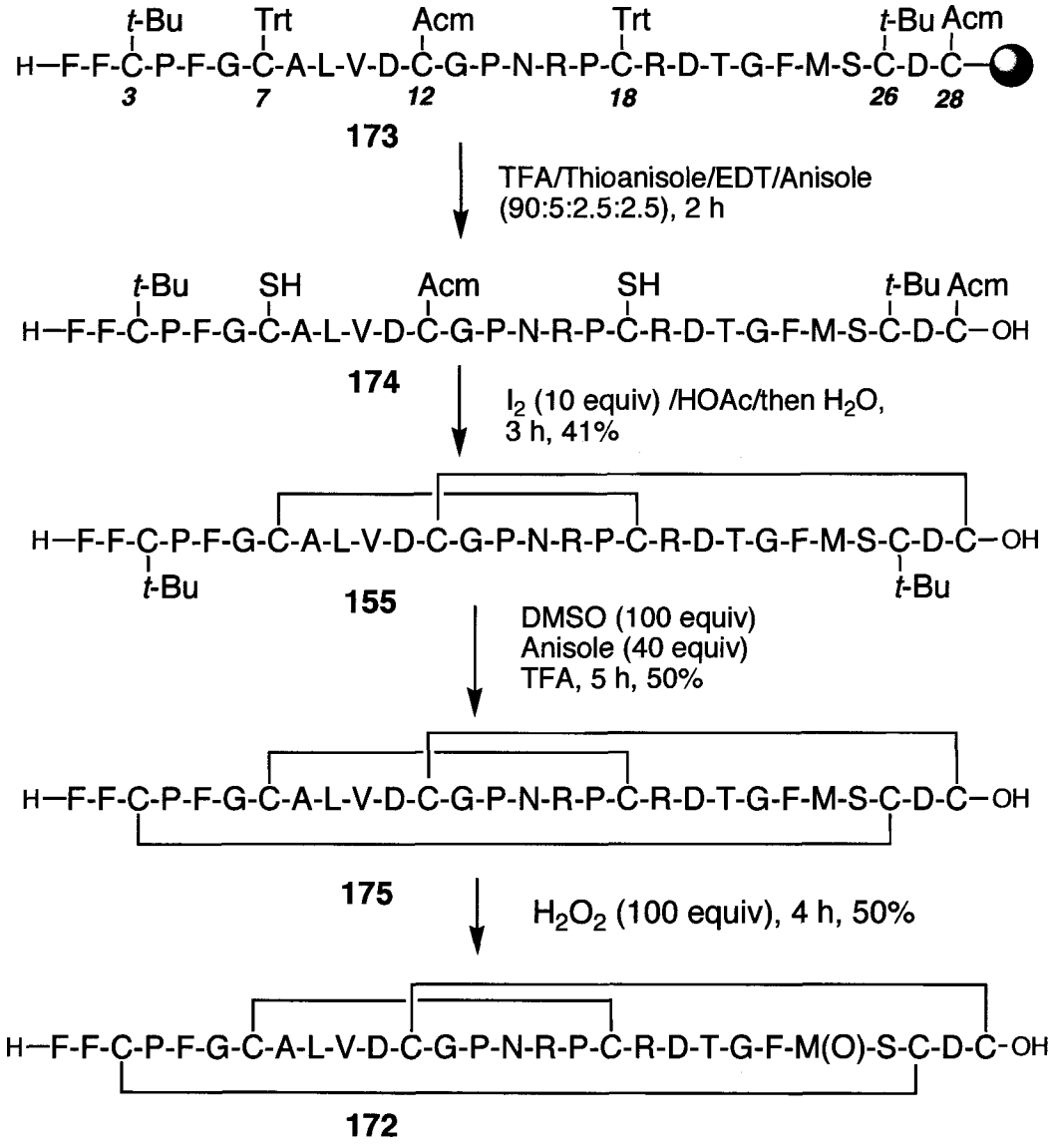


The synthetic peptide **172** and the native peptide purified from the marine sponge display the same behavior under a variety of RP-HPLC conditions (Figure 46), indicating that the peptides are identical.

**Figure 46.** Analytical RP-HPLC traces of synthetic neopetrosiamide (**172**) and the natural peptide isolated from the marine sponge (using HPLC method C listed in Chapter 5)

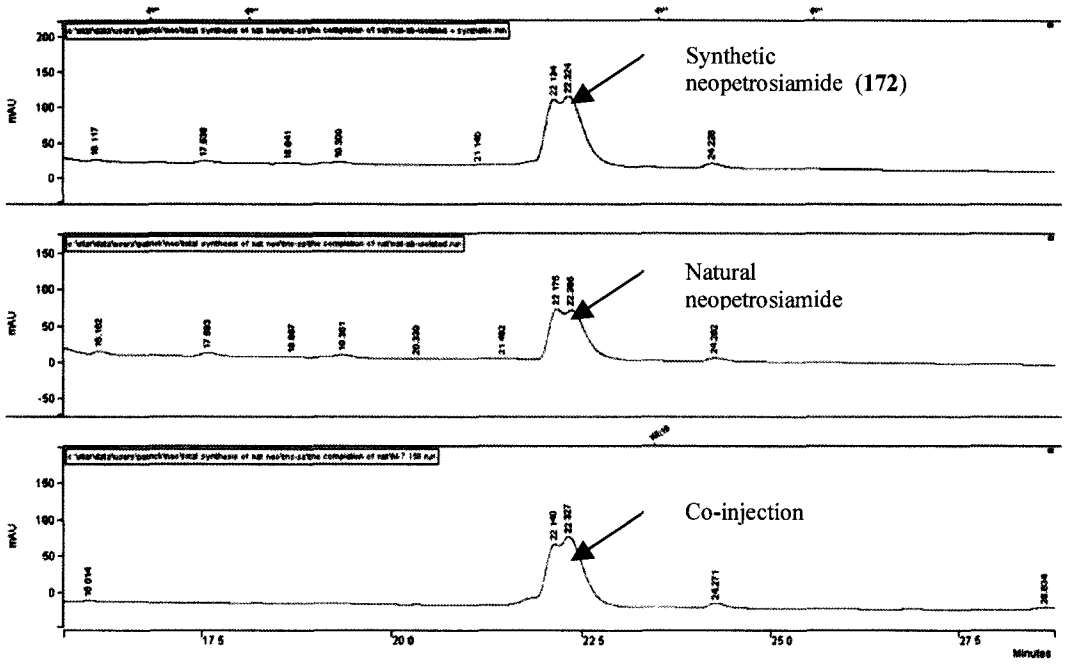


In addition, both peptides were also compared using so-called "disulfide fingerprints",[148] which are produced by a partial reduction of disulfide-rich peptides with TCEP followed by RP-HPLC analysis. As no disulfide scrambling should occur during the reduction under acidic conditions, the resulting partially reduced species from the peptide should contain the original disulfide bridges. Under the same reducing conditions, the synthetic peptide (**172**) and the native peptide display the same distribution pattern of reduced species, consistent with their chemical identity (Figure 47). Therefore, the synthetic peptide and native peptide are confirmed to be identical.

**Figure 47.** Analytical RP-HPLC trace of disulfide fingerprint of the synthetic neopetrosiamide (**172**) and the natural peptide (using HPLC method C listed in Chapter 5)

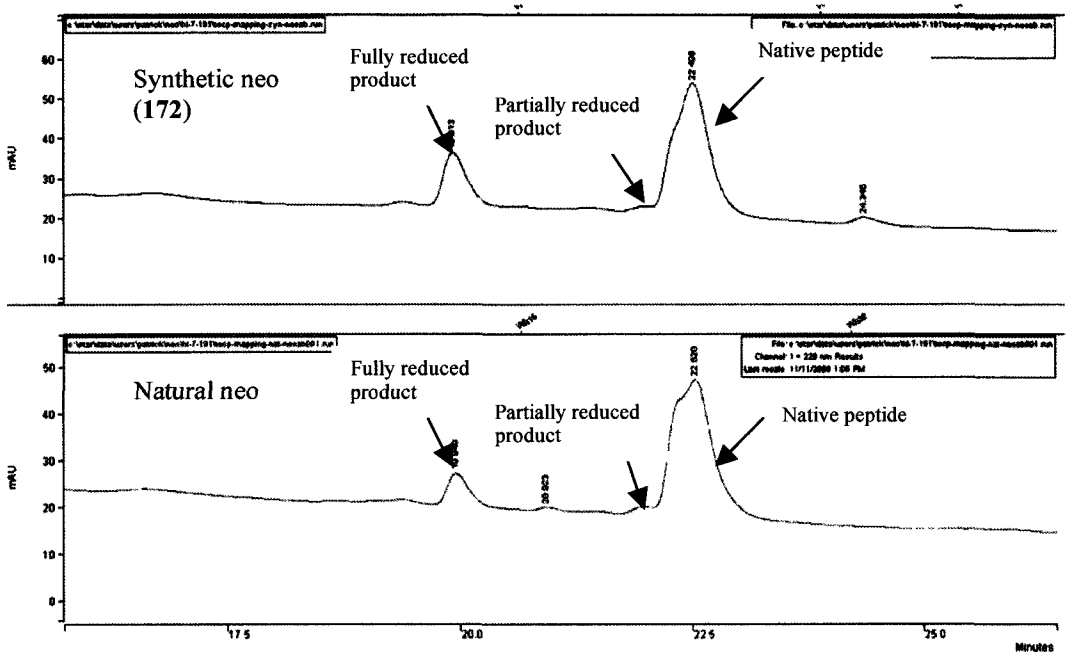


At this point, an analogue (**176**) with the revised disulfide connectivity and a norleucine at position 24 replacing the methionine sulfoxide was also prepared in the same manner as **172** (Scheme 58).

**Scheme 58.** Synthesis of norleucine analogue (**176**)

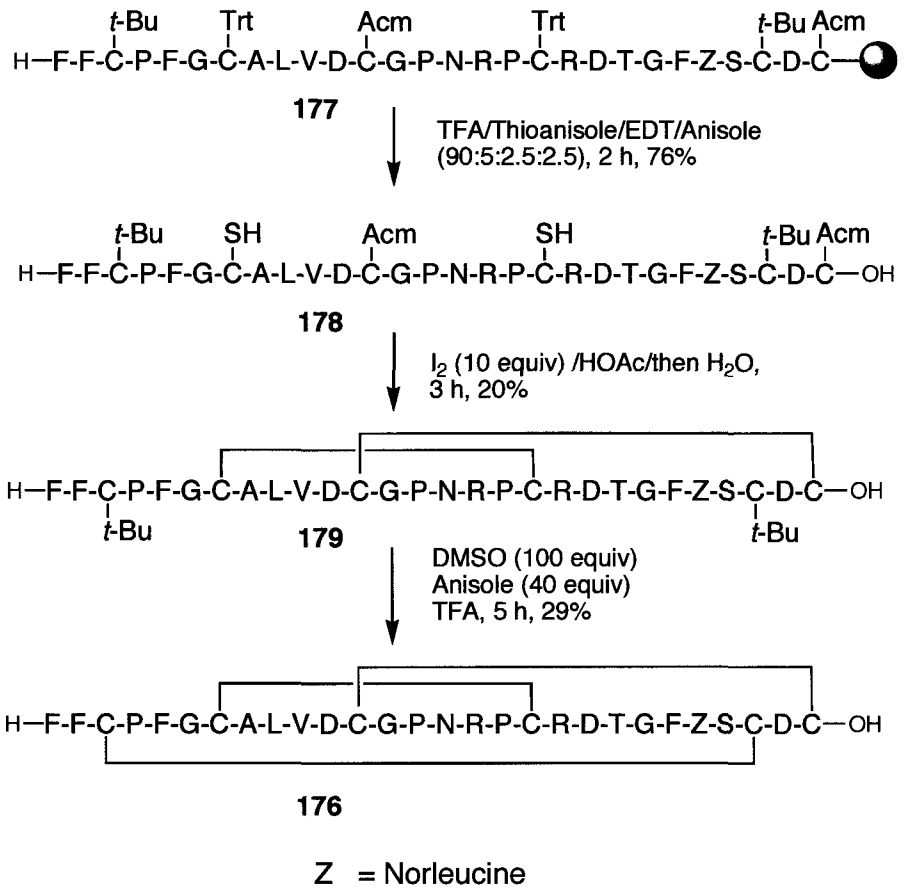


### 3.2.1.e. Biological testing of synthetic neopetrosiamides and analogues

In collaboration with Prof. Michel Roberge at the University of British Columbia, the activity of our synthetic peptides was tested using a published procedure.[149] This cell-based assay can detect compounds with low cytotoxicity that inhibit tumor cell invasion through a reconstituted basement membrane. Briefly, human colon cancer cells are cultured and deposited in a reconstituted basement membrane gel. After the peptides in a DMSO solution are added, the cells are incubated to allow invasion to take place. After incubation, the cells that fail to invade are recovered and cultured to allow their attachment to a plastic

surface. The number of live cells is quantified using the 3-(4,5-dimethylthiazol-2-yl)-2,5-diphenyltetrazolium bromide (MTT) assay. Invasion inhibition is expressed as MTT $A_{570}$ readings with high numbers indicating high invasion inhibition.

The synthetic peptide **172** displayed tumor cell invasion inhibition comparable to the native peptides isolated from the marine sponge. This further supports the structural identity of the peptides (Figure 48).

**Figure 48.** The morphology of cancer cell invasion on Matrigel

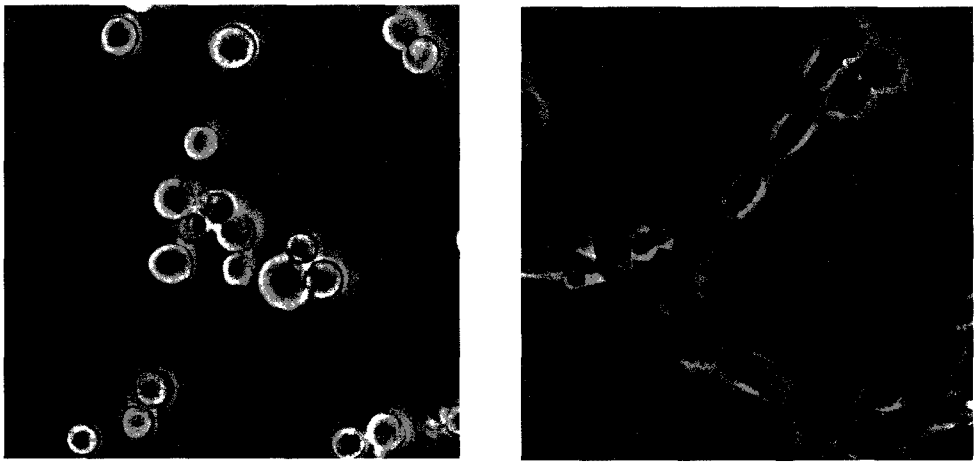

*(a) Upon the treatment with neopetrosiamide (172) in DMSO, cancer cells appear as a localized round shape, indicating the inhibition of cell invasion; (b) When treated with DMSO only in a control experiment, cancer cells display the elongated shape, suggestive of successful cell invasion.*

Neither **130**, its precursor **139**, or its analogue **141**, show any activity, which not only supports the proposal that the originally proposed disulfide connectivity of neopetrosiamide is misassigned, but also suggests that the corrected disulfide pattern is crucial for biological activity. Interestingly, the norleucine analogue **176** displays only slightly reduced activity compared with the native peptide. More surprisingly, the synthetic peptide precursor **175** with unoxidized methionine

displays the same activity as the native peptide (Figure 49). These results suggest that the methionine sulfoxide functionality is not essential for anticancer activity and the formation of methioine sulfoxide may likely arise from a non-enzymatic oxidation process, potentially during isolation.

**Figure 49.** Inhibition of cancer cell invasion by synthetic peptides and by natural neopetrosiamide (Nat)

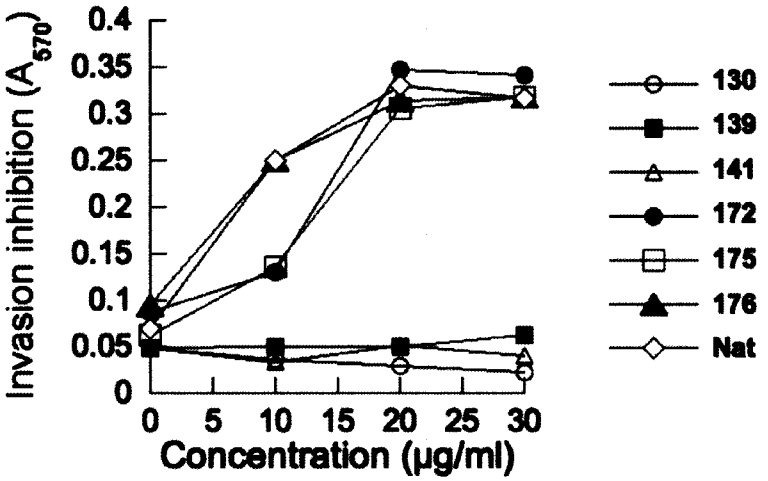


Together with HPLC analysis, disulfide bond mapping, and biological testing, the chemical synthesis of neopetrosiamides shows the disulfide connectivity of neopetrosiamide in the original proposed structure (**130**) has been misassigned and that the newly proposed structure (**172**) is correct (Figure 50). To the best of our knowledge, this work represent the first example of using chemical synthesis to revise the disulfide bond connectivity of a small disulfide rich peptide.[150, 151] This cautionary tale also shows the importance of using stepwise disulfide formation rather than directed oxidative folding to correctly obtain disulfide patterns.

**Figure 50.** Structure revision for the neopetrosiamides

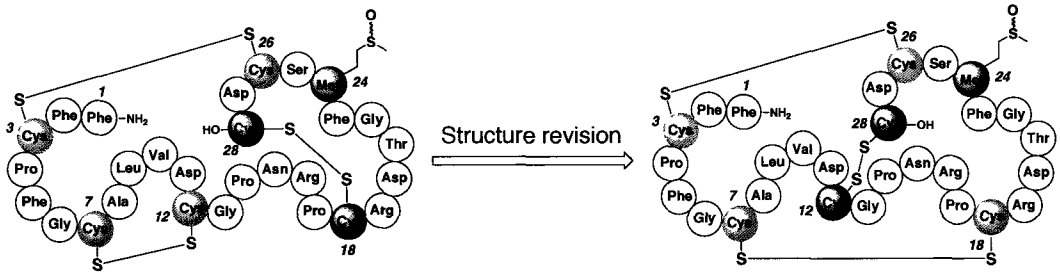


130 172

## 3.2.2. Synthesis of analogues of the structurally revised neopetrosiamide

With efficient methodology established for the synthesis of neopetrosiamides, attention was directed to the study of neopetrosiamides analogues with a view towards enhancing peptide stability, simplifying the peptide structure and studying the mode of action.

### 3.2.2.a. Neopetrosiamide analogues with modification at position 24

The interesting finding that synthetic peptide precursor **175** is fully active and norleucine analogue **176** is partially active prompted us to investigate the importance of the functionality at residue 24. Based on the surface features of the revised neopetrosiamide derived from its NMR solution structure, the methionine residue is located in a hydrophobic patch (in yellow) with the side chain protruding, which suggests it may be involved in interactions with cellular targets (Figure 51).

**Figure 51.** Position of Met on the surface of neopetrosiamide (provided by Dr. Leah Martin-Visscher) [a]

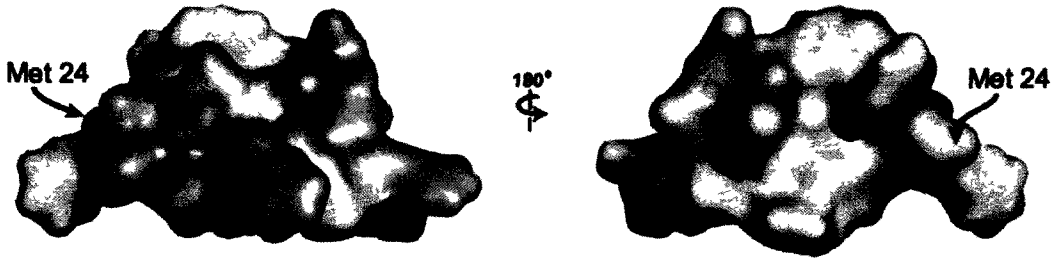


[a] *Hydrophilic region is highlighted in green and hydrophobic region is in yellow.*

In order to gain further insights to the structure-activity relationships (SAR) at this position and to find a more stable peptide that can avoid the oxidation of methionine, two other analogues were designed and synthesized. The *O*-methyl homoserine analogue (**180**) with oxygen in place of sulfur in methionine, may provide oxidative stability as well as a possible hydrogen bonding network for the biological activity. A glutamine analogue (**181**) would have similar size and could hydrogen bond. Both peptides are readily synthesized using established synthetic methodology (Figure 52). Biological tests were performed using the cell-based assay mentioned previously. Surprisingly, the *O*-methyl homoserine analogue (**180**) is inactive and glutamine analogue (**181**) shows modest activity.

**Figure 52.** The structure and biological activity of analogue **180** and **181**

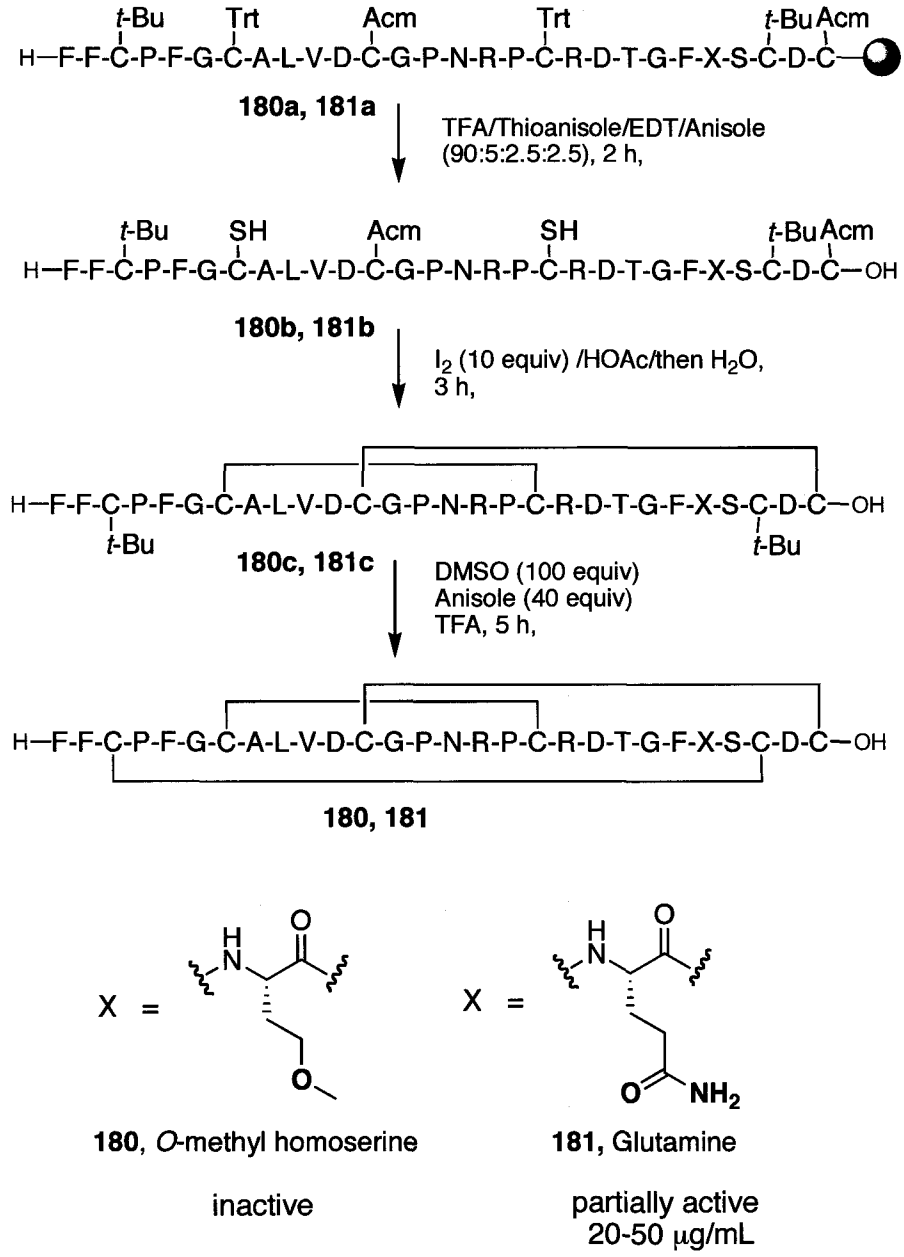


The biological testing results of analogues at position 24 indicate that the sulfoxide moiety is not essential for activity. Slight change in the size and shape of the side chain can be tolerated, as suggested by the partial activity of the norleucine analogue **176** and the glutamine analogue **181**. Interestingly, the

change in electrogenativity at the sulfur atom position in the side chain affects the biological activity dramatically. In the norleucine analogue **176**, when the sulfur atom is replaced with a carbon atom that has about the same electronegativity as sulfur (C 2.5 and S 2.5 in the Pauling scale[152]), the analogue is still active. In contrast, when the sulfur atom is replaced by the more electronegative oxygen atom (O 3.5) in the *O*-methyl homoserine analogue **180**, all activity is lost. This may be due to the incorrect binding of the peptide to a cellular target via electrostatic interactions or hydrogen bonding at this single atom position. These preliminary studies also imply that the hydrophobic region of neopetrosiamide where the methionine residue is located plays an important role for biological activity.

### 3.2.2.b. Neopetrosiamide analogues containing disulfide mimics

Given the difficulties in synthesizing multiple disulfide bonds in small peptides, it would be helpful to replace a disulfide with a non-covalent interaction, such as a hydrophobic or π-stacking interaction, Recent work in the Vederas group on replacement of a disulfide in the antimicrobial peptide leucocin A with a hydrophobic interaction produced a simplified biologically active analogue (Figure 34).[136] Hence, neopetrosiamide analogues were targeted with a pair of phenylalanine residues replacing one pair of cysteine residues. Such substitution could mimic disulfides with non-covalent hydrophobic interactions of the side chains of the two phenylalanine residues.[136]

Three analogues (**182**, **183** and **184**) with each pair of cysteines being sequentially replaced were synthesized via the one-pot oxidation procedure from corresponding linear precursors (Figure 53). After purifications, these analogues were subjected to biological testing. Unfortunately, none of them show activity. This may be due to the presence of four other phenyalanine residues in the peptide that could lead to the mismatch of hydrophobic and/or π-stacking interactions, thereby disrupting the peptide's biologically active conformation. The results indicate that the shape of the peptide is very important for activity and the disulfide cross-links (or suitable mimics) are important to maintain that shape. Further investigation can be done by replacing the disulfide with other hydrophobic residues, such as leucine, which would generate a more specific interaction, as only one leucine residue is present in the native peptide. Moreover, nature already employs this type of interaction between leucine residues, known as the "leucine zipper", in proteins that regulate gene expression.[153]

**Figure 53.** Structure of neopetrosiamide analogues with phenylalanine residues as a disulfide mimic

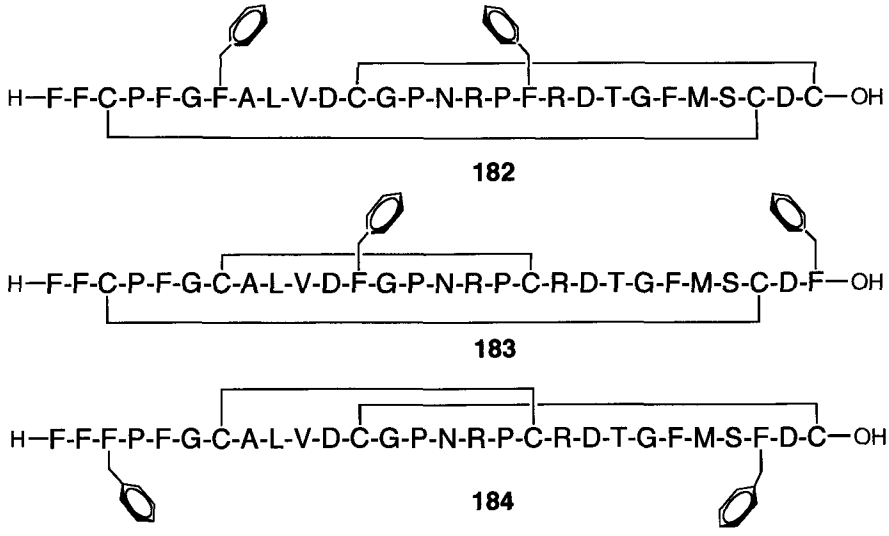

### 3.2.2.c. Neopetrosiamide analogue for study of mode of action

As described in section 3.1.5.b, a detailed mechanism of how neopetrosiamides interact with a cancer cell is still not clear[118]. In an effort to find the peptide's target, neopetrosiamide analogue **185** (Figure 55) with a fluorescent tag attached via a linker was designed and synthesized.

The solution NMR structure indicates that neopetrosiamide adopts an oblate ellipsoidal shape and has a potentially amphipathic structure due to the pronounced segregation of hydrophobic (shown in yellow) and charged (shown in green) residues (Figure 54 A). The previous investigation of the importance of the methionine sulfoxide at position 24 implies that the hydrophobic surface of the molecule might be essential for molecular recognition and biological activity. Therefore, modification on the hydrophilic region may be a reasonable choice, as this modification might not affect the binding of parent peptide onto its cellular target. The polar aspartic residues (Asp-27, Asp-20 and Asp-11) are potential modification sites (Figure 54 B), as the presence of a carboxylic acid side chain in the aspartic residue makes the attachment of a flexible linker more facile.

**Figure 54.** Surface features of neopetrosiamides (provided by Dr. Leah Martin-Visscher) *

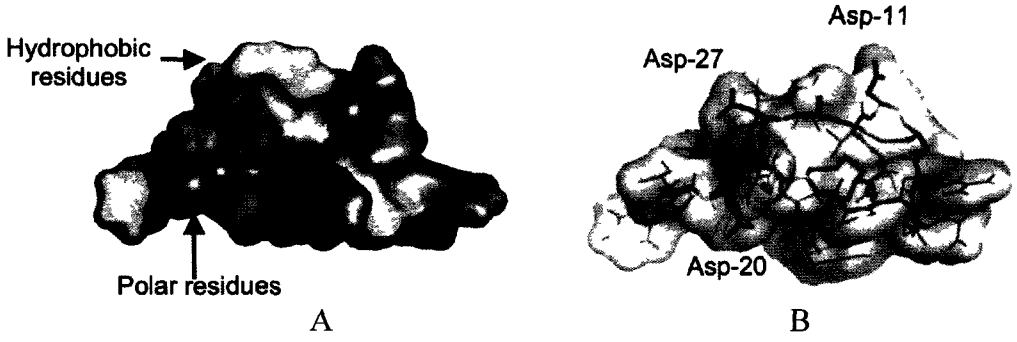


** Polar side chains are highlighted in green and hydrophobic side chains are highlighted in yellow in A; The aspartic acid side chains are highlighted in red in B.*

The neopetrosiamide analogue **175** with an unoxidized methionine at position 24 is used as a parent framework because it is as active as the natural peptide and is simpler to access. The ethylene glycol based linker **186** was selected due to its intristic water solubility. The presence of an azido group at the end of the linker allows for the use of a "click" reaction to ligate the peptide **188** and the fluorescent tag **187**. The functionalized peptide **188** can be produced via SPPS and stepwise disulfide formation using the modified aspartic acid building block **189** with the functional linker attached to the carboxylic acid side chain (Figure 55). Since there are three aspartic acid residues (Asp-27, Asp-20 and Asp-11) in neopetrosiamides, our initial goal was to synthesize three analogues with each aspartic acid residue replaced with the labeled amino acid analogue.

**Figure 55.** Retrosynthesis of neopetrosiamide analogues using "click" reaction

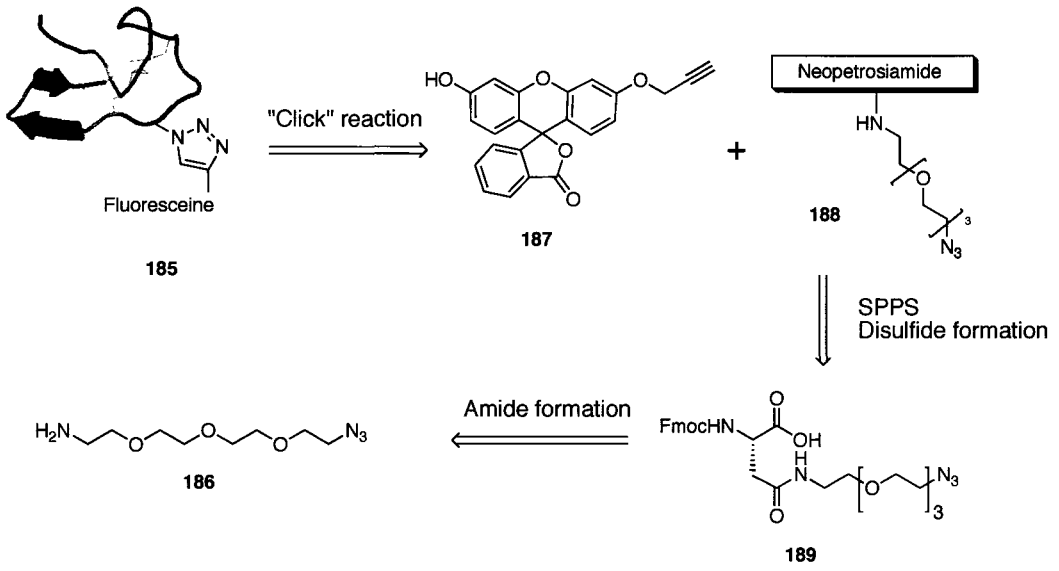


The synthesis of modified aspartic acid (**189**) begins with the coupling of Fmoc-Asp-O*t*-Bu **190** and the ethylene glycol linker **186** using PyBOP (Scheme 59). Removal of the *tert*-butyl ester protecting group with TFA affords the desired building block **189** for solid phase peptide synthesis.

**Scheme 59.** Synthesis of aspartic acid derivative (**189**)

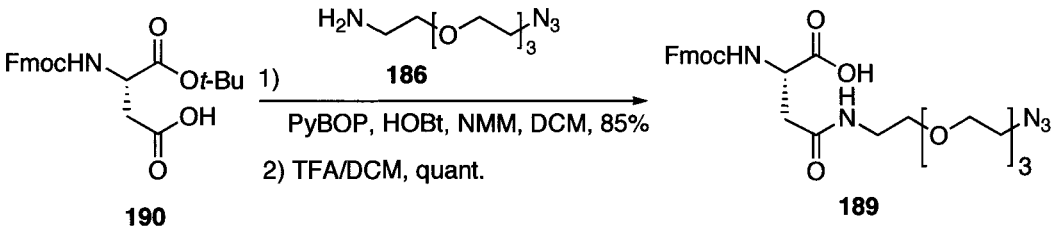


Incorporation of the modified aspartic acid **189** into the linear peptide using a peptide synthesizer followed by stepwise disulfide folding can afford the peptide precursors for the "click" reaction. Due to the presence of three aspartic acid residues (Asp11, Asp20 and Asp 27), three possible isomers could in

principle be targeted. However, the position of modification has dramatic influence on disulfide folding in solution. In the case of the Asp-27 analogue where the linker is next to the Cys 28 and Cys 26 residues, the bis-disulfide formation would not go to completion after 4 h and the third disulfide is not formed at all even under high concentration of oxidants and elevated temperature. This is likely due to the presence of the long linker in close proximity to cysteines that hinders the approach of the cysteine pairs to form the disulfide. Based on this reasoning, the Asp at position 20 is a better modification site than the other two residues, as it is not next to a cysteine residue in the linear sequence. The linear peptide **191** is assembled on a synthesizer with the modified residue at position 20 (Scheme 60). Acidic cleavage followed by the standard one-pot oxidation affords the bis-disulfide product **192**. Notably, the formation of the major desired disulfide isomer is accompanied with two minor detectable disulfide-exchange isomers. The possible reason for this side reaction is that the presence of the long linker affects the peptide conformation for correct folding and thereby promotes the undesired disulfide exchange. Interestingly, when the third disulfide is formed, no disulfide-scrambling products are observed but the oxidation of methionine is noticeable. This is possibly due to the much longer reaction time (18 h) that is required for the formation of the third disulfide.

**Scheme 60.** Synthesis of the neopetrosiamide analogue (**194**) via stepwise disulfide formation

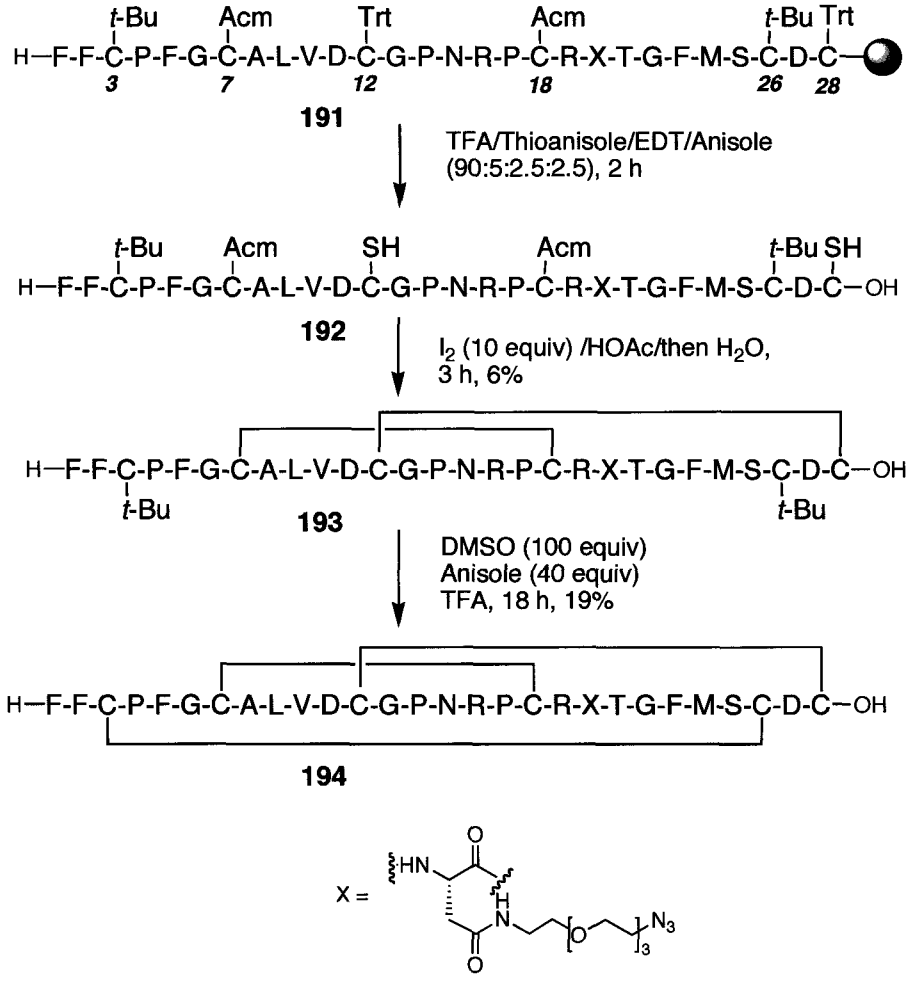


The fluorescent derivative **187** was prepared according to literature procedure.[154] The fluorescent sodium salt (**195**) reacts with acetylene bromide to give **187** in good yield (Scheme 61).

**Scheme 61.** Synthesis of fluorescent derivative (**187**)

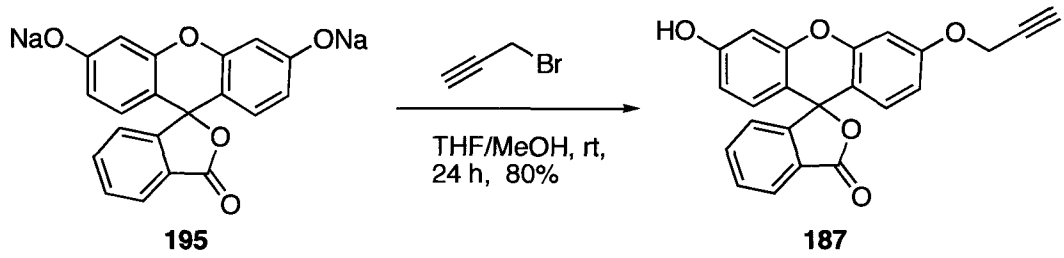


**195** **187**

With the neopetrosiamide analogue **194** and fluorescent derivative **187** available, the "click" reaction was performed.[155] The reaction of azido linked neopetrosiamide with the fluorescent derivative under high concentrations of $CuSO_4$ and sodium ascorbate in 1:1 *t*-BuOH:$H_2O$ yields the crude product **196** (Scheme 62). The desired peptide is purified by RP-HPLC and characterized by MALDI-TOF MS.

**Scheme 62.** Synthesis of **196** via the "click" reaction

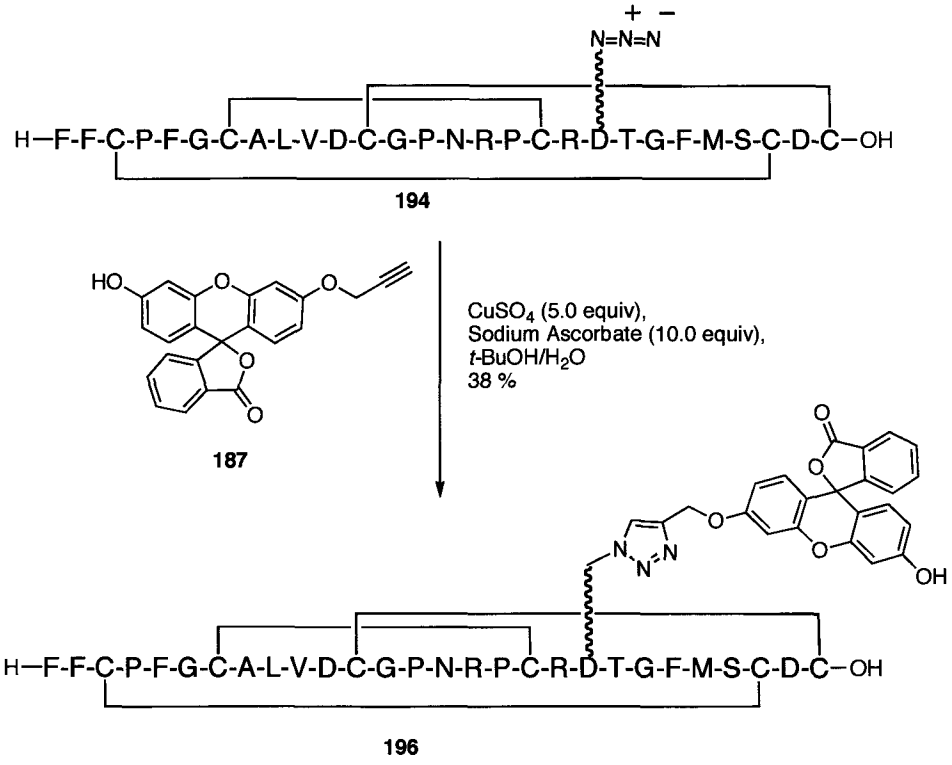

The fluorescently labeled peptide **196** and the precursor **194** were subjected to biological testing. Surprisingly, **196** is completely inactive and its precursor **194** is fully active. These results suggest the presence of the fluorescent moiety has a deleterious effect on the biological activity. The possible reason is that the ethylene glycol based linker between fluorescent tag and parent peptide is too short. Thus, when neopetrosiamde binds the cellular target, the short linker forces the attached bulky fluorescent moiety to approach the binding portion, thereby interfering with the binding of parent peptide with cellular targets. Nonetheless, the full activity of modified neopetrosiamide **194** suggests Asp-20 is an excellent site for modification. The linking methodology at this position will offer more possibilities for further investigations on target validation. Research in this direction is ongoing in the Vederas lab.

### 3.2.3. Conclusion and future work

In conclusion, the efficient total chemical synthesis of neopetrosiamides has been accomplished using solid phase peptide synthesis and subsequent stepwise disulfide formation in solution. The structure of the natural peptide has been revised and confirmed by chemical synthesis together with a combination of RP-HPLC analysis, disulfide mapping and biological activity testing. This work represents a rare example of disulfide connectivity revision in small disulfide-rich peptides using chemical synthesis. It illustrates the importance of using controlled disulfide formation rather than oxidative folding to ensure the attainment of the

correct disulfide pattern. More generally, this study provides a cautionary note to the common practice of peptide synthesis using global deprotection of many cysteine residues followed by formation of multiple disulfides through directed oxidation.

The established synthetic methodology ensures facile access to a variety of analogues with the aim of gaining insight to the structure-activity relationships, simplifying the peptide structure and studying its mode of action. The fully active analogue **175** was constructed, suggesting that the formation of methionine sulfoxide may arise from non-enzymatic processes. The stable and active analogues **176** and **181** were also discovered. Using the established synthetic methodology, further investigation at this position using other natural amino acids would provide deeper insight into how neopetrosiamide interacts with cancer cells. In studies on simplifying the peptide structure using non-covalent interactions in place of disulfides, the negative results for phenylalanine analogues (**182**, **183** and **184**) imply the importance of individual disulfide bonds and overall molecular shape to the biological activity. Further investigation will be focused on the replacement of disulfides with a pair of leucine residues, as the hydrophobic interaction between such residues is present in leucine zippers. For the mode of action study, the neopetrosiamide analogue with a fluorescent label attached through a linker was synthesized efficiently. Despite this conjugate **196** not being active, the synthetic precursor **194** with the functionalized linker attached is fully active. This interesting finding makes further investigations for

finding the cellular target possible, as this active peptide can be attached to a variety of labels through "click" chemistry.

Given the ability to synthesize a variety of neopetrosiamide analogues containing multiple disulfides, future studies may be directed towards the synthesis of a cyclic analogue of neopetrosimaide through *N*-to-*C* backbone cyclization, which could enhance peptide stability and even make the oral delivery of this peptide possible.

# Chapter 4. Summary and conclusions

Enormous progress using peptides as lead compounds in drug development has been made in the past few decades. In this thesis, the chemical synthesis and biological activity of naturally occurring cyclic peptides, which can be developed as potential antimicrobial and anticancer agents, have been demonstrated.

In the first study on an antimicrobial lantibiotic peptide, the oxidatively stable analogue (**45**) of lacticin 3147 A2, where the sulfur atoms are replaced with oxygen atoms, has been successfully synthesized via a combination of solid phase and solution phase peptide synthesis. Oxa-lacticin A2 (**45**) displays inherent activity against the Gram-positive indicator organism *Lactococcus lactis* HP. However, this analogue lacks synergistic activity with lacticin 3147 A1. This result sheds light on the importance of the sulfur atoms and further supports the proposed dual mode of action of two-peptide lantibiotics. In addition, a facile synthetic methodology via the regio- and stereoselective aziridine ring opening with oxygen nucleophiles has been developed. Due to the ease of incorporation into the peptide, these building blocks could find wide application in other medically important peptides as conformational constraints.

In an effort to synthesize the natural lantibiotic peptide (**17**), the stereoselective synthesis of methyllanthionine (125) with orthogonal protecting groups has been achieved. This synthetic methodology features the regio- and stereoselective aziridine ring opening with the thiol side chain of cysteine having

carboxyl group unprotected. The minimal use of protecting groups greatly streamlines the synthesis and enables facile access to multigram quantities for solid phase peptide synthesis. The biomimetic synthesis of *N*-terminal α-keto amide moiety has been developed via the deprotection of a Boc-protected enamine followed by hydrolysis of the resulting enamine. With these key building blocks, the total synthesis of lacticin 3147 A2 has been accomplished on solid support. This established synthetic methodology should make it possible to chemically access more lantibiotics, including those with interlocking rings, such as lacticin 3147 A1 and nisin.

In the second study, the efficient synthesis of neopetrosiamides, sponge-derived peptides with three cross-linking disulfides, has been accomplished via solid phase peptide synthesis followed by stepwise disulfide formation in solution. In the course of the total synthesis, it was found that the disulfide connectivity of neopetrosiamide had been misassigned. The revised disulfide connectivity was proposed and confirmed by chemical synthesis along with HPLC analysis, disulfide mapping and biological testing. This work emphasizes the vital role of total synthesis in the structural determination of promising natural products. This cautionary tale also shows the importance of using stepwise disulfide formation rather than directed oxidative folding to correctly synthesize disulfide-rich peptides.

Utilizing the established synthetic methodology, a variety of analogues of neopetrosiamides have been synthesized with the goal of shedding light on SAR, simplifying peptide structure and unraveling mode of action. In an effort to

elucidate the biological function of the methionine sulfoxide at position 24, it was found that the peptide (**175**) with an unoxidized methionine is fully active, suggesting that the presence of the methionine sulfoxide may be an artifact of isolation. In addition, the active analogues **176** and **181** were also discovered. To simply the peptide structure and elaborate the role of each disulfide, three analogues (**182**, **183** and **184**) where each disulfide is replaced by a non-covalent hydrophobic interaction between the side chains of a pair of phenylalanines were synthesized. Since all three analogues are inactive, the results underline the importance of the disulfide and the overall shape of the molecule to the biological activity. In order to uncover the detailed mode of action, the peptide conjugate **196** wherein a fluorescent molecule is attached to neopetrosiamide via a linker was prepared. Interestingly, this conjugate **196** is completely inactive, however, its synthetic precursor **194** containing the functionalized linker without the fluorescent label attached is fully active. This encouraging result for **194** will make it possible for further investigations to identify the precise cellular and molecular target of neopetrosiamide, as the functionalized linker in **194** will allow for the attachment of a variety of labels.

The results reported in this thesis illustrate the applications of synthetic peptides, ranging from enhancing peptide stability, confirming peptide structure, elucidating SAR, simplifying peptide structure to unraveling peptide mode of action. As demonstrated by this thesis, peptide chemistry is continuing to develop and shows excellent prospects for the future.

# Chapter 5. Experimental procedures

## 5.1. General information

### 5.1.1. Reagent, solvent and solutions

All commercially available reagents and solvents were purchased from the Aldrich Chemical Company Inc. (Madison, WI), Sigma Chemical Company (St. Louis, MO), Fisher Scientific Ltd. (Ottawa, ON) or Caledon (Georgetown, ON). All protected amino acids and SPPS resins were purchased from the Calbiochem-Novabiochem Corporation (San Diego, CA), Sigma-Aldrich Canada Ltd. (Oakville, ON), Chem Impex International Inc. (Wood Dale, IL) or VWR International (Mississauga, ON). All reagents and solvents were of American Chemical Society (ACS) grade and used without further purification. All solvents used for anhydrous reactions were dried according to Perrin *et al* and Vogel. [156,157] Tetrahydrofuran and diethyl ether were freshly distilled over sodium and benzophenone under dry argon prior to use. Dichloromethane, pyridine, and triethylamine were distilled over calcium hydride. HPLC grade methanol, acetonitrile and dimethylformamide were used without purification.

### 5.1.2. Reactions and purifications

Commercially available ACS grade solvents (>99.0% purity) were used for column chromatography without any further purification. Flash chromatography was performed according to the method of Still *et al.*[158] All reactions and fractions from column chromatography were monitored by thin

layer chromatography (TLC) using glass plates with a UV fluorescent indicator (normal $SiO_2$, Merck 60 $F_{254}$). One or more of the following methods were used for visualization: UV absorption by fluorescence quenching; iodine staining; by dipping the TLC plates in a solution of Ninhydrin:acetic acid:n-butanol (0.6 g:6 mL:200 mL); $Ce(SO_4)•4H_2O/(NH_4)MoO_{24}•4H_2O/H_2SO_4/H_2O$ (5 g:12.5 g:28 mL:472 mL) spray. Flash chromatography was performed using Merck type 60, 230-400 mesh silica gel. The removal of solvent *in vacuo* refers to evaporation under reduced pressure below 40 °C using a Buchi rotary evaporator followed by drying (<0.1 mm Hg) to a constant sample mass. Unless otherwise specified, solutions of $NH_4Cl$, $NaHCO_3$, HCl, citric acid, lithium hydroxide and sodium thiosulfate refer to aqueous solutions. Brine refers to a saturated aqueous solution of sodium chloride. In descriptions of reactions 'rt' refers to room temperature.

High performance liquid chromatography (HPLC) was performed on a Varian Prostar chromatograph equipped with a model 325 variable wavelength UV detector and a Rheodyne 7725i injector fitted with a 20 to 2000 μL sample loop. The columns used were Vydac 218TP1022 (C18, 10 $\mu$m, 2.2 cm x 25 cm), steel walled CSC-Inertsil 150A/ODS2 (5 μm, 10 × 250 mm), Varian Microsorb-MV 100-5 C18 (5 μm, 4.6 × 250 mm), Phenomenex luna C18(2) (5 μm, 100 Å, 4.6 x 250 mm, 516572-27) and Phenomenex luna C18(2) (5 μm, 100 Å, 10.0 x 250 mm, 5227280-1). All HPLC solvents were filtered with a Millipore filtration system under vacuum before use. The preparation methods are outlined in the synthesis and characterization sections.

### 5.1.3. Instruments for compound characterizations

Nuclear Magnetic Resonance (NMR) spectra were recorded on a Varian Inova 600, Inova 500, Inova 400, Inova 300 or Unity 500 spectrometer. Chemical shift values for proton and carbon NMR are reported in parts per million (ppm) downfield relative to tetramethylsilane (TMS). For $^{1}H$ NMR (300, 400, 500 or 600 MHz) spectra, δ values were referenced to $CDCl_3$ (7.26 ppm), $CD_3OD$ (3.30 ppm) or $D_2O$ (4.79 ppm), and for $^{13}C$ (75, 100, 125 or 150 MHz) spectra, δ values were referenced to $CDCl_3$ (77.0 ppm), $CD_3OD$ (49.0 ppm) as the solvents. Additional assignments were made using pulsed field gradient versions of shift correlation spectroscopy (gCOSY), heteronuclear multiple quantum coherence spectroscopy (gHMQC) and heteronuclear multiple bond correlation spectroscopy (HMBC). $^{1}H$ NMR data are reported in the following order: multiplicity (app, apparent; s, singlet; d, doublet; t, triplet; q, quartet; pent, pentet; sext, sextet and m, multiplet), number of protons, coupling constant (*J*) in Hertz (Hz) and assignment. When appropriate, a signal is preceeded by br, indicating the signal was broad. The coupling constants reported are within an error range of 0.2-0.4 Hz, and have been rounded to the nearest 0.1 Hz. All literature compounds had IR, $^{1}H$ NMR and mass spectra consistent with the assigned structures.

Mass spectra (MS) were recorded on a Kratos AEIMS-50 high resolution mass spectrometer (HRMS) or a Micromass ZabSpec Hybrid Sector-TOF positive mode electrospray ionization instruments ((ES), 0.5% solution of formic acid in MeCN:$H_2O$/1:1) or on a Perspective Biosystems Voyager™ Elite MALDI-TOF using either 4-hydroxy-α-cyanocinnamic acid (HCCA), 2,5-dihydroxybenzoic

acid (DHB) or 3,5-dimethoxy-4-hydroxycinnamic acid (sinapinic acid) as matrices. LC-MS/MS was performed on a Waters (Micromass) Q-TOF-Premier mass spectrometer coupled with a nanoAcquity UPLC system with a flow rate of 0.35 μL/min on a Waters nanoAcquity column (Atlantis 3 $\mu$m dC18, 100Å pore, 75 $\mu$m ID × 150 mm) with an in-line nanoAcquity trapping column (Symmetry 5 $\mu$m C18, 180 $\mu$m ID × 20 mm). A linear gradient from 99% solvent A (water with 0.1% formic acid) to 65% solvent B (acetonitrile with 0.1% formic acid) in 45 minutes was used. Infusion nano-electrospray MS/MS analyses were performed on a Q-TOF Premier mass spectrometer with an infusion rate of 0.5 μL/min. The collision energy was varied from 20 to 50eV with argon as the collision gas.

Infrared spectra (IR) were recorded on either a Nicolet Magna-IR 750 with Nic-Plan microscope FT-IR spectrometer or a 20SX FT-IR spectrometer. Cast refers to the evaporation of a solution on a NaCl plate.

Optical rotations were measured on a Perkin Elmer 241 polarimeter with a microcell (10 cm, 1 mL) at ambient temperature and are reported in units of $10^{-1}$ deg $cm^2$ $g^{-1}$. All reported optical rotations were referenced against air and measured at the sodium D line ($\lambda$ = 589.3 nm).

## 5.2. Experimental procedure and data for compounds

### 5.2.1. Chemical synthesis and biological testing of lacticin 3147 A2 and its analogue

**Oxa-lacticin 3147 A2 (45)**

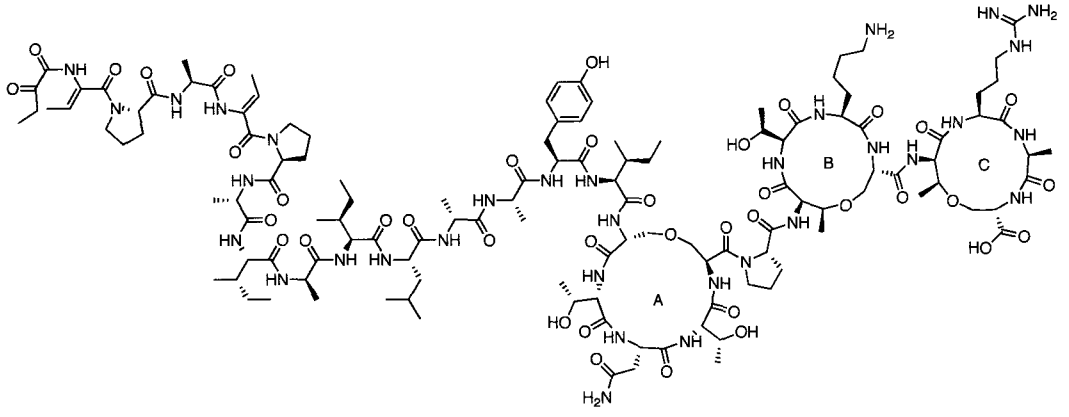

The preparation of compound **45** is described on page 175 at the end of its synthesis from compound **96**.

#### 5.2.1.a. Development of synthetic methodology for oxa-lan and derivatives

**(*S*)-2-Methyl 1-(4-nitrobenyloxycarbonyl)aziridine-2-carboxylate (52)**

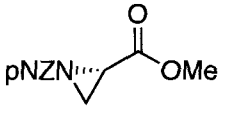

The known compound was prepared by a modified literature procedure.[88] Trifluoroacetic acid (10 mL) was added dropwise over 10 min to a solution of **55** (4.0 g, 11.63 mmol) in dichloromethane (10 mL) and methanol (10 mL) at 0 °C. The solution was stirred for 30 min at 0 °C. Volatiles were removed by azeotroping with $Et_2O$ (3 x10 mL). The residue was partitioned between $Et_2O$ (50 mL) and $H_2O$ (50 mL) and the ether layer was extracted with water (3 x10 mL).

The combined aqueous layers were basicified to pH 9 with $NaHCO_3$ at 0 °C. Ethyl acetate (100 mL) was added to the aqueous solution followed by 4-nitrobenzyl chloroformate (2.5 g, 11.63 mmol) at 0 °C. The resulting immiscible layers were warmed to room temperature and stirred vigorously for 24 h. After completion of the reaction, the two layers were separated and aqueous layer was extracted with EtOAc (3 x 20 mL). The combined organic layers were washed with brine (3 x 50 mL), dried with $Na_2SO_4$, filtered and then concentrated *in vacuo*. The crude product was further purified by flash chromatography ($SiO_2$, 4:1/Hexanes: EtOAc) to yield **52** (3.12 g, 95%) as a colorless oil. $[\alpha]_D^{25}$ -30.19° (*c* 1.00, $CHCl_3$); IR ($CHCl_3$, cast): 3516, 3082, 3007, 2956, 1744, 1607, 1523 $cm^{-1}$; $^1H$ NMR ($CDCl_3$, 500 MHz): δ 8.22 (dd, 2H, *J* = 7.00, 2.00 Hz, pNZ-H), 7.52 (dd, 2H, *J* = 7.00, 2.00 Hz, pNZ-H), 5.24 (m, 2H, -C$\underline{H_2}$-Ar), 3.75 (s, 3H, OC$\underline{H_3}$), 3.15 (dd, 1H, *J* = 3.0, 5.5 Hz, Ser-$H_\alpha$), 2.62 (dd, 1H, *J* = 3.0, 1.0 Hz, Ser-$H_\beta$), 2.52 (dd, 1H, *J* = 5.5, 1.0 Hz, Ser-$H_{\beta'}$); $^{13}C$ NMR ($CDCl_3$, 125 MHz): δ 168.5, 160.2, 147.8, 142.6, 128.5, 123.7, 66.9, 52.8, 34.8, 31.4; HRMS (ES): Calcd for $C_{12}H_{12}N_2O_6Na$ 303.0587, found 303.0588.

**(*S*)-Methyl 3-hydroxy-2-(tritylamino)propanoate (54)**

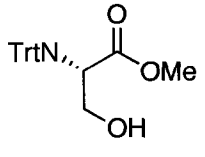


The known compound was prepared by a literature procedure.[159] To a suspension of (*S*)-serine methyl ester hydrochloride (7.5 g, 48.0 mmol) in dichloromethane

(100 mL) at 0 °C was added triethylamine (13.8 mL, 96 mmol, 2.0 equiv) dropwise followed by triphenylmethyl chloride (13.6 g, 48.0 mmol, 1.0 equiv) in dichloromethane (30.0 mL). After stirring at 4 °C for 12 h, the white precipitate was filtered under suction, and the filtrate was evaporated *in vacuo* to yield a white solid. This was dissolved in EtOAc (100 mL) and washed with saturated $NaHCO_3$ (2 x 100 mL), 10% citric acid (2 x 100 mL) and water (2 x 100 mL). The separated organic layer was dried over $Na_2SO_4$ and then concentrated *in vacuo*. The crude product was recrystallized from EtOAc-Hexanes to give **54** as a white solid (16.0 g, 92 %). mp 77-79 °C (lit.[159] mp 77-78 °C); $[\alpha]_D^{25}$ 3.60° (*c* 1.00, $CHCl_3$); IR ($CHCl_3$, cast): 3457, 3084, 3057, 3020, 2950, 1733, 1595, 1490, 1448 $cm^{-1}$; $^1H$ NMR ($CDCl_3$, 500 MHz): δ 7.51 (m, 6H, Trt-H), 7.29 (m, 6H, Trt-H), 7.21 (m, 3H, Trt-H), 3.73 (dd, 1H, $J$ = 4.5, 10.5 Hz, Ser-C$\underline{H}_a$), 3.57 (m, 2H, Ser-C$\underline{H}_b$), 3.31 (s, 3H, OC$\underline{H}_3$), 3.00-2.20 (br, 2H, O$\underline{H}$ and N$\underline{H}$); $^{13}C$ NMR ($CDCl_3$, 125 MHz): δ 173.9, 145.6, 128.8, 127.9, 126.6, 71.9, 64.9, 57.8, 51.9; HRMS (ES): Calcd for $C_{23}H_{23}NO_3Na$ 384.1570, found 384.1568.

**(*S*)-Methyl 1- tritylaziridine-2-carboxylate (55)**

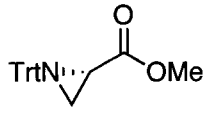


The known compound was prepared by a literature procedure.[88] Triethylamine (1.68 mL, 12.1 mmol) was added dropwise over 10 min to a stirred solution of **54** (2.0 g, 5.5 mmol) in THF (50 mL) at 0 °C, followed by dropwise addition of methanesulfonyl chloride (0.47 mL, 60 mmol). The solution was stirred at 0 °C

for a further 30 min and then refluxed for 48 h. After completion of the reaction, the solvent was removed *in vacuo*. The resulting residue was dissolved in EtOAc (60 mL) and washed with 10% citric acid (3 x 20 mL), $H_2O$ (2 x 20 mL), saturated $Na_2CO_3$ (3 x 20 mL), $H_2O$ (2 x 20 mL) and brine (20 mL). The organic layer was dried with $Na_2SO_4$, filtered and then concentrated *in vacuo*. The crude product was recrystallized from EtOAc-Hexanes to give **55** (1.8 g, 95 %) as a white solid; mp 115-117 °C (lit.[88] mp 116-118 °C); $[\alpha]_D^{25}$ -94.22° (*c* 1.00, $CHCl_3$); IR ($CHCl_3$, cast): 3057, 3031, 2951, 1748, 1595, 1489, 1448 $cm^{-1}$; $^1H$ NMR ($CDCl_3$, 500 MHz): δ 7.54 (m, 6H, Trt-H), 7.28 (m, 6H, Trt-H), 7.22 (m, 3H, Trt-H), 3.78 (s, 1H, $OC\underline{H}_3$), 2.29 (dd, 1H, $J$ = 2.0, 3.0 Hz, Ser-Hα), 1.92 (dd, 1H, $J$ = 3.0, 6.0 Hz, Ser-Hβ), 1.44 (dd, 1H, $J$ = 2.0, 6.0 Hz, Ser-Hβ); $^{13}C$ NMR ($CDCl_3$, 125 MHz): δ 171.9 143.6, 129.3, 127.6, 126.9, 74.4, 52.1, 31.7, 28.7; HRMS (ES): Calcd for $C_{23}H_{21}NO_2Na$ 366.1464, found 366.1465.

**General procedure for preparation of *N*-phthalimide serine and thereonine derivatives[92]**

To a solution of serine alkyl ester hydrochloride (1.0 equiv) and phthalic anhydride (1.0 equiv) in toluene, triethylamine (1.0 equiv) was added. The reaction mixture was refluxed under Dean-Stark conditions for 2 h. Volatiles were evaporated under reduced pressure. The residue was dissolved in EtOAc, washed with 10% citric acid, $H_2O$, saturated $NaHCO_3$ and brine. Organic layer was dried with $Na_2SO_4$, filtered and then concentrated to give the product, which was used without further purification or purified by flash chromatography.

**(*S*)-Methyl 2-(1,3-dioxoisoindolin-2-yl)-3-hydroxypropanoate (56)**

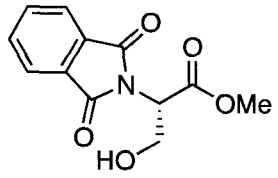

Following the general procedure for preparation of *N*-phthalimide serine and thereonine derivatives, [92] (*S*)-serine methyl ester hydrochloride (5.0 g, 32.1 mmol) was converted to the title compound **56** as a colorless oil (6.4 g, 80%). $[\alpha]_D^{25}$ 17.14° (*c* 1.10, $CHCl_3$); IR ($CHCl_3$, cast): 3476, 2956, 1773, 1745, 1714, 1612, 1468 $cm^{-1}$; $^1H$ NMR ($CDCl_3$, 400 MHz): δ 7.87 (dd, 2H, *J* = 3.2, 5.6 Hz, Ar-H), 7.75 (dd, 2H, *J* = 3.2, 5.6 Hz, Ar-H), 5.02 (dd, 1H, *J* = 4.4, 5.6 Hz, Ser-Hα), 4.20 (m, 2H, Ser-Hβ), 3.78 (s, 3H, -OC<u>H</u>$_3$); $^{13}C$ NMR ($CDCl_3$, 100 MHz): δ 168.4, 168.0, 134.4, 131.6, 123.7, 60.9, 54.6, 52.8; HRMS (ES): Calcd for $C_{12}H_{11}NO_5Na$ 272.0529, found 272.0530.

**(*S*)-Methyl 2-(1, 3-dioxoisoindolin-2-yl)-3-((*S*)-3-methoxy-2-((4-nitrobenzyloxy)carbonylamino)-3-oxoropoxy)propanoate (57)**

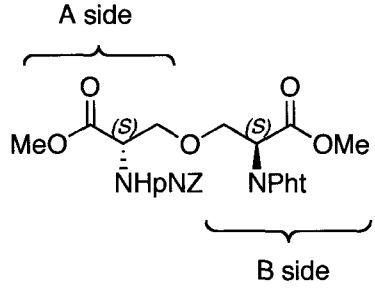


To a stirred solution of aziridine-2-carboxylate **52** (100 mg, 0.35 mmol) and **56** (174 mg, 0.7 mmol) in toluene (20 mL), was added was added $BF_3 \bullet OEt_2$ (0.22 mL, 0.175 mmol) dropwise at rt. The resulting reaction mixture was refluxed at

110 °C for 2 h. After completion of the reaction, the solvent was removed under reduced pressure. The crude product was purified by flash chromatography ($SiO_2$, 7:3/Hexanes: EtOAc) to give **57** as a colorless oil (133 mg, 72%). $[\alpha]_D^{25}$ -43.29° (*c* 0.7, $CHCl_3$); IR ($CHCl_3$, cast): 3366, 2954, 1717, 1607, 1521, 1468, 1437, 1392 $cm^{-1}$; $^1H$ NMR ($CDCl_3$, 400 MHz): δ 8.19 (d, 2H, *J* = 8.4 Hz, pNZ-H), 7.84 (dd, 2H, *J* = 5.4, 3.0 Hz, Pht-H), 7.72 (dd, 2H, *J* = 5.4, 3.0 Hz, Pht-H), 7.47 (d, 2H, *J* = 8.4 Hz, pNZ-H), 5.62 (d, 1H, *J* = 8.5 Hz, NH), 5.18 (d, 1H, *J* = 13.5 Hz, -O-C$\underline{H}_2$-Ar), 5.11 (d, 1H, *J* = 13.5 Hz, -O-C$\underline{H}_2$-Ar), 5.08 (dd, 1H, *J* = 5.0, 9.3 Hz, Hα B side), 4.40 (dt, 1H, *J* = 8.6, 3.0 Hz, Hα' A side), 4.23 (dd, 1H, *J* = 9.3, 10.7 Hz, Hβ B side), 4.09 (dd, 1H, *J* = 5.0, 10.7 Hz, Hβ B side), 4.00 (dd, 1H, *J* = 3.3, 9.5Hz, Hβ' A side), 3.68 (dd, 1H, *J* = 3.3, 9.5Hz, Hβ' A side), 3.74 (s, 3H, $OCH_3$), 3.62 (s, 3H, $OCH_3$); $^{13}C$ NMR ($CDCl_3$, 100 MHz): δ 170.0, 167.5, 167.3, 155.4, 143.7, 134.2, 131.7, 127.8, 123.6, 123.5, 70.6, 67.9, 65.3, 54.2, 52.8, 52.5, 51.1; HRMS (ES): Calcd for $C_{24}H_{23}N_3O_{11}Na$ 552.1224, found 552.1225.

**(*S*)-2-Allyl 1-(4-nitrobenzyloxycarbonyl)aziridine-2-carboxylate (58)[88]**

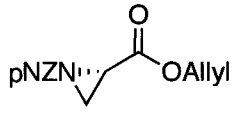


According to a similar procedure to **52**, the title compound **58** was prepared as a colorless oil (3.2 g, 77%) from **62** (5.0 g, 13.5 mmol). $[\alpha]_D^{25}$ -23.76° (*c* 1.00, $CHCl_3$); IR ($CHCl_3$, cast): 3083, 2950, 1744, 1648, 1608, 1523 $cm^{-1}$; $^1H$ NMR ($CDCl_3$, 400 MHz): δ 8.19 (d, 2H, *J* = 8.0 Hz, pNZ-H), 7.51 (d, 2H, *J* = 8.0 Hz, pNZ-H), 5.90-5.84 (m, 1H, -$CH_2C\underline{H}$=$CH_2$), 5.34-5.17 (m, 4H, -$CH_2CH$=C$\underline{H}_2$ and -

C<u>H</u>$_2$-$C_6H_4$-$NO_2$), 4.62 (m, 2H, -C<u>H</u>$_2$CH=$CH_2$), 3.16 (dd, 1H, $J$ = 3.1, 5.2 Hz, Ser-Hα), 2.64 (dd, 1H, $J$ = 3.1, 1.3 Hz, Ser-Hβ), 2.51 (dd, 1H, $J$ = 1.2, 5.2 Hz, Ser-Hβ); $^{13}$C NMR ($CDCl_3$, 125 MHz): δ 167.8, 160.1, 147.7, 142.6, 131.1, 128.4, 123.7, 119.2, 66.8, 66.4, 34.9, 31.4; HRMS (ES): Calcd for $C_{14}H_{14}N_2O_6Na$ 329.0744, found 329.0742

**(*R*)-2-Allyl 1-(4-nitrobenyloxycarbonyl)aziridine-2-carboxylate (59)[88]**

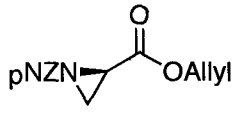


In a similar manner to that described above for **52**, compound **59** was prepared as a colorless oil (1.62 g, 80%) from **62a** (2.46 g, 6.6 mmol). $[\alpha]_D^{25}$ 22.98° (*c* 1.00, $CHCl_3$); IR ($CHCl_3$, cast): 3083, 2950, 1742, 1607, 1522 cm$^{-1}$; $^1$H NMR ($CDCl_3$, 400 MHz): δ 8.16 (d, 2H, $J$ = 8.7 Hz, pNZ-H), 7.48 (d, 2H, $J$ = 9.0 Hz, pNZ-H), 5.88-5.81 (m, 1H, -$CH_2$C<u>H</u>=$CH_2$), 5.31-5.15 (m, 4H, $CH_2$CH=C<u>H</u>$_2$ and -C<u>H</u>$_2$-$C_6H_4$-$NO_2$), 4.60 (m, 2H, -C<u>H</u>$_2$CH=$CH_2$), 3.15 (dd, 1H, $J$ = 3.1, 5.3 Hz, Ser-Hα), 2.60 (dd, 1H, $J$ = 3.1, 1.3 Hz, Ser-Hβ), 2.50 (dd, 1H, $J$ = 1.3, 5.2 Hz, Ser-Hβ); $^{13}$C NMR ($CDCl_3$, 100 MHz): δ 167.7, 160.0, 147.6, 142.6, 131.0, 128.3, 123.5, 119.0, 66.7, 66.3, 34.8, 31.3; HRMS (ES): Calcd for $C_{14}H_{14}N_2O_6Na$ 329.0744, found 329.0742.

**_N_-Triphenylmethyl-(_S_)-Serine allyl ester (61)[93]**

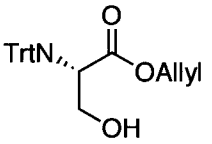


The *N*-trityl serine triethylamine salt (8.97 g, 20 mmol) was dissolved in dry MeOH (100 mL) and cesium carbonate (3.25 g, 10 mmol) was added. The resulting mixture was stirred at rt for 1 h and then concentrated *in vacuo*. The resulting cesium salt was dissolved in DMF (50 mL) and allyl bromide (1.9 mL, 22 mmol) was added dropwise at rt. The reaction mixture was stirred for 24 h and diluted with EtOAc (250 mL). The organic layer was washed with 5 % aqueous citric acid, dried over $Na_2SO_4$, and concentrated *in vacuo* to give the trityl serine allyl ester **61** (7.4 g, 96%) as a colorless oil, which was used for the next step without further purification. $[\alpha]_D^{25}$ 6.28° (*c* 1.5, $CHCl_3$); IR ($CHCl_3$, cast) 3466, 3084, 3058, 3021, 2939, 2878, 1731, 1648, 1595 $cm^{-1}$; $^1H$ NMR ($CDCl_3$, 300 MHz): δ 7.60-7.56 (m, 6H, Trt-H), 7.35-7.21 (m, 10H, Trt-H), 5.83-5.70 (m, 1H, $-CH_2-C\underline{H}=CH_2$), 5.28-5.18 (m, 2H, $-CH_2-CH=C\underline{H_2}$), 4.31- 4.11 (m, 2H, $-C\underline{H_2}-CH=CH_2$), 3.81 (m, 1H, Ser-CHα), 3.65 (m, 2H, Ser-CHβ), 2.93 (br, 2H, OH and NH); $^{13}C$ NMR ($CDCl_3$, 100 MHz): δ 173.0, 145.5, 131.5, 128.6, 127.8, 126.5, 118.3, 70.9, 65.6, 64.8, 57.7; HRMS (ES): Calcd for $C_{25}H_{25}NO_3Na$ 410.1726, found 410.1724.

**_N_-Triphenylmethyl-(_R_)-Serine allyl ester (61a)[93]**

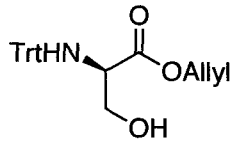


According to a similar procedure to **61**, (*R*)-trityl serine (8.0 g, 23 mmol) was converted to the title compound **61a** as a colorless oil (8.5 g, 95%). $[\alpha]_D^{25}$ 0.21° (*c* 1.0, $CHCl_3$); IR ($CHCl_3$, cast) 3454, 3057, 3031, 2934, 1731, 1595, 1490, 1448 $cm^{-1}$; $^1H$ NMR ($CDCl_3$, 500 MHz), δ 7.54 (m, 6H, Trt), 7.33-7.27 (m, 7H, Trt), 7.23-7.20 (m, 3H, Trt), 5.76-5.69 (m, 1H, $-CH_2-C\underline{H}=CH_2$), 5.26 (d, 1H, $J$ = 22.5 Hz, $-CH_2-CH=C\underline{H_2}$), 5.19 (d, 1H, $J$ = 10.5 Hz, $-CH_2-CH=C\underline{H_2}$), 4.24 (dd, 1H, $J$ = 6.0, 13.0 Hz, $-C\underline{H_2}-CH=CH_2$), 4.13 (dd, 1H, $J$ = 6.0, 13.0 Hz, $-C\underline{H_2}-CH=CH_2$), 3.76 (m, 1H, Ser-CHα), 3.60 (m, 2H, Ser-CHβ), 2.80 (br, 2H, OH and NH); $^{13}C$ NMR ($CDCl_3$, 125 MHz): δ 173.2, 145.6, 131.6, 128.7, 127.9, 126.6, 118.4, 71.0, 65.7, 64.9, 57.9; HRMS (ES): Calcd for $C_{25}H_{25}NO_3Na$ 410.1726, found 410.1725.

**(*S*)-Allyl 1- tritylaziridine-2-carboxylate (62)[88]**

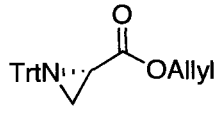


The known compound[88] was prepared according to a similar procedure to **55**, *N*-trityl serine allyl ester **61** (7.4 g, 1.9 mmol) was converted to the title compound **62** as a colorless oil (6.0 g, 86%). $[\alpha]_D^{25}$ -96.97° (*c* 1.00, $CHCl_3$); IR ($CHCl_3$, cast) 3057, 3031, 2984, 1746, 1595, 1489 $cm^{-1}$; $^1H$ NMR ($CDCl_3$, 500 MHz): δ 7.55 (m, 6H, Trt-H), 7.33-7.24 (m, 10H, Trt-H), 6.02-5.94 (m, 1H, $-CH_2-C\underline{H}=CH_2$),

5.38 (d, 1H, $J$ = 17.5 Hz, -$CH_2$-CH=C$\underline{H}_2$), 5.29 (d, 1H, $J$ = 10.5 Hz, -$CH_2$-CH=C$\underline{H}_2$), 4.72 (m, 2H, -C$\underline{H}_2$-CH=$CH_2$), 2.32 (m, 1H, Ser-Hα), 1.97 (dd, 1H, $J$ = 2.5, 6.0 Hz, Ser-Hβ), 1.46 (dd, 1H, $J$ = 2.5, 6.2 Hz, Ser-Hβ); $^{13}$C NMR ($CDCl_3$, 125 MHz): δ 171.3, 143.8, 132.2, 129.5, 127.8, 127.1, 118.7, 74.5, 65.7, 31.9, 28.9; HRMS (ES): Calcd for $C_{25}H_{23}NO_3Na$ 392.1621, found 392.1621.

**(*R*)-Allyl 1- tritylaziridine-2-carboxylate (62a)[88]**

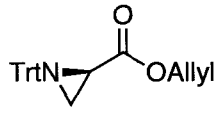


The known compound[88] was prepared according to a similar procedure to compound **55**, *N*-trityl-(*R*)-serine allyl ester **61a** (8.5 g, 22 mmol) was converted to the title compound **62a** as a colorless oil (7.6 g, 93%). $[\alpha]_D^{25}$ 73.62° (*c* 1.00, $CHCl_3$); IR ($CHCl_3$, cast) 3057, 3031, 2984, 1746, 1595, 1489 $cm^{-1}$; $^1$H NMR ($CDCl_3$, 400 MHz): δ 7.54 (m, 6H, Trt-H), 7.34-7.23 (m, 10H, Trt-H), 6.01-5.91 (m, 1H, -$CH_2$-C$\underline{H}$=$CH_2$), 5.37 (d, 1H, $J$ = 16.0 Hz, -$CH_2$-CH=C$\underline{H}_2$), 5.28 (d, 1H, $J$ = 10.4 Hz, -$CH_2$-CH=C$\underline{H}_2$), 4.70 (m, 2H, -C$\underline{H}_2$-CH=$CH_2$), 2.30 (dd, 1H, $J$ = 2.40, 1.60 Hz, Ser-Hα), 1.94 (dd, 1H, $J$ = 2.8, 6.4 Hz, Ser-Hβ), 1.40 (dd, 1H, $J$ = 1.6, 6.0 Hz, Ser-$H_6$); $^{13}$C NMR ($CDCl_3$, 100 MHz): δ 171.0, 143.5, 131.9, 129.2, 127.8, 127.5, 126.8, 118.4, 65.4, 31.6, 28.6; HRMS (ES): Calcd for $C_{25}H_{23}NO_3Na$ 392.1621, found 392.1623.

**(*2R, 3R*)-Allyl 3mehtyl-1-(4-nitrobenzyloxycarbonyl)aziridine-2-carboxylate (63)[88]**

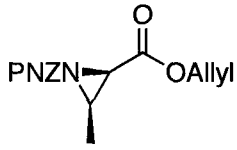


According to a similar procedure to **52**, the title compound **63** was prepared as a colorless oil (5.3 g, 80%) from **66** (8.0 g, 20.9 mmol). $[\alpha]_D^{25}$ 58.97° (*c* 1.00, $CHCl_3$); IR ($CHCl_3$, cast) 3083, 2940, 1733, 1608, 1523 $cm^{-1}$; $^1H$ NMR ($CDCl_3$, 400 MHz): δ 8.22 (d, 2H, *J* = 8.4 Hz, pNZ-H), 7.53 (d, 2H, *J* = 8.4 Hz, pNZ-H), 5.98-5.88 (m, 1H, $-CH_2C\underline{H}=CH_2$), 5.38-5.18 (m, 4H, $CH_2CH=C\underline{H}_2$ and $-C\underline{H}_2-C_6H_4-NO_2$), 4.69 (d, 2H, *J* = 6.0 Hz, $C\underline{H}_2CH=CH_2$), 3.23 (d, 1H, *J* = 6.8 Hz, CH), 2.87 (p, 1H, *J* = 6.8 Hz, $-C\underline{H}CH_3$), 1.39 (d, 3H, *J* = 6.8 Hz, $CHC\underline{H}_3$) ; $^{13}C$ NMR ($CDCl_3$, 125 MHz): δ 166.4, 161.0, 147.7, 142.3, 131.2, 128.4, 123.7, 119.1, 66.8, 66.1, 39.8, 39.0, 12.6; HRMS (ES): Calcd for $C_{15}H_{16}N_2O_6Na$ 343.0900, found 343.0912.

**(*R*)- *N*-Triphenylmethyl Threonine allyl ester (65)**

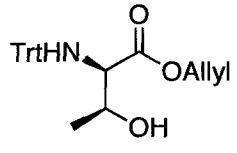


The compound was prepared by a modified literature procedure.[160] To a solution of D-threonine (5.0 g, 41.98 mmol) in toluene (100 mL), PTSA (9.58 g, 41.98 mmol) was added followed by ally alcohol (24.39 g, 419.8 mmol). The reaction was refluxed under Dean-Stark conditions for 24 h. After completion of the

reaction, the volatiles were removed *in vacuo*. The resulting residue was dissolved in EtOAc (100 mL) and cooled on ice. $Et_3N$ (21.1 mL, 151.2 mmol) was added dropwise and stirred for 10 min, followed by the addition of Trt-Cl (11.7 g, 41.97 mmol) in EtOAc (50 mL) via an addition funnel over 45 min. The reaction was stirred for 16 h at rt. The organic layer was then washed with $H_2O$ (2 x 150 mL), brine (1 x 100 mL) and dried with $Na_2SO_4$, filtered and then concentrated to yield the crude product as a light yellow sticky solid in quantitative yield (13.8 g), which was used for the next step without further purification. $[\alpha]_D^{25}$ -9.02° (*c* 2.3, $CHCl_3$); IR ($CHCl_3$, cast): 3470, 3084, 3058, 3020, 2979, 2935, 1729, 1648, 1596, 1491, 1447 $cm^{-1}$; $^1H$ NMR ($CDCl_3$, 500 MHz): δ 7.51-7.49 (m, 6H, Trt-H), 7.29-19 (m, 10H, Trt-H), 5.72-5.64 (m, 1H, $-CH_2-C\underline{H}=CH_2$), 5.21-5.16 (m, 2H, $-CH_2-CH=C\underline{H_2}$), 4.09 (dd, 1H, $J$ = 7.0, 14.0 Hz, $-C\underline{H_2}-CH=CH_2$), 3.87 (dd, 1H, $J$ = 7.0, 14.0 Hz, $-C\underline{H_2}-CH=CH_2$), 3.81 (app. d, 1H, $J$ = 6.5 Hz, Thr- $CH_\alpha$), 3.55 (br, 1H, OH), 3.42 (br, 1H, Thr-$CH_\alpha$), 2.87 (br, 1H, NH), 1.24 (d, 3H, $J$ = 6.0 Hz, Thr-$CH_3$); $^{13}C$ NMR ($CDCl_3$, 100 MHz): δ 172.8, 145.3, 131.4, 128.8, 127.7, 126.5, 118.7, 70.6, 69.7, 65.5, 62.4, 18.8; HRMS (ES): Calcd for $C_{26}H_{27}NO_3Na$ 424.1883, found 424.1880.

**(*2R, 3R*)-Allyl 3-methyl-1-tritylaziridine-2-carboxylate (66)[88]**

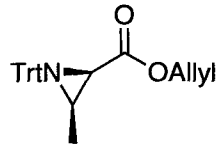


According to a similar procedure to compound **55**, the title compound **66** was prepared as a colorless oil (16.0 g, 99%) from compound **65**. $[\alpha]_D^{25}$ 98.37° (*c*

1.20, $CHCl_3$); IR ($CHCl_3$, cast) 3085, 3058, 3021, 2960, 2930, 1744, 1595, 1490, 1448$cm^{-1}$; $^1H$ NMR ($CDCl_3$, 400 MHz): δ 7.55 (m, 6H, Trt-H), 7.28-7.20 (m, 9H, Trt-H), 5.97-5.89 (m, 1H, $-CH_2-C\underline{H}=CH_2$), 5.34 (d, 1H, $J$ = 17.2 Hz, $-CH_2-CH=C\underline{H}_2$), 5.27 (d, 1H, $J$ = 10.4 Hz, $-CH_2-CH=C\underline{H}_2$), 4.67 (m, 2H, $-C\underline{H}_2-CH=CH_2$), 1.92 (d, 1H, $J$ = 6.5 Hz, Thr-Hα), 1.94 (p, 1H, $J$ = 6.5 Hz, Thr-Hβ), 1.38 (d, 3H, $J$ = 6.5 Hz, Thr-$CH_3$); $^{13}C$ NMR ($CDCl_3$, 100 MHz): δ 169.8, 143.8, 132.0, 129.3, 127.4, 126.7, 118.3, 74.8, 65.2, 35.9, 34.8, 13.2; HRMS (ES): Calcd for $C_{26}H_{25}NO_2Na$ 406.1777, found 406.1775.

**(*R*)-Methyl 2-(1,3-dioxoisoindolin-2-yl)-3-hydroxypropanoate (66a)[92]**

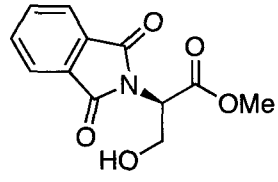


According to a similar procedure to formation of compound **56**, (*R*)-serine methyl ester hydrochloride (1.71 g, 10.9 mmol) was converted to the title compound **66a** as a colorless oil (2.2 g, 80%). $[\alpha]_D^{25}$ -17.86° (*c* 1.00, $CHCl_3$); IR ($CHCl_3$, cast): 3476, 2956, 1773, 1745, 1715, 1612, 1468 $cm^{-1}$; $^1H$ NMR ($CDCl_3$, 500 MHz): δ 7.87 (dd, 2H, $J$ = 3.0, 5.5 Hz, Ar-H), 7.58 (dd, 2H, $J$ = 3.0, 5.5 Hz, Ar-H), 5.02 (dd, 1H, $J$ = 4.5, 6.0 Hz, Ser-Hα), 4.20 (m, 2H, Ser-Hβ), 3.78 (s, 3H, $-OC\underline{H}_3$); $^{13}C$ NMR ($CDCl_3$, 125 MHz): δ 168.4, 168.0, 134.4, 131.6, 123.7, 61.0, 54.7, 52.8; HRMS (ES): Calcd for $C_{12}H_{11}NO_5Na$ 272.0529, found 272.0529.

**(*R*)-Ethyl 2-(1,3-dioxoisoindolin-2-yl)-3-hydroxypropanoate (66b)[92]**

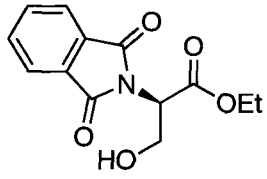

According to a similar procedure to formation of compound **56**, (*R*)-serine ethyl ester hydrochloride (2.0 g, 11.83 mmol) was converted to the title compound **66b** as a light yellow oil (2.41 g, 78%). $[\alpha]_D^{25}$ -26.63° (*c* 1.60, $CHCl_3$); IR ($CHCl_3$, cast): 3480, 2983, 1776, 1716, 1612, 1468 $cm^{-1}$; $^1H$ NMR ($CDCl_3$, 400 MHz): δ 7.83 (dd, 2H, *J* = 3.0, 5.7 Hz, Ar-H), 7.73 (dd, 2H, *J* = 3.0, 5.7 Hz, Ar-H), 5.98 (dd, 1H, *J* = 4.5, 5.4 Hz, Ser-Hα), 4.20 (m, 4H, Ser-Hβ and $C\underline{H}_2CH_3$), 3.53 (m, 1H, OH), 1.22 (t, 3H, *J* = 7.2 Hz, $CH_2C\underline{H}_3$); $^{13}C$ NMR ($CDCl_3$, 125 MHz): δ 168.0, 134.4, 131.7, 123.7, 62.1, 61.0, 54.8, 14.0; HRMS (ES): Calcd for $C_{13}H_{13}NO_5Na$ 286.0685, found 286.0684

**(2*S*,3*R*)-Methyl 2-(1,3-dioxoisoindolin-2-yl)-3-hydroxybutanoate (66c)[92]**

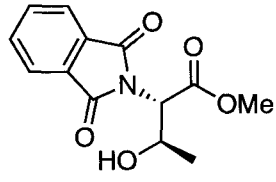

According to a similar procedure to formation of compound **56**, (*S*)-threonine methyl ester hydrochloride (3.0 g, 17.7 mmol) was coverted to the title compound **66c** as a light yellow solid (4.0 g, 86%). $[\alpha]_D^{25}$ 21.37° (*c* 1.0, $CHCl_3$); IR ($CHCl_3$, cast): 3453, 2955, 1775, 1747, 1716, 1611, 1468 $cm^{-1}$; $^1H$ NMR ($CDCl_3$, 300

MHz): δ 7.87 (dd, 2H, $J$ = 3.0, 5.4 Hz, Ar-H), 7.75 (dd, 2H, $J$ = 3.0, 5.4 Hz, Ar-H), 4.94 (d, 1H, $J$ = 4.5 Hz, Thr-Hα), 4.62 (m, H, Thr-Hβ), 4.01 (d, $J$ = 9.6 Hz, -OH), 3.75(s, 3H, -OC$\underline{H}_3$), 1.19 (d, 3H, $J$=6.6 Hz, Thr-C$\underline{H}_3$); $^{13}$C NMR ($CDCl_3$, 125 MHz): δ 168.6, 168.2, 134.5, 131.6, 123.8, 66.6, 59.1, 52.8, 20.2; HRMS (ES): Calcd for $C_{13}H_{13}NO_5Na$ 286.0685, found 286.0685.

**(2*R*,3*S*)-Methyl 2-(1,3-dioxoisoindolin-2-yl)-3-hydroxybutanoate (66d)[92]**

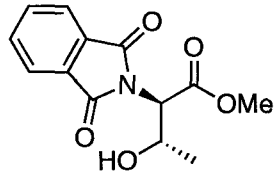


According to a similar procedure to formation of compound **56**, (*R*)-threonine methyl ester hydrochloride (3.0 g, 17.7 mmol) was converted to the title compound **66d** as a solid (3.7 g, 80%). $[\alpha]_D^{25}$ -21.96° (*c* 1.0, $CHCl_3$); IR ($CHCl_3$, cast): 3455, 2955, 1775, 1747, 1716, 1612, 1468 cm$^{-1}$; $^1$H NMR ($CDCl_3$, 500 MHz): δ 7.89 (dd, 2H, $J$ = 3.0, 5.0 Hz, Ar-H), 7.77 (dd, 2H, $J$ = 3.0, 5.0 Hz, Ar-H), 4.96 (d, 1H, $J$ = 4.0 Hz, Thr-Hα), 4.64 (m, 1H, Thr-Hβ), 3.78 (s, 3H, -OC$\underline{H}_3$), 1.21 (d, 3H, $J$ = 6.5 Hz, Thr-$CH_3$); $^{13}$C NMR ($CDCl_3$, 125 MHz): δ 168.6, 168.2, 134.5, 131.6, 123.8, 66.6, 59.1, 52.8, 20.2; HRMS (ES): Calcd for $C_{13}H_{13}NO_5Na$ 286.0685, found 286.0685.

**General procedure of the ring opening reaction of aziridine with oxygen nucleophile catalyzed by $BF_3$•$OEt_2$**

**Method A**

To a stirred solution of aziridine-2-carboxylate and the oxygen nucleophile (2.0 equiv) in toluene was added $BF_3$•$OEt_2$ (0.5 equiv) dropwise at rt. The resulting reaction mixture was refluxed at 110 °C for 2 h. After completion of the reaction, the solvent was removed under reduced pressure and the crude product was purified by flash column chromatography to provide the corresponding product.

**Method B**

To a stirred solution of aziridine-2-carboxylate and the oxygen nucleophile (2.0 equiv) in ethanol-free chloroform was added $BF_3$•$OEt_2$ (0.2 equiv) dropwise at 0 °C. The resulting reaction mixture was warmed to 40 °C and stirred for 24 h. After completion of the reaction, the solvent was removed under reduced pressure and the crude product was purified by flash column chromatography to provide the corresponding product.

For the ease of assignment, the two amino acid moieties of all ether linked bis-amino acid derivatives have been indicated:

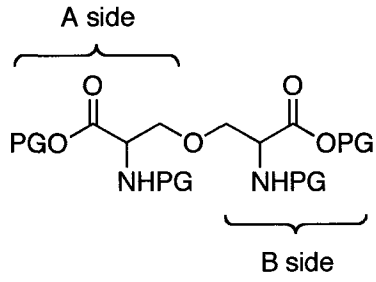

**(*R*)-Methyl 2-(1, 3-dioxoisoindolin-2-yl)-3-((*S*)-3-methoxy-2-((4-nitrobenzyloxy)carbonylamino)-3-oxopropoxy)propanoate (67a)**

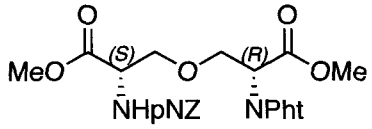


Method A was used to prepare the title compound **67a** from compound **52** (500 mg, 1.77 mmol) and **66a** (882 mg, 3.54 mmol) as a colorless oil (695 mg, 74%). $[\alpha]_D^{25}$ 69.94° (*c* 1.00, $CHCl_3$); IR ($CHCl_3$, cast): 3374, 2955, 1717, 1608, 1522 $cm^{-1}$; $^1H$ NMR ($CDCl_3$, 600 MHz): δ 8.22 (d, 2H, *J* = 8.4 Hz, pNZ-H), 7.86 (dd, 2H, *J* = 5.4, 3.0 Hz, Pht-H), 7.75 (dd, 2H, *J* = 5.4, 3.0 Hz, Pht-H), 7.52 (d, 2H, *J* = 8.4 Hz, pNZ-H), 5.69 (d, 1H, *J* = 8.4 Hz, NH), 5.22 (d, 1H, *J* = 13.8 Hz, -O-C$\underline{H_2}$-Ar), 5.19 (d, 1H, *J* = 13.8Hz, -O-C$\underline{H_2}$-Ar), 5.10 (dd, 1H, *J* = 6.0, 9.0Hz, Hα B side), 4.42 (dt, 1H, *J* = 9.0, 3.0 Hz, Hα' A side), 4.17-4.11 (m, 2H, Hβ B side), 3.88 (dd, 1H, *J* = 9.0, 3.0 Hz, Hβ' A side), 3.78 (dd, 1H, *J* = 9.0, 3.0 Hz, Hβ' A side), 3.75 (s, 3H, $OCH_3$), 3.49 (s, 3H, $OCH_3$); $^{13}C$ NMR ($CDCl_3$, 125 MHz): δ 170.0, 167.5, 167.3, 155.4, 143.7, 134.2, 131.7, 127.8, 123.7, 123.6, 123.5, 70.6, 67.9, 65.3, 54.2, 52.8, 52.5, 51.1; HRMS (ES): Calcd for $C_{24}H_{23}N_3O_{11}Na$ 552.1224, found 552.1222.

**(*S*)-Allyl 3-((*R*)-2-(1,3-dioxoisoindolin-2-yl)-3-ethoxy-3-oxopropoxy)-2-((4-nitrobenzyloxy)carbonylamino)propanoate (67b)**

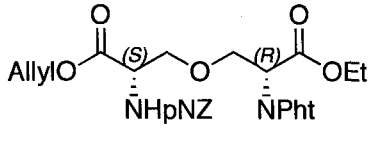

Method A was used to prepare the title compound **67b** from **58** (100 mg, 0.33 mmol) and **66b** (172 mg, 0.65 mmol) as a colorless oil (135 mg, 72%). $[\alpha]_D^{25}$ 48.28° (*c* 0.4, $CHCl_3$); IR ($CHCl_3$, cast): 3360, 2936, 1777, 1717, 1607, 1521, 1467 $cm^{-1}$; $^1H$ NMR ($CDCl_3$, 300 MHz): δ 8.20 (d, 2H, *J* = 8.7 Hz pNZ-H), 7.83 (dd, 2H, *J* = 5.4, 3.0 Hz Pht-H), 7.73 (dd, 2H, *J* = 5.4, 3.0 Hz Pht-H), 7.51 (d, 2H, *J* = 8.7 Hz pNZ-H), 5.78-5.56(m, 2H, $CH_2C\underline{H}CH_2$ and NH), 5.25-5.05 (m, 5H, $CH_2CH=C\underline{H}_2$, O-$C\underline{H}_2$-Ar and Hα B side), 4.46-4.36 (m, 3H, $C\underline{H}_2CH=CH_2$ + Hα' A side ), 4.26-4.10 (m, 4H, $OC\underline{H}_2CH_3$ + 2Hβ B side), 3.91 (dd, 1H, *J* = 3.0, 9.6 Hz, Hβ A side), 3.79 (dd, 1H, *J*=3.0, 9.6 Hz, Hβ A side), 1.22 (t, 3H, *J* = 7.2 Hz, $C\underline{H}_3$); $^{13}C$ NMR ($CDCl_3$, 100 MHz): δ 169.1, 167.2, 166.9, 155.4, 147.4, 143.7, 134.1, 131.6, 131.1, 127.8, 123.6, 123.4, 118.4, 70.7, 67.9, 65.8, 65.2, 62.0, 54.2, 51.2, 13.9; HRMS (ES): Calcd for $C_{27}H_{27}N_3O_{11}Na$ 592.1537, found 592.1537.

**(2*R*, 3*S*)-Allyl 3-((R)-2-(1, 3-dioxoisoindolin-2-yl)-3ethoxy-3-oxopropoxy)-2-((4-nitrobenzyloxy)carbonylamino)butanoate (67c)**

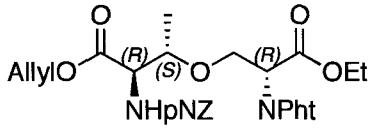


Method A was used to prepare the title compound **67c** from **63** (200 mg, 0.62 mmol) and **66b** (326 mg, 1.24 mmol) as a colorless oil (250 mg, 70%). $[\alpha]_D^{25}$ 24.85° (*c* 0.4, $CHCl_3$); IR ($CHCl_3$, cast): 3369, 2981, 1777, 1717, 1607, 1521, 1468 $cm^{-1}$; $^1H$ NMR ($CDCl_3$, 400 MHz): δ 8.17 (d, 2H, *J* = 8.4 Hz, pNZ-H), 7.84 (dd, 2H, *J* = 5.4, 3.0 Hz, Pht-H), 7.73 (dd, 2H, *J* = 5.4, 3.0 Hz, Pht-H), 7.48 (d, 2H, *J* = 9.0 Hz, pNZ-H), 5.87 (m, 1H, $CH_2C\underline{H}CH_2$), 5.55(d, 1H, *J* = 9.5 Hz, NH),

5.30 (d, 1H, $J$ = 17 Hz, $CH_2CH=C\underline{H}_2$), 5.22 (d, 1H, $J$ = 10.0 Hz, $CH_2CH=C\underline{H}_2$), 5.20 (d, 1H, $J$ = 13.8 Hz, -O-$C\underline{H}_2$-Ar), 5.14 (d, 1H, $J$ = 13.8 Hz, -O-$C\underline{H}_2$-Ar), 4.98 (dd, $J$ = 5.0, 9.1 Hz, Hα B side), 4.59 (m, 2H, $C\underline{H}_2CH=CH_2$ ), 4.28-4.11 (m, 5H, Hα' + Hβ' A side, $OC\underline{H}_2CH_3$ and Hβ B side), 3.99 (dd, 1H, $J$ = 5.1, 10.1 Hz, Hβ B side), 1.21 (t, 3H, $J$ = 7.1 Hz, $CH_2C\underline{H}_3$), 1.11 (d, 3H, $J$ = 6.3 Hz, $C\underline{H}_3$); $^{13}C$ NMR ($CDCl_3$, 100 MHz): δ 169.9, 167.4, 167.0, 156.1, 147.5, 143.8, 134.2, 131.7, 131.5, 127.8, 123.6, 123.5, 118.9, 75.3, 66.1, 65.8, 65.3, 62.0, 58.6, 51.9, 16.4, 14.0; HRMS (ES): Calcd for $C_{28}H_{29}N_3O_{11}Na$ 606.1694, found 606.1692

**(2*S*,3*R*)-Methyl 3-((*S*)-3-(allyloxy)-2-((4-nitrobenzyloxy)carbonylamino-3-oxopropoxy)-2-(1,3-dioxoisoindolin-2-yl)butanoate (67d)**

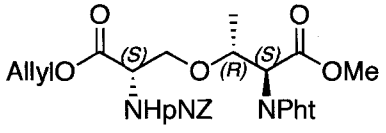


Method A was used to prepare the title compound **67d** from **58** (100 mg, 0.32 mmol) and **66c** (171 mg, 0.65 mmol) as a colorless oil (80 mg, 43%). $[\alpha]_D^{25}$ 24.25° (*c* 0.4, $CHCl_3$); IR ($CHCl_3$, cast): 3364, 2952, 1719, 1608, 1521, 1468, 2979, 1719, 1608, 1522, 1468 $cm^{-1}$; $^1H$ NMR ($CDCl_3$, 400 MHz): δ 8.22 (d, 2H, $J$ = 8.0 Hz, pNZ-H), 7.84 (dd, 2H, $J$ = 3.0, 5.5 Hz, Pht-H), 7.71 (dd, 2H, $J$ = 3.0, 5.5 Hz, Pht-H), 7.54 (d, 2H, $J$ = 8.0 Hz, pNZ-H), 6.10(d, 1H, $J$ = 8.9 Hz, NH), 5.74 (m, 1H, $CH_2C\underline{H}=CH_2$), 5.25 (d, 1H, $J$ = 13.9 Hz, -O-$C\underline{H}_2$-Ar), 5.17 (d, 1H, $J$ = 13.9 Hz, -O-$C\underline{H}_2$-Ar), 5.19 (dd, 1H, $J$ =1.4, 15.6 Hz, $CH_2CH=C\underline{H}_2$), 5.09 (dd, 1H, $J$ = 1.3, 10.4 Hz, $CH_2CH=C\underline{H}_2$), 4.73 (d, 1H, $J$ = 4.6 Hz, Hα B Side), 4.49 (m, 2H, $C\underline{H}_2CH=CH_2$), 4.38 (m, 2H, Hα' A side and Hβ B side ), 4.11 (dd, 1H, $J$ =

2.2, 8.9 Hz, Hβ' A side), 3.73 (m, 1H, Hβ' A Side), 3.71 (s, 3H, -$OCH_3$), 1.22 (d, 3H, *J* = 6.3 Hz, -$CH_3$); $^{13}C$ NMR ($CDCl_3$, 100 MHz): δ 169.3, 168.0, 167.5, 155.7, 147.3, 144.2, 134.1, 131.6, 131.4, 127.5, 123.5, 123.5, 118.1, 73.5, 69.5, 65.7, 64.9, 56.0, 54.5, 52.6, 17.8; HRMS (ES): Calcd for $C_{27}H_{27}N_3O_{11}Na$ 592.1537, found 592.1543.

**(2*R*,3*S*)-Methyl 3-((*S*)-3-(allyloxy)-2-((4-nitrobenzyloxy)carbonylamino-3-oxopropoxy)-2-(1,3-dioxoisoindolin-2-yl)butanoate (67e)**

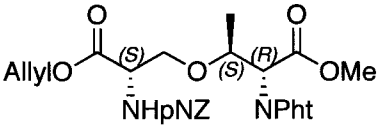


Method A was used to prepare the title compound **67e** from **58** (100 mg, 0.35 mmol) and **66c** (171 mg, 0.65 mmol) as a colorless oil (86 mg, 47%). $[\alpha]_D^{25}$ 36.16° (*c* 0.3, $CHCl_3$); IR ($CHCl_3$, cast): 3366, 2953, 1747, 1720, 1608, 1522, 1468 $cm^{-1}$; $^1H$ NMR ($CDCl_3$, 600 MHz): $^1H$ NMR ($CDCl_3$, 400 MHz,) δ 8.19 (d, 2H, *J* = 8.8 Hz, pNZ-H), 7.84 (dd, 2H, *J* = 3.2, 5.6 Hz, Pht-H), 7.73 (dd, 2H, *J* = 3.2, 5.6 Hz, Pht-H), 7.49 (d, 2H, *J* = 8.8 Hz, pNZ-H), 5.76(m, 1H, $CH_2C\underline{H}=CH_2$), 5.68 (d, 1H, *J* = 8.8 Hz, NH), 5.23-5.13 (m, 4H, O-$C\underline{H}_2$-Ar and $CH_2CH=C\underline{H}_2$), 4.73 (d, 1H, *J* = 7.2Hz, Hα B side), 4.39-4.32 (m, 4H, $C\underline{H}_2CH=CH_2$ and Hβ B side), 4.25 (dd, *J* = 5.6, 13.2 Hz, Hα' A side), 3.80 (m, 2H, Hβ' A side), 3.71 (s, 3H, -$OCH_3$), 1.35 (d, 3H, *J* = 6.0 Hz, -$CH_3$); $^{13}C$ NMR ($CDCl_3$, 100 MHz): δ 169.2, 167.7, 167.3, 155.5, 147.4, 143.8, 134.0, 131.6, 131.4, 127.8, 123.5, 123.4, 118.4, 72.7, 68.1, 65.7, 65.1, 56.0, 54.2, 52.6, 17.8; HRMS (ES): Calcd for $C_{27}H_{27}N_3O_{11}Na$ 592.1537, found 592.1536.

**(2*R*, 3*S*)-Allyl 3-((2*S*,3*R*)-3-(1,3-dioxoisoindolin-2-yl)-4-methoxy-4-oxobutan-2-yloxy)-2-((4-nitrobenzyloxy)carbonylamino)butanoate (67f)**

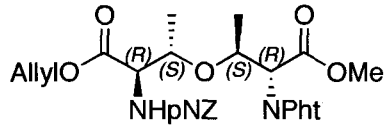


Method A was used to prepare the title compound **67f** from **63** (200 mg, 0.62 mmol) and **66c** (326 mg, 1.24 mmol) as a colorless oil (260 mg, 72%). $[\alpha]_D^{25}$ 26.87° (*c* 0.5, $CHCl_3$); IR ($CHCl_3$, cast): 3368, 2979, 1719, 1608, 1522, 1468 $cm^{-1}$; $^1H$ NMR ($CDCl_3$, 600 MHz): δ 8.22 (d, 2H, *J* = 8.5 Hz, pNZ-H), 7.84 (dd, 2H, *J* = 3.0, 5.5 Hz, Pht-H), 7.70(dd, 2H, *J* = 3.0, 5.5 Hz, Pht-H), 7.54 (d, 2H, *J* = 8.5 Hz, pNZ-H), 5.76-5.69 (m, 2H, NH and $CH_2C\underline{H}=CH_2$), 5.26 (d, 1H, *J* = 13.8 Hz, -O-$C\underline{H}_2$-Ar), 5.15 (d, 1H, *J* = 13.8 Hz, -O-$C\underline{H}_2$-Ar), 5.18 (dd, 1H, *J* = 1.2, 17.4 Hz, $CH_2CH=C\underline{H}_2$), 5.09 (dd, 1H, *J* = 1.2, 10.8 Hz, $CH_2CH=C\underline{H}_2$), 4.72 (d, 1H, *J* = 5.4 Hz, Hα B side), 4.46 (m, 2H, $C\underline{H}_2CH=CH_2$), 4.39 (p, 1H, *J* = 6.0 Hz Hα B side), 4.23-4.19 (m, 2H, Hα' and Hβ' A side), 3.73 (s, 3H, -$OCH_3$), 1.16 (d, 3H, *J* = 6.0 Hz, -$CH_3$ B side), 1.09 (d, 3H, *J* = 6.6 Hz, -$CH_3$ A side); $^{13}C$ NMR ($CDCl_3$, 125 MHz): δ 169.9, 167.6, 167.5, 156.5, 147.5, 144.3, 134.2, 131.6, 131.4, 127.6, 123.6, 123.5, 118.7, 71.1, 69.1, 65.9, 65.1, 59.2, 56.3, 52.6, 17.2, 15.7; HRMS (ES): Calcd for $C_{28}H_{29}N_3O_{11}Na$ 606.1694, found 606.1694.

**(2*R*, 3*S*)-Allyl 3-((2*R*,3*S*)-3-(1,3-dioxoisoindolin-2-yl)-4-methoxy-4-oxobutan-2-yloxy)-2-((4-nitrobenzyloxy)carbonylamino)butanoate (67g)**

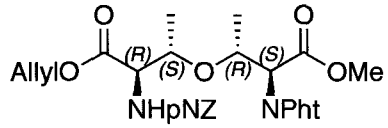

Method A was used to prepare the title compound **67g** from **63** (200 mg, 0.62 mmol) and **66d** (326 mg, 1.24 mmol) as a colorless oil (255 mg, 71%). $[\alpha]_D^{25}$ 4.33° (*c* 0.3, $CHCl_3$); IR ($CHCl_3$, cast): 3367, 2981, 1720, 1608, 1522, 1437 $cm^{-1}$; $^1H$ NMR ($CDCl_3$, 600 MHz): δ 8.22 (d, 2H, *J* = 9.0 Hz, pNZ-H), 7.86(dd, 2H, *J* = 3.0, 5.4 Hz, Pht-H), 7.74(dd, 2H, *J* = 3.0, 5.4 Hz, Pht-H), 7.52 (d, 2H, *J* = 9.0 Hz, pNZ-H), 5.90-5.84 (m, 2H, NH and $CH_2C\underline{H}=CH_2$), 5.31 (dd, 1H, *J* = 1.2, 15.6 Hz, $CH_2CH=C\underline{H}_2$), 5.22 (dd, 1H, *J* = 1.2, 11.4 Hz, $CH_2CH=C\underline{H}_2$), 5.24 (d, 1H, *J* = 13.8 Hz, -O-$C\underline{H}_2$-Ar), 5.19 (d, 1H, *J* = 13.8 Hz, -O-$C\underline{H}_2$-Ar), 4.71 (d, 1H, *J* = 5.4 Hz, Hα B side), 4.53 (dd, 2H, *J* = 1.2, 6.0 Hz $C\underline{H}_2CH=CH_2$), 4.42 (p, 1H, *J* = 6.0Hz Hα B side ), 4.27 (qd, 1H, *J* = 2.4, 6.6 Hz, Hβ' A side), 4.15 (dd, *J* = 2.4, 9.6 Hz, Hα' A side), 3.71 (s, 3H, -$OCH_3$), 1.32 (d, 3H, *J* = 6.0 Hz, -$CH_3$ B side), 1.21 (d, 3H, *J* = 6.0 Hz, -$CH_3$ A side); $^{13}C$ NMR ($CDCl_3$, 125 MHz): δ 169.9, 167.7, 167.6, 156.3, 144.2, 134.1, 131.8, 131.7, 127.7, 123.6, 123.5, 118.5, 77.0, 76.7, 73.8, 72.5, 66.0, 65.1, 59.0, 56.4, 52.6, 19.5, 19.2; HRMS (ES): Calcd for $C_{28}H_{29}N_3O_{11}Na$ 606.1694, found 606.1694.

**(2*S*,4*R*)-1-(9*H*-Fluoren-9-yl)methyl 2-methyl 4-hydroxypyrrolidine-1,2-dicarboxylate (71)**

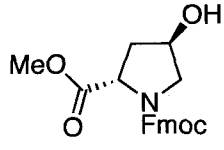


The known compound was prepared by a modified literature procedure.[161] A solution of $Na_2CO_3$ (2.09 g, 19.81 mmol) in $H_2O$ (20 mL) was added dropwise at 0 °C to a solution of HCl•H-Hyp-OMe (3.0 g, 16.5 mmol) and Fmoc-OSu (6.68 g,

19.81 mmol) in dioxane (150 mL) and $H_2O$ (30 mL). The reaction mixture was warmed to rt and stirred for 24 h. After completion of the reaction, the solvent was removed under reduced pressure. The resulting residue was dissolved in EtOAc (100 mL), washed with water (3 x 100 mL) and dried with $Na_2SO_4$. Filtration and concentration *in vacuo* yielded the crude product, which was further purified by flash chromatography ($SiO_2$, 7:1/Hexanes: EtOAc) to yield **71** as a colorless oil (5.9 g, 97%). $[\alpha]_D^{25}$ -59.76° (*c* 3.10, $CHCl_3$); IR ($CHCl_3$, cast): 3447, 3016, 2952, 1747, 1703, 1451, 1426cm$^{-1}$; $^1$H NMR ($CDCl_3$, 500 MHz, rotamers): 7.76-7.30 (m, 8H, Fmoc-H), 4.55-4.32 (m, 4H), 4.28-4.15 (m 1H, CH-Fmoc), 3.75-3.55 (m, 5H, -OC<u>H</u>$_3$ + -C<u>H</u>$_2$-), 2.56 (br, 1H, OH), 2.33 (m, 1H, CH<u>*H*</u>), 2.07 (m, 1H, C<u>*H*</u>H); $^{13}$C NMR ($CDCl_3$, 125 MHz, rotamers): δ 173.1(s), 155.0(s), 144.0(s), 141.2(s), 127.7(d), 127.0(d), 125.1(d), 119.9(d), 70.0(d), 67.7(t), 57.9(d), 55.2(t), 52.3(q), 47.2(d), 39.3(t); HRMS (ES): Calcd for $C_{21}H_{21}NO_5Na$ 390.1311, found 390.1308.

**(2*S*,4*R*)-1-(9*H*-Fluoren-9-yl)methyl 2-methyl 4-((*R*)-3-(allyloxy)-2-((4-nitrobenzyloxy)carbonylamino)-3-oxopropoxy)pyrrolidine-1,2-dicarboxylate (72a)**

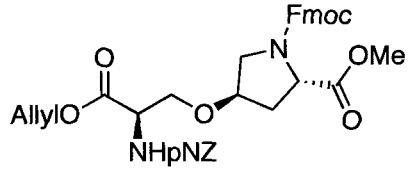


Method A was used to prepare the title compound **72a** from **59** (200 mg, 0.65 mmol) and **71** (478 mg, 1.30 mmol) as a colorless oil (270 mg, 62%). $[\alpha]_D^{25}$ -

37.90° (*c* 0.35, $CHCl_3$); IR ($CHCl_3$, cast): 3331, 2951, 1746, 1709, 1607, 1522, 1451, 1421 $cm^{-1}$; $^1H$ NMR ($CDCl_3$, 500 MHz, rotamers ) δ 8.20 (d, 2H, *J* = 11.5 Hz, pNZ-H), 7.76 (t, 2H, *J* = 7.5Hz, arom. Fmoc-H), 7.60-7.50 (m, 4H, arom. Fmoc-H and pNZ-H), 7.39 (m, 2H, arom. Fmoc-H), 7.31 (m, 2H, arom. Fmoc-H), 5.95-5.81 (m, 1H, $CH_2C\underline{H}=CH_2$), 5.66 (m, 1H, NH), 5.39-5.16 (m, 4H, $CH_2CH=C\underline{H_2}$ and O-$C\underline{H_2}$-Ar), 4.70- 4.40 (m, 9H, $CH_2$-Fmoc, $H_\alpha$ A side and $H_\beta$ A Side+ CH-Fmoc, -O-C<u>H</u>- B side and $H_\alpha$ B side), 3.75-3.50 (m, 5H, -O$C\underline{H_3}$ + CH-$C\underline{H_2}$-N- B side), 2.35 (m, 1H, OCH-CH*<u>H</u>*-CH- B side), 2.12 (m, 1H, OCH-C*<u>H</u>*H-CH- B Side); $^{13}C$ NMR ($CDCl_3$, 100 MHz, rotamers): δ 172.8, 169.4, 155.5, 154.7, 147.6, 144.0, 143.6, 141.2, 131.3, 128.0, 127.7, 127.0, 125.0, 123.7, 120.0, 119.0, 78.0, 68.9, 67.7, 66.6, 65.5, 57.8, 54.4, 52.4, 51.6, 47.2, 36.7; HRMS (ES): Calcd for $C_{35}H_{35}N_3O_{11}Na$ 696.2163, found 696.2162.

**(2*S*,4*R*)-1-(9*H*-Fluoren-9-yl)methyl 2-methyl 4-((2*S*,3*R*)-4-(allyloxy)-3-((4-nitrobenzyloxy)carbonylamino)-4-oxobutan-2-yloxy)pyrrolidine-1,2-dicarboxylate (72b)**

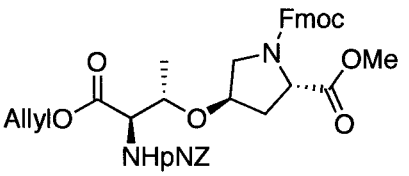


Method A was used to prepare the title compound **72b** from **63** (200 mg, 0.62 mmol) and **71** (455 mg, 1.24 mmol) as a colorless oil (200 mg, 47%). $[\alpha]_D^{25}$ -37.88° (*c* 0.8, $CHCl_3$); IR ($CHCl_3$, cast): 3423, 2952, 1731, 1710, 1607, 1522, 1451, 1421 $cm^{-1}$; $^1H$ NMR ($CDCl_3$, 400 MHz, rotamers): δ 8.20 (d, 2H, *J* = 9.0

Hz, pNZ-H), 7.76 (m, 2H, arom. Fmoc-H), 7.61-7.50 (m, 4H, arom. Fmoc-H+pNZ-H), 7.42-7.29 (m, 4H, Fmoc-H), 5.86 (m, 1H, $CH_2C\underline{H}=CH_2$), 5.48(d, 1H, $J$ = 9.0 Hz, NH), 5.33-5.18 (m, 4H, $CH_2CH=C\underline{H}_2$ and O-$C\underline{H}_2$-Ar), 4.63-4.56 (m, 2H, $C\underline{H}_2CH=CH_2$ ), 4.47-4.15 (m, 8H, $CH_2$-Fmoc, $H_a$ A side, $H_b$ A Side, CH-Fmoc, -O-C$\underline{H}$- B side and $H_a$ B side), 3.75-3.55 (m, 5H, -O$C\underline{H}_3$ and CH-$C\underline{H}_2$-N- B side), 2.32-2.26 (m, 1H, OCH-CH$\underline{H}$-CH- B side), 2.13-2.07 (m, 1H, OCH-C$\underline{H}$H-CH- B Side), 1.26-1.24 (m, 3H, -$CH_3$ A side); $^{13}$C NMR ($CDCl_3$, 100 MHz, rotamers) δ 172.8, 169.8, 156.1, 154.7, 147.6, 144.0, 143.7, 141.2, 131.3, 128.2, 127.7, 127.0, 125.1, 123.7, 119.9, 119.4, 75.5, 74.3, 67.7, 66.4, 65.5, 58.9, 57.9, 52.4, 51.7, 47.2, 37.6, 16.9; HRMS (ES): Calcd for $C_{36}H_{37}N_3O_{11}Na$ 710.2320, found 710.2315

**(*S*)-*tert*-Butyl 2-(((9*H*-fluoren-9-yl)methoxy)carbonylamino)-3-hydroxypropanoate (73)**

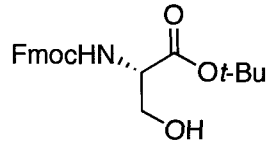


The known compound was prepared by a modified literature procedure.[161] A solution of $Na_2CO_3$ (2.57g, 24.29 mmol) in $H_2O$ (10 mL) was added dropwise at 0 °C to a solution of HCl•H-Ser-O-*t*-Bu (4.0 g, 20.4 mmol) and Fmoc-OSu (8.19 g, 24.29 mmol) in dioxane (100 mL) and $H_2O$ (40 mL). The reaction mixture was warmed to room temperature and stirred for 48 h. After completion of the reaction, the solvent was removed under reduced pressure. The resulting residue was dissolved in EtOAc (100 mL). The organic solution was washed with water

(3 x 100 mL) and dried with $Na_2SO_4$. Filtration and concentration *in vacuo* yielded the crude product, which was further purified by recrystallization from EtOAc and Hexanes to give **73** as a white solid (7.0 g, 90%). mp 127-130 °C (lit.[162] mp 130 °C); $[\alpha]_D^{25}$ 5.88° (*c* 1.20, $CHCl_3$); IR ($CHCl_3$, cast): 3425, 3066, 3007, 2978, 2889, 1720, 1517, 1450cm$^{-1}$; $^1$H NMR ($CDCl_3$, 400 MHz): 7.76 (d, 2H, *J* = 7.5 Hz, Fmoc-H), 7.60 (d, 2H, *J* = 7.1 Hz, Fmoc-H), 7.40 (t, 2H, *J* = 7.5 Hz, Fmoc-H), 7.31 (t, 2H, *J* = 7.5 Hz, Fmoc-H), 5.80 (d, 1H, *J* = 6.4 Hz, NH), 4.41 (d, *J* = 6.8 Hz, $CH_2$-Fmoc), 4.33 (br, 1H, Ser-$H_\alpha$), 4.22 (t, 1H, *J* = 6.8 Hz, CH-Fmoc), 3.93 (br, 2H, Ser-$H_\beta$), 1.49 (s, 9H, -$C(CH_3)_3$); $^{13}$C NMR ($CDCl_3$, 125 MHz): δ 169.4, 156.2, 143.7, 143.6, 141.2, 141.1, 127.6, 126.9, 124.9, 119.8, 119.8, 82.7, 67.0, 63.5, 56.5, 47.0, 27.9; HRMS (ES): Calcd for $C_{22}H_{25}NO_5Na$ 406.1624, found 406.1619.

**(*S*)-Allyl 3-((*S*)-2-(((9*H*-fluoren-9-yl)methoxy)carbonylamino)-3-*tert*-butoxy-3-oxopropoxy)-2-((4-nitrobenzyloxy)carbonylamino)propanoate (75a)**

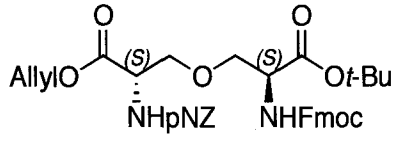


Method B was used to prepare the title compound **75a** from **58** (100 mg, 0.32 mmol) and **73** (250 mg, 0.65 mmol) as a colorless oil (80 mg, 36%). $[\alpha]_D^{25}$ 12.88° (*c* 2.0, $CHCl_3$); IR ($CHCl_3$, cast): 3335, 3067, 2978, 2938, 2880, 1726, 1607, 1522, 1478, 1451 cm$^{-1}$; $^1$H NMR ($CDCl_3$, 500 MHz): δ 8.18 (d, 2H, *J* = 8.4 Hz, pNZ-H), 7.76 (d, 2H, *J* = 8.4 Hz, Fmoc-H), 7.60 (t, 2H, *J* = 7.2 Hz, Fmoc-H), 7.47 (d, 2H, *J* = 8.4 Hz, pNZ-H), 7.40 (t, 2H, *J* = 7.2 Hz, Fmoc-H), 7.31 (t, 2H, *J*

= 8.4 Hz, Fmoc-H), 5.88 (m, 1H, $CH_2C\underline{H}=CH_2$), 5,71 (d, 1H, $J$ = 8.4 Hz, NH), 5.54 (d, 1H, $J$ = 8.4 Hz, NH), 5.29 (d, 1H, $J$ = 20.4 Hz, $CH_2CH=C\underline{H_2}$), 5.21 (d, 2H, $J$ = 15.6 Hz, $CH_2CH=C\underline{H_2}$ and O-$C\underline{H_2}$-Ar ), 5.14 (d, 1H, $J$ = 16.2 Hz, , O-$C\underline{H_2}$-Ar), 4.65 (m, 2H, $C\underline{H_2}CH=CH_2$ ), 4.57-4.34 (m, 4H, $CH_2$-Fmoc + $H_\alpha$, A side + $H_\alpha$ B side), 4.21 (t, 1H, $J$ = 7.0 Hz, CH-Fmoc), 3.98 (d, 1H, $J$ =7.5 Hz, $H_\beta$, A side), 3.86 (d, 1H, $J$ = 8,4Hz, $H_\beta$ B Side), 3.72 (m, 2H, $H_\beta$, A side and $H_\beta$ B side), 1.46(s, 9H, -$C(CH_3)_3$); $^{13}$C NMR ($CDCl_3$, 100 MHz): δ 169.4, 168.8, 155.9, 155.5, 147.6, 143.8, 143.6, 141.2, 131.3, 127.9, 127.7, 127.0, 125.0, 123.7, 119.9, 118.9, 82.7, 77.3, 77.0, 76.7, 71.8, 71.2, 67.1, 66.3, 65.4, 54.8, 54.4, 47.1, 27.9; HRMS (ES): Calcd for $C_{36}H_{39}N_3O_{11}Na$ 712.2476, found 712.2475.

**(*R*)-Allyl 3-((*S*)-2-(((9*H*-fluoren-9-yl)methoxy)carbonylamino)-3-*tert*-butoxy-3-oxopropoxy)-2-((4-nitrobenzyloxy)carbonylamino)propanoate (75b)**

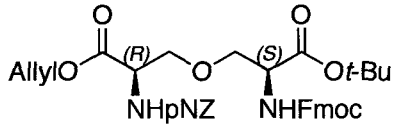


Method B was used to prepare the title compound **75b** from **59** (100 mg, 0.32 mmol) and **73** (250 mg, 0.65 mmol) as a colorless oil (82 mg, 37%). $[\alpha]_D^{25}$ 1.96° (*c* 0.7, $CHCl_3$); IR ($CHCl_3$, cast): 3326, 2978, 1726, 1607, 1523, 1478 $cm^{-1}$; $^1$H NMR ($CDCl_3$, 500 MHz): δ 8.12 (d, 2H, $J$ = 8.5 Hz, pNZ-H), 7.75 (d, 2H, $J$ = 7.5 Hz, Fmoc-H), 7.59 (d, 2H, $J$ = 7.5 Hz, Fmoc-H), 7.43 (d, 2H, $J$ = 8.5 Hz, pNZ-H), 7.39 (t, 2H, $J$ = 7.5 Hz, Fmoc-H), 7.30 (m, 2H, Fmoc-H), 5.88 (m, 1H, $CH_2C\underline{H}=CH_2$ ), 5,80 (d, 1H, $J$ = 8.0 Hz, NH), 5.61(d, 1H, $J$ = 8.0 Hz, NH), 5.32 (d, 1H, $J$ = 17.0 Hz, $CH_2CH=C\underline{H_2}$), 5.25 (d, 1H, $J$ = 8.0 Hz, $CH_2CH=C\underline{H_2}$ ),

5.21(d, 1H, *J*=13.5 Hz, O-C<u>H</u>$_2$-Ar ), 5.13 (d, 1H, *J* = 13,5 Hz, , O-C<u>H</u>$_2$-Ar), 4.65 (d, *J* = 6.0 Hz, 2H, C<u>H</u>$_2$CH=CH$_2$ ), 4.49 (d, *J* = 8.0 Hz, CH$_2$-Fmoc), 4.38(m, 2H, $H_\alpha$, A side and $H_\alpha$ B side), 4.21 (t, 1H, *J* = 7.0 Hz, CH-Fmoc), 3.97 (d, 1H, *J* = 7.0 Hz, $H_\beta$, A side), 3.86 (d, 1H, *J* = 9.5 Hz, $H_\beta$ B Side), 3.78 (d, 1H, *J* = 9.5 Hz, $H_\beta$ B side), 3,73 (d, *J* = 7.0 Hz, $H_\beta$, A side), 1.47 (s, 9H, -C(CH$_3$)$_3$); $^{13}$C NMR (CDCl$_3$, 125MHz): δ 169.4, 168.7, 155.9, 155.5, 143.8, 143.7, 143.5, 141.2, 131.3, 127.9, 127.7, 127.0, 125.0, 123.6, 120.0, 118.9, 82.7, 71.8, 71.1, 67.1, 66.3, 65.4, 54.7, 54.5, 47.1, 27.9; HRMS (ES): Calcd for $C_{36}H_{39}N_3O_{11}Na$ 712.2476, found 712.2478.

**(2*R*, 3*S*)-Allyl 3-((*S*)-2(((9*H*-fluoren-9-yl)methoxy)carbonylamino)-3-*tert*-butoxy-3-oxopropoxy)-2-((4-nitrobenzyloxy)carbonylamino)butanoate (76)**

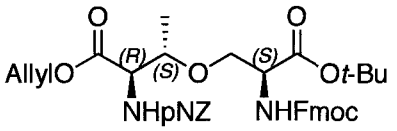


Method B was used to prepare the title compound **76** from **63** (200 mg, 0.62 mmol) and **73** (479 mg, 1.24 mmol) as a colorless oil (174 mg, 40%). $[\alpha]_D^{25}$ 12.76° (*c* 0.7, CHCl$_3$); IR (CHCl$_3$ cast) 3328, 2979, 1727, 1607, 1522, 1478, 1450 cm$^{-1}$; $^1$H NMR (CDCl$_3$, 500 MHz,) δ 8.18 (d, 2H, *J* = 9.0 Hz, PNZ-H), 7.76 (d, 2H, *J* = 7.5Hz, Fmoc-H), 7.60 (d, 2H, *J* = 7.5 Hz, Fmoc-H), 7.49 (d, 2H, *J*= 9.0 Hz, pNZ-H), 7.39 (t, 2H, *J*= 7.5 Hz, Fmoc-H), 7.30 (m, 2H, Fmoc-H), 5.90 (m, 1H, CH$_2$C<u>H</u>=CH$_2$), 5.54 (d, 2H, *J* = 9 Hz, 2 x NH), 5.33 (d, 1H, *J* = 17.5 Hz, CH$_2$CH=C<u>H</u>$_2$), 5.26 (d, 1H, *J* = 10.5 Hz, CH$_2$CH=C<u>H</u>$_2$ ), 5.24 (d, 1H, *J*=13.5 Hz,

O-C<u>H</u>$_2$-Ar ), 5.18 (d, 1H, $J$ =13.5 Hz, , O-C<u>H</u>$_2$-Ar), 4.65 (m, 2H, C<u>H</u>$_2$CH=CH$_2$ ), 4.40 (d, $J$ = 7.0 Hz, CH$_2$-Fmoc), 4.33 (m, 2H, $H_\alpha$, A side + $H_\alpha$ B side), 4.22 (t, 1H, $J$ = 7.0 Hz, CH-Fmoc), 4.09 (d, 1H, $J$= 6.5 Hz, $H_\beta$, A side), 3.74 (m, 2H, $H_\beta$ B Side), 3.78 (d, 1H, $J$=9.5Hz, $H_\beta$ B side ), 1.48 (s, 9H, -C(CH$_3$)$_3$), 1.23 (d, 3H, $J$ = 6.5 Hz, -CH$_3$); $^{13}$C NMR (CDCl$_3$, 125 MHz): δ 170.0, 168.9, 156.2, 155.8, 147.6, 143.8, 143.7, 143.6, 141.2, 131.4, 127.9, 127.7, 127.0, 125.0, 123.7, 120.0, 119.1, 82.7, 75.3, 69.2, 67.1, 66.2, 65.5, 58.6, 54.8, 47.1, 27.9, 16.6; HRMS (ES): Calcd for $C_{37}H_{41}N_3O_{11}Na$ 726.2633, found 726.2622

**(*S*)-2-(((9H-Fluoren-9-yl)methoxy)carbonylamino)-3-((R)-3-(allyloxy)-2-((4-nitrobenzyloxy)carbonylamino)-3-oxopropoxy)propanoic acid (77)**

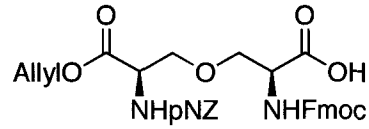


To a solution of **75b** (0.6 g, 0.87 mmol) in $CH_2Cl_2$ (10 mL) was added TFA (10 mL) followed by $PhSiH_3$ (1.0 equiv, 0.14 mL) and the reaction mixture was stirred for 2 h at rt. Volatiles were removed *in vacuo* to give a sticky white solid. The crude product was purified by silica gel chromatography (DCM:MeOH:AcOH = 20:1: 0.1) to yield **77** as a sticky white solid (494 mg, 90%). $[\alpha]_D^{25}$ 17.20° (*c* 0.65, $CHCl_3$); IR ($CHCl_3$, cast): 3320, 3067, 3020, 2950, 1724, 1608, 1522, 1451 cm$^{-1}$; $^1$H NMR ($CD_3OD$, 400 MHz): δ 8.08 (d, 2H, $J$ = 8.4 Hz, pNZ-H), 7.71 (d, 2H, $J$ = 7.6 Hz, Fmoc-H), 7.60 (m, 2H, Fmoc-H), 7.47 (d, 2H, $J$ = 8.4 Hz, pNZ-H), 7.32 (m, 2H, Fmoc-H), 7.24 (m, 2H, Fmoc-H), 5.86 (m, 1H, CH$_2$C<u>H</u>=CH$_2$), 5.27 (d,

1H, $J$ = 17.2 Hz, $CH_2CH{=}C\underline{H}_2$), 5.19 -5.10 (m, 3H, $CH_2CH{=}C\underline{H}_2$ and O-$C\underline{H}_2$-Ar ), 4.59 (m, 2H, $C\underline{H}_2CH{=}CH_2$ ), 4.42 (m, 2H, $CH_2$-Fmoc), 4.32 (m, 2H, $H_{\alpha'}$ A side and $H_{\alpha}$ B side), 4.15 (t, 1H, $J$ = 6.8 Hz, CH-Fmoc), 3.87 (m, 2H, $H_{\beta}$ A side and $H_{\beta}$ B Side), 3.72 (m, 2H, $H_{\beta}$ B side and $H_{\beta'}$ A side); $^{13}$C NMR ($CD_3OD$, 100 MHz): δ 172.2, 170.1, 157.4, 157.0, 147.6, 144.5, 144.1, 143.9, 141.3, 132.0, 127.8, 127.6, 127.0, 125.0, 123.3, 119.7, 117.5, 71.0, 70.7, 66.9, 65.8, 65.1, 54.7, 54.4; HRMS (ES): Calcd for $C_{32}H_{31}N_3O_{11}Na$ 656.18508, found 656.18429.

**(*S*)-2-(((9H-Fluoren-9-yl)methoxy)carbonylamino)-3-((2S,3R)-4-(allyloxy)-3-((4-nitrobenzyloxy)carbonylamino)-4-oxobutan-2-yloxy)propanoic acid (78)**

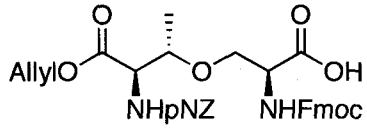


Using a procedure similar to the synthesis of compound **77**, the title compound **78** was prepared from **76** as a colorless oil (1.03 g, 87%). $[\alpha]_D^{25}$ 26.34° (*c* 0.4, $CHCl_3$); IR ($CH_2Cl_2$ cast),:3319, 3066, 2946, 1726, 1608, 1523, 1450 $cm^{-1}$; $^1$H NMR ($CD_3OD$, 400 MHz): δ 8.12 (d, 2H, $J$ = 8.4 Hz, pNZ-H), 7.71 (d, 2H, $J$ = 7.6 Hz, Fmoc-H), 7.61 (m, 2H, Fmoc-H), 7.52 (d, 2H, $J$ = 8.4 Hz, pNZ-H), 7.32 (t, 2H, $J$ = 7.2 Hz, Fmoc-H), 7.24 (t, 2H, $J$ = 7.6 Hz, Fmoc-H), 5.90 (m, 1H, $CH_2C\underline{H}{=}CH_2$ ), 5.29 (d, 1H, $J$ = 17.2 Hz, $CH_2CH{=}C\underline{H}_2$), 5.23 -5.16 (m, 3H, $CH_2CH{=}C\underline{H}_2$ and O-$C\underline{H}_2$-Ar ), 4.59 (d, 2H, $J$ = 5.6 Hz, $C\underline{H}_2CH{=}CH_2$ ), 4.34 (m, 3H, $CH_2$-Fmoc and $H_{\alpha}$ ), 4.29 (d, 1H, $J$ = 2.4 Hz , $H_{\alpha'}$), 4.16 (t, 1H, $J$ = 6.8 Hz, CH-Fmoc), 4.10(m, 1H, $H_{\beta}$), 3.78 (m, 1H, $H_{\beta}$ ) 3.68 (m, 1H, $H_{\beta}$), 1.18 (d, 3H, $J$ =

6.0 Hz, -$CH_3$); $^{13}C$ NMR ($CD_3OD$, 100 MHz): δ 172.4, 170.4, 157.6, 157.4, 147.6, 144.6, 144.1, 144.0, 141.3, 132.2, 127.8, 127.6, 127.0, 125.0, 123.3, 119.7, 117.6, 75.5, 68.8, 66.8, 65.9, 65.1, 59.3, 54.6, 14.8; HRMS (ES): Calcd for $C_{33}H_{33}N_3O_{11}Na$ 670.20073, found 670.20100.

### 5.2.1.b. Solid phase synthesis of oxygen analogue of lacticin 3147 A2 (45)

**Synthesis of ring C of oxa-lacticin (90)**

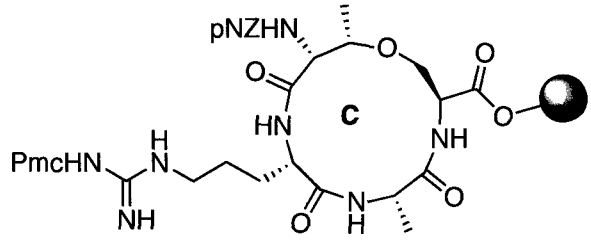


**a) General procedure for Fmoc Solid Phase Peptide Synthesis (SPPS):**

Fmoc amino acid (5.0 equiv to resin loading) and HOBt (5.0 equiv) were dissolved in DMF (10 mL) and to it, NMM (5.0 equiv) was added followed by PyBOP (4.9 equiv) and the mixture was pre-activated for 5 min. The activated amino acid solution was then transferred to pre-swelled resin and reacted for 2 h. The completion of coupling was ascertained by a negative Kaiser test and end capping was performed with 20% $Ac_2O$ in DMF for 10min. The subsequent removal of the Fmoc group was done using 20% piperidine in DMF and monitored by the absorption of the dibenzofulvene-piperidine adduct at λ = 301 nm on a UV-Vis spectrophotometer.

**b) Loading of oxa-melan on Wang resin**

Wang resin with a loading of 0.1 mmol/g was used for the synthesis. The initial loading of 0.44 mmol/g of the resin was reduced to 0.1 mmol/g to avoid any inter-strand dimerization during on resin-cyclization step.

***Formation of symmetric anhydride of* 78:** The orthogonally protected oxa-melan **78** (388.2 mg, 0.6 mmol) was dissolved in dry DCM (20 mL). Diisopropylcarbodiimide (0.3 mmole, 46.5 μL) was added and the resulting mixture was stirred for 30 min at 0 °C under argon. DCM was removed from the reaction *in vacuo* and the residue was dissolved in a minimal amount of DMF (~5 mL).

***Attachment of* 78 *to the resin:*** Wang resin (3.0 g, 1.32 mmol) was pre-swelled in DCM (20 mL) for 30 min. Preformed symmetric anhydride of **78** was added followed by DMAP (0.1 equiv relative to the desired resin loading, 0.03 mmol, 34 mg) in DMF (5 mL). The resulting solution was reacted for 2 h by shaking. The resin was washed with DMF (2 x 10 mL) and $CH_2Cl_2$ (2 x 20 mL). The rest of the free sites on-resin after loading the Oxa-melan were capped by reacting with 20% $Ac_2O$ in DMF for 30 min. The resin, thus obtained with a low loading of 0.1 mmol/g of oxa-melan, was used for further solid phase peptide synthesis.

**c) Deprotection of Allyl, Fmoc groups and cyclization to form ring C on solid support**

Fmoc SPPS was continued using PyBOP to couple Fmoc-Ala-OH (residue 27) and Fmoc-Arg(Pmc)-OH (residue 26) to the amino acid on resin to give linear fragment on resin. A solution of $Pd(PPh_3)_4$ (346.6 mg, 0.3 mmol, 1.0 equiv to resin) and $PhSiH_3$ (0.185 mL, 1.5 mmol, 5.0 equiv to resin) in (1:1) DMF/DCM

(40 mL) was reacted with resin bound peptide **88**, protected from light, for 2 h. The solution was drained and the resin was washed in the following sequence: 1) DCM (2 x 20 mL), 2) 0.5% sodium diethyldithiocarbamate in DMF (3 x 20 mL), 3) DMF (2 x 20 mL). The color of the resin changed to light yellow after washings. The Fmoc group was removed with 20% piperidine in DMF (3 x 5 mL). The resin was washed with $CH_2Cl_2$ (3 x 10 mL) and DMF (3 x10 mL). The cyclization to form ring C was done by adding a solution of PyBOP (780.45 mg, 1.5 mmol, 5.0 equiv), HOBt (202.6 mg, 1.5 mmol, 5.0 equiv) and NMM (0.329 mL, 3.0 mmol, 10.0 equiv) in DMF (40 mL) to the linear peptide **89** and reacted for 2 h. A small sample (4 mg) of resin bound **90** was cleaved by shaking with 95:2.5:2.5 (TFA: TIPS: $H_2O$) for 1 h and then filtered to remove the resin. The filtrate was concentrated *in vacuo* and precipitated with $Et_2O$ to give an off-white solid **90**. MALDI-TOF MS: Calcd for $C_{24}H_{34}N_8O_{10}$ 594.5, found 595.4 (M+H). No dimer or uncyclized linear precursor peptides were detected by MALDI-TOF MS.

**d) Removal of pNZ group on resin for subsequent solid phase peptide synthesis**

A solution of 6 M $SnCl_2$ and 1.6 mM HCl/dioxane in DMF (20 mL) was added to the resin and then reacted for 45 min. The procedure was repeated twice to ensure complete conversion. The resin was then washed with DMF (3 x 5 mL x1 min), DMF/$H_2O$ (3 x 5 mL x1 min), THF/$H_2O$ (3 x 5 mL x 1 min), DMF (3 x 5 mL x 1 min) and DCM (3 x 5 mL x 1 min) to remove excess $SnCl_2$ as well as any side

products from the deprotection. The completion of the reaction was ascertained by MALDI-TOF MS, Calcd for $C_{16}H_{29}N_7O_6$ 415.2, found 416.3 (M+H).

**Synthesis of oxa-lacticin A2 ring B (94)**

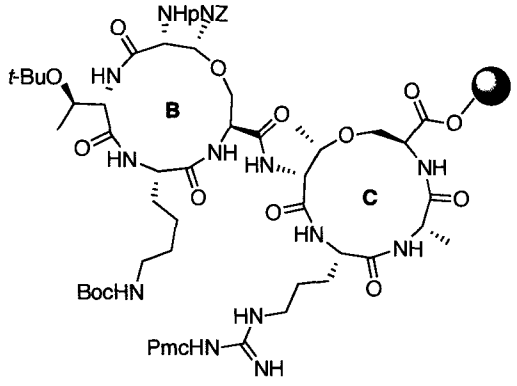


**94** was elongated using Fmoc SPPS with PyBOP to couple protected amino acids 25-23 in the following order: Fmoc-pNZ/Allyl oxa-melan (**78**), Fmoc-Lys(Boc)-OH, Fmoc-Thr(*t*-Bu)-OH. Allyl and Fmoc group were removed according to the procedure described above. Cyclization to form ring B was done with PyBOP similar to ring C. A small portion of resin (5 mg) was cleaved and analyzed by MALDI-TOF MS; Calcd for $C_{41}H_{63}N_{13}O_{16}$ 993.4, found 994.8 (M+H). No linear precursor or dimer was detected via mass spectrometry.

**Synthesis of oxa-lacticin A2 ring A (95)**

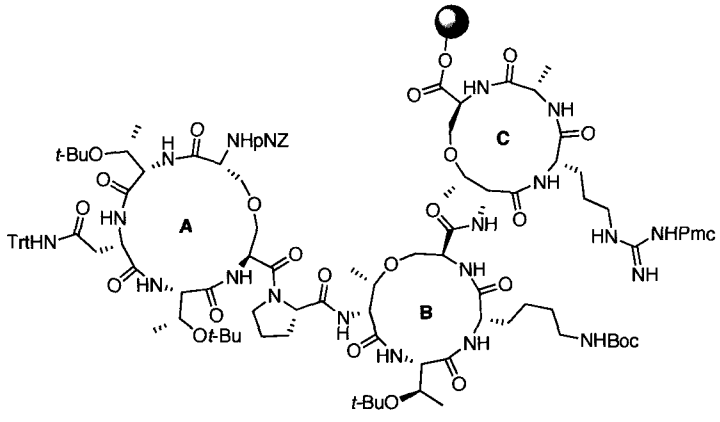

pNZ group was removed according to the same procedure described above. The residues (17-21) required for the linear portion of ring A were introduced under standard SPPS conditions using PyBOP in the order: Fmoc-Pro-OH, Fmoc-pNZ/Allyl-oxa-DAP, Fmoc-Thr(*t*-Bu)-OH, Fmoc-Asn(Trt)-OH, Fmoc-Thr(*t*-Bu)-OH. Removal of Allyl, Fmoc group and cyclization were performed in a similar manner to ring C to give **95**. A small sample of the resin was cleaved and subjected to MALDI-TOF MS analysis; Calcd for $C_{64}H_{98}N_{20}O_{26}$ 1562.6, found 1563.4 (M+H).

**Synthesis of tricyclic peptide moiety (96)**

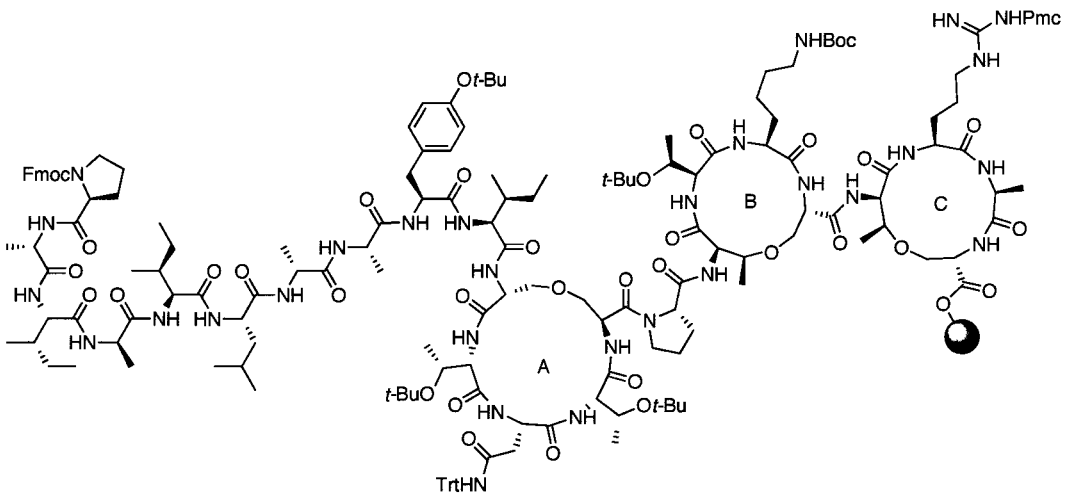


The pNZ group was removed under acidic reductive conditions as before and Fmoc-SPPS was done using PyBOP to couple amino acids 6-15 in the following order: Fmoc-Ile-OH, Fmoc-Tyr(*t*-Bu)-OH, Fmoc-Ala-OH, Fmoc-D-Ala-OH, Fmoc-Leu-OH, Fmoc-Ile-OH, Fmoc-D-Ala-OH, Fmoc-Ile-OH, Fmoc-Ala-OH, Fmoc-Pro-OH. A small sample of the resin was cleaved to give the tricyclic

peptide **96**. MALDI-TOF MS analysis: Calcd for $C_{121}H_{183}N_{29}O_{35}$ 2602.3, found 2603.3 (M+H).

**Oxa-lacticin 3147 A2 (45)**

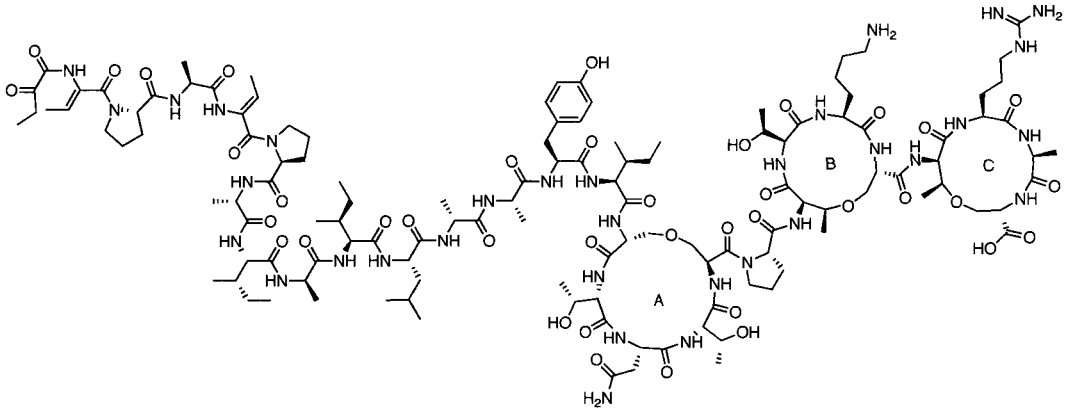


The Fmoc group of resin bound **96** (0.125 mmol) was removed using 20% piperidine/DMF (3 x 5 min) and the resin was washed with NMP (3 x 15 mL) to remove any traces of piperidine. In a separate vial, pentapeptide **34** (112 mg, 0.256 mmol) was dissolved in NMP (5 mL). To it, HOBt (35 mg, 0.256 mmol) and NMM (0.028 mL, 0.256 mmol) were added followed by PyBOP (133.1 mg, 0.256 mmol) and reacted for 5 minutes. The pre-activated solution was then transferred to resin bound peptide **96** and coupled for 7 h. The completion of reaction was ascertained by MALDI-TOF MS. No peak for the starting material was observed. The resin (300 mg) was cleaved with (97.5:2.5) TFA: TIPS (3 mL) for 3 h. The cleavage mixture was filtered to remove the resin and concentration of the filtrate *in vacuo*, followed by precipitation with cold ethyl ether and centrifugation gave crude oxa-lacticin A2 (**3**) as a white solid.

**Purification of oxa-lacticin A2:** The crude peptide was purified by reverse phase HPLC using a CSC-Inertsil 150 Å/ODS-2, 5 μm 10 x 250 mm column. The crude oxa-lacticin A2 (**45**) was dissolved in (1:1) MeCN: $H_2O$ to give a concentration of 1 mg/mL. HPLC method: Flow rate 3 mL/min, detection at 220 and 254 nm. Gradient: Starting from 20% MeCN for 5 min and ramp up to 60% over 15 min, followed by ramping down to 40% over 6 min, then 20% MeCN for 2 min. The fraction containing the desired product was collected as a broad peak ($t_R$ = 22.1 min), which was concentrated *in vacuo* and lyophilized to give relatively pure peptide. Second purification was done using an analytical column (Varian-microsorb-MV 100-5 C18, 4.6 x 250 mm). HPLC method: Flow rate 1.5 mL/min, detection at 220 and 254 nm. Gradient: starting from 20% MeCN for 5 min and first ramp up to 65% over 15 min, second ramp up to 70% over 18 min and ramp down to 20% for 2 min. The product was collected as a sharp peak ($t_R$ = 20.2 min) [Figure 1]. The fractions containing the desired product were concentrated *in vacuo* and lyophilized to give oxa-lacticin A2 (**45**) as a white solid (1.1 mg, overall yield = 0.31% [22 deprotections and couplings, 3 macrocyclizations, 3 pNZ removals and 3 allyl deprotections]. Monoisotopic MW Calcd. for $C_{126}H_{199}N_{33}O_{39}$ 2798.4, found 2799.2 (M + H) .

### 5.2.1.c. Biological Evaluation of oxa-Lacticin A2 (45)

#### (i) Synergistic activity assay:

Standard literature protocol was followed for testing the antimicrobial activity of oxa-lacticin A2 (**45**) and its parent natural peptide lacticin A1 (**16**) & A2 (**17**). Briefly, M17 agar plates (Supplemented with 10% lactose) were overlaid with soft agar, seeded with the indicator organism *L. lactis* subsp. *cremoris* HP or other Gram-positive organism of interest (100 μL fully grown culture per 10 mL soft agar). 10 μL or 5 μL of oxa-lacticin A2 and the parent lacticin 3147 A1 & A2 (dissolved in MQ-$H_2O$/ACN) were spotted and allowed to dry. The plates were then incubated at 30 °C overnight and the antibacterial activity was determined through a zone of inhibition (Figure 56). As evidenced by the panel of Gram-positive bacteria tested, oxa-lanA2 (**45**) exhibits either only independent antibacterial activity (**A** & **B**) or no biological activity (**C** to **G**). No synergistic activity similar to the parent lacticin 3147 A2 was observed.

**Figure 56.** Illustration of synergistic activity and inherent independent activity of oxa-lacticin A2 (**45**) and natural lacticin A1 (**16**) and A2 (**17**).

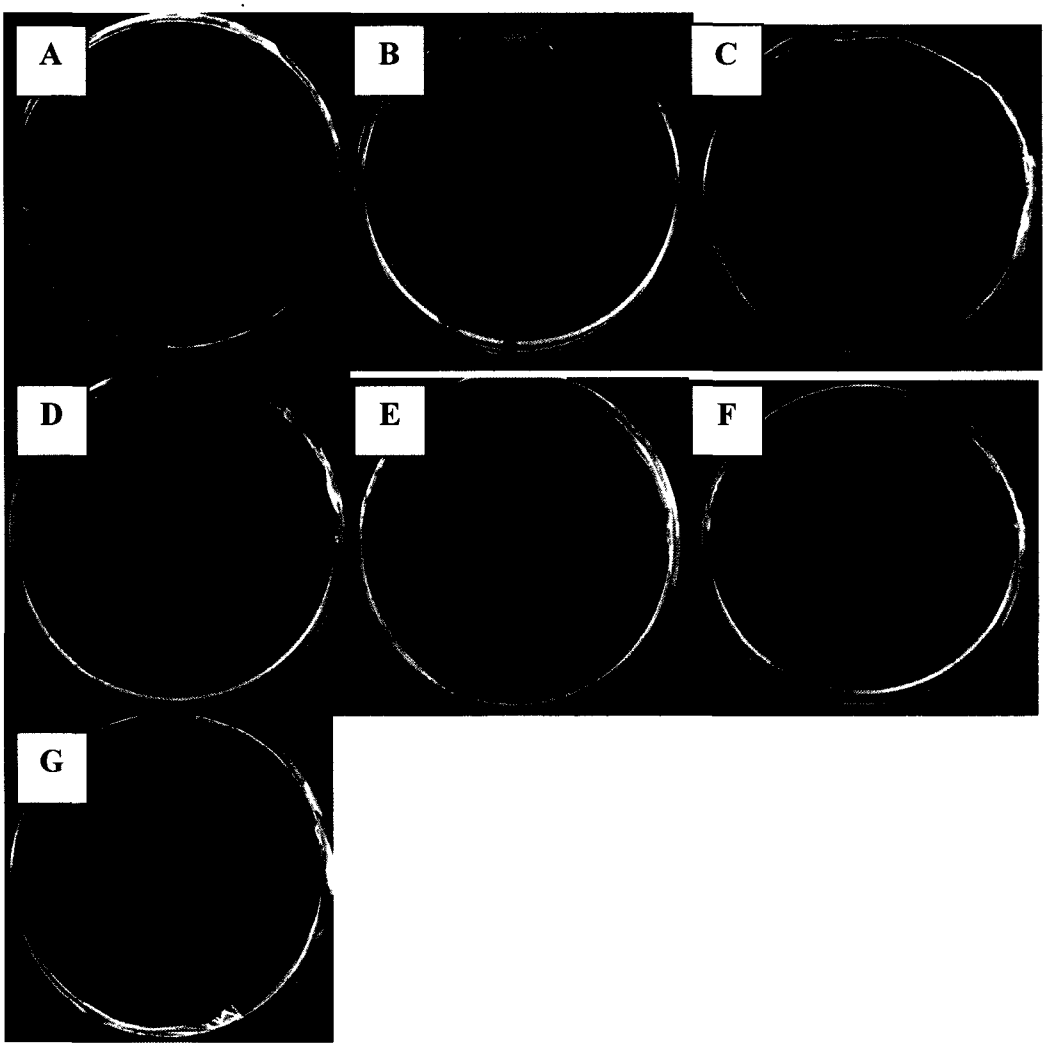


*Natural lacticin 3147 A1(**16**) & A2(**17**) are spotted on the top in all plates; natural lacticin A1(**16**) & oxa-lacticin A2 (**45**) are spotted on bottom in all plates; The panel of Gram-positive bacteria tested* (**A**) *L. lactis* subsp. *cremoris* HP (**B**) *Leuconostoc mesenteroides* Y105 (**C**) *Staphylococcus aureus* ATCC 29213 (**D**) *Enterococcus faecalis* ATCC 7080 (**E**) *Enterococcus faecium* BFE900 (**F**) *Lactobacillus sakei* 706 (**G**) *Pediococcus acidilactici* PAC 1.0.

## (ii) Synergistic activity and negative control experiment:

The test for synergistic activity was done by spotting lacticin 3147 A1 and lacticin A2 or oxa-lacticin A2 (**45**) at differing distances (1.6 to 2.4 cm). In all cases at the

concentration (200 μM) tested, oxa-lacticin A2 (**45**) showed no synergistic activity (Figure 58 **H** & **I**). A negative control experiment was performed by testing activities of the peptides against the producer organism for lacticin 3147 A1 & A2, *L. lactic* subsp. *lactis* DPC 3147. The natural A1 & A2 as well as oxa-lacticin A2 were inactive against the producer strain (Figure 58 **J**).

**Figure 57.** Synergistic activity testing at differing distances

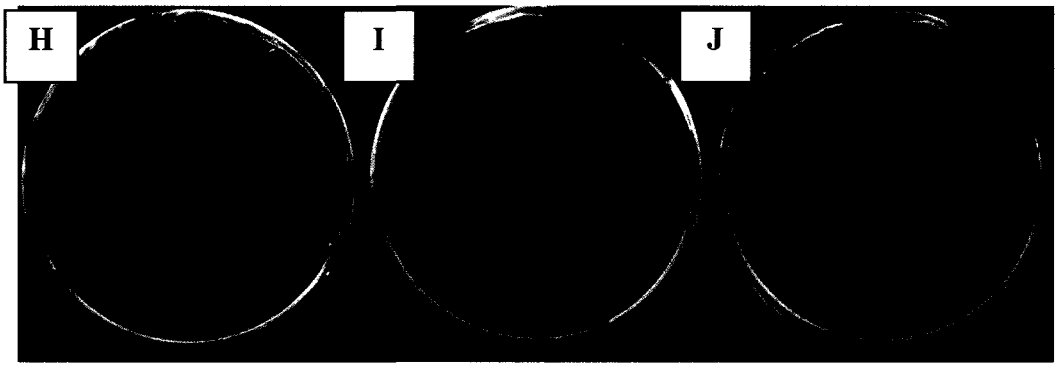


(**H**) *Synergistic activity and inherent activity between natural lacticin A1 & A2 at differing distances* (**I**) *Synergistic activity and inherent activity between natural lacticin-A1 & oxa-lancticin A2 at differing distances* (**J**) *Negative control experiment against lacticin A1 & A2 producer strain.*

(iii) **Serial dilution assay:**

A serial dilution assay was done by diluting lacticin A2 and oxa-lacticin A2 to 1 nM with MQ-water. 10 μL of solution was spotted on M17 agar plates containing the indicator organism *L. lactis* subsp. *cremoris* HP (100 μL fully grown culture per 10 mL soft agar). The plates were then incubated at 30 °C overnight and the antibacterial activity was determined through a zone of inhibition (Figure 59 **K** & **L**).

**Figure 58.** Illustration of serial dilution testing of oxa-lacticin A2 (**45**)

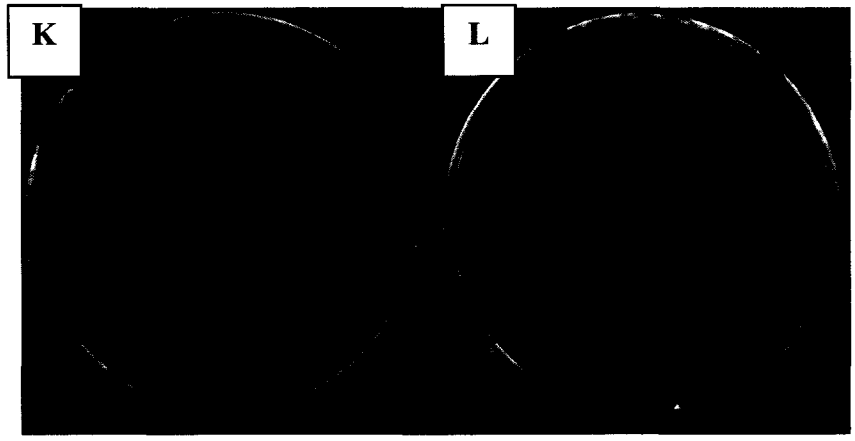


(**K**) *10-fold serial dilution of natural lacticin A2 starting at a concentration of 100 μM* (**L**) *Serial dilution of oxa-lacticin A2 (3) starting at a concentration of 200 μM.*

### 5.2.1.d. Synthesis of natural lacticin 3147 A2

**(2*S*, 3*R*)-Methyl 2-((2*S*,3*R*)-2-(tert-butoxycarbonylamino)-3-hydroxybutanamido)-3-hydroxybutanoate (100)**[163]

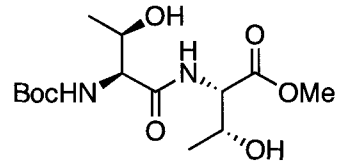


The known compound was prepared by a modified literature procedure. To a solution of Boc-Thr-OH (10.3 g, 47.1 mmol) and HCl.$NH_2$-Thr-OMe (8.0 g, 47.1 mmol) in DMF (100 mL) at -16 °C was added HOBt (7.0 g, 51.8 mmol), followed by the solution of EDCI (9.94 g, 51.8 mmol) and DIPEA (18.1 mL, 103.7 mmol) in DMF (100 mL) dropwise. The reaction mixture was stirred for 1 h at -16 °C, warmed up to rt and stirred for 20 h. The DMF solvent was removed

under *high vacuo*. The residue was dissolved in EtOAc (200 mL) and washed with 10% citric acid (3 x 50 mL), $H_2O$ (1 x 50 mL), $Na_2CO_3$ (3 x 50 mL) and brine (50 mL). The organic layer was dried with $Na_2SO_4$, filtered and then concentrated *in vacuo*. The crude product was purified by flash chromatography ($SiO_2$, 3:7/Hexanes:EtOAc) to yield **100** (9.5 g, 60%) as a light yellow oil. $[\alpha]_D^{25}$ -23.62 (*c* 1.58, $CHCl_3$); IR ($CHCl_3$, cast): 3366, 2979, 2935, 1743, 1665, 1523 $cm^{-1}$; $^1H$ NMR ($CDCl_3$, 500 MHz): δ 7.41 (d, 1H, *J* = 9.0 Hz, NH), 5.71 (d, 1H, *J* = 8.0 Hz, NH), 4.56 (dd, 1H, *J* = 9.0, 2.5 Hz, NH-C$\underline{H}_\alpha$-COOMe), 4.33 (app d, 1H, *J* = 4.0 Hz, $CH_3C\underline{H}_\beta OH$), 4.26 (app d, 1H, *J* = 4.0 Hz, $CH_3C\underline{H}_\beta OH$), 4.17 (app d, 1H, *J* = 6.5 Hz, NH-C$\underline{H}_\alpha$-CONH), 3.86 (br s, 1H, $CH_3CH_\beta O\underline{H}$), 3.75 (s, 3H, $OCH_3$), 3.63 (br s, 1H, $CH_3CH_\beta O\underline{H}$), 1.43 (s, 9H, -C($C\underline{H}_3$)$_3$), 1.19 (m, 6H, 2 x $CH_3$); $^{13}C$ NMR ($CDCl_3$, 125 MHz): δ 171.8, 171.3, 156.3, 80.4, 67.9, 67.3, 58.3, 57.7, 52.6, 28.2, 19.9, 18.1; HRMS (ES): Calcd for $C_{14}H_{26}N_2O_7Na$ 357.16322, found 357.16325.

**(*Z*)-Methyl 2-((*Z*)-2-(tert-butoxycarbonylamino)but-2-enamido)but-2-enoate (101)[74]**

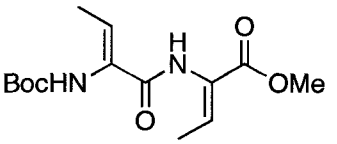


To a solution of compound **100** (7.0 g, 20.9 mmol) in DCE (350 mL), was added $Et_3N$ (17.51 mL, 125.6 mmol) followed by MsCl (6.50 mL, 83.7 mmol) dropwise. The mixture was stirred for 2 h at rt, and then DBU (18.77 mL, 125.6 mmol) was added dropwise. The reaction was stirred for 1 h at rt and then refluxed for 17 h.

The solvent was removed to give a yellow residue that was dissolved in EtOAc (200 mL) and washed with 10% citric acid (3 x 50 mL), $H_2O$ (1 x 50 mL) and brine (1 x 50 mL). The organic layer was dried with $Na_2SO_4$, filtered and then concentrated *in vacuo.* The crude product was purified by flash chromatography ($SiO_2$, 7:3/Hexanes:EtOAc) to yield **101** (3.5 g, 60%) as a yellow oil. IR ($CHCl_3$, cast): 3304, 3203, 2981, 2955, 1735, 1691, 1670, 1660, 1637 $cm^{-1}$; $^1H$ NMR ($CDCl_3$, 500 MHz): δ 7.55 (s, 1H, NH), 6.82 (q, 1H, $J$ = 6.5 Hz, Dhb-CH), 6.57 (app d, H, $J$ = 7.0 Hz Dhb-CH), 6.02 (s, 3H, NH), 3.76 (s, 3H, $OCH_3$), 1.79 (d, $J$ = 7.0 Hz, 6H, 2 x $C\underline{H}_3$) 1.47 (s, 9H -C($C\underline{H}_3$)$_3$); $^{13}C$ NMR ($CDCl_3$, 125 MHz): δ 164.9, 163.0, 153.7, 133.6, 133.3, 130.0, 125.8, 81.0, 52.3, 28.1(27.8), 14.8, 13.4; HRMS (ES) Calcd for $C_{14}H_{22}N_2O_5Na$ 321.14209, found 321.14210.

**(Z)-Methyl 2-(2-oxobutanamido)but-2-enoate (102)**

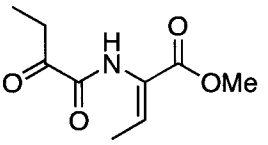


To a solution of compound **101** (107 mg, 0.36 mmol) in DCM (5 mL), was added TFA (5 mL) dropwise at rt. The mixture was stirred for 1 h at rt, and then the solvent was removed *in vacuo.* The yellow residue was dissolved in DCM (3 mL) and 5 mL of $NaHCO_3$ solution (1 N) was added to adjust pH to 5. The resulting mixture was stirred for 20 h at rt. The organic layer was separated and the aqueous layer was washed with DCM (3 x 10 mL). The organic layers were combined, dried with $Na_2SO_4$, filtered and then concentrated *in vacuo* to yield the pure **100** (44 mg, 62 %) as a colorless oil. IR ($CHCl_3$ cast): 3348, 2980, 2954,

2883, 1726, 1695, 1660, 1504 $cm^{-1}$; $^1H$ NMR ($CDCl_3$, 500 MHz): δ 8.29 (s, 1H, $NH_c$), 6.88 (q, 1H, $J$ = 7.0 Hz, =C<u>H</u>$CH_3$), 3.77 (s, 3H, O<u>C$H_3$</u>), 2.97 (q, 2H, $J$ = 7.0 Hz, -C<u>$H_2$</u>$CH_3$), 1.78 (d, 3H, $J$ = 7.0 Hz, =CHC<u>$H_3$</u>), 1.12 (t, 3H, $J$ = 7.0 Hz, -$CH_2$C<u>$H_3$</u>); $^{13}C$ NMR ($CDCl_3$, 125 MHz): δ 198.7, 164.1, 157.7, 134.9, 124.9, 52.4, 30.2, 14.9, 7.0; HRMS (ES): Calcd for $C_9H_{13}NO_4Na$, 222.07 found 222.10.

**(2*R*,3*S*)-Allyl-2-((2*S*,3*R*)-2-(*tert*-butoxycarbonylamino)-3-hydroxybutanamido)-3-hydroxybutanoate (106)[74]**

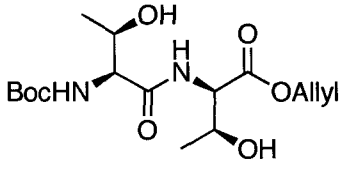


To a solution of H-D-Thr-OAllyl *p*-tolunenesulfonate salt (10.0 g, 30.2 mmol) in DCM (200 mL) was added NMM (3.0 eq., 9.96 mL, 90.6 mmol) dropwise at °C to neutralize excess acid. Boc-Thr-OH (6.61 g, 30.2 mmol) and PyBOP (15.7 g, 30.2 mmol) were added sequentially. The resulting mixture was stirred for 24 h at room temperature. The reaction solution was washed with 10% citric acid (3 x 100 mL), $H_2O$ (1 x 100 mL), 10 % $NaHCO_3$ (3 x 100 mL) and brine (100 mL). The separated organic layer was then dried with $Na_2SO_4$, filtered and then concentrated *in vacuo* to give the crude product, which was purified by flash chromatography ($SiO_2$, 3:7/Hexanes:EtOAc) to yield **106** (9.78 g, 90%) as a light yellow oil. $[\alpha]_D^{25}$ -27.43 (*c* 0.78, $CHCl_3$); IR ($CHCl_3$ cast): 3355, 2978, 2932, 1718, 1663, 1519 $cm^{-1}$; $^1H$ NMR ($CDCl_3$, 400 MHz): δ 7.26 (d, 1H, $J$ = 9.2 Hz, NH), 5.93 (m, 1H, -$CH_2$C<u>H</u>=$CH_2$), 5.56 (d, 1H, $J$ = 8.0 Hz, NH), 5.37 (dd, 1H, $J$ = 16.8, 1.2 Hz, -$CH_2$CH=C<u>H</u>H), 5.29 (dd, 1H, $J$ = 10.4, 1.2 Hz, -$CH_2$CH=CH<u>H</u>),

4.69 (m, 2H, -C$\underline{H}_2$CH=CH$_2$), 4.61 (dd, 1H, $J$ = 9.2, 2.8 Hz, NH-C$\underline{H}_\alpha$-COOAllyl), 4.38 (m, 2H, CH$_3$C$\underline{H}_\beta$OH), 4.17 (m, 1H, NH-C$\underline{H}_\alpha$-CONH), 1.47 (s, 9H, -C(C$\underline{H}_3$)$_3$), 1.24 (m, 6H, 2 x CH$_3$); $^{13}$C NMR (CDCl$_3$, 100 MHz): δ 172.1, 170.8, 156.5, 131.6, 119.3, 80.7, 68.2, 67.5, 66.6, 58.4, 57.9, 28.5, 20.2, 18.4; HRMS (ES): Calcd for $C_{16}H_{28}N_2O_7Na$ 383.17887, found 383.1787.

**(Z)-Allyl 2-((Z)-2-(tert-butoxycarbonylamino)but-2-enamido)but-2-enoate (107)[74]**

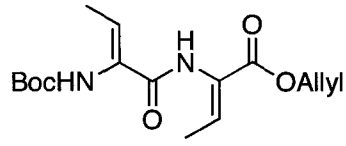


To a solution of compound **106** (9.8 g, 27.1 mmol) in DCE (500 mL) was added Et$_3$N (22.6 mL, 162.6 mmol) followed by MsCl (8.4 mL, 108.4 mmol) dropwise at rt. The mixture was stirred for 3 h at rt, and then DBU (24.3 mL, 162.6 mmol) was added dropwise. The reaction was stirred at rt for 1 h and refluxed for 20 h. The solvent was removed *in vacuo* to give a brown residue that was dissolved in EtOAc (300 mL) and washed with 10% citric acid (3 x 80 mL), H$_2$O (1 x 80 mL) and brine (1 x 80 mL). The organic layer was dried with Na$_2$SO$_4$, filtered and then concentrated *in vacuo.* The crude product was purified by flash chromatography (SiO$_2$, 7:3/Hexanes:EtOAc) to yield **107** (4.0 g, 46.0%) as a yellow oil. IR (CHCl$_3$ cast): 3268, 3127, 3004, 2983, 2968,1722, 1704, 1667, 1643 cm$^{-1}$; $^1$H NMR (CDCl$_3$, 400 MHz): δ 7.70 (br, s, 1H, NH), 6.78 (q, 1H, $J$ = 7.2 Hz, =C$\underline{H}$CH$_3$), 6.51 (q, 1H, $J$ = 6.8 Hz, =C$\underline{H}$CH$_3$), 6.41 (br, s, 1H, NH), 5.91-5.81 (m, 1H, -CH$_2$C$\underline{H}$=CH$_2$), 5.27 (d, 1H, $J$ = 15.6 Hz, -CH$_2$CH=C$\underline{H}$H), 5.18 (d, 1H, $J$ = 10.4

Hz, -$CH_2CH$=$CH\underline{H}$), 4.59 (m, 2H, -$C\underline{H}_2CH$=$CH_2$), 1.74-1.71 (m, 6H, 2 x $CH_3$), 1.39 (s, 9H, -$C(C\underline{H}_3)_3$); $^{13}C$ NMR ($CDCl_3$, 100 MHz): δ 164.1, 163.2, 153.8, 134.1, 131.8, 130.0, 129.5, 126.0, 118.3, 80.7, 65.7, 28.1, 14.7, 13.3; HRMS (ES): Calcd for $C_{16}H_{26}N_2O_5$ 325.1758, found 325.1754

**(*Z*)-2-((*Z*)-2-(*tert*-Butoxycarbonylamino)but-2-enamido)but-2-enoic acid (108)[74]**

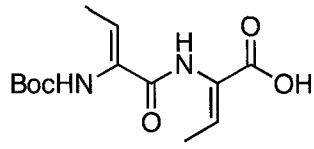


To a solution of compound **107** (1.7 g, 5.24 mmol) in degassed DCM (200 mL), was added $PhSiH_3$ (1.29 mL, 10.48 mmol) followed by $Pd(Ph_3P)_4$ (605.5 mg, 0.524 mmol) at rt. The reaction was stirred in the absence of light for 2 h. The solvents were removed *in vacuo*. The resulting crude product was purified using flash chromatography ($SiO_2$, 30:1:0.1/ DCM:MeOH:Acetic acid) to yield **103** (1.30 g, 87.8 %) as a pale pink solid. IR ($CHCl_3$ cast) 3276, 2980, 2935, 2455, 1703, 1643, 1502 $cm^{-1}$; $^1H$ NMR ($CD_3OD$, 400 MHz): 6.84 (q, 1H, $J$ = 7.2 Hz, C=C$\underline{H}CH_3$), 6.46 (q, 1H, $J$ = 7.2 Hz, C=C$\underline{H}CH_3$), 1.77(d, 3H, $J$ = 7.2 Hz, C=CHC$\underline{H}_3$), 1.76 (d, 3H, $J$ = 7.2 Hz, C=CHC$\underline{H}_3$), 1.46 (s, 9H, -$C(C\underline{H}_3)_3$); $^{13}C$ NMR ($CD_3OD$, 125 MHz): δ 167.5, 166.7, 156.2, 136.5, 132.0, 130.1, 128.7, 81.3, 28.6, 14.3, 13.2; HRMS (ES): Calcd. for $C_{13}H_{20}N_2NaO_5$ 307.12644, found 307.12657.

**(*Z*)-Allyl 2-((*R*)-2-((*S*)-1-((*Z*)-2-((*Z*)-2-(*tert*-butoxycarbonylamino)but-2-enamido)but-2-enoyl)pyrrolidine-2-carboxamido)propanamido)but-2-enoate (109)[74]**

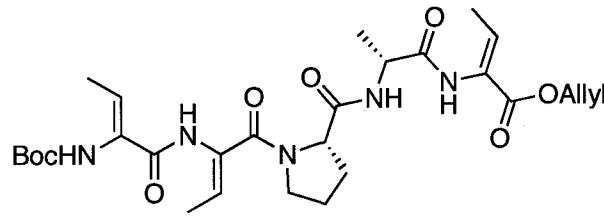


To a solution of Boc-Pro-D-Ala-Dhb-OAllyl (**80**) (100 mg, 0.24 mmol) in DCM (2 mL) was added TFA (2 mL). The resulting mixture was stirred at rt for 1 h. Removal of solvent *in vacuo* gave the deprotection product as a colorless oil. Without further purification, the residue was dissolved in DCM (5 mL). NMM (0.079 mL, 0.72 mmol) was added at 0 °C followed by a solution of **108** (68.1 mg, 0.24 mmol), HOBt (38.9 mg, 0.288 mmol) and DIC (0.0427 mL, 0.288 mmol) in DCM (5 mL). The reaction mixture was then allowed to warm to rt and stirred for 16 h. The solvent was removed *in vacuo*. The crude product was purified by flash chromatography ($SiO_2$, 8:2/EtOAc:Acetone) to yield **109** (0.1 g, 69%) as a colorless oil. $[\alpha]_D^{25}$ -106.18 (*c* 0.5, $CHCl_3$); IR ($CHCl_3$, cast): 3283, 2978, 2939, 2876, 2453, 1720, 1663, 1640, 1505 $cm^{-1}$; $^1H$ NMR ($CDCl_3$, 600 MHz): δ 8.23 (s, 1H, NH), 8.04 (s, 1H, NH), 7.89 (d, 1H, $J$ = 8.4 Hz, NH), 6.76 (q, 1H, $J$ = 7.2 Hz, Dhb-CH), 6,63 (q, 1H, $J$ = 6.6 Hz, Dhb-CH), 6.52 (br s, 1H, NH), 5.87 (m, 1H, $CH_2C\underline{H}=CH_2$), 5.45 (q, 1H, $J$ = 7.2 Hz, Dhb-CH), 5.29 (dd, 1H, $J$ = 17.4, 1.2 Hz, $CH=C\underline{H_2}$), 5.18 (dd, 1H, $J$ = 10.2, 1.2 Hz, $CH=C\underline{H_2}$), 4.57

(m, 2H, C<u>H</u>$_2$-CH=CH$_2$), 4.50-4.45 (m, 2H, Ala-H$_\alpha$ and Pro-H$_\alpha$), 3.90-3.89 (m, 1H, Pro-H$_\alpha$), 3.55-3.50 (m, 1H, Pro-H$_{\alpha'}$), 2.28-2.14 (m, 2H, Pro-H$_\beta$), 1.95-1.91 (m, 2H, Pro-H$_\gamma$), 1.74 (d, 3H, $J$ = 6.6 Hz, Dhb-CH$_3$), 1.722 (d, 3H, $J$ = 6.6 Hz, Dhb-CH$_3$), 1.718 (d, 3H, $J$ = 7.2 Hz, Dhb-CH$_3$), 1.49 (d, 3H, $J$ = 7.2 Hz, Ala-CH$_3$), 1.45 (s, 9H, -C(C<u>H</u>$_3$)$_3$); $^{13}$C NMR (CDCl$_3$, 100 MHz): δ 171.9, 171.2, 167.1, 164.5, 164.0, 154.0, 135.7, 133.3, 132.1, 130.7, 129.1, 126.9, 117.9, 117.8, 80.8, 65.4, 61.4, 49.7, 41.8, 29.9, 28.1, 24.4, 23.4, 16.9, 13.5, 11.6; HRMS (ES): Calcd for $C_{28}H_{41}N_5O_8Na$ 598.28473, found 598.28501.

**(*Z*)-2-((*R*)-2-((*S*)-1-((*Z*)-2-((*Z*)-2-(*tert*-Butoxycarbonylamino)but-2-enamido)but-2-enoyl)pyrrolidine-2-carboxamido)propanamido)but-2-enoic acid (110)[74]**

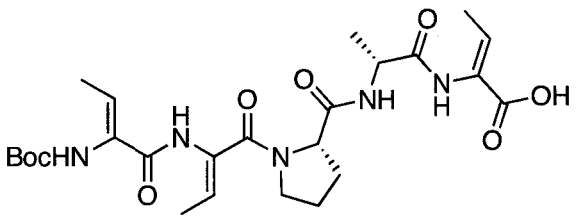


To a solution of compound **109** (1.0 g, 1.73 mmol) in degassed $CH_2Cl_2$ (200 mL) was added $PhSiH_3$ (0.428 mL, 3.46 mmol) followed by $Pd(Ph_3P)_4$ (199.9 mg, 0.173 mmol). The resulting mixture was stirred for 2 h in the absence of light at rt. The solvent was removed *in vacuo* and the crude product was purified by flash chromatography ($SiO_2$, 10:1:0.1 / DCM: MeOH: HOAc) to yield **110** (700 mg, 77%) as an off-white solid. $[\alpha]_D^{25}$ -121.73 (*c* 0.4, $CHCl_3$); IR ($CHCl_3$, cast): 3283, 2982, 2942, 2880, 1713, 1664, 1638, 1534 cm$^{-1}$; $^1$H NMR ($CDCl_3$, 500 MHz): δ 8.40 (br s, 1H, NH), 8.18 (br s, 1H, NH), 8.03 (app d, 1H, $J$ = 7.5 Hz, NH), 6.82

(br s, 1H, NH), 6.78 (q, 1H, $J$ = 7.5 Hz, Dhb-CH), 6.66 (q, 1H, $J$ = 7.5 Hz, Dhb-CH), 5.44 (br d, 1H, Dhb-CH), 4.54-4.47 (m, 2H, Ala-$H_\alpha$ and Pro-$H_\alpha$), 3.91-3.86 (m, 1H, Pro-$H_\delta$), 3.57-3.52 (m, 1H, Pro-$H_{\delta'}$), 2.27-2.16 (m, 2H, Pro-$H_\beta$), 1.97-1.91 (m, 2H, Pro-$H_\gamma$), 1.73 (d, 6H, $J$ = 7.5 Hz, 2 x Dhb-$CH_3$), 1.71 (d, 3H, $J$ = 7.5 Hz, Dhb-$CH_3$), 1.52 (d, 3H, $J$ = 7.5 Hz, Ala-$CH_3$), 1.45 (s, 9H, -C($C\underline{H}_3$)$_3$); $^{13}$C NMR ($CDCl_3$, 100 MHz): δ 172.1, 171.4, 167.7, 167.0, 164.3, 154.7, 136.9, 133.9, 130.3, 128.9, 126.7, 80.9, 61.3, 50.2, 49.8, 30.0, 28.2, 24.3, 20.7, 16.9, 14.1, 13.4, 11.7; HRMS (ES): Calcd for $C_{25}H_{37}N_5O_8Na$ 558.25343, found 558.25313.

**(2*R*,3*R*)-Allyl 1-(2,4-dinitrophenylsulfonyl)-3-methylaziridine-2-carboxylate (118)[88]**

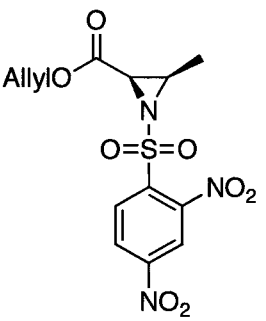


TFA (30 mL) was added dropwise at 0 °C to a solution of **66** (25 g, 65.2 mmol) in DCM (30 mL) and MeOH (20 mL). The solution was stirred for 30 min at rt. Volatiles were removed by azeotroping with $Et_2O$ (3 x 20 mL). The residue was partitioned between $Et_2O$ (50 mL) and $H_2O$ (50 mL) and the ether layer was extracted with water (3 x 50 mL). The combined aqueous layers were basified to pH 9 with $NaHCO_3$ at 0 °C. Ethyl acetate (200 mL) was added to the aqueous solution followed by 2-nitrobenzenesulfonyl chloride (19.1 g, 71.7 mmol) at 0 °C.

The resulting immiscible layers were warmed to room temperature and stirred vigorously for 24 h. After completion of the reaction, the two layers were separated and the aqueous layer was extracted with EtOAc (3 x 100 mL). The combined organic layers were washed with brine (3 x 50 mL), dried with $Na_2SO_4$, filtered and then concentrated *in vacuo*. The crude product was further purified by flash chromatography ($SiO_2$, 10:1/Hexanes: EtOAc) to yield **118** (12 g, 50%) as a light yellow oil. $[\alpha]_D^{25}$ 21.29° (*c* 0.85, $CHCl_3$); IR ($CHCl_3$, cast): 3105, 3042, 2941, 1752, 1648, 1607, 1555, 1542 $cm^{-1}$; $^1H$ NMR ($CDCl_3$, 400 MHz): δ 8.65 (dd, 1H, *J* = 2.0, 0.4 Hz, Ar-H), 8.59(dd, 1H, *J* = 8.8, 2.4 Hz, Ar-H), 8.54 (dd, 1H, *J* = 8.8, 0.4 Hz, Ar-H), 5.97-5.87 (m, 1H, $-CH_2C\underline{H}=CH_2$), 5.36 (d, 1H, *J* = 15.6 Hz, $-CH_2CH=C\underline{H}H$), 5.3 (d, 1H, *J* = 10.4 Hz, $-CH_2CH=CH\underline{H}$), 4.71-4.68 (m, 2H, $-C\underline{H}_2CH=CH_2$), 3.80 (d, 1H, *J* = 7.6 Hz, $H_\alpha$), 3.48 (qd, 1H, *J* = 5.6, 7.6 Hz, $H_\beta$), 1.46 (d, 2H, *J* = 5.6 Hz $-CH_3$); $^{13}C$ NMR ($CDCl_3$, 100 MHz): δ 164.5, 150.2, 148.4, 137.4, 133.2, 130.9, 126.9, 120.1, 119.3, 66.5, 43.8, 43.1, 12.2; HRMS (ES): Calcd for $C_{13}H_{13}N_3O_8SNa$ 394.03156, found 394.03164.

**2-((2*S*,3*S*)-4-(Allyloxy)-3-(2,4-dinitrophenylsulfonamido)-4-oxobutan-2-ylthio)acetic acid (122)**

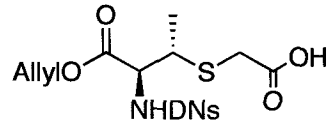


To a solution of **118** (32 mg, 0.086 mmol) in $CDCl_3$ (1 mL) was added mercaptoacetic acid (6 μL, 0.086 mmol) followed by $BF_3 \bullet OEt_2$ (21.6 μL, 0.172 mmol) at rt. The resulting mixture was stirred for 12 h. Removal of solvent *in*

*vacuo* afforded a yellow oil as a crude product, which was purified by a preparative TLC plate ($SiO_2$, 3:7:0.1/EtOAc:Hexanes:HOAc) to give **122** (18 mg, 45%) as a yellow oil. $[\alpha]_D^{25}$ 63.69° (*c* 0.8, $CHCl_3$); IR ($CHCl_3$, cast): 3318, 3105, 3038, 2930, 2689, 1739, 1649, 1606, 1552, 1540 $cm^{-1}$; $^1H$ NMR ($CDCl_3$, 400 MHz): δ 8.74 (d, 1H, *J* = 2.0 Hz, Ar-H), 8.51(dd, 1H, *J* = 8.8, 2.4 Hz, Ar-H), 8.28 (d, 1H, *J* = 8.8 Hz, Ar-H), 6.83 (d, 1H, *J* = 9.2 Hz, NH), 5.74-5.64 (m, 1H, -$CH_2CH$=$CH_2$), 5.23-5.17 (m, 2H, -$CH_2CH$=$CH2$), 4.46-4.38 (m, 3H, -$CH_2CH$=$CH_2$ and $H_a$), 3.71 (q, 1H, *J* = 3.2 Hz, $H_a$), 3.31 (q, 2H, *J* = 16 Hz -$SCH_2$-), 1.48 (d, 3H, *J* = 3.2 Hz –$CH_3$); $^{13}C$ NMR ($CDCl_3$, 100 MHz): δ 174.6, 168.8, 149.6, 147.7, 139.7, 131.9, 130.5, 127.0, 120.8, 119.9, 66.8, 61.6, 42.6, 32.1, 18.8; HRMS (ES): Calcd for $C_{15}H_{16}N_3O_{10}S_2$ 462.0283, found 462.0277.

**(*R*)-2-(((9*H*-Fluoren-9-yl)methoxy)carbonylamino)-3-mercaptopropanoic acid (123)**

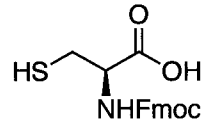


The compound was prepared by a modified literature procedure.[161] To a solution of HCl•$NH_2$-Cys-OH (25 g, 142 mmol) in water (200 mL) and dioxane (250 mL), was added Fmoc-OSu (52.8 g, 156 mmol) followed by $Na_2CO_3$ (15.0 g, 142 mmol) at rt. The resulting mixture was stirred for 24 h at rt. Removal of solvent *in vacuo* gave an oily residue that was dissolved in water (200 mL). The solution was acidified with 10% citric acid to pH 3 followed by extraction into EtOAc (3 x 200 mL). The combined organic layers were dried with $Na_2SO4$. Filtration and

concentration *in vacuo* gave the product **123** (43 g, 90%) as a white solid without further purification. $[\alpha]_D^{25}$ -4.47° (*c* 1.27, MeOH); IR (MeOH, cast): 3317, 3064, 3019, 2950, 2572, 1696, 1536 $cm^{-1}$; $^1H$ NMR ($CDCl_3$, 400 MHz): δ 7.75 (d, 2H, *J* = 7.6 Hz, Fmoc-H), 7.64(t, 2H, *J* = 5.2 Hz, Fmoc-H), 7.35 (t, 2H, *J* = 7.2 Hz, Fmoc-H), 7.28 (t, 2H, *J* = 7.2 Hz, Fmoc-H), 4.88 (br s, 2H, NH and $H_\alpha$), 4.34 (d, 2H, *J* = 7.2 Hz Fmoc-$CH_2$-), 4.19 (t, 1H, *J* = 5.6 Hz, Fmoc-CH), 3.30 (m, 1H, SH), 2.93-2.84 (m, 2H, $H_\beta$); $^{13}C$ NMR ($CDCl_3$, 100 MHz rotamer): δ 173.4, 158.4, 145.3(145.1), 142.6, 128.8, 128.1, 126.2, 120.9, 68.0, 57.7, 26.9 ; HRMS (ES): Calcd for $C_{18}H_{16}NO_4S$ 342.0806, found 342.0805

**(*R*)-2-(((9*H*-Fluoren-9-yl)methoxy)carbonylamino)-3-((2*S*,3*S*)-4-(allyloxy)-3-(2,4-dinitrophenylsulfonamido)-4-oxobutan-2-ylthio)propanoic acid (125)**

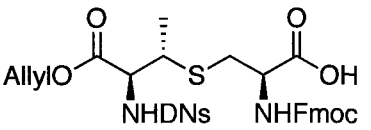


To a solution of **118** (3.0 g, 8.07 mmol) in $CHCl_3$ (70 mL) was added Fmoc-Cys-OH (3.32 g, 9.69 mmol) followed $BF_3 \bullet OEt_2$ (2.4 mL, 19.36 mmol). The resulting mixture was stirred for 24 h. Removal of solvent *in vacuo* afforded a yellow oil as a crude product, which was purified by flash chromatography ($SiO_2$, 3:7:0.1/EtOAc:Hexanes:HOAc) to give **125** (1.84 g, 32%) as a yellow oil. $[\alpha]_D^{25}$ -17.50° (*c* 0.2, $CHCl_3$); IR ($CHCl_3$, cast): 3331, 3102, 3021, 2930, 1723, 1605, 1552 $cm^{-1}$; $^1H$ NMR ($CDCl_3$, 600 MHz): δ 8.67 (s, 1H, DNs-H), 8.45(dd, 1H, *J* = 8.4, 2.4 Hz, DNs-H), 8.25 (d, 1H, *J* = 8.4 Hz, DNs-H), 7.76 (d, 2H, *J* = 7.8 Hz,

Fmoc-H), 7.58 (m, 2H, Fmoc-H), 7.40 (t, 2H, $J$ = 7.2 Hz, Fmoc-H), 7.30 (t, 2H, $J$ = 7.2 Hz, Fmoc-H), 6.67 (d, 1H, $J$ = 9.0 Hz, NH), 5.70 (m, 1H, $CH_2C\underline{H}=CH_2$), 5,64 (d, 1H, $J$ = 8.4 Hz, NH), 5.19 (d, 2H, $J$ = 18.0 Hz, $CH_2CH=C\underline{H_2}$), 5.17 (d, 2H, $J$ = 10.8 Hz, $CH_2CH=C\underline{H_2}$), 4.60 (app d, 1H, $J$ = 5.4 Hz, $H_\alpha$ B side), 4.48-4.39 (m, 4H, Fmoc-$CH_2$ and O-$C\underline{H_2}$-Ar), 4.34 (d, 1H, $J$ = 7.2 Hz, $H_\alpha$ A side), 4.23 (t, 1H, $J$ = 6.6 Hz, CH-Fmoc), 3.51 (br, 1H, $H_\beta$ A side), 3.06 (dd, 1H, $J$ = 13.2, 3.6 Hz, $H_\beta$ B Side), 2.90 (dd, 1H, $J$ = 13.2, 5.4 Hz, $H_\beta'$ B Side), 2.36 (s, 9H, $-C(CH_3)_3$), 1.42 (d, 3H, $J$ = 6.6 Hz, $-CH_3$); $^{13}C$ NMR ($CDCl_3$, 125 MHz): δ 173.7, 169.1, 155.9, 149.7, 147.7, 143.6, 143.5, 141.3, 139.6, 132.0, 130.6, 127.8, 127.1, 125.0, 120.9, 120.06, 120.04, 67.4, 66.9, 61.7, 53.4, 47.0, 43.4, 33.6, 19.6; HRMS (ES): Calcd for $C_{31}H_{30}N_4O_{12}S_2Na$ 737.11939, found 737.11900.

## 5.2.2. Chemical synthesis of neopetrosiamides and analogues

### 5.2.2.a. General experimental procedure

#### a). General procedure for automated solid phase peptide synthesis (SPPS) using ABI 433A

The peptide synthesis was completed on preloaded resin using an ABI-433A peptide synthesizer (Applied Biosystems) with UV monitoring capability (Perkin Elmer), detecting at 301 nm using standard *FastMoc* 0.1 mmole protocol. In the method employed, 10 equivalents of Fmoc amino acids were used with respect to the resin loading. Peptide couplings were done by mixing a solution of Fmoc-amino acid (in NMP) with a solution of HBTU, HOBt and DIPEA in DMF and pre-activated for 2.1 minutes. The activated solution was then transferred to the pre-swelled resin and allowed to react for 9.3 minutes. End capping was

performed with a solution of $Ac_2O$, HOBt and DIPEA in NMP. Removal of the Fmoc group was done by using 22% piperidine in NMP and monitored by the absorption of dibenzofulvene-piperidine adduct at $\lambda$ = 301 nm on a UV-Vis spectrophotometer. The overall coupling cycle time for each amino acid was approximately 50 minutes. The following side chain protecting groups were employed for the peptide synthesis: Fmoc-Cys(Acm)-OH, Fmoc-Cys(Trt)-OH, Fmoc-Cys(*t*-Bu)-OH, Fmoc-Asp(*t*-Bu)-OH, Fmoc-Ser(*t*-Bu)-OH, Fmoc-Thr(*t*-Bu)-OH, Fmoc-Asn(Trt)-OH, Fmoc-Arg(Pmc)-OH. For cleavage, the resulting peptidyl resin was treated with a fresh mixture of TFA: Thioanisole: EDT: Anisole (90: 5: 3: 2, v/v/v/v, 10 mL/g peptidyl resin) for 1.5 – 2 h at room temperature. The solution was then filtered through a plug of cotton into cold diethyl ether. The white precipitate was collected by centrifugation and washed with cold ether. The crude peptide was then purified by RP-HPLC. Fractions containing the appropriate mass by MALDI-TOF MS were pooled, concentrated, lyophilized and re-purified to homogeneity.

**b). General procedure for stepwise disulfide formation and methionine oxidation**

**(1). Formation of bis-disulfide bond**

To the linear Cys protected peptide in acetic acid (peptide concentration: 0.5 mg/mL) was added 10 equivalent of iodine in methanol for the first disulfide bond formation. After 1 h of stirring at rt, water (20% of reaction solution volume) was added to facilitate the second disulfide bond formation. The extent of reaction completion was monitored by MALDI-TOF MS. After the reaction was complete,

a 0.1 M ascorbic acid solution was added until the solution became colorless. The mixture was concentrated *in vacuo* and purified by RP-HPLC. Fractions containing the desired peptide were pooled and lyophilized.

**(2). Formation of tris-disulfide bond:**

The oxidation solution was prepared at room temperature by dissolving DMSO (100 equiv) and anisole (4 equiv) in TFA. The bicyclic peptide with *t*-Bu protecting groups on the two remaining Cys residues was dissolved in the oxidizing reagent to give a concentration of 0.1 mg/mL. The resulting mixture was stirred for 5 h at room temperature and then diluted with water. The solution was concentrated *in vacuo* and purified by RP-HPLC. Fractions containing the desired product, as confirmed by RP-HPLC and MALDI-TOF MS, were pooled and lyophilized.

**(3). Formation of methionine sulfoxide**

The tricyclic peptide was dissolved in water to a concentration of 0.5 mg/mL. To the reaction mixture was added a 30 % hydrogen peroxide solution (100 equiv). The reaction was allowed to proceed for 4 h at room temperature. The mixture was then freeze-dried. The crude product was purified by RP-HPLC and characterized by analytical HPLC and MALDI-TOF MS.

**c). General methods for HPLC analysis and purification**

HPLC methods used are listed as follows:

**Method A** (preparative column): Flow rate 10.0 mL/min, detection at 220 and 254 nm. Gradient: starting from 10% MeCN/90% $H_2O$ (0.05% TFA) for 5

min and first ramp up to 30% over 5 min, second ramp up to 60% over 16 min, then ramp up to 80% over 6 min, ramp down to 10% for 1 min.

**Method B** (semi-preparative column): Flow rate 3.0 mL/min, detection at 220 and 254 nm. Gradient: starting from 10% MeCN/90% $H_2O$ (0.05% TFA) for 5 min and first ramp up to 30% over 5 min, second ramp up to 60% over 28 min, ramp down to 10% for 1 min and continue to 10% for 1 min.

**Method C** (analytical column): Flow rate 1.5 mL/min, detection at 220 and 254 nm. Gradient: starting from 20% MeCN/90% $H_2O$ (0.05% TFA) for 5 min and first ramp up to 65% over 15 min, second ramp up to 70% over 18 min and ramp down to 20% for 2 min.

**Method D** (analytical column):: Flow rate 1.5 mL/min, detection at 220 and 254 nm. Gradient: starting from 10% MeCN/90% $H_2O$ (0.05% TFA) for 5 min and first ramp up to 30% over 5 min, second ramp up to 35% over 15 min, third ramp up to 60% over 10 min, and ramp down to 10% for 5 min.

**Method E** (analytical column):: Flow rate 1.5 mL/min, detection at 220 and 254 nm. Gradient: starting from 10% MeCN/90% $H_2O$ (0.05% TFA) for 5 min and first ramp up to 30% over 5 min, second ramp up to 60% over 28 min, and ramp down to 10% for 1 min and continue 10% for 1 min.

**d). General procedure for disulfide mapping analysis using MS-based method**

**Partial reductions and stepwise alkylation**

**(1) Partial reduction with TCEP**

**Method A**: A peptide solution (2.0 mg/mL in 50% MeCN) was incubated with an equivalent volume of 20 mM TCEP, 0.2 M citrate buffer, pH 3.0, at 25 °C for 3 min. The reaction was stopped by immediate injection on a Varian Microsorb-MV 100-5 C18 column (5 μm, 4.6 × 250 mm), eluted with HPLC method C. Partially reduced species were collected manually.

**Method B**: A peptide solution (2.0 mg/mL in 50% MeCN) was incubated with 25 equiv (relative to peptide) of 100 mM TCEP, 0.1 M citrate buffer, pH 3.0, at 4 °C for 4 h. The reaction was stopped by immediate injection on a Varian Microsorb-MV 100-5 C18 column (5 μm, 4.6 × 250 mm), eluted with HPLC method C. Partially reduced species were collected manually.

**(2) General method for Nem alkylation:**

A solution of 60 mM Nem (same volume as collected HPLC fraction) in 0.2 M citrate buffer, pH 3, was added directly to collected fractions containing partially reduced peptides. The mixture was incubated for 2 h at rt and the Nem alkylated product was purified on a Varian Microsorb-MV 100-5 C18 column (5 μm, 4.6 × 250 mm), eluted with HPLC method C. The product was collected manually and characterized by MALDI-TOF MS.

**(3) General method of complete reduction and alkylation with Nmm:**

The fraction containing Nem-alkylated peptide was treated with the same volume of 20 mM TCEP, 0.2 M citrate buffer, pH 3.0, for 1 h at room temp. To the reaction mixture, the same volume of 60 mM Nmm in 0.2 M citrate buffer was added, after which the reaction was incubated 2 h at room temperature. The reaction was then terminated by injection on RP-HPLC. The fully labeled peptide was purified on a Varian Microsorb-MV 100-5 C18 column (5 μm, 4.6 × 250 mm), eluted with HPLC method C. The pure peptides were then subjected to LC-MS/MS analysis.

**Enzymatic digestion:**

**(1) Trypsin digestion:** Digestion was performed by sequencing grade modified trypsin, using a peptide/enzyme ratio of 20:1 (mol/mol). Peptides were dissolved in 100 mM ammonium bicarbonate buffer (pH = 8) at a concentration of 3 μg/μL, and the reaction mixture was incubated at 30 °C for 1 h. After incubation, samples were acidified to pH = 2 using 10% TFA and desalted by a Millipore $C_{18}$ ZipTip pipette tip. The crude sample was analyzed by LC-MS/MS without further purification.

**(2) Endoproteinase Asp-*N* digestion:** Enzymatic digestion was done using a peptide/enzyme ratio of 10:1 (mass/mass). Peptides were dissolved in 50 mM sodium phosphate buffer (pH = 8) at a concentration of 5 μg/μL, and the reaction mixture was incubated at 37 °C for 22 h. After incubation, samples were

acidified to pH = 2 using 10% TFA and desalted by a Millipore $C_{18}$ ZipTip pipette tip. The sample was analyzed by LC-MS/MS without further purification.

### 5.2.2.b. Experimental procedure and data for compounds

**Tris-disulfide peptide with methionine sulfoxide (130)**

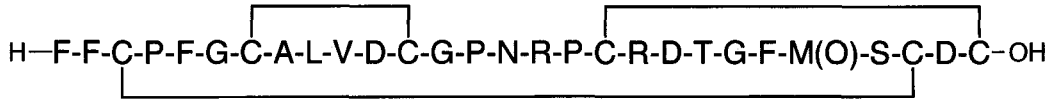


The neopetrosiamides with originally proposed disulfide connectivity (**130**) was obtained by $H_2O_2$ oxidation of the tricyclic peptide (**139**) according to the general method for sulfoxide formation. The crude peptide was purified by the semi-preparative RP-HPLC using method B ($t_R$ = 22.7 min) to give **130** as a white powder (1.6 mg, 61.3% relative to 2.6 mg of the tricyclic peptide). MALDI-TOF (MS) cald. for $C_{129}H_{184}N_{35}O_{39}S_7$ $(M + H)^+$ 3071.1. Found 3071.6 $(M + H)^+$.

**Tris-disulfide peptide (139)**

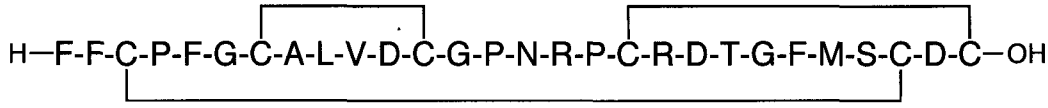


The introduction of the third disulfide bond was achieved by DMSO oxidation of the bis-disulfide peptide **154** according to the general method for tris-disulfide bond formation. The crude peptide was purified by semi-preparative RP-HPLC using method B ($t_R$ = 26.7 min) to give **139** as a white powder (3.5 mg, 55.1%

relative to 6.6 mg of the bicyclic peptide). MALDI-TOF (MS) cald. for $C_{129}H_{184}N_{35}O_{38}S_7$ $(M + H)^+$ 3055.1. Found 3055.3 $(M + H)^+$.

**Tris-disulfide norleucine analogue (141)**

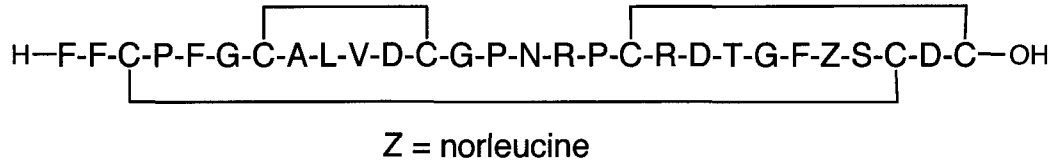


The introduction of the third disulfide bond was achieved by DMSO oxidation of the bicyclic peptide **159** according to the general method for tris-disulfide bond formation. The crude peptide was purified by semi-preparative RP-HPLC using method B ($t_R$ = 25.3 min) to give **141** as a white powder (2 mg, 29.6% relative to 7.0 mg of the bicyclic peptide). MALDI-TOF (MS): cald. for $C_{130}H_{186}N_{35}O_{38}S_6$ $(M + H)^+$ 3037.1. Found 3036.8 $(M + H)^+$.

**Linear neopetrosiamide for oxidative folding (148)**

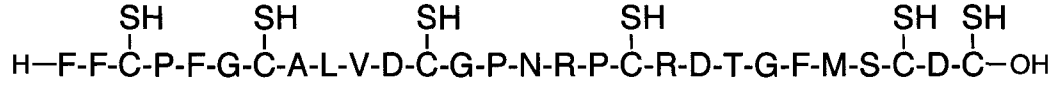


The linear peptide **148** was synthesized on a preloaded $H_2N$-Cys(Trt)-2-ClTrt resin (0.62 mmol/g) on a 0.1 mmol scale using the automated peptide synthesizer according to the general method for solid phase peptide synthesis. The thiol side chains of cysteines are protected with trityl groups. After acidic cleavage, the crude peptide was washed thoroughly with cold ether to give **148** as a white

powder (150 mg). The peptide was used for oxidative folding directly without further purification. MALDI-TOF (MS): cald. for $C_{129}H_{190}N_{35}O_{38}S_7$ $(M + H)^+$ 3061.2 found 3061.4 $(M + H)^+$

**Linear peptide (Cys 3, 26-*t*-Bu, Cys 18, 28-Acm) (153)**


Peptide **153** was synthesized on a preloaded $H_2N$-Cys(Acm)-2-ClTrt resin (0.84 mmol/g) on a 0.1 mmol scale using the automated peptide synthesizer according to the general method for solid phase peptide synthesis. Protection of the cysteine residues was Cys 3, 26-*t*-Bu, Cys 7, 12-Trt, Cys 18, 28-Acm. The crude peptide was purified by preparative RP-HPLC (Vydac 218TP1022 C18, 10 $\mu$m, 2.2 cm x 25 cm) using method A ($t_R$ = 20.1 min) to give **153** as a white powder (33 mg, 9.9 % relative to the resin loading). MALDI-TOF (MS): cald. for $C_{143}H_{216}N_{37}O_{40}S_7$ $(M + H)^+$ 3315.3. found 3315.8 $(M + H)^+$.

**Bis-disulfide peptide (154)**

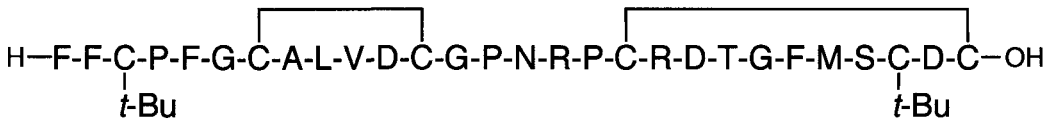


Peptide **154** was synthesized according to the general method for bis-disulfide bond formation from the linear peptide **153.** The crude peptide was purified by

semi-preparative RP-HPLC using method B ($t_R$ = 27.1 min) to give **154** as a white powder (4.0 mg, 52.3% relative to 8.0 mg of the linear peptide). MALDI-TOF (MS): cald. for $C_{137}H_{202}N_{35}O_{38}S_7$ $(M + H)^+$ 3169.2. Found 3169.3 $(M + H)^+$.

**Bis-disulfide peptide (155)**

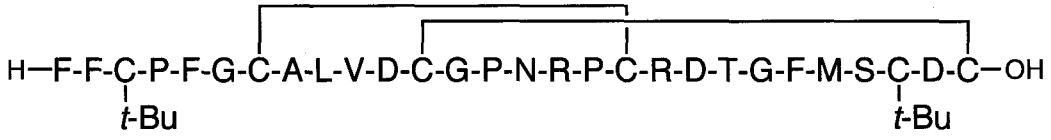


Peptide **155** was synthesized according to the general method for bis-disulfide bond formation from the linear peptide **175.** The crude peptide was purified by semi-prep RP-HPLC using method B ($t_R$ = 27.3 min) to give **155** as a white powder (3.5 mg, 40.6% relative to 9 mg of the linear peptide). MALDI-TOF (MS): cald. for $C_{137}H_{202}N_{35}O_{38}S_7$ $(M + H)^+$ 3169.2. Found 3169.5 $(M + H)^+$.

**Linear peptide (Cys 3, 26-*t*-Bu, Cys 7, 28-Acm) (156a)**

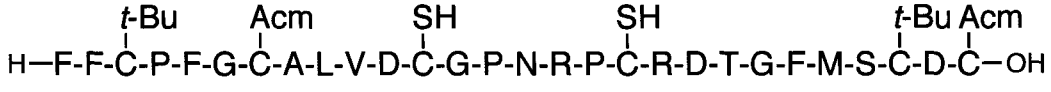


Linear peptide **156a** was synthesized on a preloaded $H_2N$-Cys(Acm)-2-ClTrt resin (0.84 mmol/g) on a 0.1 mmol scale using the automated peptide synthesizer according to the general method for solid phase peptide synthesis. Protection of the cysteine residues was Cys 3, 26-*t*-Bu Cys 12, 18-Trt; Cys 7, 28-Acm. The

crude peptide was used in the next step without further purification. MALDI-TOF (MS) cald. for $C_{143}H_{216}N_{37}O_{40}S_7$ $(M + H)^+$ 3315.3. Found 3315.5 $(M + H)^+$.

**Bis-disulfide peptide (156)**

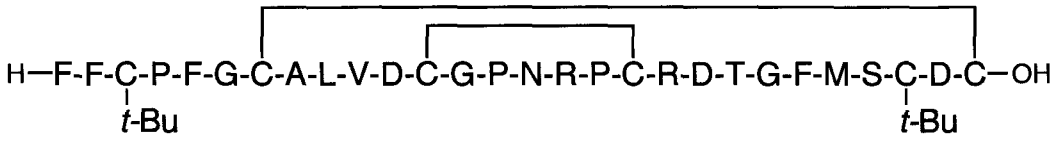


Peptide **156** was synthesized according to the general method for bis-disulfide bond formation from the linear peptide **156a.** The crude peptide was purified by semi-prep RP-HPLC using method B ($t_R$ = 26.5 min) to give **156** as a white powder (3.0 mg, 15.7% relative to 20 mg of the crude linear peptide). MALDI-TOF (MS): cald. for $C_{137}H_{202}N_{35}O_{38}S_7$ $(M + H)^+$ 3169.2. Found 3169.3 $(M + H)^+$.

**Linear norleucine analogue (Cys 3, 26-*t*-Bu, Cys 18, 28-Acm) (158)**

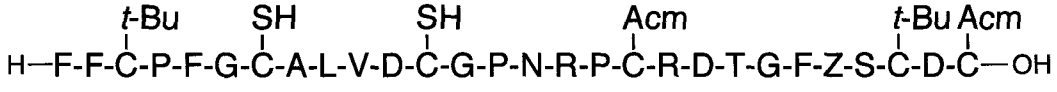


Z = norleucine

Linear peptide **158** was synthesized on a preloaded $H_2N$-Cys(Acm)-2-ClTrt resin (0.84 mmol/g) on a 0.1 mmol scale using the automated peptide synthesizer according to the general method for solid phase peptide synthesis. Protection of the cysteine residues was Cys 3, 26-*t*-Bu; Cys 7, 12-Trt; Cys 18, 28-Acm. The crude peptide (250 mg, 75.8% relative to the resin loading) was used in the next

step without further purification. MALDI-TOF (MS): cald. for $C_{144}H_{218}N_{37}O_{40}S_6$ $(M + H)^+$ 3297.4. Found 3297.8 $(M + H)^+$.

**Bis-disulfide norleucine analogue (159)**

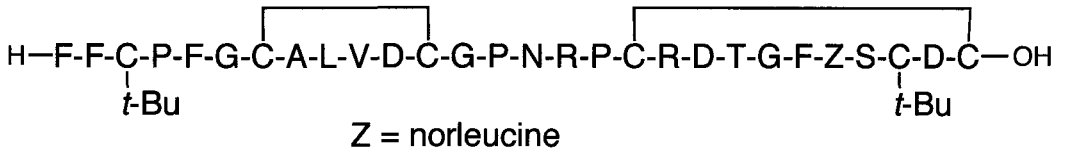


Peptide **159** was synthesized according to the general method for bis-disulfide bond formation from the linear peptide **158.** The crude peptide was purified by semi-preparative RP-HPLC using method B ($t_R$ = 27.1 min) to give **159** as a white powder (20.0 mg, 20.9 % relative to 100 mg of the crude linear peptide). MALDI-TOF (MS): cald. for $C_{138}H_{204}N_{35}O_{38}S_6$ $(M + H)^+$ 3151.3. Found 3151.4 $(M + H)^+$.

**Tris-disulfide peptide having methionine sulfoxide (172)**

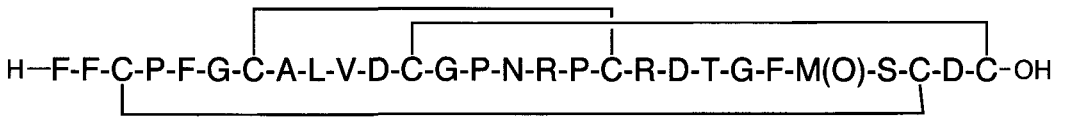


The neopetrosiamide with the revised disulfide connectivity (**172**) was synthesized by $H_2O_2$ oxidation of the tricyclic peptide (**175**) according to the general method for sulfoxide formation. The crude peptide was purified by semi-preparative RP-HPLC using method B ($t_R$ = 24.1 min) to give **172** as a white

powder (3.0 mg, 50.0% relative to 6.0 mg of the tricyclic peptide). MALDI-TOF (MS): cald. for $C_{129}H_{184}N_{35}O_{39}S_7$ $(M + H)^+$ 3071.1. Found 3071.5 $(M + H)^+$.

**Linear peptide (Cys 3,26-*t*-Bu, Cys 12, 28-Acm) (174)**

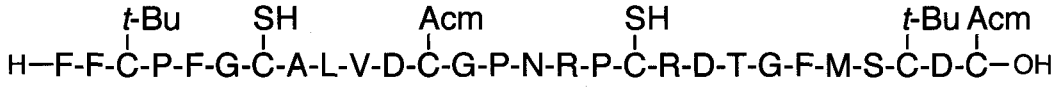


Linear peptide **174** was synthesized on a preloaded $H_2N$-Cys(Acm)-2-ClTrt resin (0.85 mmol/g) on a 0.1 mmol scale using the automated peptide synthesizer according to the general method for solid phase peptide synthesis. Protection of the cysteine residues was Cys 3, 26-*t*-Bu; Cys 7,18-Trt; Cys 12,28-Acm. The crude peptide was purified by semi-preparative RP-HPLC using method B ($t_R$ = 26.1 min) to give **174** as a white powder (12 mg, 10.9% relative to 110 mg of dried crude linear peptide). MALDI-TOF (MS): cald. for $C_{143}H_{216}N_{37}O_{40}S_7$ $(M + H)^+$ 3315.3. Found 3315.6 $(M + H)^+$.

**Tris-disulfide peptide (175)**

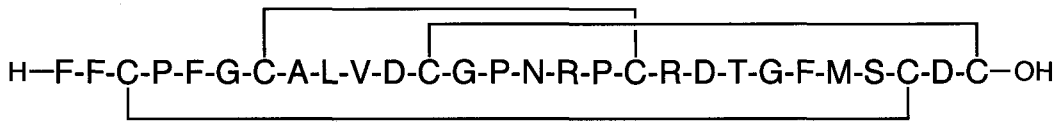


The introduction of the third disulfide bond was achieved by DMSO oxidation of the bicyclic peptide **155** according to the general method for tris-disulfide bond

formation. The crude peptide was purified by semi-preparative RP-HPLC using method B ($t_R$ = 29.6 min) to give **175** as a white powder (10 mg, 50 % relative to 20 mg of the bicyclic peptide). MALDI-TOF (MS): cald. for $C_{129}H_{184}N_{35}O_{38}S_7$ $(M + H)^+$ 3055.1. Found 3054.9 $(M + H)^+$.

**Linear norleucine analogue (Cys 3, 26-*t*-Bu, Cys 12, 28-Acm) (178)**


Linear peptide **178** was synthesized on a preloaded $H_2N$-Cys(Acm)-2-ClTrt resin (0.85 mmol/g) on a 0.1 mmol scale using the automated peptide synthesizer according to the general method for solid phase peptide synthesis. Protection of the cysteine residues was Cys 3, 26-*t*-Bu; Cys 7, 18-Trt; Cys 12, 28-Acm. The crude peptide (150 mg, 75.8% relative to the resin loading) was used in the next step without further purification. MALDI-TOF (MS): cald. for $C_{144}H_{218}N_{37}O_{40}S_6$ $(M + H)^+$ 3297.4. Found 3297.8 $(M + H)^+$.

**Tris-disulfide norleucine analogue (176)**

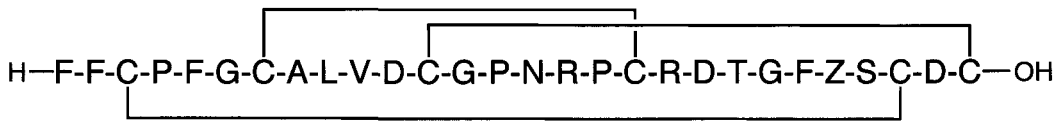


The introduction of the third disulfide bond was achieved by DMSO oxidation of the bicyclic peptide **179** according to the general method for tris-disulfide bond

formation. The crude peptide was purified by analytical RP-HPLC using method D ($t_R$ = 29.9 min) to give **176** as a white powder (1.2 mg, 29% relative to 3 mg of the bicyclic peptide). MALDI-TOF (MS): cald. for $C_{130}H_{186}N_{35}O_{38}S_6$ $(M + H)^+$ 3037.1. Found 3036.8 $(M + H)^+$.

**Bis-disulfide norleucine analogue (179)**

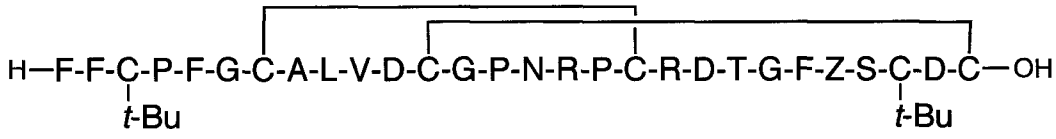


Peptide **179** was synthesized according to the general method for bis-disulfide bond formation from the linear peptide **178.** The crude peptide was purified by semi-preparative RP-HPLC using method B ($t_R$ = 26.2 min) to give **179** as a white powder (4.8 mg, 20 % relative to 24 mg of the crude linear peptide). MALDI-TOF (MS): cald. for $C_{138}H_{204}N_{35}O_{38}S_6$ $(M + H)^+$ 3151.3. Found 3151.7 $(M + H)^+$.

**Linear O-methyl homoserine analogue (Cys 3, 26-*t*-Bu, Cys 7, 18-Acm) (180b)**

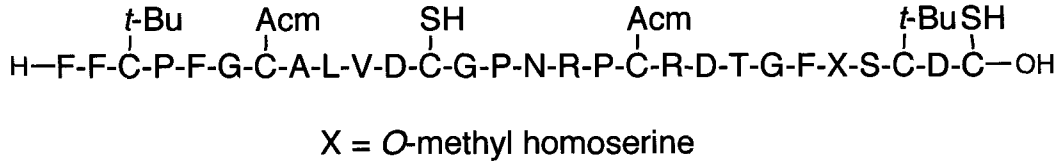

Linear peptide **180b** was synthesized on a preloaded $H_2N$-Cys(Trt)-2-ClTrt resin (0.62 mmol/g) on a 0.1 mmol scale using the automated peptide synthesizer according to the general method for solid phase peptide synthesis. Protection of the cysteine residues was Cys 3, 26-*t*-Bu; Cys 7, 18-Trt; Cys 12, 28-Acm. The crude peptide (150 mg, 45.4% relative to the resin loading) was used in the next step without further purification. MALDI-TOF (MS): cald. for $C_{143}H_{216}N_{37}O_{41}S_6$ $(M + H)^+$ 3299.4. Found 3299.5 $(M + H)^+$.

**Bis-disulfide norleucine analogue (180c)**

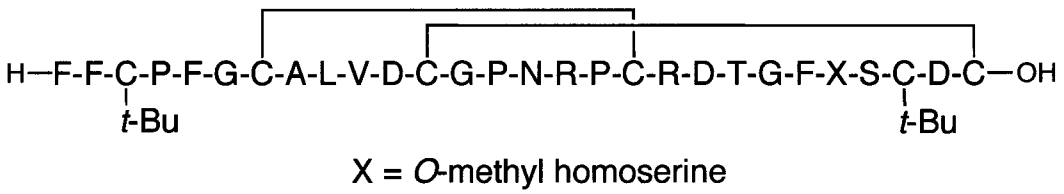


Peptide **180c** was synthesized according to the general method for bis-disulfide bond formation from the linear peptide **180b.** The crude peptide was purified by semi-preparative RP-HPLC using method B ($t_R$ = 24.8 min) to give **180c** as a white powder (22 mg, 23.2 % relative to 100 mg of the crude linear peptide). MALDI-TOF (MS): cald. for $C_{137}H_{202}N_{35}O_{39}S_6$ $(M + H)^+$ 3153.3 Found 3153.9 $(M + H)^+$.

**Tris-disulfide norleucine analogue (180)**

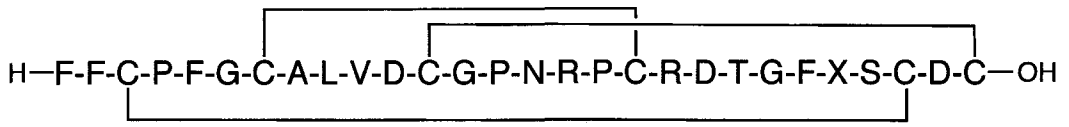


X = *O*-methyl homoserine

The introduction of the third disulfide bond was achieved by DMSO oxidation of the bicyclic peptide **180c** according to the general method for tris-disulfide bond formation. The crude peptide was purified by semi-preparative RP-HPLC using method B ($t_R$ = 25.18 min) to give **180** as a white powder (1.0 mg, 26.3% relative to 4 mg of the bicyclic peptide). MALDI-TOF (MS): cald. for $C_{129}H_{184}N_{35}O_{39}S_6$ $(M + H)^+$ 3039.1 Found 3038.8 $(M + H)^+$.

**Linear glutamine analogue (Cys 3, 26-*t*-Bu, Cys 7, 18-Acm) (181b)**


X = glutamine

Linear peptide **181b** was synthesized on a preloaded $H_2N$-Cys(Trt)-2-ClTrt resin (0.62 mmol/g) on a 0.1 mmol scale using the automated peptide synthesizer according to the general method for solid phase peptide synthesis. Protection of the cysteine residues was Cys 3, 26-*t*-Bu; Cys 7, 18-Trt; Cys 12, 28-Acm. The crude peptide (160 mg, 48.3% relative to the resin loading) was used in the next step without further purification. MALDI-TOF (MS): cald. for $C_{143}H_{215}N_{38}O_{41}S_6$ $(M + H)^+$ 3312.4. Found 3312.5 $(M + H)^+$.

**Bis-disulfide norleucine analogue (181c)**

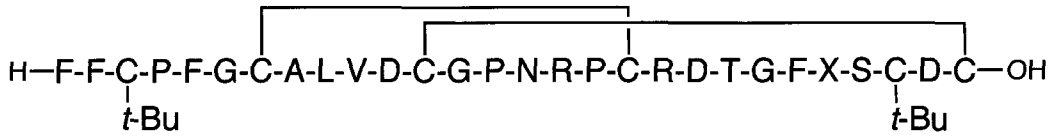


X = glutamine

Peptide **181c** was synthesized according to the general method for bis-disulfide bond formation from the linear peptide **181b.** The crude peptide was purified by semi-preparative RP-HPLC using method B ($t_R$ = 24.0 min) to give **181c** as a white powder (7.6 mg, 5.3 % relative to 150 mg of the crude linear peptide). MALDI-TOF (MS): cald. for $C_{137}H_{201}N_{36}O_{39}S_6$ $(M + H)^+$ 3166.3. Found 3166.8 $(M + H)^+$.

**Tris-disulfide norleucine analogue (181)**

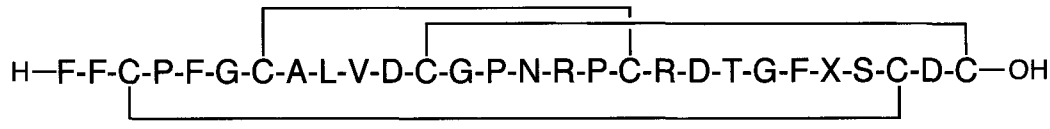


X = glutamine

The introduction of the third disulfide bond was achieved by DMSO oxidation of the bicyclic peptide **181c** according to the general method for tris-disulfide bond formation. The crude peptide was purified by analytical RP-HPLC using method C ($t_R$ = 20.9 min) to give **181** as a white powder (1.2 mg, 27.0% relative to 4.6 mg of the bicyclic peptide). MALDI-TOF (MS): cald. for $C_{129}H_{183}N_{36}O_{39}S_6$ $(M + H)^+$ 3052.1. Found 3052.8 $(M + H)^+$.

**Linear peptide (C7F, C18F) (182a)**

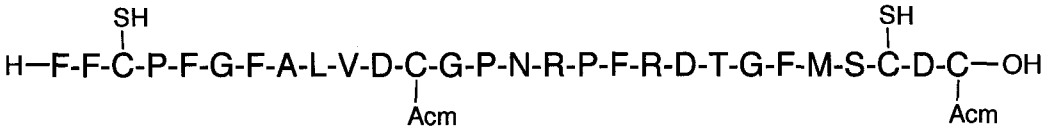


Linear peptide **182a** was synthesized on a preloaded $H_2N$-Cys(Acm)-2-ClTrt resin (0.32 mmol/g) on a 0.1 mmol scale using the automated peptide synthesizer according to the general method for solid phase peptide synthesis. Protection of the cysteine residues was Cys 3, 26-*t*-Bu and Cys 12, 28-Acm. The crude peptide (300 mg, 91.1% relative to the resin loading) was used in the next step without further purification. MALDI-TOF (MS): cald. for $C_{147}H_{209}N_{37}O_{40}S_5$ $(M + H)^+$ 3291.3. Found 3291.8 $(M + H)^+$.

**Bis-disulfide analogue (C7F, C18F) (182)**

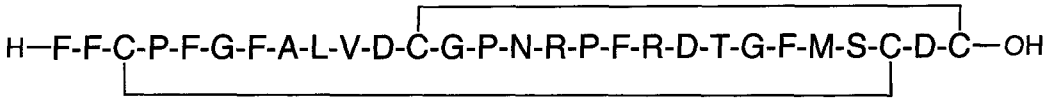


Peptide **182** was synthesized according to the general method for bis-disulfide bond formation from the linear peptide **182a.** The crude peptide was purified by semi-preparative RP-HPLC using method B ($t_R$ = 26.5 min) to give **182** as a white powder (4.8 mg, 3.3 % relative to 150 mg of the crude linear peptide). MALDI-

TOF (MS): cald. for $C_{141}H_{194}N_{35}O_{38}S_5$ $(M + H)^+$ 3145.2. Found 3145.4 $(M + H)^+$.

**Linear peptide (C12F, C28F) (183a)**

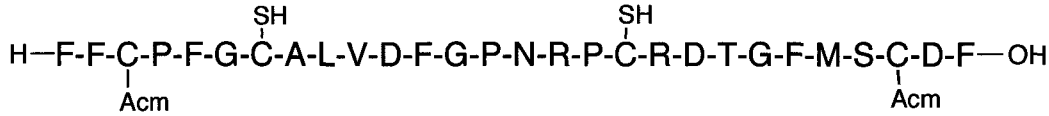


Linear peptide **183a** was synthesized on a preloaded Fmoc-Phe-Wang (0.6 mmol/g) on a 0.1 mmol scale using the automated peptide synthesizer according to the general method for solid phase peptide synthesis. Protection of the cysteine residues was Cys 3,26-Acm and Cys 7,18-Trt. The crude peptide (205 mg, 62.3% relative to the resin loading) was used in the next step without further purification. MALDI-TOF (MS): cald. for $C_{147}H_{209}N_{37}O_{40}S_5$ $(M + H)^+$ 3291.3. Found 3291.8 $(M + H)^+$.

**Bis-disulfide analogue (C12F, C28F) (183)**

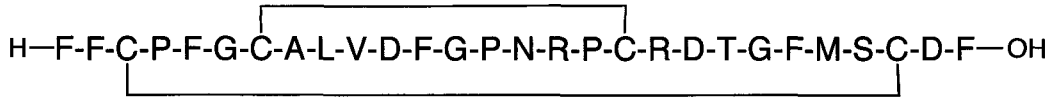


Peptide **183** was synthesized according to the general method for bis-disulfide bond formation from the linear peptide **183a.** The crude peptide was purified by

semi-preparative RP-HPLC using method B ($t_R$ = 26.5 min) to give **183** as a white powder (3.7 mg, 28.6% relative to 30 mg of the crude linear peptide). MALDI-TOF (MS): cald. for $C_{141}H_{194}N_{35}O_{38}S_5$ $(M + H)^+$ 3145.2. Found 3145.8 $(M + H)^+$.

**Linear peptide (C3F, C26F) (184a)**

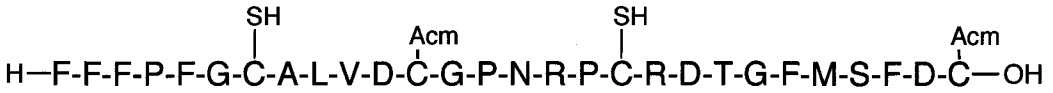


Linear peptide **184a** was synthesized on a preloaded $H_2N$-Cys(Acm)-2-ClTrt resin (0.82 mmol/g) on a 0.1 mmol scale using the automated peptide synthesizer according to the general method for solid phase peptide synthesis. Protection of the cysteine residues was Cys 12,28-Acm and Cys 7,18-Trt. The crude peptide (130 mg, 39.5% relative to the resin loading) was used in the next step without further purification MALDI-TOF (MS): cald. for $C_{147}H_{209}N_{37}O_{40}S_5$ $(M + H)^+$ 3291.3. Found 3291.6 $(M + H)^+$.

**Bis-disulfide analogue (C3F, C26F) (184)**

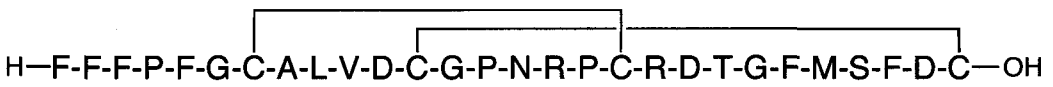


Peptide **184** was synthesized according to the general method for bis-disulfide bond formation from the linear peptide **184a.** The crude peptide was purified by

semi-preparative RP-HPLC using method B ($t_R$ = 27.3 min) to give **184** as a white powder (4.1 mg, 14.3% relative to 30 mg of the crude linear peptide). MALDI-TOF (MS): cald. for $C_{141}H_{194}N_{35}O_{38}S_5$ $(M + H)^+$ 3145.2. Found 3145.0 $(M + H)^+$.

**3'-hydroxy-6'-(prop-2-ynyloxy)-3*H*-spiro[isobenzofuran-1,9'-xanthen]-3-one (187)**

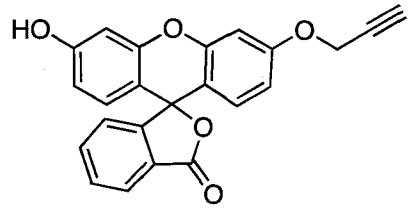


The known compound was prepared by a literature procedure.[154] To a solution of fluorescein sodium salt (2.25 g, 6.0 mmol) in a mixture of THF/MeOH (20 mL: 20 mL), was added propargyl bromide solution (6.72 mL, 120 mmol, 20 equiv) in toluene at rt. The resulting mixture was stirred overnight. Removal of solvent *in vacuo* gave the crude product as a yellow residue. The crude product was purified by flash chromatography ($SiO_2$, EtOAc: Hexanes = 2:8) to afford **187** as a yellow solid (1.77 g, 80%). IR ($CHCl_3$, cast), 3379, 3264, 3108, 3067, 2934, 2121, 1721, 1667, 1611, 1505 $cm^{-1}$; $^1H$ NMR ($CD_3OD$, 600 MHz): δ 7.97 (d, 1H, $J$ = 7.8 Hz Ar-H), 7.69 (m, 2H, Ar-H), 7.13 (d, 1H, $J$ = 7.2 Hz Ar-H), 6.88 (d, 1H, $J$ = 2.0 Hz Ar-H), 6.69-6.51 (m, 5H, Ar-H), 4.72 (d, 2H, $J$ = 2.4 Hz, -O-C$\underline{H_2}$-), 2.94 (t, 1H, $J$ = 2.4 Hz, terminal alkyne-H); $^{13}C$ NMR ($CD_3OD$, 100 MHz): δ 171.4, 161.1, 160.8, 154.4, 153.9, 153.8, 136.6, 131.1, 130.1, 130.0, 128.0, 125.8, 125.2, 113.6,

113.27, 113.25, 111.1, 103.6, 103.2, 79.2, 77.3, 56.9; HRMS (ES): Calcd for $C_{23}H_{14}O_5Na$ 393.0733, found 393.0732.

**(*S*)-*tert*-butyl 15-(((9*H*-fluoren-9-yl)methoxy)carbonylamino)-1-azido-13-oxo-3,6,9-trioxa-12-azahexadecan-16-oate (188)[74]**

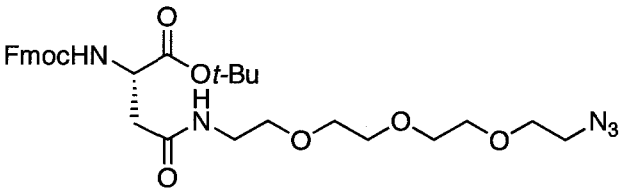


To a solution of Fmoc-Asp-O*t*-Bu (1.036 g, 2.52 mmol) in DCM (20 mL) was added NMM (0.27 mL, 2.52 mmol) and HOBt (0.34 g, 2.52 mmol) followed by PyBOP (1.311 g, 2.52 mmol). The resulting mixture was stirred for 10 min at room temperature. The 11-azido-3,6,9 trioxaundecan-1-amine (0.5 mL, 2.52 mmol) was added to the solution and the resulting reaction mixture was stirred for 12 h. Removal of solvent *in vacuo* gave an oily residue that was taken up in EtOAc (100 mL). The organic solution was then washed with $H_2O$ (3 x 50 mL), 10% citric acid (3 x 50 mL), $H_2O$ (50 mL), saturated $NaHCO_3$ (3 x 50 mL) and brine (50 mL), and dried with $Na_2SO4$. Filtration and concentration *in vacuo* gave the crude product which was purified by flash chromatography ($SiO_2$, EtOAc: Hexanes = 9: 1) to give **188** as a colorless oil (1.29 g, 85 %). $[\alpha]_D^{25}$ 10.7° (*c* 0.6, $CHCl_3$); IR ($CHCl_3$, cast): 3324, 2976, 2928, 2872, 2105, 1724, 1659, 1533 $cm^{-1}$; $^1H$ NMR ($CDCl_3$, 500 MHz): δ 7.70 (d, 2H, *J* = 7.5 Hz, Fmoc-H), 7.56 (t, 2H, *J* = 4.5 Hz, Fmoc-H), 7.33 (t, 2H, *J* = 7.5 Hz, Fmoc-H), 7.25 (t, 2H, *J* = 7.5 Hz, Fmoc-H), 6.30 (app s, 1H, NH), 6.12 (d, 1H, *J* = 8.5 Hz, NH), 4.44 (m, 1H, $H_\alpha$),

4.36 (m, 1H, Fmoc-$CH_2$), 4.27 (m, 1H, Fmoc-$CH_2$), 4.17 (t, 2H, $J$ = 2.5 Hz, Fmoc-CH), 3.59-3.52 (m, 12H, -$C\underline{H}_2C\underline{H}_2$-O), 3.38(m, 2H, NH-$C\underline{H}_2$-$CH_2$-O-), 3.30 (t, 2H, $J$ = 5.0 Hz, $H_\alpha$), 2.82 (dd, $J$ = 15.0, 5.0 Hz, -$CH_2$-$C\underline{H}_2$-$N_3$), 2.66 (dd, 1H, $J$ = 15.5, 4.0 Hz, -$CH_2$-$C\underline{H}_2$-$N_3$), 1.43 (s, 9H, -$C(CH_3)_3$); $^{13}$C NMR ($CDCl_3$, 125 MHz, rotamer): δ 170.0, 169.8, 156.1, 143.9(143.8), 141.2, 127.6, 127.0, 125.2(125.1), 119.9, 82.1, 70.56, 70.49, 70.41, 70.2, 69.9, 69.6, 67.0, 51.4, 50.5, 47.1, 39.2, 37.8, 27.9; HRMS (ES): Calcd for $C_{31}H_{41}N_5O_8Na$ 634.2847, found 634.2841.

**(*S*)-15-(((9*H*-Fluoren-9-yl)methoxy)carbonylamino)-1-azido-13-oxo-3,6,9-trioxa-12-azahexadecan-16-oic acid (189)[82]**

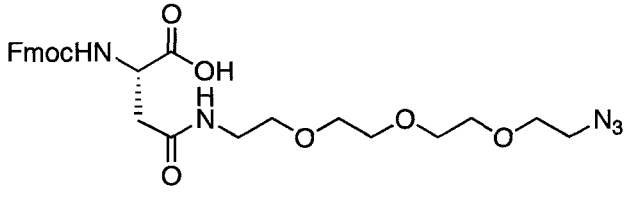


To a solution of **188** (1.2 g, 1.96 mmol) in DCM (10 mL) was added TFA (10 mL). The resulting mixture was stirred at room temperature for 1 h. Removal of solvent *in vacuo* gave the product as a colorless oil (1.0 g, 98%). The product was used for next step without further purification. $[\alpha]_D^{25}$ 23.88° (*c* 0.36, $CHCl_3$); IR ($CHCl_3$, cast): 3322, 3066, 2924, 2874, 2576, 2107, 1719, 1546 $cm^{-1}$; $^1$H NMR ($CDCl_3$, 500 MHz): δ 7.75 (d, 2H, $J$ = 7.5 Hz, Fmoc-H), 7.60 (m, 2H, Fmoc-H), 7.39 (t, 2H, $J$ = 5.0 Hz, Fmoc-H), 7.30 (t, 2H, $J$ = 7.5 Hz, Fmoc-H), 6.94 (app s, 1H, NH), 6.31 (d, 1H, $J$ = 7.5 Hz, NH), 4.63 (m, 1H, $H_\alpha$), 4.45-4.32 (m, 2H, Fmoc-$CH_2$), 4.21 (t, 1H, $J$ = 7.0 Hz, Fmoc-CH), 3.66-3.34 (m, 16H, -$CH_2CH_2$-

and $H_6$), 2.94 (dd, $J$ = 15.0, 4.0 Hz, -$CH_2$-$C\underline{H}_2$-$N_3$), 2.81 (dd, 1H, $J$ = 15.0, 6.0 Hz, -$CH_2$-$C\underline{H}_2$-$N_3$); $^{13}C$ NMR ($CDCl_3$, 125 MHz rotamer): δ172.6, 171.4, 156.2, 143.7(143.6), 141.3(141.2), 127.7, 127.1, 125.1, 119.9, 70.6, 70.4, 70.36(70.34), 69.9, 69.8, 69.1, 67.4, 50.9, 50.6(50.5), 47.0, 39.7, 37.8; HRMS (ES): Calcd for $C_{27}H_{33}N_5O_8Na$ 578.2221, found 578.2223.

**Linear Asp20N3 analogue (Cys 3, 26-*t*-Bu, Cys 7, 18-Acm) (192)**

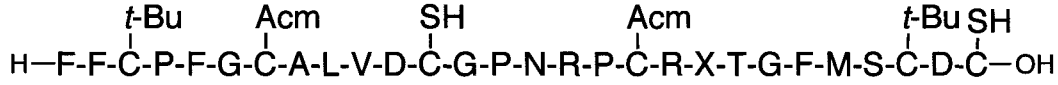


X = aspartic acid derivative

Linear peptide **192** was synthesized on a preloaded $H_2N$-Cys(Trt)-2-ClTrt resin (0.62 mmol/g) on a 0.1 mmol scale using the automated peptide synthesizer according to the general method for solid phase peptide synthesis. Protection of the cysteine residues was Cys 3, 26-*t*-Bu; Cys 7, 18-Trt; Cys 12, 28-Acm. The crude peptide (200 mg, 56.8% relative to the resin loading) was used in the next step without further purification. MALDI-TOF (MS): cald. for $C_{151}H_{232}N_{41}O_{42}S_7$ $(M + H)^+$ 3515.5. Found 3515.7 $(M + H)^+$.

**Bis-disulfide Asp20N3 analogue (193)**

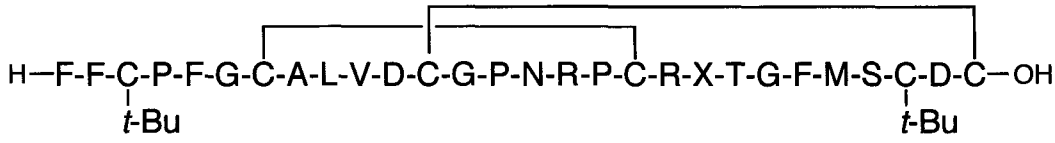


Peptide **193** was synthesized according to the general method for bis-disulfide bond formation from the linear peptide **192.** The crude peptide was purified by semi-preparative RP-HPLC using method B ($t_R$ = 26.7 min) to give **193** as a white powder (10 mg, 5.8 % relative to 180 mg of the crude linear peptide). MALDI-TOF (MS): cald. for $C_{145}H_{218}N_{39}O_{40}S_7$ $(M + H)^+$ 3369.4. Found 3369.2 $(M + H)^+$.

**Tris-disulfide Asp20N3 analogue (194)**

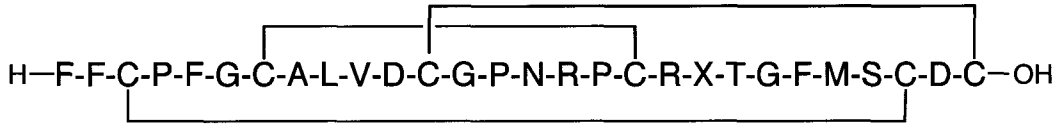


The introduction of the third disulfide bond was achieved by DMSO oxidation of the bicyclic peptide **193** according to the general method for tris-disulfide bond formation. The reaction took 18 h for completion. The crude peptide was purified by semi-preparative RP-HPLC using method B ($t_R$ = 28.9 min) to give **194** as a white powder (1.0 mg, 18.8% relative to 5.5 mg of the bicyclic peptide). MALDI-

TOF (MS): cald. for $C_{137}H_{200}N_{39}O_{40}S_7$ $(M + H)^+$ 3255.2. Found 3255.4 $(M + H)^+$.

**The fluorescent conjugate (196)**[155]

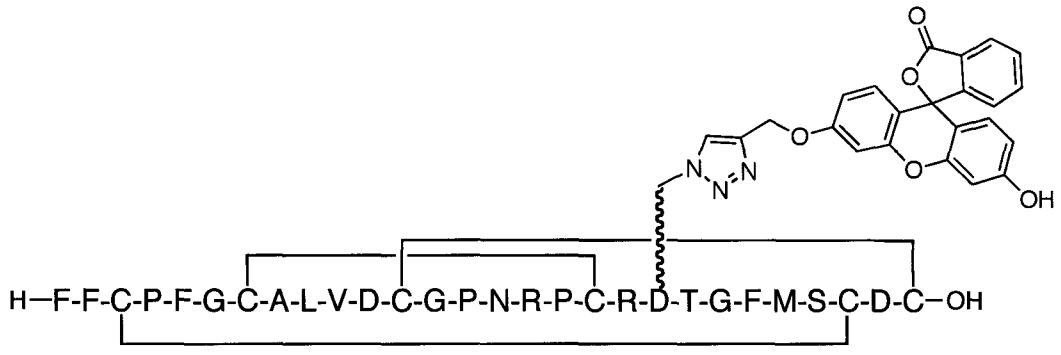


The neopetrosiamide analogue **194** (0.6 mg, 0.184 μmol) was dissolved in the mixture of *t*-BuOH (0.2 mL) and $H_2O$ (0.2 mL) at rt. The fluorescent derivative **187** (0.2 mg, 0.552 μmol, 3.0 equiv relative to starting material) was added followed by 0.1 N $CuSO_4$ (5.0 equiv, 9.2 μL) and 0.2 N sodium ascorbate (10 equiv, 9.2 μL). The resulting mixture was stirred for 22 h at rt, in the absence of light (covered by a tin foil). The reaction progress was monitored by MALDI-TOF-MS. Once the reaction was complete, crude peptide was purified directly by semi-preparative RP-HPLC using method B ($t_R$ = 31.2 min) to give **196** as a white solid (0.25 mg, 38%). MALDI-TOF (MS): cald. for $C_{160}H_{214}N_{39}O_{45}S_7$ $(M + H)^+$ 3625.3. Found 3625.2 $(M + H)^+$.

### 5.2.2.c. Disulfide mapping experiment and results

#### (1). Norleucine analogue (141) having originally proposed disulfide connectivity

Partial reduction with TCEP in citric acid buffer (pH = 3) was performed according to general method A. Two partially reduced species were manually collected and subjected to the first alkylation using the general method for Nem alkylation. The complete reduction of the two Nem-alkylated species was done with TCEP. One species (**160**) was subjected to MS/MS sequencing directly without the second alkylation to give the disulfide connectivity of **161** (Figure 59). Upon complete reduction, the other species was treated with Nmm according to the general method to give the fully labeled linear peptide **162**. MS/MS sequencing revealed the disulfide connectivity of **163** (Figure 60).

**Figure 59.** MS/MS sequencing and disulfide connectivity deduction of **161**

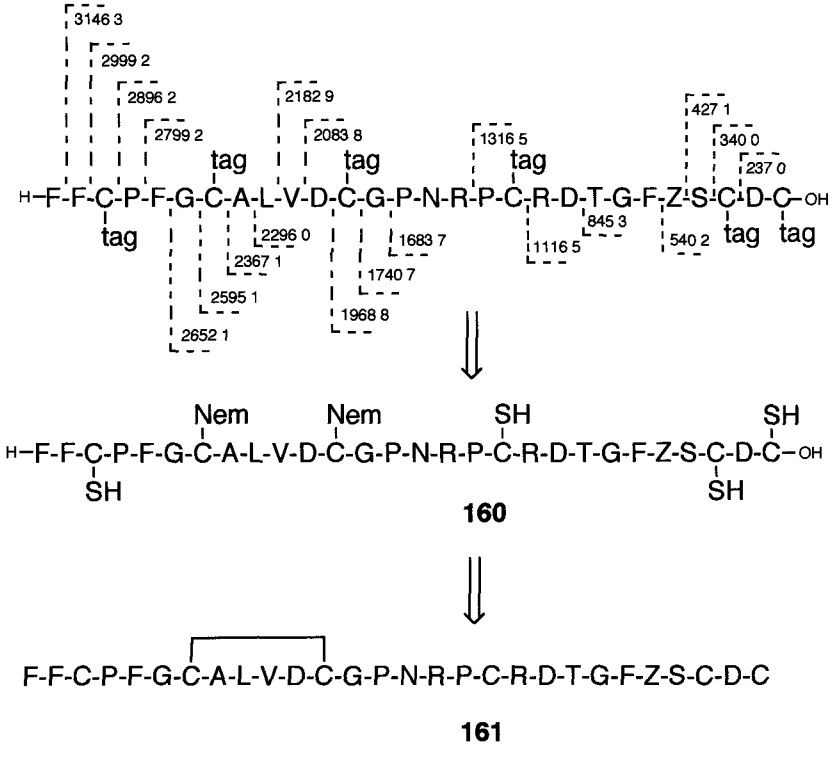

**Figure 60.** MS/MS sequencing and disulfide connectivity deduction of **163**

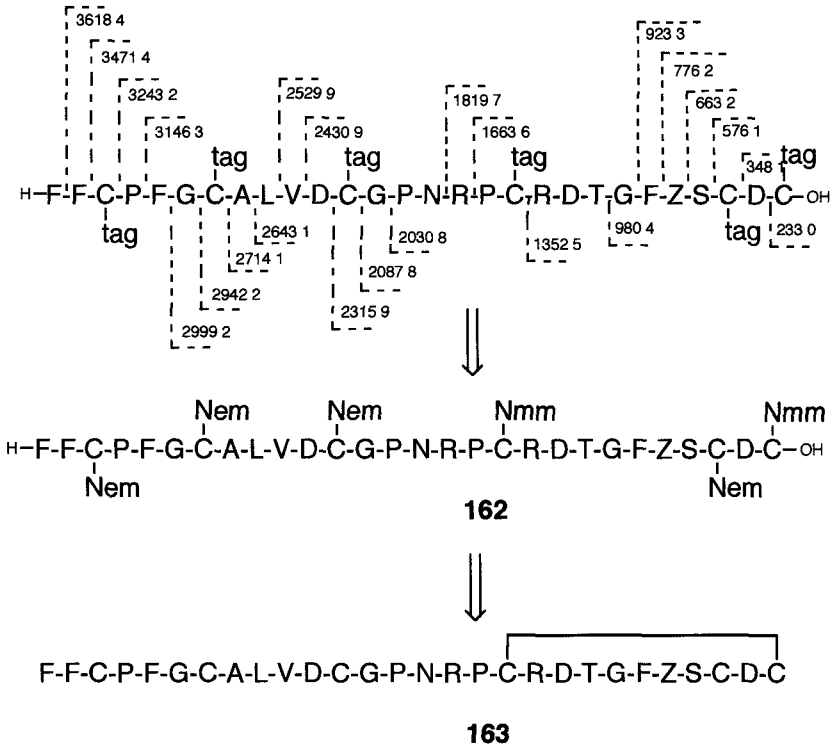


**(2). Synthetic neopetrosiamides (130) having originally proposed structure**

Partial reduction with TCEP in citric acid buffer (pH = 3) was performed according to general method A. The partially reduced species were manually collected and subjected to the first alkylation using the general method for Nem alkylation. The complete reduction of the Nem alkylated species followed by the second alkylation with Nmm gave the linear labeled species. Enzymatic digestion of these species with trypsin followed by MS/MS sequencing revealed the linear sequence of fragments. The individual disulfide connectivities were deduced as shown in Figure 61 and Figure 62

**Figure 61.** MS/MS sequencing and disulfide connectivity deduction of **166**

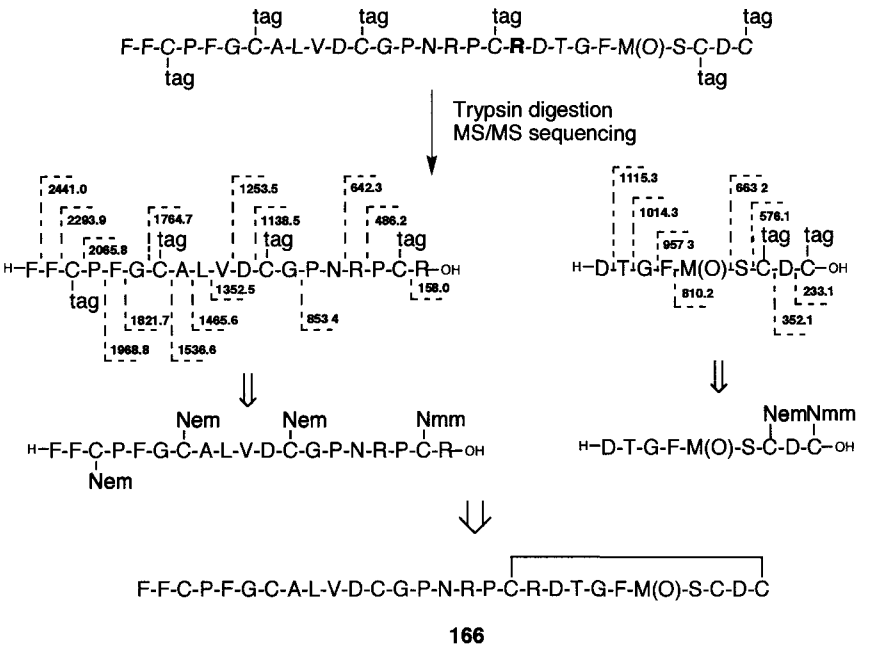


166

**Figure 62.** MS/MS sequencing and disulfide connectivity deduction of **167**

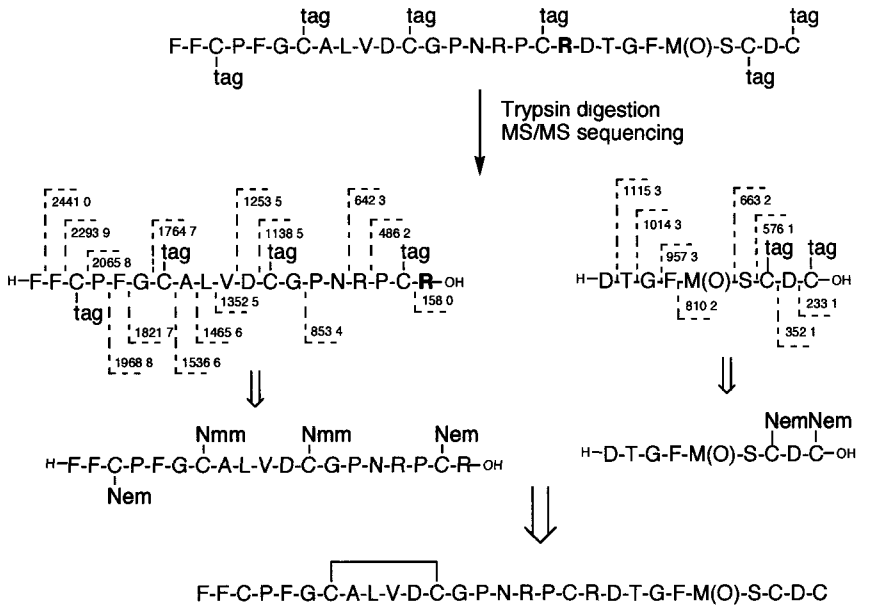


167

**(3). Natural neopetrosiamide from marine sponge**

The connectivity was confirmed by the combination of the partial reduction and enzymatic digestion.

Partial reduction with TECP and isolation of the intermediates was done according to method B. A typical HPLC trace is shown in Figure 63. Notably, only one partially reduced species was generated.

**Figure 63.** HPLC trace of partial reduction of natural neopetrosiamide with TCEP

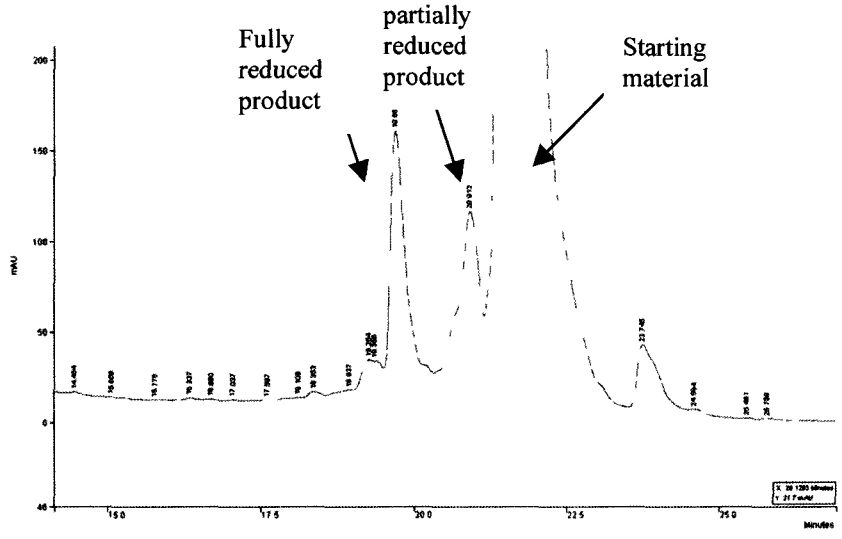


The partially reduced species was alkylated with Nem according to the general method A. Full reduction with TCEP followed by a second alkylation with Nmm gave the linear labeled species **168**. MS/MS sequencing of **168** revealed the disulfide connectivity of **169** (Figure 64).

**Figure 64.** MS/MS sequencing and disulfide connectivity deduction of **169**

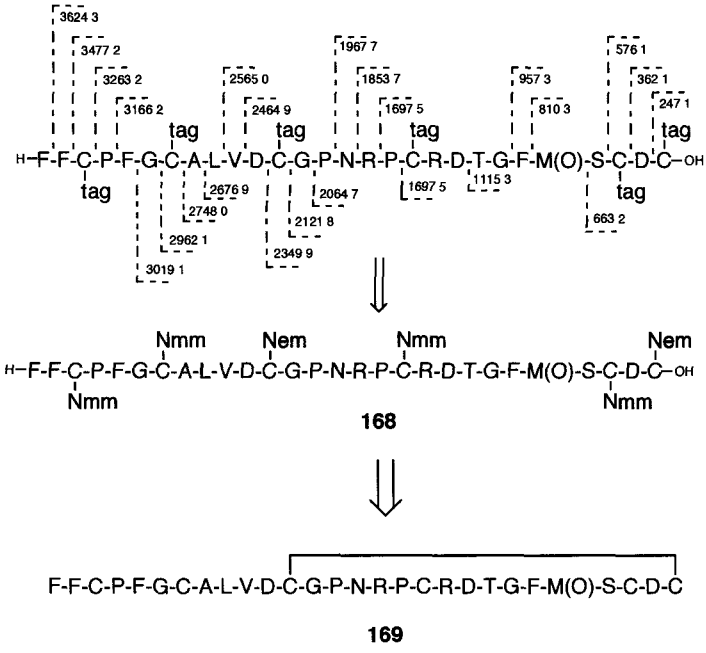


The enzymatic digestion of natural neopetrosiamides was done using endoproteinase Asp-*N* according to the general method. The enzymatic cleavage product (**170**) was subjected to LC-MS/MS analysis. The disulfide connectivity of **171** was revealed as shown in Figure 65.

**Figure 65.** MS/MS sequencing of enzymatically digested product and disulfide connectivity deduction of **171**

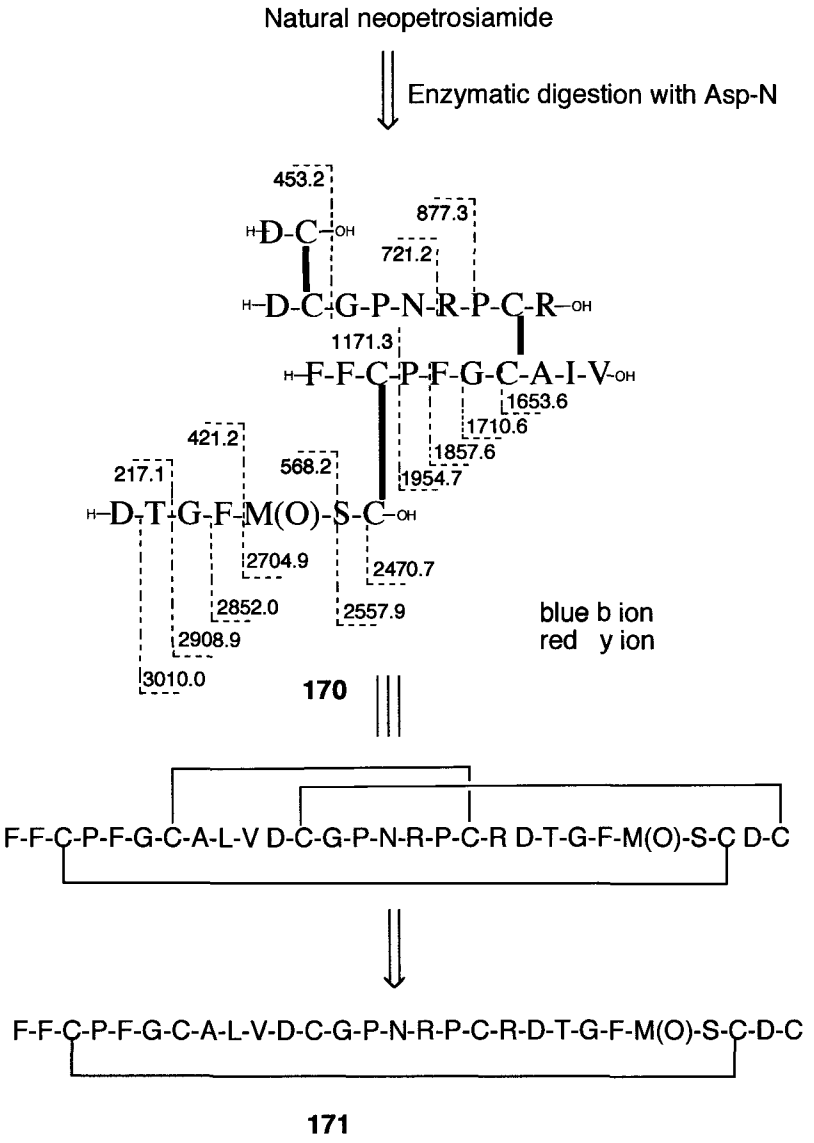


**(4). Synthetic neopetrosiamide having the revised disulfide connectivity**

The synthetic peptide (**172**) was treated with endoproteinase Asp-*N* according to the general method to yield the digested product. This species was subjected to

LC-MS/MS analysis. The MS/MS sequencing shown below confirmed the connections of three pairs of disulfides (highlighted in orange)

**Figure 66.** MS/MS sequencing and disulfide connectivity deduction of **172**

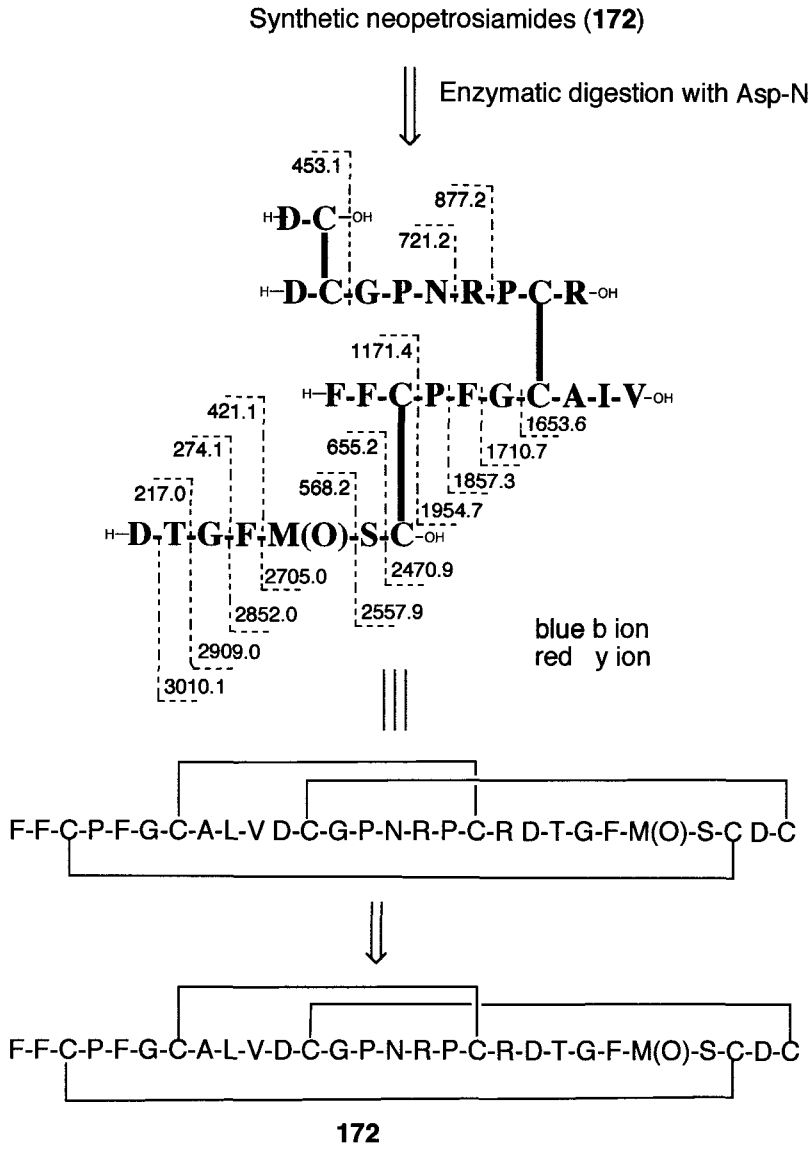

# Chapter 6. References

1. Lee, H. J.; Macbeth, A. H.; Pagani, J. H.; Young, W. S., Oxytocin: The great facilitator of life. *Prog. Neurobiol.* **2009,** *88*, 127-151.
2. Holt, N. F.; Haspel, K. L., Vasopressin: A review of therapeutic applications. *J. Cardiothorac. Vasc. Anesth.* **2010,** *24*, 330-347.
3. Bedoyere, G. D. L., The discovery of penicillin. *Evans Brothers Ltd: London.* **2005.**
4. Vlieghe, P.; Lisowski, V.; Martinez, J.; Khrestchatisky, M., Synthetic therapeutic peptides: science and market. *Drug Discov. Today* **2010,** *15*, 40-56.
5. Marx, V., Watching peptide drugs grow up. *Chem. Eng. News* **2005,** *83*, 17-24.
6. Marx, V., Roche's Fuzeon challenge. *Chem. Eng. News* **2005,** *83*, 16-17.
7. Gracia, S. R.; Gaus, K.; Sewald, N., Synthesis of chemically modified bioactive peptides: recent advances, challenges and developments for medicinal chemistry. *Future Med. Chem.* **2009,** *1*, 1289-1310.
8. Sable, C. A.; Strohmaier, K. M.; Chodakewitz, J. A., Advances in antifungal therapy. *Annu. Rev. Med.* **2008,** *59*, 361-379.
9. Craik, D. J.; Cemazar, M.; Daly, N. L., The chemistry and biology of cyclotides. *Curr. Opin. Drug Discov. Dev.* **2007,** *10*, 176-184.
10. Daly, N. L.; Craik, D. J., Design and therapeutic applications of cyclotides. *Future Med. Chem.* **2009,** *1*, 1613-1622.

11. Williams, J. A.; Day, M.; Heavner, J. E., Ziconotide: an update and review. *Expert Opin. Pharmacother.* **2008,** *9*, 1575-1583.

12. Willey, J. M.; van der Donk, W. A., Lantibiotics: Peptides of diverse structure and function. *Annu. Rev. Microbiol.* **2007,** *61*, 477-501.

13. Nagao, J. I.; Asaduzzaman, S. M.; Aso, Y.; Okuda, K.; Nakayama, J.; Sonomoto, K., Lantibiotics: Insight and foresight for new paradigm. *J. Biosci. Bioeng.* **2006,** *102*, 139-149.

14. Chatterjee, C.; Paul, M.; Xie, L. L.; van der Donk, W. A., Biosynthesis and mode of action of lantibiotics. *Chem. Rev.* **2005,** *105*, 633-683.

15. Smith, L.; Hillman, J. D., Therapeutic potential of type A (I) lantibiotics, a group of cationic peptide antibiotics. *Curr. Opin. Microbiol.* **2008,** *11*, 401-408.

16. Li, J. W. H.; Vederas, J. C., Drug discovery and natural products: end of an era or an endless frontier? *Science* **2009,** *325*, 161-165.

17. Demain, A. L., Antibiotics: natural products essential to human health. *Med. Res. Rev.* **2009,** *29*, 821-842.

18. Levy, S. B.; Marshall, B., Antibacterial resistance worldwide: causes, challenges and responses. *Nat. Med.* **2004,** *10*, S122-S129.

19. Overbye, K. M.; Barrett, J. F., Antibiotics: where did we go wrong. *Drug Discov. Today* **2005,** *10*, 45-52.

20. Alekshun, M. N.; Levy, S. B., Molecular mechanisms of antibacterial multidrug resistance. *Cell* **2007,** *128*, 1037-1050.

21. Talbot, G. H.; Bradley, J.; Edwards, J. E.; Gilbert, D.; Scheld, M.; Bartlett, J. G., Bad bugs need drugs: an update on the development pipeline from the Antimicrobial Availability Task Force of the Infectious Diseases Society of America (vol 42, pg 657, 2006). *Clin. Infect. Dis.* **2006,** *42*, 1065-1065.

22. Cotter, P. D.; Hill, C.; Ross, R. P., Bacteriocins: developing innate immunity for food. *Nat. Rev. Microbiol.* **2005,** *3*, 777-788.

23. Riley, M. A.; Wertz, J. E., Bacteriocins: evolution, ecology, and application. *Annu. Rev. Microbiol.* **2002,** *56*, 117-137.

24. Draper, L. A.; Ross, R. P.; Hill, C.; Cotter, P. D., Lantibiotic immunity. *Curr. Protein Pept. Sci.* **2008,** *9*, 39-49.

25. Klaenhammer, T. R., Bacteriocins of lactic-acid bacteria. *Biochimie* **1988,** *70*, 337-349.

26. Daw, M. A.; Falkiner, F. R., Bacteriocins: nature, function and structure. *Micron* **1996,** *27*, 467-479.

27. Nes, I. F.; Yoon, S. S.; Diep, D. B., Ribosomally synthesiszed antimicrobial peptides (Bacteriocins) in lactic acid bacteria: A review. *Food Sci. Biotechnol.* **2007,** *16*, 675-690.

28. Martin-Visscher, L. A. Examining the structure, fuction and mode of action of bacteriocins from lactic acid bacteria. Ph.D. Thesis, University of Alberta, Edmonton, 2010.

29. Fukase, K.; Kitazawa, M.; Sano, A.; Shimbo, K.; Horimoto, S.; Fujita, H.; Kubo, A.; Wakamiya, T.; Shiba, T., Synthetic study on peptide antibiotic

Nisin .5. total synthesis of Nisin. *Bull. Chem. Soc. Jpn.* **1992,** *65*, 2227-2240.

30. Sailer, M.; Helms, G. L.; Henkel, T.; Niemczura, W. P.; Stiles, M. E.; Vederas, J. C., $^{15}N$- and $^{13}C$-labeled media from *Anabaena* Sp for universal isotopic labeling of Bacteriocins - NMR resonance assignments of Leucocin-A from *Leuconostoc-gelidum* and Nisin-A from *Lactococcus-lactis*. *Biochemistry* **1993,** *32*, 310-318.

31. Cotter, P. D.; Hill, C.; Ross, R. P., Bacterial lantibiotics: strategies to improve therapeutic potential. *Curr. Protein Pept. Sci.* **2005,** *6*, 61-75.

32. Kruszewska, D.; Sahl, H. G.; Bierbaum, G.; Pag, U.; Hynes, S. O.; Ljungh, A., Mersacidin eradicates methicillin-resistant *Staphylococcus* aureus (MRSA) in a mouse rhinitis model. *J. Antimicrob. Chemother.* **2004,** *54*, 648-653.

33. Jung, G., Lantibiotics - Ribosomally synthesized biologically-active polypeptides containing sulfide bridges and alpha-beta-didehydroamino Acids. *Angew. Chem. Int. Edit. Engl.* **1991,** *30*, 1051-1068.

34. Aranha, C.; Gupta, S.; Reddy, K. V. R., Contraceptive efficacy of antimicrobial peptide Nisin: in vitro and in vivo studies. *Contraception* **2004,** *69*, 333-338.

35. Martin, N. I.; Sprules, T.; Carpenter, M. R.; Cotter, P. D.; Hill, C.; Ross, R. P.; Vederas, J. C., Structural characterization of lacticin 3147, a two-peptide lantibiotic with synergistic activity. *Biochemistry* **2004,** *43*, 3049-3056.

36. Dischinger, J.; Josten, M.; Szekat, C.; Sahl, H. G.; Bierbaum, G., Production of the Novel Two-Peptide Lantibiotic Lichenicidin by *Bacillus licheniformis* DSM 13. *PLoS One* **2009,** *4*.

37. Lawton, E. M.; Ross, R. P.; Hill, C.; Cotter, P. D., Two-peptide lantibiotics: a medical perspective. *Mini-Rev. Med. Chem.* **2007,** *7*, 1236-1247.

38. Ryan, M. P.; Flynn, J.; Hill, C.; Ross, R. P.; Meaney, W. J., The natural food grade inhibitor, lacticin 3147, reduced the incidence of mastitis after experimental challenge with *Streptococcus dysgalactiae* in nonlactating dairy cows. *J. Dairy Sci.* **1999,** *82*, 2625-2631.

39. Stergiou, V. A.; Thomas, L. V.; Adams, M. R., Interactions of nisin with glutathione in a model protein system and meat. *J. Food Prot.* **2006,** *69*, 951-956.

40. Wilson-Stanford, S.; Kalli, A.; Hakansson, K.; Kastrantas, J.; Orugunty, R. S.; Smith, L., Oxidation of lanthionines renders the lantibiotic Nisin inactive. *Appl. Environ. Microbiol.* **2009,** *75*, 1381-1387.

41. Oman, T. J.; van der Donk, W. A., Follow the leader: the use of leader peptides to guide natural product biosynthesis. *Nat. Chem. Biol.* **2010,** *6*, 9-18.

42. Bierbaum, G.; Sahl, H. G., Lantibiotics: Mode of action, biosynthesis and bioengineering. *Curr. Pharm. Biotechnol.* **2009,** *10*, 2-18.

43. Kuipers, A.; Meijer-Wierenga, J.; Rink, R.; Kluskens, L. D.; Moll, G. N., Mechanistic dissection of the enzyme complexes involved in biosynthesis

of Lacticin 3147 and Nisin. *Appl. Environ. Microbiol.* **2008,** *74*, 6591-6597.

44. Li, B.; Yu, J. P. J.; Brunzelle, J. S.; Moll, G. N.; van der Donk, W. A.; Nair, S. K., Structure and mechanism of the lantibiotic cyclase involved in nisin biosynthesis. *Science* **2006,** *311*, 1464-1467.

45. Cotter, P. D.; O'Connor, P. M.; Draper, L. A.; Lawton, E. M.; Deegan, L. H.; Hill, C.; Ross, R. P., Posttranslational conversion of L-serines to D-alanines is vital for optimal production and activity of the lantibiotic lacticin 3147. *Proc. Natl. Acad. Sci. U. S. A.* **2005,** *102*, 18584-18589.

46. Majer, F.; Schmid, D. G.; Altena, K.; Bierbaum, G.; Kupke, T., The flavoprotein MrsD catalyzes the oxidative decarboxylation reaction involved in formation of the peptidoglycan biosynthesis inhibitor mersacidin. *J. Bacteriol.* **2002,** *184*, 1234-1243.

47. Breukink, E.; de Kruijff, B., Lipid II as a target for antibiotics. *Nat. Rev. Drug Discovery* **2006,** *5*, 321-332.

48. Martin, N. I.; Breukink, E., Expanding role of lipid II as a target for lantibiotics. *Future Microbiol.* **2007,** *2*, 513-525.

49. de Kruijff, B.; van Dam, V.; Breukink, E., Lipid II: A central component in bacterial cell wall synthesis and a target for antibiotics. *Prostaglandins Leukotrienes and Essential Fatty Acids* **2008,** *79*, 117-121.

50. Chatterj.A. N; Perkins, H. R., Compounds formed between nucleotides related to biosynthesis of bacterial cell wall and Vancomycin. *Biochem. Biophys. Res. Commun.* **1966,** *24*, 489-94.

51. Molinari, H.; Pastore, A.; Lian, L. Y.; Hawkes, G. E.; Sales, K., Structure of Vancomycin and a Vancomycin D-Ala-D-Ala complex in solution. *Biochemistry* **1990,** *29*, 2271-2277.

52. Hasper, H. E.; Kramer, N. E.; Smith, J. L.; Hillman, J. D.; Zachariah, C.; Kuipers, O. P.; de Kruijff, B.; Breukink, E., An alternative bactericidal mechanism of action for lantibiotic peptides that target lipid II. *Science* **2006,** *313*, 1636-1637.

53. Breukink, E.; Wiedemann, I.; van Kraaij, C.; Kuipers, O. P.; Sahl, H. G.; de Kruijff, B., Use of the cell wall precursor lipid II by a pore-forming peptide antibiotic. *Science* **1999,** *286*, 2361-2364.

54. Hsu, S. T. D.; Breukink, E.; Tischenko, E.; Lutters, M. A. G.; de Kruijff, B.; Kaptein, R.; Bonvin, A.; van Nuland, N. A. J., The nisin-lipid II complex reveals a pyrophosphate cage that provides a blueprint for novel antibiotics. *Nat. Struct. Mol. Biol.* **2004,** *11*, 963-967.

55. Breukink, E., A lesson in efficient killing from two-component lantibiotics. *Mol. Microbiol.* **2006,** *61*, 271-273.

56. Wiedemann, I.; Bottiger, T.; Bonelli, R. R.; Wiese, A.; Hagge, S. O.; Gutsmann, T.; Seydel, U.; Deegan, L.; Hill, C.; Ross, P.; Sahl, H. G., The mode of action of the lantibiotic lacticin 3147 - a complex mechanism involving specific interaction of two peptides and the cell wall precursor lipid II. *Mol. Microbiol.* **2006,** *61*, 285-296.

57. Pattabiraman, V. R.; McKinnie, S. M. K.; Vederas, J. C., Solid-supported synthesis and biological evaluation of the lantibiotic peptide

bis(desmethyl) lacticin 3147 A2. *Angew. Chem. Int. Ed. Engl.* **2008,** *47*, 9472-9475.

58. Oman, T. J.; van der Donk, W. A., Insights into the mode of action of the two-peptide lantibiotic haloduracin. *ACS Chem. Biol.* **2009,** *4*, 865-874.

59. Brotz, H.; Bierbaum, G.; Leopold, K.; Reynolds, P. E.; Sahl, H. G., The lantibiotic mersacidin inhibits peptidoglycan synthesis by targeting lipid II. *Antimicrob. Agents Chemother.* **1998,** *42*, 154-160.

60. Fukase, K.; Kitazawa, M.; Sano, A.; Shimbo, K.; Fujita, H.; Horimoto, S.; Wakamiya, T.; Shiba, T., Total synthesis of peptide antibiotic Nisin. *Tetrahedron Lett.* **1988,** *29*, 795-798.

61. Fukase, K.; Wakamiya, T.; Shiba, T., Synthetic study on peptide antibiotic Nisin .2. the synthesis of ring-B. *Bull. Chem. Soc. Jpn.* **1986,** *59*, 2505-2508.

62. Fukase, K.; Oda, Y.; Kubo, A.; Wakamiya, T.; Shiba, T., Synthetic study on peptide antibiotic Nisin .4. synthesis of ring D-E. *Bull. Chem. Soc. Jpn.* **1990,** *63*, 1758-1763.

63. Fukase, K.; Kitazawa, M.; Wakamiya, T.; Shiba, T., Synthetic study on peptide antibiotic Nisin .3. synthesis of ring-C. *Bull. Chem. Soc. Jpn.* **1990,** *63*, 1838-1840.

64. Harpp, D. N.; Gleason, J. G., Organic sulfur chemistry .10. selective desulfurization of disulfides - scope and mechanism. *J. Am. Chem. Soc.* **1971,** *93*, 2437-2445.

65. Ross, A. C.; Liu, H. Q.; Pattabiraman, V. R.; Vederas, J. C., Synthesis of the lantibiotic lactocin S using peptide cyclizations on solid phase. *J. Am. Chem. Soc.* **2010,** *132*, 462-463.

66. Martin, N. I., Concise Preparation of Tetra-orthogonally protected (*2S,6R*)-lanthionines. *J. Org. Chem.* **2009,** *74*, 946-949.

67. Paul, M.; van der Donk, W. A., Chemical and enzymatic synthesis of lanthionines. *Mini-Rev. Org. Chem.* **2005,** *2*, 23-37.

68. Bregant, S.; Tabor, A. B., Orthogonally protected lanthionines: Synthesis and use for the solid-phase synthesis of an analogue of nisin ring C. *J. Org. Chem.* **2005,** *70*, 2430-2438.

69. Matteucci, M.; Bhalay, G.; Bradley, M., Cystine mimetics - solid phase lanthionine synthesis. *Tetrahedron Lett.* **2004,** *45*, 1399-1401.

70. Mustapa, M. F. M.; Harris, R.; Bulic-Subanovic, N.; Elliott, S. L.; Bregant, S.; Groussier, M. F. A.; Mould, J.; Schultz, D.; Chubb, N. A. L.; Gaffney, P. R. J.; Driscoll, P. C.; Tabor, A. B., Synthesis of orthogonally protected lanthionines. *J. Org. Chem.* **2003,** *68*, 8185-8192.

71. Nakajima, K.; Oda, H.; Okawa, K., Studies on 2-aziridinecarboxylic acid .9. Convenient synthesis of optically-active S-alkylcysteine, threo-S-alkyl-beta-methylcysteine, and lanthionine derivatives via the ring-opening reaction of aziridine by several thiols. *Bull. Chem. Soc. Jpn.* **1983,** *56*, 520-522.

72. Narayan, R. S.; VanNieuwenhze, M. S., Versatile and stereloselective syntheses of orthogonally protected beta-methylcysteine and beta-methyllanthionine. *Org. Lett.* **2005,** *7*, 2655-2658.

73. Cobb, S. L.; Vederas, J. C., A concise stereoselective synthesis of orthogonally protected lanthionine and beta-methyllanthionine. *Org. Biomol. Chem.* **2007,** *5*, 1031-1038.

74. Pattabiraman, V. R.; Stymiest, J. L.; Derksen, D. J.; Martin, N. I.; Vederas, J. C., Multiple on-resin olefin metathesis to form ring-expanded analogues of the lantibiotic peptide, lacticin 3147 A2. *Org. Lett.* **2007,** *9*, 699-702.

75. Ghalit, N.; Rijkers, D. T. S.; Kemmink, J.; Cees, V. B.; Liskamp, R. M. J., Pre-organization induced synthesis of a crossed alkene-bridged nisin Z DE-ring mimic by ring-closing metathesis. *Chem. Commun.* **2005**, 192-194.

76. Ghalit, N.; Reichwein, J. F.; Hilbers, H. W.; Breukink, E.; Rijkers, D. T. S.; Liskamp, R. M. J., Synthesis of bicyclic alkene-/alkane-bridged nisin mimics by ring-closing metathesis and their biochemical evaluation as lipid II binders: toward the design of potential novel antibiotics. *ChemBioChem* **2007,** *8*, 1540-1554.

77. Ghalit, N.; Poot, A. J.; Furstner, A.; Rijkers, D. T. S.; Liskamp, R. M. J., Ring-closing alkyne metathesis approach toward the synthesis of alkyne mimics of thioether A-, B-, C-, and DE-ring systems of the antibiotic nisin Z. *Org. Lett.* **2005,** *7*, 2961-2964.

78. Ghalit, N.; Kemmink, J.; Hilbers, H. W.; Versluis, C.; Rijkers, D. T. S.; Liskamp, R. M. J., Step-wise and pre-organization induced synthesis of a crossed alkene-bridged nisin Z DE-ring mimic by ring-closing metathesis. *Org. Biomol. Chem.* **2007,** *5*, 924-934.

79. Allen, F. H.; Kennard, O.; Watson, D. G.; Brammer, L.; Orpen, A. G.; Taylor, R., Tables of bond lengths determined by X-ray and neutron-diffraction .1. bond lengths in organic-compounds. *J. Chem. Soc.-Perkin Trans. 2* **1987**, S1-S19.

80. Glowka, M. L.; Parthasarathy, R., Structure of DL-lanthionine monohydrate - Hydrogen-bonding patterns in amino-acid crystal-structures. *Acta Crystallogr. Sect. C-Cryst. Struct. Commun.* **1986,** *42*, 620-623.

81. Liu, H. Q.; Pattabiraman, V. R.; Vederas, J. C., Synthesis and biological activity of oxa-lacticin A2, a lantibiotic analogue with sulfur replaced by oxygen. *Org. Lett.* **2009,** *11*, 5574-5577.

82. Liu, H. Q.; Pattabiraman, V. R.; Vederas, J. C., Stereoselective syntheses of 4-oxa diaminopimelic acid and its protected derivatives via aziridine ring opening. *Org. Lett.* **2007,** *9*, 4211-4214.

83. Zhou, P. C., B.; Davis, F. A., Asymmetric syntheses with aziridinecarboxylate and aziridinephosphonate building blocks. In *Aziridines and Epoxides in Organic Synthesis*, Yudin, A. K., Ed. Wiley-VCH: Weiheim, Germany, 2006; p 89.

84. Hu, X. E., Nucleophilic ring opening of aziridines. *Tetrahedron* **2004,** *60*, 2701-2743.

85. McKeever, B.; Pattenden, G., Total synthesis of trunkamide A, a novel thiazoline-based prenylated cyclopeptide metabolite from *Lissoclinum* sp. *Tetrahedron* **2003,** *59*, 2713-2727.

86. Ho, M. F.; Wang, W. H.; Douvlos, M.; Pham, T.; Klock, T., Synthesis of an ethylene-glycol cross-linked amino-acid. *Tetrahedron Lett.* **1991,** *32*, 1283-1286.

87. Nakajima, K.; Neya, M.; Yamada, S.; Okawa, K., Studies on 2-aziridinecarboxylic acid .6. Synthesis of beta-alkoxy-alpha-amino acids via ring-opening reaction of aziridine. *Bull. Chem. Soc. Jpn.* **1982,** *55*, 3049-3050.

88. McKeever, B.; Pattenden, G., Total synthesis of the cytotoxic cyclopeptide mollamide, isolated from the sea squirt *Didemnum molle. Tetrahedron* **2003,** *59*, 2701-2712.

89. Isidro-Llobet, A.; Guasch-Camell, J.; Alvarez, M.; Albericio, F., p-Nitrobenzyloxycarbonyl (pNZ) as a temporary N-alpha-protecting group in orthogonal solid-phase peptide synthesis - Avoiding diketopiperazine and aspartimide formation. *Eur. J. Org. Chem.* **2005**, 3031-3039.

90. Polt, R.; Szabo, L.; Treiberg, J.; Li, Y. S.; Hruby, V. J., General-methods for alpha-O-Ser/Thr or beta-O-Ser/Thr glycosides and glycopeptides - solid-phase synthesis of O-glycosyl cyclic enkephalin analogs. *J. Am. Chem. Soc.* **1992,** *114*, 10249-10258.

91. Szabo, L.; Li, Y. S.; Polt, R., O-Glycopeptides - a Simple beta-stereoselective glycosidation of serine and threonine via a favorable hydrogen-bonding pattern. *Tetrahedron Lett.* **1991,** *32*, 585-588.

92. Bose, A. K., *Organic Synthesis*. Wiley & Sons: New York, 1973; Vol. V, p 973-974.

93. Bayo, N.; Jimenez, J. C.; Rivas, L.; Nicolas, E.; Albericio, F., Solid-phase synthesis of the cyclic lipononadepsipeptide [N-Mst(Ser1), D-Ser4, L-Thr6, L-Asp8, L-Thr9]syringotoxin. *Chem. Eur. J.* **2003,** *9*, 1096-1103.

94. Kuethe, J. T.; Marcoux, J. F.; Wong, A.; Wu, J.; Hillier, M. C.; Dormer, P. G.; Davies, I. W.; Hughes, D. L., Stereoselective preparation of a cyclopentane-based NK1 receptor antagonist bearing an unsymmetrically substituted Sec-Sec ether. *J. Org. Chem.* **2006,** *71*, 7378-7390.

95. Tomasini, C.; Vecchione, A., Novel synthesis of 4-carboxymethyl 5-alkyl/aryl oxazolidin-2-ones by rearrangement of 2-carboxymethyl 3-alkyl/aryl N-tert-butoxycarbonyl aziridines. *Org. Lett.* **1999,** *1*, 2153-2156.

96. Ferraris, D.; Drury, W. J.; Cox, C.; Lectka, T., "Orthogonal" Lewis acids: Catalyzed ring opening and rearrangement of acylaziridines. *J. Org. Chem.* **1998,** *63*, 4568-4569.

97. Osterkamp, F.; Wehlan, H.; Koert, U.; Wiesner, M.; Raddatz, P.; Goodman, S. L., Synthesis and biological evaluation of dianhydrohexitol integrin antagonists. *Tetrahedron* **1999,** *55*, 10713-10734.

98. Zhu, X. M.; Schmidt, R. R., Efficient synthesis of differently protected lanthionines via beta-bromoalanine derivatives. *Eur. J. Org. Chem.* **2003**, 4069-4072.

99. Pattabiraman, V. R. Chemical Synthesis of Lantibiotics and Their Analogues. Ph.D. Thesis, University of Alberta, Edmonton, 2008.

100. Garneau, S.; Ference, C. A.; van Belkum, M. J.; Stiles, M. E.; Vederas, J. C., Purification and characterization of brochocin A and brochocin B(10-43), a functional fragment generated by heterologous expression in *Carnobacterium piscicola. Appl. Environ. Microbiol.* **2003,** *69*, 1352-1358.

101. Fukuyama, T.; Cheung, M.; Jow, C. K.; Hidai, Y.; Kan, T., 2,4-dinitrobenzenesulfonamides: A simple and practical method for the preparation of a variety of secondary amines and diamines. *Tetrahedron Lett.* **1997,** *38*, 5831-5834.

102. Mao, H.; Joly, G. J.; Peeters, K.; Hoornaert, G. J.; Compernolle, F., Synthesis of 1-deoxymannojirimycin analogues using N-tosyl and N-nosyl activated aziridines derived from 1-amino-1-deoxyglucitol. *Tetrahedron* **2001,** *57*, 6955-6967.

103. Di Bussolo, V.; Checchia, L.; Romano, M. R.; Pineschi, M.; Crotti, P., Stereoselective synthesis of 2,3-unsaturated 1,6-oligosaccharides by means of a glycal-derived allyl epoxide and N-nosyl aziridine. *Org. Lett.* **2008,** *10*, 2493-2496.

104. Miller, S. C.; Scanlan, T. S., oNBS-SPPS: A new method for solid-phase peptide synthesis. *J. Am. Chem. Soc.* **1998,** *120*, 2690-2691.

105. Huang, Z.; Derksen, D. J.; Vederas, J. C., Preparation and use of cysteine orthoesters for solid-supported synthesis of peptides. *Org. Lett.* **2010,** *12*, 2282-2285.

106. Barlos, K.; Gatos, D.; Schafer, W., Synthesis of prothymosin alpha (Pro T-Alpha) - a protein consisting of 109 amino-acid-residues. *Angew. Chem. Int. Edit. Engl.* **1991,** *30*, 590-593.

107. Barlos, K.; Chatzi, O.; Gatos, D.; Stavropoulos, G., 2-Chlorotrityl chloride resin - studies on anchoring of Fmoc-amino acids and peptide cleavage. *Int. J. Pept. Protein Res.* **1991,** *37*, 513-520.

108. Li, X. Q.; Kawakami, T.; Aimoto, S., Direct preparation of peptide thioesters using an Fmoc solid-phase method. *Tetrahedron Lett.* **1998,** *39*, 8669-8672.

109. Vazquez, J. V.; Qushair, G.; Albericio, F., Qualitative colorimetric tests for solid phase synthesis. In *Combinatorial Chemistry, Pt B*, Academic Press Inc: San Diego, 2003; Vol. 369, pp 21-35.

110. WHO Cancer. http://www.who.int/mediacentre/factsheets/fs297/en/ (Access date July 8, 2010),

111. CDC number of deaths for leading causes of death. http://www.cdc.gov/nchs/fastats/lcod.htm (Access date July 8, 2010),

112. Avendano, C.; Menendez, J. C., *Medicinal Chemistry of Anticancer Drugs*. 1st Ed.; Elsevier Science: 2008; p 1.

113. Molinski, T. F.; Dalisay, D. S.; Lievens, S. L.; Saludes, J. P., Drug development from marine natural products. *Nat. Rev. Drug Discov.* **2009,** *8*, 69-85.

114. Newman, D. J.; Cragg, G. M., Natural products as sources of new drugs over the last 25 years. *J. Nat. Prod.* **2007,** *70*, 461-477.

115. Williams, D. E.; Austin, P.; Diaz-Marrero, A. R.; Van Soest, R.; Matainaho, T.; Roskelley, C. D.; Roberge, M.; Andersen, R. J., Neopetrosiamides, peptides from the marine sponge *Neopetrosia* sp. that inhibit amoeboid invasion by human tumor cells. *Org. Lett.* **2005,** *7*, 4173-4176.

116. Friedl, P., Prespecification and plasticity: shifting mechanisms of cell migration. *Curr. Opin. Cell Biol.* **2004,** *16*, 14-23.

117. Wolf, K.; Mazo, I.; Leung, H.; Engelke, K.; von Andrian, U. H.; Deryugina, E. I.; Strongin, A. Y.; Brocker, E. B.; Friedl, P., Compensation mechanism in tumor cell migration: mesenchymal-amoeboid transition after blocking of pericellular proteolysis. *J. Cell Biol.* **2003,** *160*, 267-277.

118. Austin, P.; Heller, M.; Williams, D. E.; McIntosh, L. P.; Vogl, A. W.; Foster, L. J.; Andersen, R. J.; Roberge, M.; Roskelley, C. D., Release of membrane-bound vesicles and inhibition of tumor cell adhesion by the peptide neopetrosiamide A. *PLoS One* **2010,** *5*, 1-14.

119. Armishaw, C. J.; Alewood, P. F., Conotoxins as research tools and drug leads. *Curr. Protein Pept. Sci.* **2005,** *6*, 221-240.

120. Schulz, A.; Kluver, E.; Schulz-Maronde, S.; Adermann, K., Engineering disulfide bonds of the novel human beta-defensins hBD-27 and hBD-28: Differences in disulfide formation and biological activity among human beta-defensins. *Biopolymers* **2005,** *80*, 34-49.

121. Sollod, B. L.; Wilson, D.; Zhaxybayeva, O.; Gogarten, J. P.; Drinkwater, R.; King, G. F., Were arachnids the first to use combinatorial peptide libraries? *Peptides* **2005,** *26*, 131-139.

122. Bulaj, G., Integrating the discovery pipeline for novel compounds targeting ion channels. *Curr. Opin. Chem. Biol.* **2008,** *12*, 441-447.

123. Wu, J.; Watson, J. T., A novel methodology for assignment of disulfide bond pairings in proteins. *Protein Sci.* **1997,** *6*, 391-398.

124. Walewska, A.; Skalicky, J. J.; Davis, D. R.; Zhang, M. M.; Lopez-Vera, E.; Watkins, M.; Han, T. S.; Yoshikami, D.; Olivera, B. M.; Bulaj, G., NMR-based mapping of disulfide bridges in cysteine-rich peptides: Application to the mu-Conotoxin SxIIIA. *J. Am. Chem. Soc.* **2008,** *130*, 14280-14286.

125. Rosengren, K. J.; Daly, N. L.; Plan, M. R.; Waine, C.; Craik, D. J., Twists, knots, and rings in proteins - Structural definition of the cyclotide framework. *J. Biol. Chem.* **2003,** *278*, 8606-8616.

126. Gray, W. R., Disulfide structures of highly bridged peptides - a New strategy for analysis. *Protein Sci.* **1993,** *2*, 1732-1748.

127. Wu, W.; Huang, W.; Qi, R. F.; Chou, Y. T.; Torng, E.; Watson, J. T., 'Signature sets', minimal fragment sets for identifying protein disulfide

structures with cyanylation-based mass mapping methodology. *J. Proteome Res.* **2004,** *3*, 770-777.

128. Goransson, U.; Craik, D. J., Disulfide mapping of the cyclotide kalata B1 - Chemical proof of the cyclic cystine knot motif. *J. Biol. Chem.* **2003,** *278*, 48188-48196.

129. Liu, H. Q.; Boudreau, M. A.; Zheng, J.; Whittal, R. M.; Austin, P.; Roskelley, C. D.; Roberge, M.; Andersen, R. J.; Vederas, J. C., Chemical synthesis and biological activity of the neopetrosiamides and their analogues: Revision of disulfide bond connectivity. *J. Am. Chem. Soc.* **2010,** *132*, 1486-1487.

130. Moroder, L.; Musiol, H. A.; Gotz, M.; Renner, C., Synthesis of single- and multiple-stranded cystine-rich peptides. *Biopolymers* **2005,** *80*, 85-97.

131. Moroder, L.; Besse, D.; Musiol, H. J.; RudolphBohner, S.; Siedler, F., Oxidative folding of cystine-rich peptides vs regioselective cysteine pairing strategies. *Biopolymers* **1996,** *40*, 207-234.

132. Tam, J. P.; Lu, Y. A.; Yang, J. L.; Chiu, K. W., An unusual structural motif of antimicrobial peptides containing end-to-end macrocycle and cystine-knot disulfides. *Proc. Natl. Acad. Sci. U. S. A.* **1999,** *96*, 8913-8918.

133. Stymiest, J. L.; Mitchell, B. F.; Wong, S.; Vederas, J. C., Synthesis of oxytocin analogues with replacement of sulfur by carbon gives potent antagonists with increased stability. *J. Org. Chem.* **2005,** *70*, 7799-7809.

134. Muttenthaler, M.; Nevin, S. T.; Grishin, A. A.; Ngo, S. T.; Choy, P. T.; Daly, N. L.; Hu, S. H.; Armishaw, C. J.; Wang, C. I. A.; Lewis, R. J.; Martin, J. L.; Noakes, P. G.; Craik, D. J.; Adams, D. J.; Alewood, P. F., Solving the alpha-Conotoxin folding problem: efficient selenium-directed on-resin generation of more potent and stable nicotinic acetylcholine receptor antagonists. *J. Am. Chem. Soc.* **2010,** *132*, 3514-3522.

135. Derksen, D. J.; Stymiest, J. L.; Vederas, J. C., Antimicrobial leucocin analogues with a disulfide bridge replaced by a carbocycle or by noncovalent interactions of allyl glycine residues. *J. Am. Chem. Soc.* **2006,** *128*, 14252-14253.

136. Derksen, D. J.; Boudreau, M. A.; Vederas, J. C., Hydrophobic interactions as substitutes for a conserved disulfide linkage in the type IIa bacteriocins, leucocin A and pediocin PA-1. *ChemBioChem* **2008,** *9*, 1898-1901.

137. Escher, S. E.; Sticht, H.; Forssmann, W. G.; Rosch, P.; Adermann, K., Synthesis and characterization of the human CC chemokine HCC-2. *J. Pept. Res.* **1999,** *54*, 505-513.

138. Cuthbertson, A.; Indrevoll, B., Regioselective formation, using orthogonal cysteine protection, of an alpha-conotoxin dimer peptide containing four disulfide bonds. *Org. Lett.* **2003,** *5*, 2955-2957.

139. Annis, I.; Chen, L.; Barany, G., Novel solid-phase reagents for facile formation of intramolecular disulfide bridges in peptides under mild conditions. *J. Am. Chem. Soc.* **1998,** *120*, 7226-7238.

140. Maruyama, T.; Ikeo, T.; Ueki, M., A rapid and facile method for the preparation of peptide disulfides. *Tetrahedron Lett.* **1999,** *40*, 5031-5034.

141. Soll, R.; Beck-Sickinger, A. G., On the synthesis of orexin A: A novel one-step procedure to obtain peptides with two intramolecular disulphide bonds. *J. Pept. Sci.* **2000,** *6*, 387-397.

142. Kamber, B.; Hartmann, A.; Eisler, K.; Riniker, B.; Rink, H.; Sieber, P.; Rittel, W., The Synthesis of cystine peptides by iodine oxidation of S-trityl-cysteine and S-acetamidomethyl-cysteine peptides. *Helv. Chim. Acta* **1980,** *63*, 899-915.

143. Akaji, K.; Fujino, K.; Tatsumi, T.; Kiso, Y., Total synthesis of human insulin by regioselective disulfide formation using the silyl chloride sulfoxide method. *J. Am. Chem. Soc.* **1993,** *115*, 11384-11392.

144. Szabo, I.; Schlosser, G.; Hudecz, F.; Mezo, G., Disulfide bond rearrangement during regioselective oxidation in $PhS(O)Ph/CH_3SiCl_3$ mixture for the synthesis of alpha-conotoxin GI. *Biopolymers* **2007,** *88*, 20-28.

145. Bach, R. D.; Dmitrenko, O.; Thorpe, C., Mechanism of thiolate-disulfide interchange reactions in biochemistry. *J. Org. Chem.* **2008,** *73*, 12-21.

146. Akaji, K.; Tatsumi, T.; Yoshida, M.; Kimura, T.; Fujiwara, Y.; Kiso, Y., Disulfide bond formation using the silyl chloride sulfoxide system for the synthesis of a cystine peptide. *J. Am. Chem. Soc.* **1992,** *114*, 4137-4143.

147. Duenas, E. T.; Keck, R.; De Vos, A.; Jones, A. J. S.; Cleland, J. L., Comparison between light induced and chemically induced oxidation of rhVEGF. *Pharm. Res.* **2001,** *18*, 1455-1460.

148. Bulaj, G.; Zhang, M. M.; Green, B. R.; Fiedler, B.; Layer, R. T.; Wei, S.; Nielsen, J. S.; Low, S. J.; Klein, B. D.; Wagstaff, J. D.; Chicoine, L.; Harty, T. P.; Terlau, H.; Yoshikami, D.; Olivera, B. M., Synthetic mu O-conotoxin MrVIB blocks TTX-resistant sodium channel Na(V)1.8 and has a long-lasting analgesic activity. *Biochemistry* **2006,** *45*, 7404-7414.

149. Roskelley, C. D.; Williams, D. E.; McHardy, L. M.; Leong, K. G.; Troussard, A.; Karsan, A.; Andersen, R. J.; Dedhar, S.; Roberge, M., Inhibition of tumor cell invasion and angiogenesis by motuporamines. *Cancer Res.* **2001,** *61*, 6788-6794.

150. Nishio, H.; Inui, T.; Nishiuchi, Y.; De Medeiros, C. L. C.; Rowan, E. G.; Harvey, A. L.; Katoh, E.; Yamazaki, T.; Kimura, T.; Sakakibara, S., Chemical synthesis of dendrotoxin-I: revision of the reported structure. *J. Pept. Res.* **1998,** *51*, 355-364.

151. Cotton, J.; Crest, M.; Bouet, F.; Alessandri, N.; Gola, M.; Forest, E.; Karlsson, E.; Castaneda, O.; Harvey, A. L.; Vita, C.; Menez, A., A potassium-channel toxin from the sea anemone *Bunodosoma granulifera*, an inhibitor for Kv1 channels - Revision of the amino acid sequence, disulfide-bridge assignment, chemical synthesis, and biological activity. *Eur. J. Biochem.* **1997,** *244*, 192-202.

152. Smith, M. B.; March, J., *Advanced Organic Chemistry: Reactions, Mechanisms and Structures*. 5th Ed.; John Wiley & Sons, Inc: New York, 2001; p 14.

153. Landschulz, W. H.; Johnson, P. F.; McKnight, S. L., The Leucine Zipper - a Hypothetical Structure common to a new class of DNA-binding proteins. *Science* **1988,** *240*, 1759-1764.

154. Derbre, S.; Roue, G.; Poupon, E.; Susin, S. A.; Hocquemiller, R., Annonaceous acetogenins: The hydroxyl groups and THF rings are crucial structural elements for targeting the mitochondria, demonstration with the synthesis of fluorescent squamocin analogues. *ChemBioChem* **2005,** *6*, 979-982.

155. Huang, B. H.; Desai, A.; Tang, S. Z.; Thomas, T. P.; Baker, J. R., The synthesis of a c(RGDyK) targeted SN38 prodrug with an indolequinone structure for bioreductive drug release. *Org. Lett.* **2010,** *12*, 1384-1387.

156. Perrin, D. D.; Armarego, W. L. F., *Purification of Laboratory Chemicals*. 3rd Ed.; Pergamon Press: New York, 1993.

157. Vogel, A., *Vogel's Textbook of Practical Organic Chemistry*. 4th Ed.; Wiley & Sons Inc: New York, 1978.

158. Still, W. C.; Kahn, M.; Mitra, A., Rapid chromatographic technique for preparative separations with moderate resolution. *J. Org. Chem.* **1978,** *43*, 2923-2925.

159. Baldwin, J. E.; Spivey, A. C.; Schofield, C. J.; Sweeney, J. B., Amino-acid synthesis via ring-opening of N-sulfonyl aziridine-2-carboxylate esters with organometallic reagents. *Tetrahedron* **1993,** *49*, 6309-6330.

160. Xia, Z. P.; Smith, C. D., Efficient synthesis of a fluorescent farnesylated ras peptide. *J. Org. Chem.* **2001,** *66*, 5241-5244.

161. Lewis, I.; Bauer, W.; Albert, R.; Chandramouli, N.; Pless, J.; Weckbecker, G.; Bruns, C., A novel somatostatin mimic with broad somatotropin release inhibitory factor receptor binding and superior therapeutic potential. *J. Med. Chem.* **2003,** *46*, 2334-2344.

162. Ginisty, M.; Gravier-Pelletier, C.; Le Merrer, Y., Chemical investigations in the synthesis of O-serinyl aminoribosides. *Tetrahedron: Asymmetry* **2006,** *17*, 142-150.

163. Wang, D. X.; Liu, H. Q.; Lin, H.; Tian, G. J., Solid-phase synthesis of Mannich-base hybridized cyclopeptides. *Tetrahedron Lett.* **2003,** *44*, 4793-4795.

# Appendix: Synthesis and enzymatic study of oxa-DAP derivatives

## A. 1. Background

The increasing bacterial resistance to conventional antibiotics continues to stimulate interest in new strategies for disrupting bacterial cell wall biosynthesis. As depicted in section 2.1.4., *meso*-Diaminopimelic acid (*meso*-DAP) (**A1**) is involved in the cross-linking of the peptidoglycan layers of virtually all Gram-negative bacteria, whereas its metabolic product, L-lysine, is used analogously in many Gram-positive organisms.[1] The biosynthetic pathways to *meso*-DAP (**A1**) and L-lysine are shown in Figure A-1.[2] The enzymes involved in this pathway provide potential targets for the development of new antibiotics with low mammalian toxicity because mammals do not make DAP or L-lysine and therefore require L-lysine in their diet.[3]

**Figure A-1.** Bacterial biosynthetic pathway to *meso*-DAP (**A1**) and L-lysine

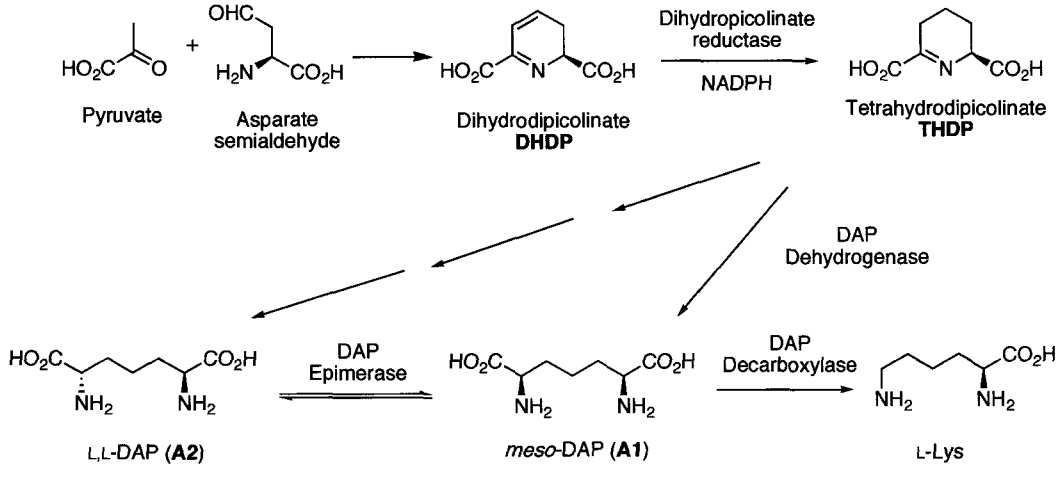

One of these biosynthetic enzymes, DAP epimerase, catalyzes the reversible conversion of L,L-DAP (**A2**) to *meso*-DAP (**A1**) without the use of metals, cofactors or reducible keto or imino functional groups. DAP epimerase belongs to the class pyridoxal 5'-phosphaste (PLP)-independent amino acid racemase, which includes aspartic racemase, glutamase racemase and proline racemase.[4] An unusual " two base" mechanism has been proposed for DAP epimerase, which involves two active-site cysteine residues as a thiol-thiolate pair to deprotonate the α-carbon of the substrate and reprotonate from the opposite side (Figure A-2). Detailed mechanistic insight has been obtained from crystallographic data.[5]

**Figure A-2.** Proposed mechanism for the interconversion of L,L-DAP and *meso* DAP by DAP epimerase.

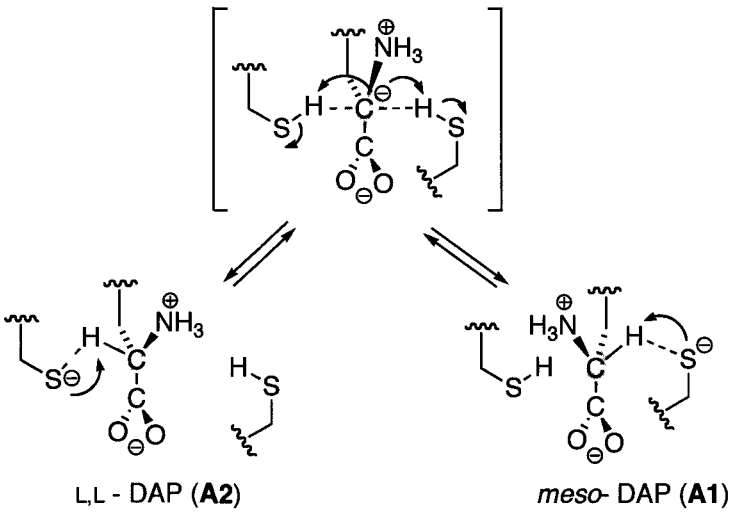


DAP epimerase exhibits very strict substrate specificity. It only accepts *meso*-DAP and L,L-DAP as substrates, and not D,D-DAP. This suggests the stereochemistry at the nonreacting (distal) carbon is crucial for substrate

recognition. In addition, *meso*-lanthionine (**A3**), which has a sulfur atom instead of a $CH_2$ group at the 4-position, is also not accepted by the enzyme.[6] Presumably, due to the significant differences in bond lengths (1.53Å vs 1.80Å) and bond angles (109° vs 101°) of C-C-C and C-S-C bonds between the natural substrate and the sulfur analogue, *meso*-lanthionine (**A3**) apparently cannot be accommodated in the very tight active site of this epimerase (Figure A-3). However, we proposed that L,L-oxa-DAP (**A4**), with the $CH_2$ at the 4-position in DAP replaced with an oxygen atom, could be a substrate or inhibitor as the predicted bond lengths (1.53Å vs 1.43Å) and bond angles (109° vs 111.4°) of C-C-C and C-O-C bonds are more comparable.[7] In this context, we decided to stereoselectively synthesize the novel DAP analogue and test the activity towards the DAP epimerase.

**Figure A-3.** Structures of L,L-DAP, *meso*-lanthionine and L,L-oxa-DAP

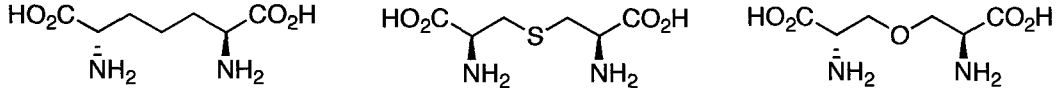


L,L-DAP **A2** | *meso*-lanthionine **A3** | L,L-oxa-DAP **A4**

## A. 2. Results and discussions

Utilizing the established synthetic methodology for oxa-lan derivatives, the stereoselective synthesis of oxygen analogues of L,L-DAP and *meso* DAP can be achieved via the azirdine ring opening with the hydroxyl side chain of the serine followed by global deprotection.[8] The fully protected L,L-oxa-DAP (**57**) and *meso*-oxa-DAP (**67a**) are prepared via the stereoselective ring opening

reaction as described in section 2.2.1.a.. Global deprotection of the fully protected L,L- and *meso*-oxa-DAP derivatives are attempted using 6N HCl. Unfortunately, this provides only the partially deprotected product with the pNZ group still attached as suggested by NMR and mass spectrometry. This is possibly due to the acidic stability of the pNZ group.[9] Simple hydrogenolytic deprotection of the remaining pNZ gives the completely deprotected L,L-DAP (**A4**). The *meso*-oxa-DAP (**A5**) isomer is also prepared in the same manner as L,L-DAP (**A4**) (Scheme A-1).

**Scheme A-1.** Global deprotection of the fully protected oxa-DAP derivatives

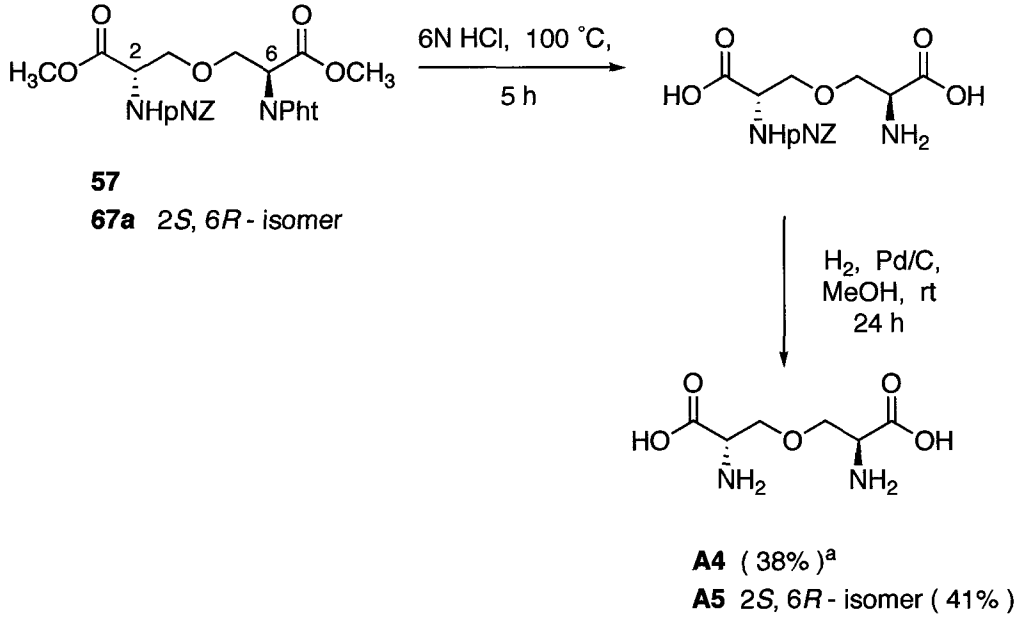


**57**
**67a** 2*S*, 6*R* - isomer

**A4** ( 38% )[a]
**A5** 2*S*, 6*R* - isomer ( 41% )

a. Isolated yields over two steps after cationic ion exchange column

The inhibition studies with DAP epimerase are performed using a coupled enzyme assay at pH 7.8. In the assay, *meso*-DAP (**A1**) produced by DAP epimerase from L,L-DAP (**A2**) is transformed by DAP-dehydrogenase to produce L-THDP (**A6**) with generation of NADPH, which is monitored

spectrophotometrically (Scheme A-2).[4] The results show that neither L,L-oxa-DAP (**A4**) nor *meso*-oxa-DAP (**A5**) displays any inhibition of DAP epimerase.

**Scheme A-2.** Spectrophotometric coupled assay for DAP epimerase activity.

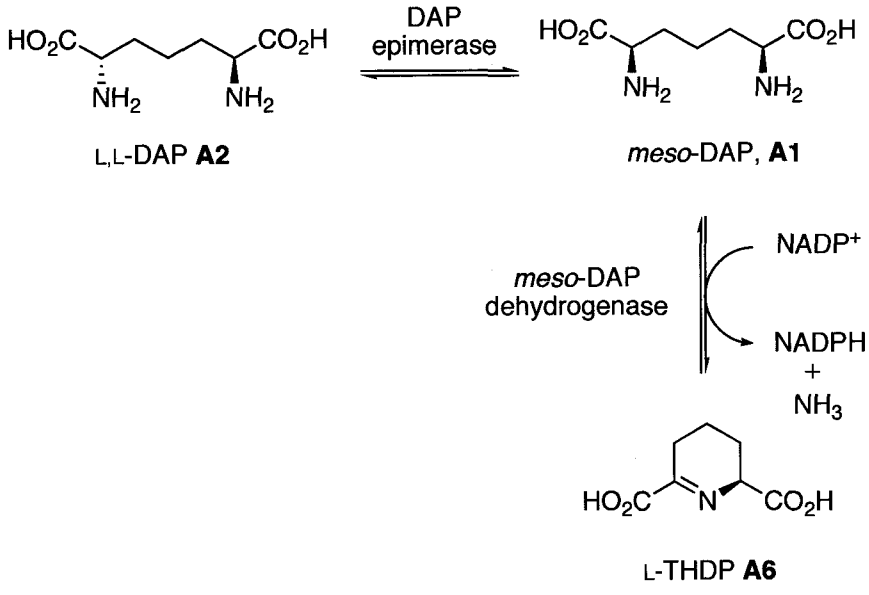


To study the substrate specificity, the couple enzyme assay is not suitable, as *meso*-oxa-DAP (**A5**) cannot be transformed by DAP-dehydrogenase to the corresponging oxygen analogue of L-THDP (**A7**) with the production of NADPH (Scheme A-3). This result is confirmed by the UV assay wherein the synthetic *meso*-oxa-DAP (**A5**) is treated with DAP-dehydrogenase and results in no change in UV absorbance.

**Scheme A-3.** Testing of *meso*-oxa-DAP as a substrate for *meso*-DAP dehydrogenase

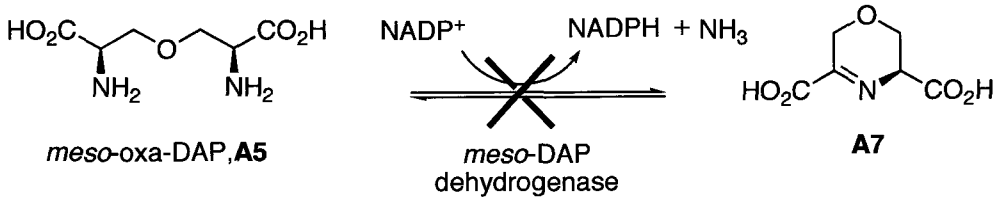

Therefore, the substrate test for DAP epimerase is done in deuterated solvents, which allow for using NMR and mass spectrometry to monitor the exchange of the α-hydrogen with a deuterium by the epimerase.[10, 11] Incubation of L,L-oxa-DAP (**A4**) with DAP epimerase in deuterated Tris buffer results in the change of the integral for the α-hydrogen in the $^1$H NMR spectrum due to incorporation of deuterium at the α-position. This demonstrates that DAP epimerase accepts L,L-oxa-DAP (**A4**) as a substrate. Initial velocity for the enzymatic reaction could be obtained by monitoring the change in integral values for the α-proton of **A4** and **A2** in separate reactions as a function of time. L,L-oxa-DAP (**A4**) exhibits an initial velocity that is 26% of that of the natural substrate L,L-DAP (**A2**) (Figure A-4).

**Scheme A-4.** Time course of epimerization of L,L-DAP (**A2**) and L,L-oxa-DAP (**A4**) catalyzed by DAP epimerase.

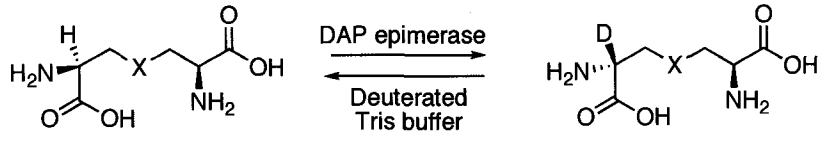


**A2** X= $CH_2$ L,L-DAP
**A4** X= O L,L-Oxa-DAP

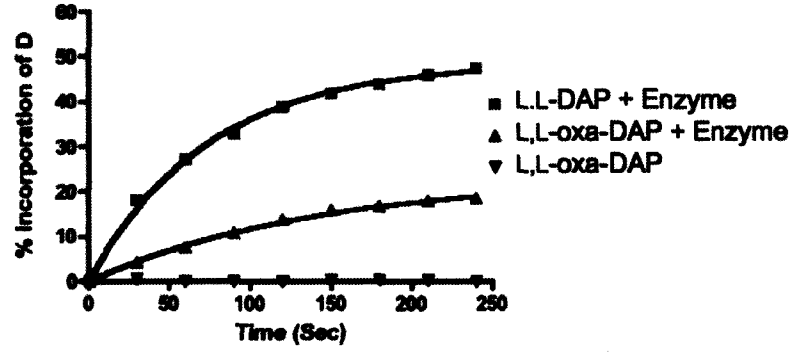


*As both meso and L,L-isomers are substrates/products and there is an isotope effect for removal of a-hydrogen, the conversion to deuterated product slows as the reaction proceeds.*

The observed results suggest that although oxygen analogues of DAP show no inhibition of DAP epimerase, DAP epimerase accommodates the substitution of an oxygen atom for a methylene group at the 4-position in its natural substrate. The presence of a polar oxygen atom appears to disrupt the tight hydrophobic interactions in the closed enzyme active site and renders the poor binding of oxa-DAP to the enzyme.

## A. 3. Conclusions

In conclusion, the novel oxa-DAP analogues (**A4** and **A5**) have been synthesized via the stereoselective aziridine ring opening methodology. The substrate and inhibition study for DAP epimerase suggest the oxygen analogue (**A4**) can be used by the enzyme as an effective substrate and it shows no inhibition activity. This study further highlights the tight substrate specificity of DAP epimerase and gives further insight into the structural features of the enzyme activate site.

## A. 4. Experimental procedures

### (2*S*, 6*S*)-3,3-oxybis(2-aminopropanoic acid) (A4)

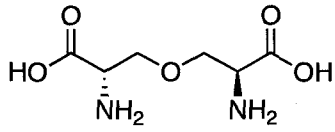

To a solution of **57** (250 mg, 0.473 mmol) in chloroform (5ml) was added 6N HCl (60 mL). The reaction mixture was refluxed for 5 h. After washing with $Et_2O$ (3 x 30 ml), the aqueous layer was concentrated to yield a yellow oil. The oil was dissolved in MeOH (50 ml), followed by addition of 10% Pd/C (10 mg). The reaction mixture was stirred for 12 h at room temperature. The reaction mixture was filtered through celite and the filtrate was concentrated *in vacuo* to give the crude product as a green oil. The crude product was purified by ion-exchange chromatography (Biorad AG 50W-X8 hydrogen form resin) by loading with distilled $H_2O$, flushing 3 column volume with de-ionized water, followed by elution with $NH_4OH$ (2N) to give the title compound (**A4**) as a white powder after lyophilyzation (27 mg, 38% over two steps); $[\alpha]_D^{25}$ -6.72° (*c* 0.18, $H_2O$); IR ($CHCl_3$ cast): 2942 (br), 1596, 1521 $cm^{-1}$; $^1H$ NMR ($D_2O$, 500 MHz): δ 3.98 (dd, 2H, $J$ = 4.0, 10.5 Hz, $H_\beta$), 3.94 (dd, 2H, $J$ = 3.0, 4.0 Hz, $H_\alpha$), 3.88 (dd, 2H, $J$ = 3.0, 10.5 Hz, $H_{\beta'}$); $^{13}C$ NMR ($CDCl_3$, 100 MHz) δ 173.6, 70.1, 55.2; HRMS (ES): Calcd for $C_6H_{12}N_2O_5Na$ 215.0638, found 215.0638.

**(*S*)-2-amino-3-((*R*)-2-amino-2-carboxyethoxy)propanoic acid (A5)**

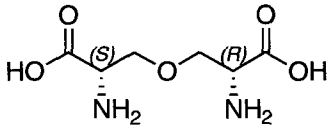

In similar manner to **A4**, the title compound **A5** was prepared starting from **67a** as a white powder (70 mg, 41% over two steps), $[\alpha]_D^{25}$ 0.0° (*c* 0.35, $H_2O$); IR ($CHCl_3$ cast): 3383, 3300-2042 (br), 1643 $cm^{-1}$; $^1H$ NMR ($D_2O$, 500 MHz): δ 3.93(m, 6H, -$CHCH_2$-); $^{13}C$ NMR ($CDCl_3$, 125 MHz): δ 172.9, 70.0, 55.5; HRMS (ES): Calcd for $C_6H_{12}N_2O_5Na$ 215.0638, found 215.0639

**Enzymatic kinetics using NMR assay:**

Enzymatic reactions were performed by incubating 27 μL (0.6 mg/mL solution) of active DAP epimerase from *Haemophilus influenzae* with the substrates (5.2 mM, 0.0026 mmol) in deuterated Tris buffer (0.1 M Tris, 1 mM DTT, 1 mM EDTA, pD7.8, final volume 0.5 mL). The reactions were initiated by adding enzyme and time course $^1H$-NMR spectra was recorded at 27°C on a 600 MHz NMR instrument at specified time intervals. The experiments were repeated to obtain duplicated results. A $^1H$-NMR spectrum of substrate without enzyme was recorded as a control. The $^1H$-NMR spectra showed a continuous decrease in the integral value at 3.94 ppm (L,L-oxa-DAP) and 3.76 ppm (L,L-DAP) originating from the exchange of $H_\alpha$ to deuterium. Furthermore, the $^1H$-NMR spectra also showed the change of splitting pattern of $H_\beta$ (L,L-oxa-DAP) due to the

incorporation of deuterium at the α position. The $^{13}$C-NMR and MS were also recorded to confirm the incorporation of deuterium into the substrate.

**Calculation of the initial velocity of the enzymatic reaction**

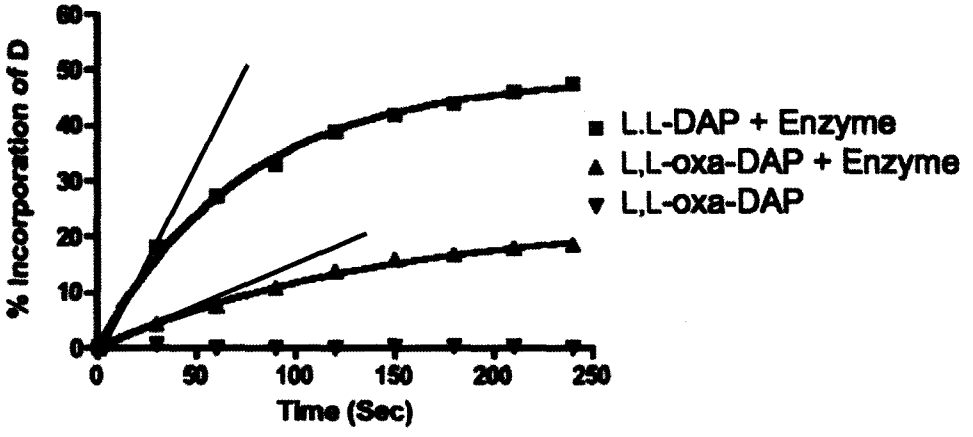


**Equation A-1.** The percentage incorporation of deuterium in L,L-oxa-DAP

% Incorporation of D = ($2H_\alpha$ - integration of remaining $H_\alpha$)/$2H_\alpha$

Values obtained for the incorporation of deuterium were graphed against time. Curve fitting (Figure 10) was done by the equation $Y = -e^{kx}$ using Prism software. The initial velocity was calculated from the data in the linear portion of the graph (Figure 10) using the equation Y = KX. The values of 0.485 Unit* (L,L-DAP) and 0.128 Unit (L,L-oxa-DAP) were obtained according to the corresponding slopes. Based on the ratio of the slope values, L,L-oxa-DAP showed an initial velocity that is 26% of that of the natural substrate L,L-DAP.

**Unit is defined as the percentage of deuterium product formed per second.*

## A. 5. References

1. van Heijenoort, J., Recent advances in the formation of the bacterial peptidoglycan monomer unit. *Nat. Prod. Rep.* **2001,** *18*, 503-519.

2. Cox, R. J.; Sutherland, A.; Vederas, J. C., Bacterial diaminopimelate metabolism as a target for antibiotic design. *Bioorg. Med. Chem.* **2000,** *8*, 843-871.

3. Vederas, J. C., 2005 Alfred Bader Award Lecture Diaminopimelate and lysine biosynthesis - An antimicrobial target in bacteria. *Can. J. Chem.-Rev. Can. Chim.* **2006,** *84*, 1197-1207.

4. Wiseman, J. S.; Nichols, J. S., Purification and properties of diaminopimelic acid epimerase from *Escherichia-coli*. *J. Biol. Chem.* **1984,** *259*, 8907-8914.

5. Pillai, B.; Cherney, M. M.; Diaper, C. M.; Sutherland, A.; Blanchard, J. S.; Vederas, J. C.; James, M. N. G., Structural insights into stereochemical inversion by diaminopimelate epimerase: An antibacterial drug target. *Proc. Natl. Acad. Sci. U. S. A.* **2006,** *103*, 8668-8673.

6. Lam, L. K. P.; Arnold, L. D.; Kalantar, T. H.; Kelland, J. G.; Lanebell, P. M.; Palcic, M. M.; Pickard, M. A.; Vederas, J. C., Analogs of diaminopimelic acid as inhibitors of *meso*-diaminopimelate dehydrogenase and LL-diaminopimelate epimerase. *J. Biol. Chem.* **1988,** *263*, 11814-11819.

7. Allen, F. H.; Kennard, O.; Watson, D. G.; Brammer, L.; Orpen, A. G.; Taylor, R., Tables of bond lengths determined by X-ray and neutron-

diffraction .1. Bond lengths in organic-compounds. *J. Chem. Soc.-Perkin Trans. 2* **1987**, S1-S19.

8. Liu, H. Q.; Pattabiraman, V. R.; Vederas, J. C., Stereoselective syntheses of 4-oxa diaminopimelic acid and its protected derivatives via aziridine ring opening. *Org. Lett.* **2007,** *9*, 4211-4214.

9. Shields, J. E.; Carpenter, F. H., Synthesis of a heptapeptide sequence derived from bovine insulin. *J. Am. Chem. Soc.* **1961,** *83*, 3066-3070.

10. Campbell, I. D., Nmr-Studies of Enzymes. *Fresenius Zeitschrift Fur Analytische Chemie* **1986,** *324*, 437-441.

11. Petersen, B. O.; Krah, M.; Duus, J. O.; Thomsen, K. K., A transglycosylating 1,3(4)-beta-glucanase from *Rhodothermus marinus* NMR analysis of enzyme reactions. *Eur. J. Biochem.* **2000,** *267*, 361-369.